THE GENOMIC BASIS AND SPATIAL SCALE OF VARIATION IN THERMAL RESPONSES OF ATLANTIC COD (*GADUS MORHUA*)

by

Rebekah Alice Oomen

Submitted in partial fulfilment of the requirements
for the degree of Doctor of Philosophy

at

Dalhousie University
Halifax, Nova Scotia
March, 2019

For my parents, who sparked my interest in the natural world
and have supported me every day since,

and

for Thomas Torgersen, a friend and fellow lover of jazz and fishes
whose memory continues to inspire me.

TABLE OF CONTENTS

List Of Tables

List Of Figures

Abstract

The thesis investigates the genomic basis and spatial scale of variation in thermal responses of Atlantic cod (*Gadus morhua*), with the over-arching aim of improving our understanding of plastic and evolutionary responses to environmental change in natural populations. It advances our understanding of how cod will respond to global climate change, how cod populations will respond differently depending on the local conditions to which they are adapted, and the genomic mechanisms of local adaptation with gene flow. We first review the potential of RNA sequencing as a tool to study the complex responses of non-model organisms to the environment and illustrate how it can help us understand plastic and evolutionary responses to global environmental change in fishes. We rear cod larvae at a range of temperatures in the laboratory and find, using RNA sequencing, changes in gene expression consistent with a severe cellular stress response at both ambient and forecasted (+2°C and +4°C) temperatures. Earlier onset of the transcriptomic stress response is observed at higher temperatures and is not explained by differences in degree-days among treatments. The stress response is accompanied by faster growth and an increase in mortality that suggests a reduction in fitness at higher temperatures. This knowledge fills a critical gap in our understanding of how marine fish larvae respond to warmer temperatures. We then use a common-garden-gradient approach to compare thermal responses in larval cod growth and survival among six genetic crosses originating from a single fjord system. We disentangle the effects of fine-scale environmental heterogeneity between inner and outer fjord areas, and genetic divergence between coexisting ecotypes, to better understand the genetic basis of cryptic diversity in thermal responses of cod. We find genetic divergence in plasticity at a microgeographic (<20 km^2) scale that is unprecedented in a marine species lacking physical barriers to dispersal. Finally, we combine common-garden experiments conducted on cod larvae from four locations with large-scale RNA sequencing and genotyping to characterize variation in gene expression means and thermal plasticities, growth reaction norms, and survival. The observed variation is consistent with adaptive divergence at macro- (~1300 km) and micro-geographic (<20 km^2) spatial scales along coastal Norway. Our findings suggest that local adaptation at a macrogeographic scale characterized by moderate gene flow is largely manifest by low-level differentiation located throughout the genome. However, local adaptation at a micro-geographic scale with high potential for gene flow is mainly attributable to blocks of tightly linked genes in the form of chromosomal inversions. We present the first experimental evidence for the putative adaptive functions of three large chromosomal inversions that are polymorphic throughout the species range and show evidence of within-generation experimental selection against specific genotypes. These novel empirical investigations will aid our understanding of how climate change will affect the population dynamics and distributions of cod and other marine fishes and enable effective management of harvested species with high gene flow.

List Of Abbreviations And Symbols Used

°C – degrees Celsius
CPM – counts per million
DE – differential expression/differentially expressed
DP – differentially plastic
dph – days post hatch
F – fjord ecotype
FDR – false discovery rate
FLØ – Flødevigen
FPKM – fragments per kilobase mapped
GO – gene ontology
H – Helgeland
HEL – Helgeland
I – inner Risør
LG – linkage group
logFC – log2(fold change)
MDS – multi-dimensional scaling
N – North Sea ecotype
NOR – North Sea
O – outer Risør
PC – principal component
RIS – Risør
RNA seq – RNA sequencing
SD – standard deviation
SEM – standard error of the mean
SNP – single nucleotide polymorphism
TVE – Tvedestrand
WBA – Western Baltic

Acknowledgements

Firstly, I want to thank Halvor Knutsen for taking the time to sit down for a chat during his visit to the Biology Department in September 2011. He delivered a seminar entitled 'Mechanisms behind fine-scaled population structure in Atlantic cod', which could have been the title of this thesis. On the second day of his visit, we decided that we would aim for me to travel to Norway to undertake my PhD research. I'm so glad that we did. Halvor, you have been a steady rock of support ever since and a pleasure to get to know. A huge thank you also goes to Esben Moland Olsen, whose amazing field skills and wealth of knowledge about the local cod ecology not only made this work possible, but a total pleasure. To Sissel Jentoft, who took me under the Cod Sequencing fin and provided me all kinds of support during the latter half of this journey, thank you. To all of you – our collaboration has been fantastic and I'm so looking forward to its continuation.

The greatest thanks goes to my advisor Jeff Hutchings, who has been endlessly inspiring over the course of my graduate student career. It's difficult to overstate the positive impact that his vision and support has had on me. Not least, thanks Jeff for giving me the time and the space to develop my independence as a researcher and for encouraging me to pursue new challenges in academia and in life. As the apparent complexity of my study system and thesis project grew, I'm so grateful that you provided the opportunity for me to see it through to a satisfying endpoint (or pit stop, rather). I also want to thank Paul Bentzen and Christophe Herbinger for helpful advice and stimulating discussion that guided my thesis, as well as Mark Johnston for comments on the review paper.

To everyone at the Institute of Marine Research, Flødevigen, I couldn't have done this without your overwhelming, collective support. Special thanks to Petter Baardsen, Stian Stiansen, Rune Johansen, Hanne Sannaes, Kim Halvorsen, Tonje Sørdalen, Mats Huserbråten, Albert Fernández Chacón, Susanna Huneide Thorbjørnsen, Jon Albretsen, Ida Mellerud, Enrique Blanco Gonzalez, and Heidi Fiskaa Thygesen. Thanks also to the fantastic students who chose to spend their work experience weeks and co-op terms with me in the lab – Kjell Elias, Ben, Fredericke, Jonas og Jonas. A very special thanks goes to the amazing team that made the beast of an experiment in 2014 possible: Nancy Roney, Elisabeth Juliussen, and David Rivas-Sánchez. Nancy, thank you for your invaluable friendship and tireless enthusiasm. Elisabeth, thank you for many years of exceptional and hard work.

I could not have found a better home during the second half of my PhD than the Centre for Ecological and Evolutionary Synthesis at the University of Oslo. Thank you to everyone who contributed to this supportive, stimulating, and engaging environment. Special thanks to my RNA-seq mentor Monica Solbakken, delightful office mate Helle Baalsrud, and saviour Ole K. Tørresen, as well as Paul Berg and Kjetill Jakobsen for sharing their cod wisdom. I also want to thank Bastiaan Star for diving into this project with me with the kind of enthusiasm a late-stage PhD student could really use and Asbjørn Vøllestad for his enduring support. Big thanks to Morten, Spyros, Ave, Nanna, Marianne, and Lex for all your support in the lab, on the nodes, and beyond. Thanks also to Kari, Gry, Tore, and the whole CEES admin team for a ton of support. I want to acknowledge the work of the Norwegian Sequencing Centre and the Research Computing Services group at USIT who operate the Abel Supercomputing Cluster. Thanks also to Audun Slettan for lending lab equipment and Tor Birkeland and Bobben for IT support. Last but not least, a huge thank you to Nils Christian Stenseth for forming this wonderful academic community, welcoming me into it, and providing me with fantastic opportunities and advice.

I gratefully acknowledge the Natural Sciences and Engineering Research Council, Research Council of Norway, European Regional Development Fund, Killam Trust, Nova Scotia Research and Innovation Trust, Prediction and Observation of the Marine Environment network, Robert and Ella Wenzins Endowment, Dalhousie University, Institute of Marine Research, and Centre for Ecological and Evolutionary Synthesis for financial support.

The first of what will be many thanks goes to the James S. McDonnell Foundation, Santa Fe Institute, and all the Postdocs in Complexity for broadening and enriching my mind in my final year.

Most of all, thanks to my family who tolerated some very ill timed deadlines and supported me from afar: Tamara, Ben, Deborah, Lili, Lachlan, my mom for infusing me with her creative spirit, and my dad for being my research cheerleader. Thanks to my Kampenjazz family and all the musicians from Oslo and abroad that have kept my heart, soul, and brain in the best possible shape. Finally, to my partners in love, life, and friendship: Sigve, Mads, Stine, Kristine, Kathrine, and Matthew, you have made these the best years of my life.

Chapter 1: Introduction

1.1 Local Adaptation

The 'modern synthesis' (Huxley 1942) of Darwin's theory of evolution and Mendel's laws of genetic inheritance eventually led to an understanding that when the forces of natural selection vary in space, populations can adapt to local environments (Williams 1966). Local adaptation produces genetically differentiated populations with traits that can differ in both mean phenotype and phenotypic plasticity (the range of phenotypes expressed by a genotype under different environmental conditions; Bradshaw 1965). Therefore, spatial environmental heterogeneity can lead to variation in morphology, life history, physiology, and behaviour among populations, as well as how these phenotypes change in response to changes in the environment. This genetic variation contributes to the observed global diversity in traits and their plasticities, one consequence of which is that environmental change will affect locally adapted populations differently (Hoffmann *et al.* 2015).

Adaptive divergence is counteracted by the homogenizing effects of gene flow: swamping of locally adapted alleles and reduced fitness of immigrants (Wright 1931; Bulmer 1972; Lenormand 2002). In addition to the extent of gene flow and the strength of selection, the migration-selection balance (Felsenstein 1976) depends on demographic factors, such as population abundance and sex ratio, as well as genetic factors, such as frequencies of adaptive variants and genome organization. Despite a large body of empirical and theoretical work describing the interplay between some demographic, genetic, and environmental variables, there are many unresolved questions that prevent us from predicting the conditions under which local adaptation occurs in nature and the impact of environmental change on wild populations (Hansen *et al.* 2012). In addition to being fundamental questions in evolutionary biology, they are of major concern for scientists worldwide due to the unprecedented threat of global climate change

(Bernatchez 2016) and have been identified as top priorities for molecular ecological research (Andrew *et al.* 2013).

1.2 Adaptation with Gene Flow

When gene flow is low, neutral processes, such as isolation by distance and genetic drift, play a large role in shaping genetic structure (Wright 1931; Allendorf *et al.* 2010). Additionally, theoretical groundwork laid as early as the 1930s led to the traditional assumption that local adaptation is negligible in species with high dispersal capabilities because gene flow is likely to overpower selection (reviewed by Tigano & Friesen 2016). Together, these assumptions imply a relatively small role for local adaptation in generating biological diversity. Yet, as molecular technologies improve, empirical studies are increasingly challenging the assumption that high gene flow precludes adaptation (Tigano & Friesen 2016). For example, early population genetic studies of marine species tended to find a lack of structure across broad spatial scales using allozyme markers, with notable exceptions (reviewed by Hilbish 1996) at times revealed by common-garden experiments (Conover 1998). Nonetheless, the majority of evidence fuelled a long-held view of marine species as large panmictic units. Further support for this assumption came from neutral microsatellite markers routinely used to delineate population structure for fisheries management (Ward 2000; Kapuscinski & Miller 2007). However, this view gradually shifted as empirical studies demonstrating local adaptation in a variety of physiological and morphological traits piled up and it became clear that adaptive divergence could occur over contemporary timescales (Conover 1998; Conover *et al.* 2006). With decreasing costs of genotyping and increasing numbers of samples and molecular markers, there are now numerous examples of local adaptation in the face of high gene flow (e.g., Nielsen *et al.* 2009; Clarke *et al.* 2010; Limborg *et al.* 2012; Milano *et al.* 2014; reviewed by Nosil *et al.* 2009). Yet, its underlying mechanisms and the spatial scales at which it can occur remain poorly understood.

1.3 Genomic Basis of Adaptation

A mechanistic understanding of adaptation requires knowledge of at least the specific selective pressure, the phenotypic trait undergoing selection, and the genetic basis of that trait to be known, in the context of demographic processes. Despite several calls for using integrated approaches to address these (e.g., Pörtner *et al.* 2006; Dalziel *et al.* 2009; Lowe *et al.* 2017; Oomen & Hutchings 2017), progress has been slow for non-model species. The advent of large-scale genotyping (e.g., single nucleotide polymorphisms [SNPs]) and next-generation sequencing (e.g., RAD sequencing, RNA sequencing, long-read sequencing) technologies coupled with advances in big data handling and bioinformatic software is enabling the characterization of genome-wide variation in large samples with little or no prior genomic resources. As a consequence of this revolution, it is more feasible to isolate the genetic basis of adaptive traits. For example, Jones et al. (2012) identified the genomic basis of parallel adaptation to fresh water in threespine sticklebacks (*Gasterosteus aculeatus*) and, in doing so, made several revelations about the roles of standing genetic variation, non-coding regulatory elements, and genetic and genomic architecture in adaptive evolution. Indeed, genetic and genomic architecture has emerged as a key mechanism involved in adaptation in the face of gene flow (Nosil *et al.* 2009; Tigano & Friesen 2016). Therefore, investigating the genomic basis of adaptation, especially in species with high connectivity, has great potential to yield new insights into adaptation and other eco-evolutionary processes, with direct relevance for wildlife conservation and management.

1.4 Spatial Scale of Adaptation

Of major concern for wildlife management is the spatial scale at which adaptive variation exists and its distribution relative to spatially heterogeneous selection pressures. Conservation and management practices are frequently implemented geographically (Coates *et al.* 2018) and often rely on identifying units considered to represent distinct genetic components as targets for conservation (Ryder 1986; reviewed by Fraser & Bernatchez 2001). This approach is aimed at preserving intraspecific diversity, which bolsters the adaptive potential of a species and therefore its ability to evolve in response to environmental change (Hoffmann & Sgrò 2011). Intraspecific diversity is also, on

average, just as important as species diversity for maintaining broader ecological processes and ecosystem services (Roches *et al.* 2018). Therefore, failing to account for spatially structured adaptive variation in conservation and management plans can erode both the population of interest and ecosystem functioning as a whole.

Importantly, in the absence of reproductive barriers, gene flow depends on geographic barriers, including the distance between populations relative to their dispersal capabilities. Consequently, gene flow varies across the range of a species (but see Pujolar *et al.* 2014). Because the primary factors driving adaptation are expected to vary with gene flow (Nosil *et al.* 2009), different genomic mechanisms might underlie adaptation at different spatial scales.

1.5 Anthropogenic Selection

Global wildlife is experiencing unprecedented threats from anthropogenic sources. The most widespread and urgent danger is that of rising and increasingly variable temperatures (Hoffmann *et al.* 2015). Mean temperatures have already risen 1°C in recent decades and are expected to increase 3-6°C globally, coupled with increased magnitude and frequency of thermal extremes (IPCC 2013). The extent of these changes will vary locally, along with a host of other co-varying and interacting variables (e.g., precipitation, sea level rise, storm activity). Under these circumstances, populations and species will disperse to more favourable environments (if available), cope with new environmental conditions through phenotypic plasticity, adapt if there is sufficient time and genetic variation to do so, or perish (Williams *et al.* 2008). Much attention has been focused in recent years on predicting these outcomes (Evans & Hofmann 2012; Pinsky *et al.* 2013; Valladares *et al.* 2014; Brito-Morales *et al.* 2018), which will inform effective conservation strategies while also highlighting emerging resources for potential sustainable exploitation.

Although true of any species that experiences variation in the types or strengths of selective agents throughout their range (which is most, if not all, species), identifying the

spatial scale of adaptation is particularly important for harvested species, which typically undergo intense, directional, and spatially varying selection (Kuparinen & Merilä 2007). Overharvested populations already suffer from reduced genetic diversity (Pinsky & Palumbi 2014). The compounded effects of harvesting and climate change call for urgent implementation of an adaptive approach to management (Pinsky & Mantua 2014; Pinsky & Byler 2015; Bernatchez 2016).

1.6 Genomic Reaction Norms

Genomic technologies provide extraordinary opportunities for unraveling the demographic and adaptive processes that form the basis of adaptive evolutionary management (Hoffmann *et al.* 2015; Bernatchez *et al.* 2017), notwithstanding challenges in doing so (Coates *et al.* 2018; Waples & Lindley 2018). However, population genetic studies typically neglect to examine the phenotypic traits potentially undergoing selection (Cushman 2014; de Villemereuil *et al.* 2016). More traditional experimental approaches, such as common-garden and reciprocal transplant experiments, are unmatched for their ability to disentangle genetic and environmental (i.e., plastic) effects on phenotypes (de Villemereuil *et al.* 2016). Yet, plasticity is not merely a nuisance to be controlled for, but a key mechanism of organismal responses to environmental change. Plasticity can be quantified as a 'norm of reaction' (*sensu* Woltereck 1909) by measuring phenotypes across an environmental gradient. Combining such measures with a common-garden design offers a powerful approach for detecting genetic variation in plasticity (Hutchings 2011; Oomen & Hutchings 2015a), which is in itself a heritable trait for selection to act upon to produce an adaptive response to environmental change (Nussey *et al.* 2005; Murren *et al.* 2014). Further integrating common-garden-gradient experiments with genomics facilitates adaptive and functional insights into genetically based variation in phenotypes and phenotypic responses. Thus, this powerful approach is capable of bridging across several levels of biological organization and multiple time scales of environmental responses.

Transcriptomics (the study of the collection of genes expressed in a particular condition; Wang *et al.* 2009) provide a key bridge in this regard, by linking genes to phenotypes. Because of its presumed influence on physiological, morphological, behavioural, and life-history traits, gene expression is considered a putatively adaptive phenotype itself. Expression profiles can therefore inform the design of conservation units (Hansen 2010; Vandersteen Tymchuk *et al.* 2010) and biomarkers for sub-lethal stress (Akbarzadeh *et al.* 2018), as well as monitor organism condition in the wild (reviewed by Evans & Hofmann 2012). In the context of the experimental framework outlined above, transcriptomics enables the construction of genomic norms of reaction. Genomic reaction norms characterize the molecular basis of phenotypic plasticity and identify candidate genetic variants underlying adaptive phenotypes, thus adding important pieces to the genotype-phenotype-environment puzzle (Aubin-Horth & Renn 2009; Shama *et al.* 2016).

1.7 Fishes and the Marine Environment

Common-garden experiments have been extensively employed on fishes, owing to their relative ease of handling compared to other vertebrates, the ecological and socioeconomic value of wild fish populations globally, the aquaculture industry, and their use as model systems for medical and genetic research (reviewed by (Conover & Baumann 2009; Hutchings 2011; Oomen & Hutchings 2015a). Concurrently, marine systems have emerged as ideal models to study local adaptation with gene flow, due to their typically high effective population sizes and at least one highly dispersive life stage (e.g., a pelagic egg or larvae stage) often making the effects of genetic drift and isolation by distance negligible (Allendorf *et al.* 2010; Tigano & Friesen 2016). Finally, the marine environment faces perhaps the most egregious list of threats from anthropogenic global change, including rising temperatures, acidification, habitat alteration, pollution, and changes in salinity and dissolved oxygen concentrations (IPCC 2013; Hoffmann *et al.* 2015), all compounded by widespread overharvesting (Hutchings 2000; Worm *et al.* 2009). As the health of the planet depends on the health of its oceans, there is an urgent

need for a better understanding of how marine species and ecosystems will respond to global change and marine fishes represent an ideal system for such studies.

1.8 Atlantic Cod

"The fish that changed the world" (Kurlansky 1997), Atlantic cod (*Gadus morhua*; hereafter, 'cod') is a marine fish of global biological, socioeconomic, and historical importance. Its widespread abundance in north-temperate waters, cold tolerance, and resistance to disease made it ideal for exploitation and trade, which has been maintained for at least a millennium (Star *et al.* 2017). Yet, cod are not as impervious to human impact as was long assumed. Today, they represent a textbook example of overexploitation. The collapse of the Northern cod stock off the coast of Newfoundland in the 1980s and subsequent fishing moratorium is thought to be the largest numerical loss of a vertebrate in Canadian history (1.5-2.5 million reproductive individuals) and, at the time, caused the greatest job loss in Canadian history (Hutchings & Rangeley 2011). The Northern cod have not recovered decades later and the abundances of populations in the Northwest Atlantic and parts of the Northeast Atlantic are at or near historical lows (Hutchings & Rangeley 2011; ICES 2018).

Despite having high dispersal capabilities and limited apparent physical barriers to gene flow, there is increasing evidence that cod are adapted to local selective pressures and that the spatial scale of adaptation is much smaller than previously believed (e.g. (Hutchings *et al.* 2007; Olsen *et al.* 2008; Bradbury *et al.* 2010, 2014, Berg *et al.* 2015, 2017, Oomen & Hutchings 2015b, 2016; Barth *et al.* 2017). Temperature has emerged as a particularly important driver of local adaptation in cod (Hutchings *et al.* 2007; Bradbury *et al.* 2010, 2014, Oomen & Hutchings 2015b, 2016), which is unsurprising given its critical role in physiological performance in ectotherms (Huey & Berrigan 2001; Clarke & Fraser 2004). Therefore, the variety of thermal regimes experienced across the distribution of cod is expected to promote adaptive divergence in plastic responses to temperature, reflecting differences in short- and long-term responses by cod to environmental change. Indeed, substantial genetic variability in reaction norms for larval

growth and survival in response to temperature have been found at both large (>600-800 km; Hutchings *et al.* 2007; Oomen & Hutchings 2016) and relatively small (<200 km; Oomen & Hutchings 2015b) spatial scales in the Northwest Atlantic among groups of cod that experience different thermal regimes during the larval stage. However, whether adaptive divergence in thermal plasticity exists at even smaller spatial scales is unknown, as is the molecular basis of this localized thermal adaptation. Management of cod fisheries is implemented geographically. Therefore, identifying spatial scales at which local adaptation occurs is critical to the viability of this species, as is characterizing how cod adapted to local environments will respond differently to ongoing directional environmental change.

From a population genetics perspective, cod are the most well studied commercial fish (Reiss *et al.* 2009). Despite this, the whole genome sequence of cod constructed during the high-throughput revolution (Star *et al.* 2011; Tørresen *et al.* 2017) has led to several new revelations about its evolutionary history and contemporary adaptation, including: 1) a lack of Major Histocompatibility Complex II (the core of the adaptive immune system in vertebrates; (Star *et al.* 2011; Star & Jentoft 2012), making cod a new model system for immunological research, 2) the characterization of several distinct ecotypes living in partial sympatry (e.g., Kirubakaran *et al.* 2016; Knutsen *et al.* 2018; Barth *et al.* 2019; Sodeland *et al.* in review), and 3) the existence of four large chromosomal inversion polymorphisms associated with migratory behaviour and/or environmental clines throughout the range (Bradbury *et al.* 2010, 2014, Berg *et al.* 2015, 2016, 2017; Kirubakaran *et al.* 2016; Sodeland *et al.* 2016; Barth *et al.* 2017; Sinclair-Waters *et al.* 2018). These findings set a rich foundation on which to explore the genomic basis and spatial scale of adaptation under gene flow.

1.9 Objectives and Summary

The aim of this thesis is improve our understanding of plastic and evolutionary responses to environmental change in natural populations. Specifically, my goal is to identify the molecular basis and spatial scale of genetic variation in thermal responses of Atlantic

cod. This thesis consists of four main chapters, followed by a brief synthesis and concluding remarks.

Chapter 2 comprises a critical literature review and synthesis. The potential of whole transcriptome sequencing (RNA sequencing) as a tool to study the complex responses of non-model organisms to the environment is being realized in a rapidly growing body of literature on fishes. In this chapter, we merge the disparate bodies of ecological, aquacultural, and medical genetic research on this topic by critically reviewing studies that utilize RNA-seq to study the responses of fishes to continuous abiotic environmental variables (salinity, temperature, dissolved oxygen concentration, and pH). By doing so, we illustrate how this emerging technology can help us understand plastic and evolutionary responses to global environmental change in fishes.

Despite the body of work described in Chapter 2, the molecular architecture underlying thermal responses is still largely unknown, especially during early life. In Chapter 3, we use RNA sequencing of laboratory-reared cod larvae to provide evidence of changes in gene expression consistent with a severe cellular stress response at both ambient and forecasted (+2°C and +4°C) temperatures. Earlier onset of the transcriptomic stress response is observed at higher temperatures, as well as faster growth and an increase in mortality that suggests a reduction in fitness. This knowledge fills a critical gap in our understanding of how marine fish larvae respond to warmer temperatures.

In chapter 4, we use a common-garden approach to compare thermal responses in larval cod growth and survival among six genetic crosses originating from a single fjord system <20 km^2. We disentangle the effects of fine-scale environmental heterogeneity between the inner and outer fjord areas and genetic divergence between coexisting ecotypes to better understand the genetic basis of variable thermal responses in cod and the minimum spatial scale at which such variation exists. Genetic variation in plasticity at such a small spatial scale is unprecedented in a marine species lacking physical barriers to dispersal and has important implications for the management of such species in the face of environmental change.

In Chapter 5, we combine common-garden experiments with large-scale RNA sequencing and SNP genotyping of cod larvae to characterize variation in gene expression means and thermal plasticities, growth reaction norms, and survival consistent with adaptive divergence at macro- (~1300 km) and micro-geographic (<20 km^2) spatial scales along coastal Norway. We present the first experimental evidence for the putative adaptive functions of three large chromosomal inversions that are polymorphic throughout the species range and show evidence of within-generation experimental selection against specific genotypes. Overall, these findings suggest that local adaptation at a macrogeographic scale characterized by moderate gene flow is largely manifest by low-level differentiation located throughout the genome. However, local adaptation at a micro-geographic scale with high potential for gene flow is mainly attributable to blocks of tightly linked genes in the form of chromosomal inversions.

The novel empirical investigations described in Chapters 3 to 5 will aid our understanding of how climate change will affect the population dynamics and distributions of cod and other marine fishes and enable effective management of harvested species with high gene flow.

1.10 Thesis Structure

This thesis is largely publication based, with each of the main chapters representing a stand-alone body of research. Chapter 2 has been published in a peer-reviewed journal under a Creative Commons Attribution 4.0 International (CC BY 4.0) license. Thus, Jeffrey Hutchings and I, Rebekah Oomen, own the copyright for Oomen and Hutchings (2017). Chapter 3 and Appendix B are, at the time of writing, undergoing peer review as two companion manuscripts. Chapters 4 and 5 will be submitted for peer review, though perhaps not in their current organization. All literature cited in this thesis is listed in a single reference section. I affirm that data collection and analysis for each chapter was conducted by myself, in some cases with the help of others, and that I wrote each chapter with input from my coauthors. I use the pronoun ‘we’ throughout the remainder of this

thesis to reflect the contributing authors. The author contributions are described in detail for each manuscript below:

Chapter 2: Rebekah Oomen and Jeffrey Hutchings conceived and designed the study. Rebekah Oomen collected, analyzed, and interpreted the data. Rebekah Oomen wrote the manuscript. Both authors revised the manuscript.

Chapter 3: Rebekah Oomen and Jeffrey Hutchings conceived and designed the study. Jeffrey Hutchings, Halvor Knutsen, and Nils Chr. Stenseth contributed funds. Esben Moland Olsen and Halvor Knutsen managed wild fish collection and supervised the fish rearing experiment. Rebekah Oomen conducted the fish rearing experiment, molecular laboratory work, and data analyses. Sissel Jentoft managed the RNA sequencing. Rebekah Oomen, Sissel Jentoft, and Jeffrey Hutchings interpreted the results. Rebekah Oomen wrote the manuscript with feedback from all authors.

Chapter 4: Rebekah Oomen and Jeffrey Hutchings conceived and designed the study. Jeffrey Hutchings, Halvor Knutsen, and Esben Moland Olsen contributed funds. Esben Moland Olsen and Halvor Knutsen organized the wild fish collection and supervised the fish rearing experiment. Rebekah Oomen, Elisabeth Juliussen, Esben Moland Olsen, and Halvor Knutsen carried out the wild fish collection. Rebekah Oomen led the fish rearing experiment and molecular laboratory work, which were carried out with Elisabeth Juliussen. Elisabeth Juliussen measured the larvae and conducted the microsatellite marker summary statistics and Hardy-Weinberg tests. Rebekah Oomen conducted all other data analyses. Elisabeth Juliussen wrote some of the Methods and Rebekah Oomen wrote the rest of the manuscript. Sissel Jentoft, Esben Moland Olsen, Halvor Knutsen, and Jeffrey Hutchings provided feedback on the manuscript.

Chapter 5: Rebekah Oomen and Jeffrey Hutchings conceived and designed the study. Jeffrey Hutchings, Halvor Knutsen, and Esben Moland Olsen contributed funds. Esben Moland Olsen and Halvor Knutsen organized the wild fish collection and supervised the fish rearing experiments. Rebekah Oomen conducted the fish rearing experiments,

molecular laboratory work, and data analyses. Elisabeth Juliussen assisted with the rearing experiments and molecular laboratory work for the 2014 experiment and measured the larvae for the 2014 and 2015 experiments. Sissel Jentoft managed the RNA sequencing. Bastiaan Star performed the SNP calling and principal component analyses and contributed to the Methods. Rebekah Oomen wrote the rest of the manuscript. Sissel Jentoft, Esben Moland Olsen, Halvor Knutsen and Jeffrey Hutchings provided feedback on the manuscript.

Appendix B: Rebekah Oomen and Jeffrey Hutchings designed the study. Jeffrey Hutchings, Halvor Knutsen, and Nils Chr. Stenseth contributed funds. Esben Moland Olsen and Halvor Knutsen managed wild fish collection and supervised the fish rearing experiment. Rebekah Oomen conducted the fish rearing experiment, molecular laboratory work, and data analyses. Sissel Jentoft managed the RNA sequencing. Rebekah Oomen, Sissel Jentoft, and Jeffrey Hutchings interpreted the results. Rebekah Oomen wrote the manuscript with feedback from all the authors.

Chapter 2: Transcriptomic Responses to Environmental Change in Fishes: Insights from RNA Sequencing

Published as: Oomen RA, Hutchings JA (2017) Transcriptomic responses to environmental change in fishes: insights from RNA sequencing. *FACETS*, **2**, 610–641.

2.1 Abstract

The need to better understand how plasticity and evolution affect organismal responses to environmental variability is paramount in the face of global climate change. The potential of utilizing RNA-sequencing (RNA-seq) to study complex responses by non-model organisms to the environment is evident in a rapidly growing body of literature. This is particularly true of fishes for which research has been motivated by their ecological importance, socioeconomic value, and increased use as model species for medical and genetic research. Here, we review studies that have utilized RNA-seq to study transcriptomic responses to continuous abiotic variables to which fishes have likely evolved a response and that are predicted to be affected by climate change (e.g., salinity, temperature, dissolved oxygen concentration, pH). Field and laboratory experiments demonstrate the potential for individuals to respond plastically to short- and long-term environmental stress and reveal molecular mechanisms underlying developmental and transgenerational plasticity, as well as adaptation to different environmental regimes. We discuss experimental, analytical, and conceptual issues that have arisen from this work and suggest avenues for future study.

2.2 Introduction

There are two primary mechanisms by which animal populations might alter phenotypes in response to environmental change. Plasticity (the ability of a genotype to produce different phenotypes, depending on environmental conditions; Bradshaw 1965) shifts the trait phenotype along a "norm of reaction" (*sensu* Woltereck 1909) defined by the genotype. Evolutionary (i.e., genetic) change occurs when selection acts on standing genetic variation to alter allele frequencies. These mechanisms are not mutually exclusive; for example, plasticity can facilitate adaptive evolutionary change to new environments (Ghalambor *et al.* 2007, 2015) and the magnitude and direction of plastic responses can themselves evolve in response to selection (Bradshaw 1965; Schlichting 1986; Lande 2009; Chevin *et al.* 2010). The need to better understand how plasticity and evolution will affect the responses of wildlife to environmental variability is intensifying as the magnitude and inevitability of global climate change becomes increasingly clear (Merilä & Hendry 2014).

As with other challenges related to climate change, technological advances will likely play a key role in addressing its effect on global biodiversity. Transcriptomics (the study of all the genes expressed at a particular moment; Wang et al. 2009) has been used to unravel the relationships between environment, genotype, and phenotype in natural populations for over a decade. Hybridization-based microarrays have traditionally been the dominant method for characterizing genome-wide expression levels in ecological studies (Alvarez *et al.* 2015). However, RNA-seq is being increasingly utilized as next-generation sequencing technologies become more accessible (refer to Box 1 for an outline of some of the key features and limitations of these two methodologies in the context of this review). Although still in relative infancy, a remarkably rapidly growing body of literature has capitalized on the advantages of RNA-seq to study how fishes (the most speciose of vertebrates) are impacted by environmental change. This work is motivated by the ecological and socioeconomic value of wild fish populations globally, the aquaculture industry, and their popularity as model systems for medical and genetic research. Yet, a unique feature of RNA-seq as it applies to ecological questions about

global change is the sheer diversity of species whose investigation is unlocked through *de novo* transcriptome assembly. An ISI Web of Science search using the keywords "fish" and "RNA-seq*" from 2008 (when the first studies utilizing the term "RNA-seq" were published) returned 605 articles, the majority (61%) of which were published in the previous 2 years. Of the 420 studies remaining after excluding those that focussed on organisms other than fishes, many examined the effects of diseases (56), parasites (7), pollutants (45), and diet (19) (see Qian et al. 2014). While these topics are relevant to the discussion of responses to environmental change because of interactions between biotic and abiotic factors, herein we focus solely on direct responses by fishes to well-studied abiotic environmental variables: to which animals have evolved a response, but to which changes in climate are expected to alter the conditions they naturally experience. Although this might seem unduly restrictive, such studies proffer unique opportunities to advance our understanding of plastic and evolutionary responses to environmental change. In addition, they are often accompanied by specific challenges that we feel can be ameliorated by an early critical review of this rapidly expanding field.

After including an additional 6 studies not detected by the keyword search, the resultant 52 studies investigated the responses of a remarkably diverse 38 fish species to one or more of the following factors: temperature (24), salinity (20), dissolved oxygen concentration (11), and pH (7) (Table 2.1), all of which are expected to be affected in the coming decades as a result of global climate warming. Water temperatures are increasing across most of the globe, while pH and dissolved oxygen concentration are declining (IPCC 2013). Salinity is increasing in some freshwater and oceanic environments where evaporation outpaces precipitation (IPCC 2013; Settele et al. 2014) and decreasing in some tropical and high latitudes due to increased precipitation and sea ice melt (Durack et al. 2012). We review these studies in the context of how RNA-seq can inform our understanding of plastic and evolutionary responses to environmental change in fishes. We note that it is premature to draw firm conclusions based on the limited body of work thus far, especially considering variation among the tissues and time points sampled as these can drastically impact expression. However, in the interest of inspiring future investigations of this nature, we draw some tentative inferences based on comparative

results across studies. We also highlight some of the experimental, analytical, and conceptual issues that have arisen in the early days of using RNA-seq to study wild populations.

Box 1: Key features and limitations of microarrays, expressed sequence tags (ESTs), and RNA-sequencing.

Traditional hybridization- (microarrays) and sequence- (expressed sequence tag [EST]) based transcriptomic methods suffer from some technical limitations (reviewed by Wang et al. 2009). For microarrays, which involve hybridizing fluorescently labeled complementary DNA (cDNA) with probes affixed to a solid surface (Schena *et al.* 1995), these include dependence on *a priori* knowledge of genome sequence and a narrow quantification range that is constrained by 1) high background noise generated by nonspecific hybridization (Okoniewski & Miller 2006) and 2) fluorescent signal saturation for highly abundant transcripts. Statistical treatment of microarray data has advanced to address many of its initial limitations, therefore microarrays might still be an appropriate and cost-effective choice for quantifying differential expression in known transcripts if a microarray for the species of interest (or one closely related) is available. While high-throughput expressed sequence tag methods have largely overcome the limitations of microarrays through direct cDNA sequencing, they utilize outdated, time-, cost-, and labour-intensive Sanger sequencing technology. Further, because the tag sequences are short, incomplete transcripts, many are unable to be annotated even if a complete reference genome is available (Costa *et al.* 2010) and it is not possible to distinguish between alternative splice isoforms or different alleles (Wang *et al.* 2009).

Advances in high-throughput sequencing technology have revolutionized transcriptomics with the advent of deep RNA sequencing (RNA-seq). A rapid, cost-effective method, RNA-seq is able to determine suites of genes expressed in a particular environment, including their sequences with single base-pair resolution, and their relative abundance with far greater precision than previous techniques (Wang *et al.* 2009). Without the need for a reference genome, RNA-seq provides a relatively accessible mode for studying the complex responses of non-model organisms to the

Box 1 (continued):

environment. The ability of RNA-seq to distinguish allelic and splice variants adds another layer of valuable information for this purpose. Because it allows determination of both quantitative (i.e., differential expression levels) and qualitative (i.e., sequence) variation in gene expression, RNA-seq has the potential to enable researchers to begin to disentangle the relative contributions of transcript abundance, allelic variants and alternative splicing to phenotypic change. Transcript sequences can be used to identify single nucleotide polymorphisms (SNPs) within coding regions either *de novo* (given sufficient coverage; van Belleghem et al. 2012, Gayral et al. 2013, Lopez-Maestre et al. 2016) or with the aid of a reference genome (Piskol *et al.* 2013). Although the ability of *de novo* SNP discovery to exhaustively detect all SNPs is uncertain, those identified in transcripts are arguably likely to have a direct functional impact (Lopez-Maestre *et al.* 2016). Variation in these SNPs can then be inexpensively and efficiently characterized in large-scale ecological and evolutionary studies (e.g., Romiguier et al. 2014). Further, mRNA sequences can inform us about putative downstream protein structure and function with no prior knowledge about particular genes.

RNA-seq is not without its own technical biases (e.g., fragmentation [Sendler et al. 2011] and PCR [Aird et al. 2011] biases during sample preparation), computational limitations (e.g., difficulties of assembling and aligning short reads [Engström et al. 2013]), and logistical constraints (e.g., high costs prohibiting adequate levels of replication [Table 1]). We address some of these concerns as they pertain to this review in the discussion, where we also recommend workflows that combine multiple methods when appropriate. We anticipate that current drawbacks of RNA-seq will be ameliorated by technological and computational advances in the near future. Nevertheless, RNA-seq can be leveraged through considered experimental design to be a promising tool to address the question of how animal populations will respond to global climate change.

2.3 Plastic Responses to Environmental Change

Plastic responses to global climate change have been documented in morphological, behavioural, physiological, and life-history traits in a variety of fishes (reviewed by Crozier and Hutchings 2014). Plasticity can be characterized by the time lag between the environmental cue and the change in phenotype (Padilla & Adolph 1996), which can range from an immediate response to one expressed later in development, or even across multiple generations (i.e., transgenerational plasticity; Salinas and Munch 2012). In this section, we discuss both short- and long-term within-generation responses, as well as non-genetic change that can occur across generations.

2.3.1 Short-Term, Acute Responses

Many experiments have investigated physiological responses to short-term (herein defined as 1-120 h), often extreme conditions, usually with the aim of discovering 'tolerance' genes for breeding or aquaculture (e.g., Liu et al. 2013, Xia et al. 2013, Ao et al. 2015, Sun et al. 2015). These challenge studies reveal genes involved in short-term stress responses, many of which quickly return to baseline levels with no consequences to fitness (van Straalen & Feder 2012). These genes are arguably less likely to be targets for selection during the expected gradual, directional environmental shifts associated with climate change (Kassahn *et al.* 2007; Logan & Somero 2010).

Nonetheless, these studies can be informative about the way environmental signals are integrated and how response pathways evolve, and might help us to understand the resiliency of populations in the face of extreme weather events that are expected to increase in frequency and magnitude (Rahmstorf & Coumou 2011). An extensive and rapid response of the transcriptome to high salinity was found in euryhaline medaka (*Oryzias latipes*; Wong et al. 2014) and Asian seabass (*Lates calcarifer*; Xia et al. 2013). A high degree of overlap between the genes involved in signalling the osmoregulatory stress response and those related to other stressors, such as handling (Wong *et al.* 2014),

bacterial infection, and fasting (Xia *et al.* 2013), is consistent with the hypothesis that these signalling networks evolved in parallel. Metabolic pathways were widely repressed in response to stress in Asian seabass but not in medaka, while immune genes were upregulated (particularly those involved in innate immunity) and downregulated in both studies.

With respect to short-term heat stress, heat shock proteins (molecular chaperones that aid in protein folding and degradation) are upregulated in the majority of fishes studied, including hybrid catfish (*Ictalurus* sp.; Liu et al. 2013), snow trout (*Schizothorax richardsonii*; Barat et al. 2016), Iberian freshwater fishes (*Squalius torgalensis* and *Squalius carolitertii*; Jesus et al. 2016), longfin smelt (*Spirinchus thaleichthys*; Jeffries et al. 2016), and tambaqui (*Colossoma macropomum*; Prado-Lima and Val 2016). This is consistent with vast numbers of molecular studies on eurythermal fishes (reviewed by Tomanek et al. 2010). In contrast, stenothermal fishes (e.g., cold-adapted polar or warm-adapted tropical species) typically lack an inducible heat shock response (Logan and Buckley 2015). Constitutive expression of heat-shock proteins has been observed using microarrays in several polar species (e.g., Antarctic plunderfish [*Harpagifer antarcticus*], Thorne et al. 2010; Antarctic emerald notothen [*Trematomus bernacchii*], Buckley and Somero 2009]), in which denaturation or slow folding of proteins at extremely cold temperatures is hypothesized. However, RNA-seq revealed that heat shock proteins were actually downregulated in an Antarctic nototheniid (*Pagothenia borchgrevinki*) after short-term heat exposure (Bilyk and Cheng 2014; but see Huth and Place 2016*a*), consistent with an earlier quantitative-PCR (qPCR) study on *H. antarcticus* (Clark et al. 2008). These studies point towards the existence of yet another heat coping mechanism that warrants further study. As with osmoregulatory stress, the effect of heat stress on metabolic processes varied among species (Table 2.1). Notably, metabolism was strongly upregulated in the heat-stressed catfish (Liu *et al.* 2013) and delta smelt (*Hypomesus transpacificus*; Jeffries et al. 2016), species known for their high thermal tolerance, whereas a lack of metabolic response was observed in *P. borchgrevinki* (Bilyk & Cheng 2014). Such evidence of contrasting responses to heat stress in cold- and warm-adapted

fishes sheds light on how adaptive divergence can alter the contents of the genomic tool kits with which species can respond to contemporary thermal stress.

In the model zebrafish (*Danio rerio*), acute cold stress has repeatedly been associated with large shifts in transcriptional regulation (Long et al. 2013, 2015, Hu et al. 2015a, Hung et al. 2016). This stress response substantially overlaps with that induced by hypoxia, both involving the upregulation of many genes involved in oxygen transport (Long *et al.* 2013, 2015). Hypoxia tolerance has been associated with variation in the expression of genes involved in a variety of processes, including the regulation of epithelial permeability (Sun *et al.* 2015) and repression of cellular apoptosis (Yuan *et al.* 2016) in channel catfish (*Ictalurus punctatus*), avoiding cerebral inflammation in the large yellow croaker (*Larimichthys crocea*; Ao et al. 2015) and lipid utilization in a hybrid striped bass (*Morone* sp.; Beck et al. 2016).

This limited collation of studies suggests a global coordination of stress response in teleost fishes combined with the regulation of stress-specific genes dependent on species-specific adaptations.

2.3.2 Long-Term, Chronic Responses

After the initial stress response, how do fishes adjust physiologically (i.e., acclimatize) during prolonged exposure to new environmental conditions? Given that climate change will involve sustained alteration of the environment, the genes and pathways identified in long-term experiments (herein defined as 1-4 weeks) are more likely to be involved in some form of a plastic response that has fitness consequences (either adaptive or maladaptive) (Smith *et al.* 2013).

The general stress response is less apparent following prolonged exposure to increased salinity, consistent with the hypothesis that acclimation is common (Table 2.1). A vast array of genes and pathways has been proposed to enable prolonged salinity tolerance, including those involved in ion transport (Lam *et al.* 2014; Wang *et al.* 2014; Gu *et al.*

2015; Nguyen *et al.* 2016), blood pressure regulation and fat metabolism (Xu *et al.* 2015), and both innate and adaptive immunity (Norman et al. 2014*a*; Norman et al. 2014*b*).

The mechanisms by which long-term hypoxia leads to reproductive impairment in the marine medaka (*Oryzias melastigma*) have been determined through sex-specific brain transcriptome sequencing (Lai et al. 2016*a*) coupled with gonadal microRNA profiling (Lai et al. 2016*b*; Tse et al. 2016). Hypoxia-responsive microRNAs (small non-coding RNAs which can post-transcriptionally modulate gene expression; Carrington and Ambros 2003) were associated with the upregulation of steroidogenic enzymes and hormone receptors in the ovary (Lai et al. 2016*b*) and diverse cellular processes including epigenetic modifications in the testes (Tse *et al.* 2016).

Heat-shock proteins and immune-related genes associated with the short-term heat stress response are likewise upregulated during prolonged heat exposure in crimson spotted rainbowfish (*Melanotaenia duboulayi*; Smith et al. 2013), redband trout (*Oncorhynchus mykiss gairdneri*; Narum and Campbell 2015), and half-smooth tongue sole (*Cynoglossus semilaevis*; Guo et al. 2016) while metabolic processes continue to be one of the most enriched categories of dysregulated genes during long-term heat stress in these studies. However, immunity-related genes comprise a much smaller proportion of differentially expressed transcripts in rainbowfish when compared to short-term challenge studies in other species. Further, both the number of differentially expressed transcripts and the expression levels of stress response genes decreased over the 4-week duration of the study on redband trout (Narum & Campbell 2015), suggesting acclimation to heat stress. Limited evidence from microarrays cautions that even if the stress response decreases following acclimation in heat-tolerant species, maintenance costs for homeostasis might be higher at warmer temperatures (Logan and Buckley 2015): energetically-costly protein biosynthesis and active ion transport were upregulated in the longjaw mudsucker (*Gillicthys mirablis*) after three weeks of heat exposure, while HSPs were largely absent (Logan and Somero 2010). Less energy for foraging, growth, and reproduction would be available to species with such a response.

If similar biological processes characterize the majority of dysregulated pathways in both acute and long-term responses to environmental change, then challenge experiments might reliably be used to uncover the general physiological processes underlying long-term plastic responses. However, there is evidently potential for acclimation to decrease the magnitude of the plastic response and it is not clear whether the same genes are involved at different times during the response.

2.3.3 Developmental Plasticity

Environmental conditions experienced earlier in life can both alter subsequent phenotypes and impact future plastic responses to the environment through epigenetic mechanisms (i.e., those which "cause chromosome-bound, heritable changes to gene expression that are not dependent on changes to DNA sequence"; Deans and Maggert 2015). This developmental plasticity or acclimation can enhance persistence in new and variable environments and result in novel phenotypes that can facilitate adaptation (West-Eberhard 2003).

For example, through RNA-seq, we are beginning to better understand the mechanisms underlying the ability of thermal acclimatization to shift the breadth and optima of thermal performance later in life (*sensu* Fry and Hart 1948). Embryonic exposure to thermal extremes appears to enhance the response of adult zebrafish to cold temperatures, surprisingly resulting in greater swimming performance regardless of the direction of the extreme (Scott & Johnston 2012). The improved acclimation capacity of the warm-incubated fish was explained by differential expression of genes involved in energy metabolism, blood vessel development, and muscle contraction and remodelling, which corresponded with differences in muscle area and composition (Figure 2.1). It would be interesting to know whether the cold-incubated fish (which were not sequenced) achieved acclimation *via* the same transcriptional modifications. In a separate study, RNA-seq revealed the molecular basis of "rapid cold hardening" (Kelty and Lee 2001), whereby brief exposure to mild cold improved larval survival in the face of severe cold stress (Long *et al.* 2013). Promoter switching and alternative splicing emerged as major

mechanisms enabling cold tolerance in fishes, consistent with previous studies on a wide range of stressors in other taxa, although the functional significance of different isoforms remains to be investigated.

2.3.4 Transgenerational Plasticity

Non-genetic parental influences on offspring phenotype can facilitate acclimation across generations (Mousseau & Fox 1998). Evidence of such transgenerational effects in fishes suggests that they might play a major role in enabling fish populations to cope with environmental change (Salinas & Munch 2012; Miller *et al.* 2012; Hurst *et al.* 2012; Donelson *et al.* 2012), particularly in species that have less capacity for acclimation as adults because they have evolved in a relatively stable environment (e.g., coral reef fishes; Munday et al. 2012). Veilleux *et al.* (2015) explored the molecular basis of this phenomenon, using RNA-seq in a common reef fish (*Acanthochromis polyacanthus*), by evaluating gene expression and metabolic performance in response to increased temperature both within and across generations. Differential expression was greater in transgenerationally-exposed fish, which had improved aerobic scope, compared to developmentally-exposed fish, for which performance was reduced relative to the controls (Figure 2.2). The biological processes associated with the developmental response to temperature were also part of the transgenerational response (e.g., metabolism, immunity, and stress response), as were genes previously found to respond to short-term thermal challenge (e.g., apoliproteins; Podrabsky and Somero 2004, Kassahn et al. 2007), suggesting a link between short-term, developmental, and transgenerational thermal stress responses in fishes. Interestingly, heat shock proteins were largely absent from both developmental and transgenerational treatments, suggesting that they might not be good predictors of thermal acclimation capacity.

The epigenetic mechanisms involved in regulating the developmental and transgenerational thermal responses above are unknown. In another study, microRNA sequencing has revealed a specific epigenetic effect of hypoxia that causes trangenerational reproductive impairments in male marine medaka (Tse *et al.* 2016).

Sequencing of microRNAs is therefore another promising avenue for understanding how gene expression is fine-tuned by epigenetic mechanisms in response to environmental factors throughout development and across generations. The epigenetic mechanisms responsible for regulating developmental and transgenerational plasticity are of substantial interest given their considerable potential to improve our understanding of the capacity of fishes to cope with rapid environmental change.

2.3.5 Responses to Multiple Stressors

Climate change is altering many environmental variables simultaneously (IPCC 2013). Considering that multiple stressors can have complex interactive effects (Schulte 2004), studies examining the combined effects of heat and other stressors on fishes are highly relevant to predictions of fish responses to global climate change.

Heat stress suppressed the immune system of Mozambique tilapia (*Oreochromis mossambicus*) infected with a bacterial pathogen, apparently through metabolic constraints imposed by limited oxygen (Wang *et al.* 2016). Among the 2000+ differentially expressed genes, rates of synonymous and nonsynonymous substitutions based on SNPs identified from the *O. mossambicus* transcriptome and the closely related, but less disease-resistant, Nile tilapia (*Oreochromis niloticus*) revealed signs of positive selection in *O. mossambicus* for 43 genes involved in the immune response and oxidative respiration. These findings suggest that *O. mossambicus* has evolved superior disease resistance relative to *O. niloticus*, yet its immune system is impaired by heat stress. A better understanding of how temperature mediates infection in fishes, many of which have unusual or poorly understood immunological strategies (Buonocore & Gerdol 2016), is urgent as climate change increases the incidence of disease outbreaks globally (Brander 2007).

Along with rising temperatures, acidification driven by increases in dissolved carbon dioxide is a major threat to fishes (Pörtner et al. 2004). A long-term dual-stressor time-series experiment on the Antarctic notothenioid *P. borchgrevinki* suggests that, when

occurring in tandem, these shifts can produce distinct responses when compared to heat stress alone (Huth and Place 2016*a*). Huth and Place (2016*a*, 2016*b*) demonstrated an inflammatory response to increased temperatures and pCO_2 that lasted at least 7 days, along with an increase in rates of cell death followed by gradual acclimation to near basal expression levels by 56 days, in two Antarctic notothenioids. However, the degree of response was reduced overall in *P. borchgrevinki* compared to *T. bernacchii*, suggesting that sensitivity to environmental perturbation varies among these closely related cold specialists. In contrast, the long-term response of Amazonian tambaqui to these dual stressors was dominated by molecular chaperones and metabolic and developmental processes (Prado-Lima & Val 2016).

The interaction between multiple abiotic stressors has been explored using RNA-seq from a developmental perspective with respect to the extent to which variation in prior exposure along one environmental axis influences the response along a different axis. Although developmental cold exposure has been reported to protect larval zebrafish against future cold stress, it was associated with decreased tolerance to lethal hypoxia, while prior exposure to mild hypoxia improved both hypoxia and cold tolerance (Long *et al.* 2015). Genes involved in oxygen transport were mainly associated with this process, revealing molecular mechanisms underlying the hypothesis that oxygen limitation is the primary determinant of thermal tolerance in fishes (Pörtner 2002). Somewhat less intuitively, acclimation to different salinities activated different strategies to cope with cold tolerance in milkfishes (*Chanos chanos*), whereby seawater-acclimated milkfish were more cold-tolerant than those acclimated to fresh water (Hu *et al.* 2015a). The seawater-acclimated fish upregulated a suite of genes related to increasing the energy budget, whereas freshwater-acclimated fish reduced energy loss by downregulating genes involved in basal metabolism.

These studies highlight the fact that previous exposure and interactions between multiple stressors can have substantial and perhaps surprising consequences on fitness and are thus critical to understanding fish responses to our changing climate.

2.4 Evolutionary Responses to Environmental Change

While individual and transgenerational plasticity can help organisms cope with environmental change in the short term (e.g., fewer than five generations), responding to ongoing climatic shifts will involve evolution because traits are not necessarily plastic and/or reaction norms will no longer be adaptive in the new environment (Visser 2008). Though empirical evidence is scarce relative to that of plastic responses (Merilä & Hendry 2014), rapid evolution in response to environmental change has been documented in a variety of taxa (e.g., Bradshaw and Holzapfel 2001, Umina et al. 2005, Derry and Arnott 2007, Charmantier et al. 2008), including fishes (reviewed by Crozier and Hutchings 2014). This section summarizes what has been learned about adaptive responses to environmental change in fishes from RNA-seq experiments.

2.4.1 Identifying Candidate Genes for Adaptation

A primary aim of transcriptomics is to identify candidate genes for adaptation, i.e., those genes with large impacts on fitness under different environmental conditions (Feder & Mitchell-Olds 2003). This "discovery-driven" approach proved powerful early on in the study of genomic reaction norms (Aubin-Horth and Renn, 2009). RNA-seq offers an advantage for candidate gene discovery because of its unbiased nature and lack of necessity for prior information (Wang *et al.* 2009). The studies described previously identified numerous candidate genes that are potential targets for selection in response to changes in temperature, salinity, and dissolved oxygen concentration. Armed with such information, researchers can develop functional markers to monitor for a contemporary response to climate change (Hoffmann & Willi 2008) or screen broadly across a species range to predict the potential for adaptation (Hoffmann & Sgrò 2011). The unique opportunities proffered by RNA-seq have yet to be fully taken advantage of with regards to the evolutionary effects of environmental change on fishes, but this avenue of research holds great potential.

2.4.2 Intraspecific Variation in Transcriptomes

Transcriptomic variation at the population level can reveal how gene expression evolves in response to local environmental regimes. Zhang *et al.* (2015) compared the transcriptomes of two ecotypes of scaleless carp (*Gymnocypris przewalskii*) from saline and freshwater lakes. Of the many thousands of genes that were differentially expressed, they used sequence information to narrow in on just 242 protein-coding genes that showed signs of strong positive selection. The authors concluded that relatively few genes, chiefly those involved in ion regulation and the immune response, play critical roles in the shift from saline to freshwater habitats in fishes. An acclimation experiment comparing native freshwater to anadromous saltwater threespine stickleback (*Gasterosteus aculeatus*) also revealed many genes potentially underlying salinity adaptation (Wang *et al.* 2014). Finally, a rare study examining the effects of elevated pH on a fish transcriptome described how changes in gene expression played a key role in the relatively recent shift of Amur ide (*Leuciscus waleckii*) from fresh water to extreme alkalinity in a soda lake (Xu *et al.* 2013). Further research is needed to determine whether the intraspecific variation in expression described for the wild-caught fish used in these studies has a genetic (as opposed to epigenetic) basis, thereby representing adaptive evolution. This could be achieved through traditional labour-intensive common-garden experiments or some genetic inferences could perhaps be gleaned more readily by examining allele-specific expression patterns.

2.4.3 Population-level Variation in Transcriptional Plasticity

In addition to shifting the mean phenotype (i.e., reaction norm elevation), evolutionary responses to environmental change can alter the shape of the plastic response (i.e., reaction norm slope) (Bradshaw 1965; Lande 2009; Chevin *et al.* 2010). In fishes, there is evidence from common-garden experiments of population- and family-level variation in plastic responses to each of the environmental variables discussed thus far (reviewed by Hutchings 2011 and Oomen and Hutchings 2015). These experiments are extremely useful for detecting adaptation when combined with measures of fitness, however they do not tell us about the genetic mechanisms underlying plastic responses.

RNA-seq allows us to bridge the gap between genotype and phenotype by linking genetic variation directly to differences in gene expression and then to phenotypic responses observed in the lab. Such a complete chain has yet to be made within the scope of the present review. Narum and Campbell (2015) came the closest when they found population-specific patterns of plasticity in response to heat stress among desert and montane redband trout. The desert population exhibited greater differential expression (in both the number of genes and the magnitude of the fold-change) compared to either the montane population or their F1 cross (Figure 2.3), although all populations showed evidence of acclimation during the 28-day experiment. Heat shock proteins were not upregulated as much in the desert trout when compared to the montane trout, while many genes involved in metabolic and cellular processes were highly upregulated, suggesting that the desert trout have evolved complex and specialized molecular mechanisms to cope with heat stress. The F1 cross generally exhibited intermediate expression patterns between the two populations, consistent with additive genetic variation, although a greater number of shared differentially expressed genes with the maternal montane trout suggests a possible maternal or dominant effect at some genes.

While this novel experiment provides considerable insight into the molecular basis of thermal adaptation, corresponding physiological and other phenotypic measurements would be extremely valuable in understanding how changes in individual gene expression are related to fitness. Further, the inclusion of multiple temperatures in such an experiment would allow for direct quantification of thermal plasticity within populations. This approach was used by Morris et al. (2014) to compare levels of transcriptomic thermal plasticity, as determined by microarrays, between ancestral marine and derived freshwater threespine stickleback populations. More plastic genes were detected in the derived freshwater populations, supporting the hypothesis that if greater environmental variability is encountered following colonization of new habitats, it will drive the evolution of greater plasticity relative to the ancestral population.

2.4.4 Family-level Variation in Transcriptional Plasticity

In addition to population-level variation in transcriptional plasticity, studies in fishes have shown differences in patterns of gene expression at the family level. Norman *et al.* (2014a) used a quantitative trait locus (QTL) approach to reveal the genetic basis underlying the correlation between salinity tolerance and differential expression of immune genes among families of Arctic char (*Salvelinus alpinus*). Interestingly, the majority of QTL associated with ion transport were located near differentially expressed genes, suggesting that cis-regulatory elements (non-coding DNA that regulates transcription of nearby genes) are involved in controlling their expression. Concomitantly, the majority of differentially expressed genes were not associated with QTL, suggesting that they might be controlled by trans-regulatory elements (those on distant genes). That genetically-based differences in gene expression were found within a lab-bred strain suggests that there might be substantial variation in transcription within populations.

Knowledge of the extent to which such transcriptional variation is heritable is thus far rather limited, as attempts to quantify heritability of gene expression are rare. Critically, the ability of a population or species to respond evolutionarily to environmental change depends on the amount of heritable genetic variation it possesses for adaptive traits (Hoffmann & Sgrò 2011). In a unique example, McCairns *et al.* (2016) used crimson-spotted rainbowfish of known pedigree to demonstrate moderate levels of heritability for transcription and transcriptional plasticity in thermal responses of candidate genes that were previously identified using RNA-seq (Smith *et al.* 2013). Abundant family-level variation in plasticity for most genes suggests that substantial heritable variation in plasticity might exist within fish populations for selection to act upon to produce an adaptive evolutionary response to climate change.

2.5 Challenges and Directions for Future Research

The application of RNA-seq to study non-model systems is still in its infancy and care must be taken not to overlook its limitations in the rush to adopt the technology (Costa *et*

al. 2013; Todd *et al.* 2016). In this section, we describe some of the experimental, analytical, and conceptual challenges raised specifically by the body of work described herein and highlight some avenues of future exploratory and confirmatory analyses. For further detail about technical and analytical issues surrounding RNA-seq experiments in general, we refer the reader to several discussions on the topic (Fang & Cui 2011; Ozsolak & Milos 2011; Sendler *et al.* 2011; Costa *et al.* 2013; Conesa *et al.* 2016).

2.5.1 Experimental Protocols and Sampling Design

Gene expression is extremely sensitive in that it can potentially change very quickly and in response to slight environmental variability. This can make sampling protocols challenging, as any manipulations that fish experience between the environment of interest (whether in the field or laboratory) and the preservation of tissue for RNA extraction can affect gene expression. Depending on the research question, it might be prudent to collect a control sample for handling or transfer stress (e.g., Wong et al. 2014) or avoid feeding prior to sampling (e.g., Liu et al. 2013).

Although relatively inexpensive from an input:output (cost:amount of data generated) perspective, the substantive financial, laboratory, and computational resources required for RNA-seq appear to have limited experimental design in terms of sample sizes and numbers of replicates and treatments. Indeed, of the studies included here, nearly half did not include true biological replicates (at best, samples were pooled within groups to create a single library for RNA-sequencing), consistent with the dearth of replication observed in ecological and evolutionary studies in general (Todd *et al.* 2016). St. Laurent et al. (2013) concluded that as few as three biological replicates can be sufficient to detect small differences in expression in a model system, while Robles et al. (2012) found that at least six are necessary when dealing with low count data (e.g., when using a multiplex sequencing strategy). However, the increased biological variation inherent in studies on non-model organisms essentially means that the more biological replication, the better, as it is the only way to cope with the unique statistical challenges of controlling for false positives during such highly parallelized significance testing while retaining the ability to

detect lowly expressed transcripts. Although few replicates can still produce significant results, they will be biased towards genes with large log-fold changes, and these are not necessarily the most relevant for fitness (Smith *et al.* 2013; Evans 2015).

Few of the experimental RNA-seq studies published to date included biological replicates within tank replicates, which is necessary for estimating variation due to random tank effects. This might be partly explained by the difficulty of such computations with currently available differential expression analysis software. However, a few experiments dispersed replicates among tanks to eliminate tank variation as a confounding factor (e.g., Narum and Campbell 2015, Prado-Lima and Val 2016). Studies measuring multiple time points are also uncommon because they require multiplying sample sizes, yet they are key to distinguishing between short-term stress and long-term acclimation responses (e.g., Narum and Campbell 2015, Xu et al. 2015, Huth and Place 2016*a*, 2016*b*). The number of individual and tank replicates required is extremely dependent on the amount of biological variation within and between groups, which can be difficult to anticipate as it will likely be extremely case-specific. However, the development of tools to help predict the power of various experimental designs based on data from pilot experiments (e.g., Scotty [Busby et al. 2013]; reviewed by Todd et al. 2016) and future decreases in the cost of RNA-seq will likely facilitate more robust and complex experiments. Alternatively, the utility of RNA-seq to explore uncharacterized genomes can be leveraged to design custom microarrays (Alvarez *et al.* 2015) for expansion of experimental designs or to reduce the bioinformatic challenges associated with follow-up experiments. Kusakabe et al. (2017) took advantage of both RNA-seq and microarrays, combined with QTL mapping, qPCR, whole genome sequencing, and a genome scan, to confidently identify candidate genes for salinity adaptation in threespine stickleback. Notably, the direction and magnitude of expression differences for the genes identified by transcriptome analysis were similar between the RNA-seq and microarray results.

2.5.2 Bioinformatic Analysis

The technological limitations of RNA-seq are not of as great concern when compared to the analytical ones, as our ability to generate data vastly surpasses our ability to interpret it. Key areas for improvement in this regard are bioinformatic and genomic resources. Differential expression analysis programs capable of handling mixed-effects models are needed to control for variation due to random (e.g., tank) effects. Biological interpretation of large differentially expressed gene lists remains a major obstacle, although gene set enrichment analyses, which groups genes based on common biological function, location, or regulation (Subramanian *et al.* 2005), have become a popular aid in their distillation to major functional categories (e.g., Liu et al. 2013, Long et al. 2013, Gu et al. 2015). However, there is often a focus on only the largest or most-expected functional categories, potentially ignoring important biological processes involving fewer genes and providing opportunity for reporting bias and subjective interpretation of results.

When the goal is to identify a reduced set of the most promising candidate genes, complementary methods utilizing the high resolution sequence data, such as testing for positive selection through comparing rates of synonymous and nonsynonymous substitutions (e.g., Kavembe et al. 2015, Zhang et al. 2015, Wang et al. 2016), can be helpful. Although underutilized in ecological genomics, gene network construction offers a promising alternative for functional analysis based on the notion that genes with a higher degree of connectedness have a greater impact on fitness through involvement in multiple cellular pathways (i.e., hub genes; Costanzo et al. 2010). Although incorporation of differential expression data improves these networks by taking co-expression into account (Fu *et al.* 2014), it is not necessary because they are built using databases of known gene interactions (Evans 2015). If specific (i.e., candidate) genes are the unit of interest, validation of gene expression using additional samples (either more biological replicates from the same experiment or, ideally, samples from a different population or incidence of environmental exposure) would be an asset to reduce the potential for false positives.

A lack of reference data for functional annotation is one of the biggest challenges facing RNA-seq analysis in an ecological context, a consequence of the fact that annotations are

based on homologies with genes from a few model species and environmental conditions (Pavey *et al.* 2012). For example, over half of the transcripts differentially expressed in the heat stress response of crimson spotted rainbowfish could not be annotated (Smith *et al.* 2013). Pavey et al. (2012) proposed alleviating this problem by creating a database of ecological annotations (*sensu* Landry and Aubin-Horth 2007), allowing for cross-referencing genes and associated environmental variables across studies and species. Such a database could be populated with results from functional assays (i.e., experiments which demonstrate that a gene has a measureable effect on a particular phenotype), such as targeted gene knockdown or overexpression, as these become available. For example, Hu et al. (2015) confirmed the cold-responsive functions of novel *cis*-regulatory elements discovered using RNA-seq by exposing mutant and wild-type transgenic zebrafish embryos to different temperatures. Ecological annotations would complement the current practice of using the Gene Ontology (www.geneontology.org) to annotate genes according to cellular component, molecular function, and biological process. However, genes associated experimentally with particular environmental variables need not necessarily be annotated to serve as functional markers for ecological studies of environmental adaptation.

2.5.3 Conceptual Challenges

Most criticisms of RNA-seq can justifiably pertain to transcriptomics in general. For example, inferring physiological function from gene expression data is inherently problematic due to transcriptional noise (caused by nonspecific initiation of transcription by RNA polymerase II; Struhl 2007) and time lags between environmental exposure, transcriptional response, and physiological and fitness consequences (for a detailed discussion see van Straalen and Feder 2012). With respect to its utility in discovering candidate genes of major consequence for environmental adaptation, the main criticisms (as proposed by Feder and Walser 2005) are: 1) that such genes are rare, therefore the wide net approach of transcriptomics may not be the most effective, 2) that differences in gene expression levels do not necessarily correlate with differences in fitness, and 3) that post-transcriptional and -translational modifications mean that mRNA abundance is not a

good predictor of protein abundance, which is more relevant for fitness and can also be examined directly to address questions of environmental plasticity and adaptation (see Papakostas et al. 2014 and Mäkinen et al. 2016 for examples in the European grayling [*Thymallus thymallus*]). While these issues have persisted to some extent for a decade, ongoing developments from systems-level experiments, advancing bioinformatic techniques, and additional gene functional analyses will continue to improve prospects (reviewed by Evans 2015).

Specifically, increasing our ability to detect lowly expressed genes, as described in the previous section, and dedicating more effort towards interpreting these and moderately-differentially expressed transcripts will advance efforts to better understand the genetic basis of plastic and evolutionary responses to environmental change (e.g., Smith et al. 2013), as plasticity need not be great to have fitness consequences.

Experiments that directly link gene expression with physiological and other phenotypic traits, particularly measures of fitness, are of vital importance for understanding how transcriptomic variation ultimately affects populations and species. One approach involves following individuals after non-destructive RNA sampling (potentially at many points during development) through to reproduction or mortality, thereby providing a more comprehensive and concrete view of how the environment interacts with development to alter gene expression and, ultimately, fitness. For example, Evans et al. (2011) combined nonlethal sampling of sockeye salmon (*Oncorhynchus nerka*) gill tissue and microarray expression profiling with telemetry to identify transcriptional signatures of mortality during subsequent upstream migration. In a related experiment, microarray expression profiles from nonlethal samples were compared between time-matched moribund and surviving wild-caught salmon after being held for one week at warm, ecologically-relevant temperatures (Jeffries et al. 2012). Such approaches also address a caveat of most experimental RNA-based studies in which mortality occurs: that only the survivors are sampled.

Another issue inherent in 'omics' approaches in general is the difficulty of testing the hypothesis that a putative candidate gene is indeed of major consequence for environmental adaptation (Evans 2015). In addition to functional validation, candidate genes derived from laboratory studies could be validated in the field, such as through broad-scale screening of wild populations coupled with *a priori* predictions regarding the expected distributions of variants based on environmental data. A conceptually similar approach was employed to identify those RNA-seq-derived candidate genes for thermal adaptation that occur in the same molecular pathways as genes showing signs of climate-mediated selection in the wild (McCairns et al. 2016). Notwithstanding the difficulty of controlling for background genetic variation in such studies on wild populations, although feasible in some systems (e.g., ancestral *versus* derived populations; Barrett et al. 2008), they can independently corroborate the role of candidate genes in adaptation and contribute to a mechanistic understanding of the impact of genotype on fitness (*sensu* Dalziel et al. 2009).

2.6 Conclusion

The popularity of using RNA-seq to study environmental responses in natural populations has increased rapidly over the past few years and represents a promising method, alone or with other transcription quantification techniques as part of a "unifying workflow" (Alvarez *et al.* 2015), to understand the effects of environmental change on global biodiversity. Field and laboratory experiments on both model and non-model fishes have already provided much insight into the potential for individuals to respond plastically to short- and long-term environmental stress and for populations and species to evolve in the face of shifting environmental regimes. Numerous candidate genes for environmental adaptation have been identified for further study and myriad fish species not mentioned here have recently had their transcriptomes characterized (e.g., Li et al. 2015, Salem et al. 2015, Salisbury et al. 2015, Yue et al. 2015, Fan et al. 2016, Kolder et al. 2016). Coupling this potential with ongoing technological and bioinformatic advances will lead to rapid developments in this field in the coming years. In particular, we expect an even greater broadening of the taxonomical and geographical representation of non-model

study species and an increase in downstream analyses that utilize the sequence information to further test specific hypotheses derived from initial exploratory approaches. We also hope to see more studies being interpreted in an ecological or evolutionary context, as this would greatly facilitate their application to the global climate crisis.

2.7 Tables

Table 2.1: Research in which RNA-seq was utilized to study the effect of continuous, abiotic environmental variables on fishes. The number of biological replicates is given with the number of individuals pooled within each replicate denoted in parentheses when applicable. Key processes involved in responses include both those of focal interest to the authors and those to which the greatest number of dysregulated genes were annotated, to a maximum of five processes. Arrows indicate the relationship between environmental and response variables, where applicable. Identical superscripts between the 'Experimental comparison' and 'Environmental variable/challenge' columns denote which comparisons were made with which variables when multiple options are present within a study. Asterisks denote that the challenge was conducted in combination with a bacterial infection.

Species	Tissue	Number of biological replicates	Experimental comparison	Environmental variable/challenge	Key processes involved in response	Reference
Temperature only						
Acanthochromis polyacanthus	liver	4-5	developmental, transgenerational	temperature(↑)	metabolism(↑), immune response(↑ ↓), stress response(↑ ↓), tissue development(↑), transcriptional regulation(↑)	(Veilleux et al. 2015)
Cynoglossus semilaevi	gill, liver, muscle	3	long-term	temperature(↑)	protein processing(↑), cell morphogenesis(↑), autophagy(↑), immune response(↓), hypoxic signalling(↑)	(Guo et al. 2016)
Hypomesus transpacificus	whole larvae	5	short-term, interspecific	temperature(↑)	metabolism(↑), protein synthesis(↑), inducible transcription factors(↑), osmoregulation	(Jeffries et al. 2016)
Ictalurus sp.	gill, liver	1 (3)	short-term	temperature(↑)	oxygen transport(↑), protein folding/degradation(↑), metabolic process(↑), cytoskeletal organization(↑), protein synthesis(↓)	(Liu et al. 2013)
Melanotaenia duboulayi	liver	6	long-term	temperature(↑)	immune response(↑), stress response(↑), developmental process(↑), metabolism(↓)	(Smith et al. 2013)
Oncorhynchus mykiss gairdneri	gill	3 (3)	long-term, intraspecific	temperature(↑)	stress response(↑), metabolism(↑), cellular process, response to stimuli	(Narum and Campbell 2015)
Pagothenia borchgrevinki	liver	3	short-term	temperature(↑)	cell cycle(↓), ribosome biogenesis(↓), protein biosynthesis(↓)	(Bilyk and Cheng 2014)
Schizothorax richardsonii	liver	1 (3)	short-term	temperature(↑)	response to stimulus(↑ ↓), metabolic process(↑ ↓), protein folding and degradation(↑), immune response(↑), lipid metabolism(↑)	(Barat et al. 2016)
Spirinchus thaleichthys	whole larva	5	short-term, interspecific	temperature(↑)	stress response(↑), protein folding and degradation(↑), DNA damage(↑), aerobic metabolism(↑), osmoregulation	(Jeffries et al. 2016)

Species	Tissue	Number of biological replicates	Experimental comparison	Environmental variable/challenge	Key processes involved in response	Reference
Squalius carolitertii	muscle, liver, fin	1	short-term, interspecific	temperature(↑)	regulation of transcription(↑), RNA metabolism(↑), protein folding and degradation(↑), oxidation-reduction(↑↓)	(Jesus et al. 2016)
Squalius torgalensis	muscle, liver, fin	1	short-term, interspecific	temperature(↑)	protein folding and degradation(↑), cell division(↓), DNA and RNA metabolism(↓), ribosome biogenesis(↓)	(Jesus et al. 2016)
Cyprinus carpio haematopterus	brain, liver, spleen, gill, muscle	1 (3)	long-term	temperature(↓)	protein localization and transport, cellular processes, signal transduction, genetic information processing, metabolism	(Liang et al. 2015)
Danio rerio	whole larvae	2 (50)	short-term	temperature(↓)	transcription(↑), metabolism(↑↓), transport(↑↓), phosphorylation(↑↓), cell motility(↓)	(Hung et al. 2016)
Danio rerio	whole larvae	1 (50)	developmental, short-term	temperature(↓)	RNA splicing/localization(↑), ribosome biogenesis(↑), protein catabolism(↑), metabolism(↓), oxidation-reduction process(↓)	(Long et al. 2013)
Danio rerio	brain, heart, liver, intestine, muscle, gill, spleen, kidney	1 (20)	short-term	temperature(↓)	transcriptional regulation(↑), microtubule-based processes(↑), mRNA splicing(↑), proteolysis(↑), oxidation-reduction process(↓)	(Hu et al. 2015)
Danio rerio	muscle	4	developmental, long-term	temperature(↓)	metabolism(↑), oxidation-reduction process(↑), angiogenesis(↑), muscle contraction and remodelling(↑↓), translation(↓)	(Scott and Johnston 2012)
Lates calcarifer	muscle	1 (8)	long-term, intraspecific	temperature (↓Northern; ↑Southern)	Northern: microtubule-based process(↑), response to stress(↑); Southern: complement system(↓), celular stress reponse(↑)	(Newton et al. 2013)
Neogobius melanostomus	liver	3	short-term, interspecific	temperature(↑↓)	temperature(↑): cell cycle(↓), DNA replication(↓); temperature(↓): carboxylic acid metabolism(↑), amino acid transport(↑); protein catabolism(↑)	(Wellband and Heath 2017)
Proterorhinus semilunaris	liver	3	short-term, interspecific	temperature(↑↓)	temperature(↑): immune response(↑); temp(↓): detection of stimulus(↑), cell signaling(↑), regulation of gene expression(↑), immune response(↑)	(Wellband and Heath 2017)
Salinity only						
Gymnocypris przewalskii	gill, kidney	6	intraspecific	salinity	response to stimulus, immune response, ion transport, cellular water absorption, neuroendocrine system	(Zhang et al. 2015)
Oryzias melastigma	brain, liver, gonads	1 (10)	interspecific	salinity	ion transport, signalling, cell adhesion, metabolism	(Lai et al. 2015 b)

Species	Tissue	Number of biological replicates	Experimental comparison	Environmental variable/challenge	Key processes involved in response	Reference
Anguilla japonica	corpuscle of Stannius gland	2	long-term	salinity(↑)	calcium metabolism(↑↓), blood pressure regulation(↑↓), ion transport(↑↓), cell adhesion(↑), morphogenesis(↑)	(Gu et al. 2015)
Anguilla japonica	gill	2	long-term	salinity(↑)	intracellular signaling cascade(↑), phosphate metabolic process(↑), regulation of cell proliferation(↑), cell adhesion(↑)	(Lai et al. 2015 a)
Anguilla japonica	esophagus	1	long-term	salinity(↑)	ion transport, cellular permeability	(Takei et al. 2017)
Gasterosteus aculeatus	kidney	3	long-term, intraspecific	salinity(↑)	ion transport, cellular water absorption	(Wang et al. 2014)
Gasterosteus aculeatus	gill	10	short-term	salinity(↑)	ATP production(↑), signaling(↑), osmoregulation(↑), cellular permeability(↑)	(Kusakabe et al. 2017)
Gasterosteus aculeatus	brain	88-108	short-term	salinity(↑)	hyperosmotic response, immune response	(Ishikawa et al. 2017)
Lateolabrax maculatus	liver	3	long-term	salinity(↑)	metabolites and ion transporters(↑), energy metabolism(↑), signal transduction(↑↓), immune response(↑↓), structure reorganization(↑)	(Zhang et al. 2017)
Lates calcarifer	intestine	1 (3)	short-term	salinity(↑)	immune response(↑↓), signal transduction(↑↓), metabolism(↓), ribosome biosynthesis(↓)	(Xia et al. 2013)
Oreochromis mossambicus	gill	1 (4)	long-term	salinity(↑)	ion transport(↑), cell cycle(↑), metabolism(↑), signalling(↑↓), cellular remodelling(↓)	(Lam et al. 2014)
Oreochromis niloticus	hepatopancreas	1 (8)	long-term	salinity(↑)	amino acid, sterol, and protein metabolism(↑), immune response(↑↓), lipid metabolism(↓), signal transduction(↑)	(Xu et al. 2015)
Oryzias latipes	intestine	5	short-term	salinity(↑)	protein phosphorylation, transcription regulation(↑), cell adhesion, signal transduction	(Wong et al. 2014)
Pangasianodon hypophthalmus	gill, kidney, intestine	1 (3)	long-term	salinity(↑)	apoptosis(↑), energy metabolism(↑), ion transport(↑↓), cellular reorganization(↑), signal transduction(↑↓)	(Nguyen et al. 2016)
Salvelinus alpinus	gill	6	long-term	salinity(↑)	ion transport(↑↓), immune response(↑↓), cell cycle(↑), stress response(↑), developmental process(↓)	(Norman et al. 2014 a)
Salvelinus alpinus	gill	6	long-term, intraspecific	salinity(↑)	immune response(↑↓), regulation of protein transport(↑)	(Norman et al. 2014 b)
Alosa pseudoharengus	gill	3	long-term, intraspecific	salinity(↑↓)	Landlocked/salinity(↓): freshwater ion uptake(↑), cellular permeability(↑); Anadramous/salinity(↑): ion secretion(↑))	(Velotta et al. 2017)
Gasterosteus aculeatus	gill	5	long-term, intraspecific	salinity(↑↓)	ion transport(↑↓), carbohydrate metabolism(↑↓), lipid metabolism(↑↓), rRNA processing(↓; salinity(↓) only),	(Gibbons et al. 2017)

Species	Tissue	Number of biological replicates	Experimental comparison	Environmental variable/challenge	Key processes involved in response	Reference
					epithelial cell migration(↑ ↓)	
Dissolved oxygen only						
Ictalurus punctatus	gill	n/a	short-term	dissolved oxygen(↓)	cellular permeability	(Sun et al. 2015)
Ictalurus punctatus	gill	n/a	short-term	dissolved oxygen(↓)	apoptosis(↓)	(Yuan et al. 2016)
Larimichthys crocea	brain	6	short-term	dissolved oxygen(↓)	neuro-endocrine-immune system(↑ ↓), glycolysis(↑), protein synthesis(↓), aerobic metabolism(↓)	(Ao et al. 2015)
Megalobrama amblycephala	liver, gill	1 (3)	long-term	dissolved oxygen(↓)	hypoxic signalling(↑), angiogenesis, coagulation, DNA damage signaling and repair, metabolism	(Li et al. 2015)
Morone sp.	hepatopancreas	3 (3)	short-term, long-term	dissolved oxygen(↓)	lipid utilization(↑ ↓), metabolism(↑ ↓), autophagy(↑), apoptosis(↓)	(Beck et al. 2016)
Oryzias melastigma	brain, liver, gonads	1	long-term	dissolved oxygen(↓)	regulatory miRNAs of unknown biological function	(Lau et al. 2014)
Oryzias melastigma	gonad	2 (3)	long-term	dissolved oxygen(↓)	stress response, cell cycle, epigenetic modification, sugar metabolism, cell motility	(Tse et al. 2016)
Oryzias melastigma	brain	2 (3)	long-term	dissolved oxygen(↓)	brain development(↑ ↓), nervous system development(↑ ↓), synaptic transmission(↑ ↓), axon guidance(↑ ↓), potassium ion transport(↑ ↓)	(Lai et al. 2016 a)
Oryzias melastigma	gonad	2 (3)	long-term	dissolved oxygen(↓)	steroidogenesis(↑)	(Lai et al. 2016 b)
pH only						
Leuciscus waleckii	gill, liver, kidney	1 (9-10)	intraspecific	pH(↑)	metabolism(↑), immune response(↑), response to stimulus(↑ ↓), oxidation-reduction process(↑ ↓), signalling	(Xu et al. 2013)
Sebastes caurinus	muscle	3-4	long-term, interspecific	pH(↓)	transcriptional regulation(↑), signalling(↑), stress response(↑)	(Hamilton et al. 2017)
Sebastes mystinus	muscle	2-3	long-term, interspecific	pH(↓)	muscle contraction(↑ ↓), signalling(↑ ↓), metabolism(↑ ↓), cellular structure(↑ ↓), transcription(↑ ↓)	(Hamilton et al. 2017)
Multiple stressors						
Oreochromis mossambicus	spleen	1 (6)	long-term	temperature(↑)*	oxygen metabolism(↑ ↓), energy metabolism(↑ ↓), hypoxic signalling(↑), immune response(↑ ↓)	(Wang et al. 2016)
Chanos chanos	brain, gill, liver, kidney	1 (8)	developmental[a], long-term[a]	salinity[a], temperature[a](↓)	metabolism(↑ ↓)	(Hu et al. 2015)

Species	Tissue	Number of biological replicates	Experimental comparison	Environmental variable/challenge	Key processes involved in response	Reference
Danio rerio	whole larvae	1 (50)	developmental[c], short-term[d]	temperature[a](↓), dissolved oxygen[a](↓)	oxidation-reduction process(↑), oxygen transport(↑), hemoglobin biosynthesis(↑), ion transport(↑), fatty acid biosynthesis(↑)	(Long et al. 2015)
Colossoma macropomum	muscle	1 (6)	short-term, long-term	temperature(↑), pH(↓)	metabolism(↑↓), development(↑), cellular organization(↑), macromolecule biosynthesis(↑↓), translation(↓)	(Prado-Lima and Val 2016)
Pagothenia borchgrevinki	gill	5	long-term	temperature(↑), pH(↓)	immune response(↑), stress response(↑↓), cell proliferation(↓), cell death(↑), protein folding and degradation(↑)	(Huth and Place 2016 a)
Trematomus bernacchii	gill	5	long-term	temperature(↑), pH(↓)	immune response(↑), cell death(↑),carbohydrate and lipid metabolism(↑↓), signal transduction(↓), cell proliferation(↓)	(Huth and Place 2016 b)
Alcolapia grahami	gill	5	long-term, interspecific	pH(↑), salinity(↑), temperature(↑), dissolved oxygen(↑↓)	energy metabolism(↑), ion transport(↑), stress response(↑), immune response(↑), osmoregulation(↑↓)	(Kavembe et al. 2015)

2.8 Figures

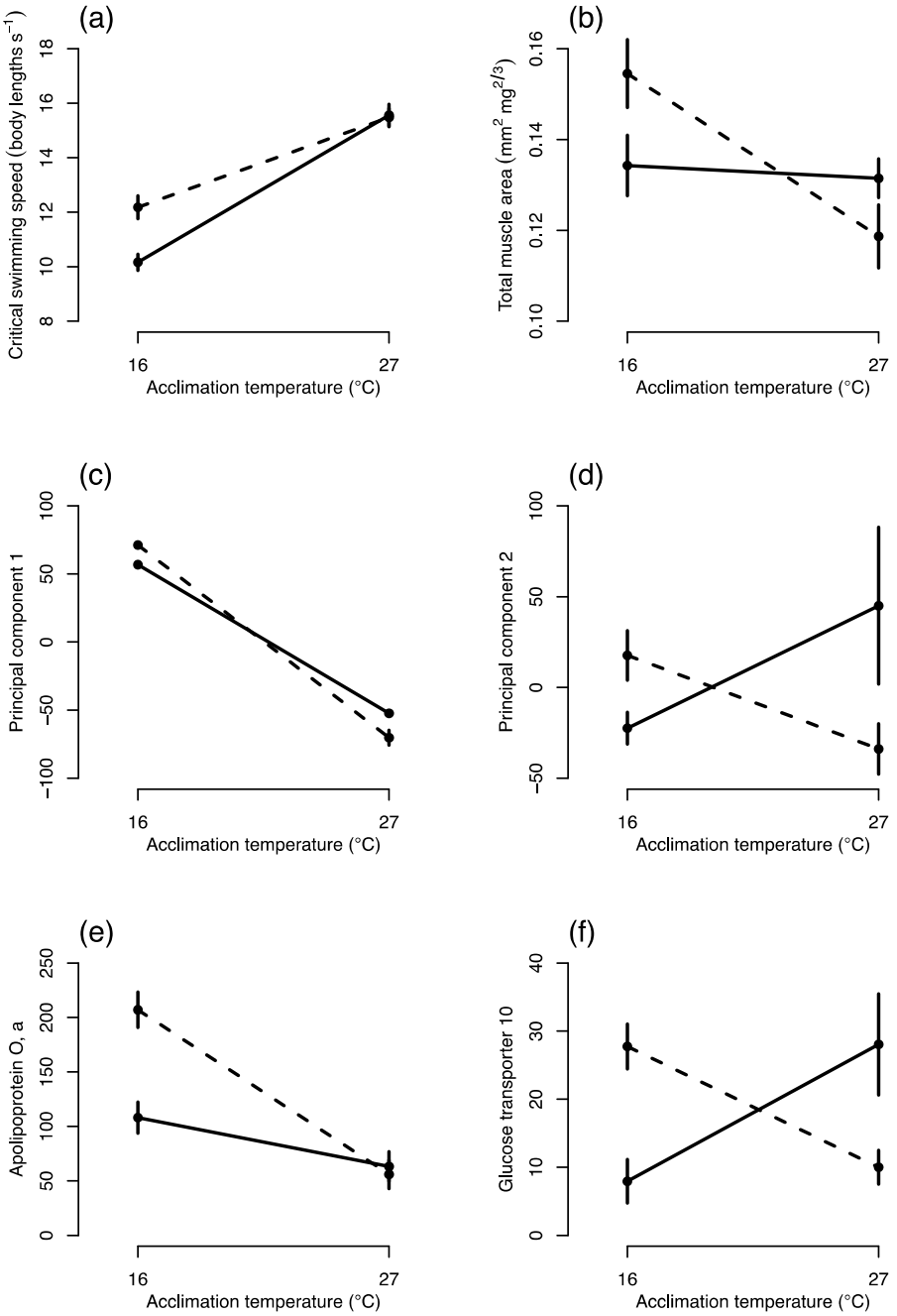

Figure 2.1: Effect of embryonic temperature (solid line=27°C; dashed line=32°C) and long-term acclimation temperature on adult zebrafish (*Danio rerio*) (a) swimming performance, (b) muscle phenotype, (c) and (d) primary transcriptional responses as identified by principal components analysis, and (e) and (f) transcription of genes representative of those involved in the primary transcriptional responses, given in normalized read counts (means ± SEM). Some error bars are too small to be seen (redrawn from Scott and Johnston 2012).

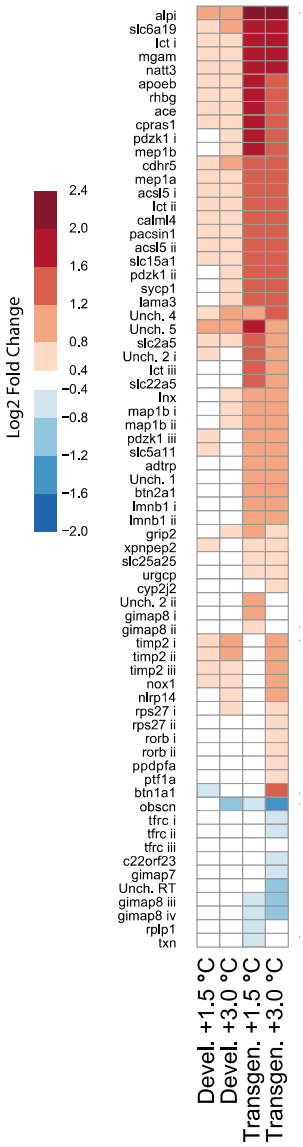

Figure 2.2: Heatmap of contigs differentially expressed (adjusted $P<0.05$) between spiny chromis damselfish (*Acanthochromis polyacanthus*) developmentally or transgenerationally exposed to +1.5°C or +3.0°C and the controls (+0.0°C) (modified from Veilleux et al. 2015).

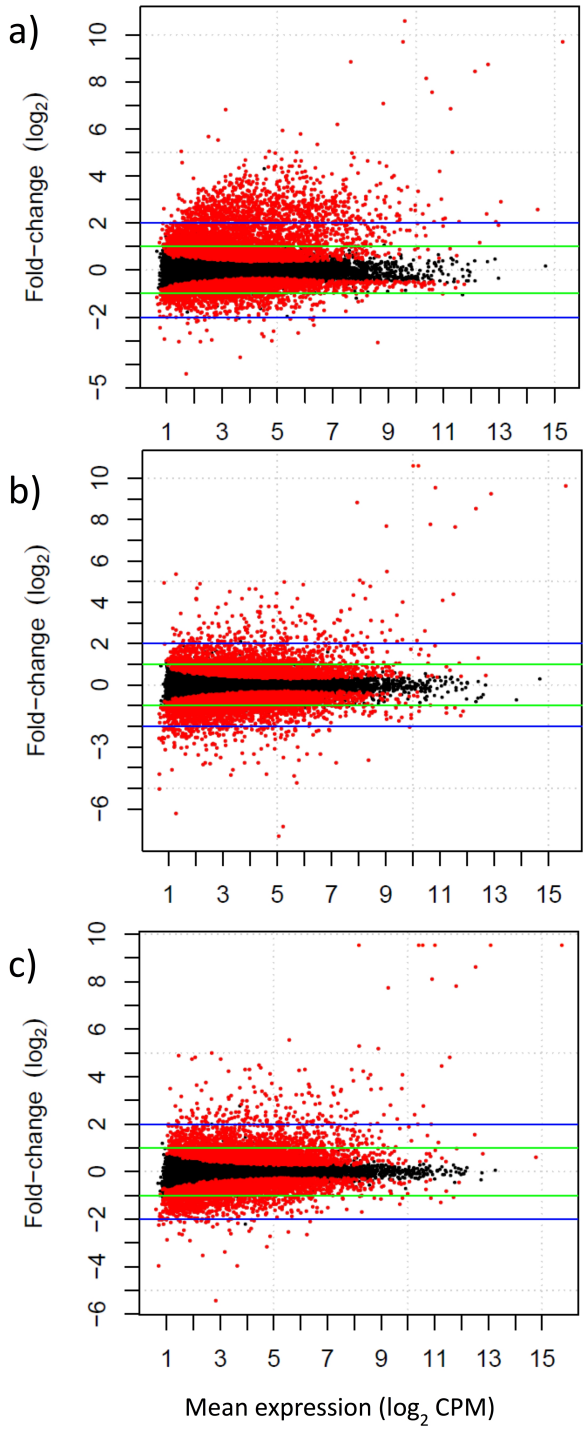

Figure 2.3: Differential expression of (a) a desert strain, (b) an F1 cross, and (c) a montane strain of redband trout (*Oncorhynchus mykiss gairdneri*) exposed to heat stress versus those held at control temperatures. Significant differentiation (FDR≤0.05) is indicated in red. Green and blue lines represent ≥ 2-fold and ≥ 4-fold changes, respectively (original source: Narum and Campbell 2015).

Chapter 3: Ocean Warming Affects the Molecular Stress Response of a North Temperate Marine Fish

Supplementary materials for this chapter are located in Appendix A.
A companion manuscript is located in Appendix B.

3.1 Abstract

Temperature profoundly affects ectotherm physiology. Although differential thermal responses influence fitness, thus driving population dynamics and species distributions, the molecular architecture underlying these responses is unknown, especially early in life. Here, using RNA-sequencing of laboratory-reared Atlantic cod (*Gadus morhua*) larvae of wild origin, we find changes in gene expression consistent with a severe cellular stress response at both ambient and projected (+2°C and +4°C) temperatures. Earlier onset of the transcriptomic response was evident at higher temperatures; concomitant increased growth and mortality suggests a reduction in fitness. Here, we present the first study of transcriptomic responses to temperature by ectothermic vertebrate larvae beyond the critical first-feeding stage, a time when organisms begin balancing the energetic demands of growth, foraging, development, and maintenance. Linking the molecular basis of a thermal response to key fitness-related traits is fundamentally important to predicting how global warming will affect ectotherms.

3.2 Introduction

Temperature has profound effects on ectotherm physiology, impacting metabolic and developmental rates (Clarke & Fraser 2004), aerobic scope (Clark *et al.* 2013), and inducing cellular stress responses (Schulte 2014). The resulting phenotypic and fitness consequences ultimately drive population dynamics and species distributions (Pörtner 2002; Schulte *et al.* 2011). Despite clear links to individual fitness and population viability, the molecular mechanisms underlying thermal plasticity are poorly understood (Logan & Buckley 2015). This is especially true of early life stages, which encompass critical periods for survival and development and are particularly sensitive to temperature (Pörtner & Farrell 2008). Ectothermic larvae typically tolerate a narrower range of temperatures than later life stages and these tolerances often more accurately reflect the climatic boundaries within which species successfully colonize (Abele 2012). Further, the influence of temperature during development has consequences for thermal tolerances and acclimation capacities later in life (Scott & Johnston 2012). Thus, understanding the effects of temperature during early development at the molecular level is critical for determining the physiological limitations of ectotherms and predicting their individual and population responses to global climate change.

Most investigations of responses to thermal extremes at the molecular level have narrowly focused on heat shock proteins (Chen *et al.* 2018). Recent advances in transcriptomics of non-model species (i.e., those which lack genomic tools and resources) have broadened the interpretation of thermal responses beyond the heat shock response to the highly complex genome-wide suite of processes that affect an organism's performance near the edges of their thermal range (Logan & Buckley 2015; Kingsolver & Woods 2016). While energetically costly heat shock proteins have been shown to improve short-term survival, sustained overexpression can have trade-offs, reducing the energy available for growth, development, and reproduction (Tomanek 2010). Therefore, the extent and duration of gene and protein expression in response to sub-lethal thermal stress, and associated fitness consequences, can have profound impacts on ectotherm populations experiencing climate warming (Kingsolver & Woods 2016).

Knowledge of how the transcriptomic thermal response impacts and interacts with growth and development of ectotherms in early life is limited; most studies have been undertaken on juveniles and adults (Moyano *et al.* 2017). Among transcriptomic studies of early life-stage thermal plasticity in ectothermic vertebrates, none has extended beyond the stage of first feeding, the critical point at which organisms must begin to balance the energetic demands of foraging, growth, development, and maintenance. Microarray studies investigating responses to warming in (pre-feeding) fish larvae have had limited time points (n=2) and do not link variation in gene expression to survival (Long *et al.* 2012; Meier *et al.* 2014), despite fitness measures being critical to the interpretation of how thermal responses affect individuals and populations.

Nonetheless, these studies have revealed dysregulation of thousands of genes in response to temperature increases of 3°C (Meier *et al.* 2014) and 6°C (Long *et al.* 2012). For example, in a study of larval zebrafish (*Danio rerio*) 96 hours post-fertilization, differential expression of 2860 temperature-responsive genes was coupled with inhibitory effects of thermal extremes on larval development (Long *et al.* 2012). Seemingly contrary evidence from the invertebrate realm suggests that 2°C of warming accelerates normal developmental transcription patterns in larvae of the coral *Acropora palmata*, although the fitness implications are unclear (Polato *et al.* 2013).

We hypothesize that small temperature increases concordant with those predicted to occur over the next century (IPCC 2013) are likely to cause vast shifts in gene expression, associated fitness and, consequently, population viability. Here, we use RNA-sequencing to investigate the effects of ambient and projected global shifts in temperature (+2°C and +4°C) on genome-wide expression patterns during early development of Atlantic cod (*Gadus morhua*), a widely distributed marine eurytherm with a thermally and developmentally sensitive pelagic larval phase. A comprehensive experimental design, comprising several temperatures and time points (beyond the critical stage of first feeding), allows us to characterize the transcriptomic response to warming in larval fish and evaluate the relationship between the thermal response and developmental time.

Further, we quantify growth and survival reaction norms to understand the fitness implications of the transcriptomic response. In doing so, the present study contributes to our understanding of the physiological limitations of ectotherms during early life and provides a resource for functional studies of temperature-responsive genes during early development.

3.3 Results

3.3.1 Differential Gene Expression Between Each Temperature at Each Time Point Relative to the Baseline

We raised laboratory-hatched cod larvae of wild origin at three temperatures (9°C, 11°C, and 13°C). We sampled a total of three larvae across two tank replicates at each temperature at 2, 14, and 29 days post hatch (dph), and an additional three larvae from the hatching tank at 0 dph (prior to transfer to temperature treatments) to serve as a baseline sample (n=30). Differential expression analysis of 51,075 *de novo* assembled transcripts revealed that genomic expression varied among time points and temperatures, with a time-by-temperature interaction (Figure 3.1; Appendix A Table S1; for assembly details see Appendix B). At 2 dph, no difference in expression was observed at 9°C relative to the baseline sample taken prior to transfer (0 dph at 9°C), indicating a lack of response to transfer or major change in development over this brief time period. At the same time point, 10 and 3,646 differentially expressed genes were detected at 11°C and 13°C, respectively, suggesting a minimal response to a short-term 2°C increase in temperature, but a comparatively substantive response to a short-term 4°C increase. At 14 dph, the number of differentially expressed genes increased to 94 at 9°C and 5,121 at 11°C, while they declined to 294 at 13°C. At 29 dph, the greatest number of differentially expressed genes was observed at 9°C (4,276), although many were still detected at higher temperatures (1,229 and 1,068 at 11°C and 13°C, respectively).

There was substantial overlap among temperatures at which genes were differentially expressed relative to the baseline. At 2 dph, all 10 genes that were differentially expressed at 11°C were also differentially expressed at 13°C (Figure 3.2a), representing a

common transcriptomic response to short-term warming. At 14 dph, most of the differentially expressed genes at 9°C were also detected at 11°C, and many of these were also detected at 13°C (Figure 3.2b), perhaps representing a common developmental trajectory. Substantial numbers of differentially expressed genes were common between each set of temperatures (617-673) and among all three temperatures (495) at 29 dph (Figure 3.2c).

There were differences between time points in which genes were differentially expressed relative to the baseline. Relatively little overlap between 2 and 14 dph at 13°C (55/294 genes at 14 dph; Figure 3.2e) suggests a major shift in transcription across this time period. Many new genes were differentially expressed at 29 dph relative to earlier time points, while some were also common to those detected at 14 dph (all temperatures) and 2 dph (13°C only) (Figure 3.2d-f).

3.3.2 Differential Expression Between Temperatures

Direct tests for differential expression between temperatures within time points confirm that short-term exposure to 11°C (2°C increase) had little or no detectable impact on gene expression levels, while short-term exposure to 13°C (4°C increase) upregulated thousands of genes (Table S1). After 2 weeks of exposure, 1,507 and 2,324 genes were upregulated at 11°C relative to 9°C and 13°C, respectively, while only 4 differentially expressed genes were detected between 9°C and 13°C. There were essentially no detectable differences in expression between temperatures after 4 weeks of exposure, suggesting that the responses to long-term exposure to different temperatures were similar.

3.3.3 Differential Expression over Time

Direct tests for differential expression between time points within temperature treatments indicate a gradual shift in expression at 9°C, with a greater change in expression during the latter half of the experiment and the majority of differentially expressed genes detected only in pairwise tests between 0/2 and 29 dph (Table S1). The numbers of up-

and downregulated genes both increased over time, but more genes were upregulated overall. A drastic shift in expression was observed between 2 and 14 dph at 11°C, with nearly twice as much upregulation as downregulation. This was followed primarily by downregulation between 14 and 29 dph, where the number of differentially expressed genes was about half as many as between the previous time points. At 13°C, expression largely decreased between 2 and 14 dph, then remained relatively constant between 14 and 29 dph.

3.3.4 Temporal Shift in Common Transcriptomic Response

The differential expression analyses described herein specify a transcriptomic response characterized by vast upregulation that occurs earlier at higher temperatures, followed by downregulation of a portion of this response (except at 9°C, for which no time point subsequent to the peak of the response was available). This is exemplified by the greatest differences in gene expression relative to the baseline being observed at D2-13°C (i.e., 2 dph and 13°C), D14-11°C, and D29-9°C. The majority (2,448) of these differentially expressed genes overlapped among all three responses, while 985 and 891 additionally overlapped between D29-9°C and D14-11°C, and D14-11°C and D2-13°C, respectively (Figure S1a). The GO terms associated with these differentially expressed genes overlapped even more, with 5,902/8,655 common among all three samples (Figure S1b). This suggests earlier onset of a common transcriptomic response as temperature increases, along with some temperature- or time-specific gene expression.

Importantly, these temporal differences in gene expression levels do not correspond to differences in growing degree days. The magnitude of the common transcriptomic responses, in terms of both the numbers of differentially expressed genes and their log fold-changes, peaked at different degree days (Figure 3.3), in addition to different experimental time points (Figure 3.1).

3.3.5 Gene Ontology Enrichment Analysis

Although the number of significantly enriched GO terms differed between two enrichment methods, BiNGO (Maere *et al.* 2005) and ClueGO (Bindea *et al.* 2009), they showed similar patterns across temperatures and times (Table S2). After 2 days of exposure, the few upregulated genes at 11°C were enriched for cellular respiration according to BinGO, as were the genes upregulated at 9°C after 14 days of exposure (Supplementary data 1).

Genes that were upregulated during the peak of the common transcriptomic response (i.e., at D2-13°C, D14-11°C, and D29-9°C) were enriched for 305, 334, and 307 (BiNGO) and 1,545, 1,756, and 1,595 (ClueGO) GO terms, respectively (Table S2). Most of the BiNGO-enriched terms were associated with development and oogenesis, cellular respiration and metabolism (particularly lipid metabolism), gene expression regulation, cell cycle activity, and protein folding, metabolism, and localization (Supplementary data 1). The number of terms related to the cell cycle decreased with temperature, whereas the number of terms related to energy and protein metabolism increased with temperature. The same ClueGO-enriched GO category was the largest category D2-13°C, D14-11°C, and D29-9°C, consisting of 141-198 enriched GO terms (Figure 3.4). Most of these were involved in cell cycle regulation (e.g., cell cycle checkpoint [GO: 75], regulation of cell cycle [GO: 51726]) including cell cycle arrest (GO: 7050, 71156) and protein metabolism (e.g., protein catabolic process [GO: 30163], proteolysis [GO: 6508]). Other GO terms within this upregulated enrichment group were associated with a response to hypoxia (GO: 36293, 36294, 61418, 70482, 71453, 71456), antigen presentation (GO: 2474, 19884, 48002), and autophagy (GO: 6914, 10506).

Among the next largest GO enrichment groups were those dominated by protein biosynthesis, metabolism, transport and localization, energy metabolism including cellular respiration, chromatin and histone modification, DNA repair, regulation of transcription and translation, responses to hormonal stimuli, cellular/mitochondrial organization and autophagy/mitophagy, and adaptive immune and viral responses (Figure 3.4). These GO groups were represented by similar numbers and types of GO terms at D2-13°C, D14-11°C, and D29-9°C, although there were fewer terms associated with

metabolic processes at D29-9°C. Further, a large GO group associated with brain and nervous system development at D29-9°C (25 terms, Group194) was absent from the warmer temperatures (although 4 [D2-13°C] and 6 [D14-11°C] of these terms were enriched in clusters related to other processes) and a group of heart developmental processes was larger at D29-9°C (20 terms) compared to D2-13°C and D14-11°C (8 terms each).

Among these commonly upregulated responses at D2-13°C, D14-11°C, and D29-9°C, those enriched GO terms unique to D2-13°C included more terms related to metabolism and energy production, whereas those unique to D29-9°C included more terms related to development, cell cycle processes, and the immune system (Supplementary data 2). Those enriched GO terms unique to D14-11°C contained intermediate amounts of metabolic and cell cycle-related terms relative to the other treatments. The numbers of enriched GO terms for upregulated genes associated with the endoplasmic-reticulum-associated protein degradation (ERAD) pathway (11, 15, and 22) and apoptotic signalling pathways (10, 16, and 22) increased with temperature for D29-9°C, D14-11°C, and D2-13°C, respectively. Enriched GO terms specifically related to oxidative stress were only present at D2-13°C (4) and D14-11°C (6). Genes upregulated at D2-13°C, D14-11°C, and D29-9°C were characterized by similar numbers of enriched GO terms related to cell cycle arrest (2-3), neuron death (3-4), cellular responses to heat (2-5), hypoxia (7-8), and stress in general (9-11). In contrast, the numbers of enriched GO terms explicitly associated with the immune system (31, 25, and 19) and the Wnt signalling pathways (14, 9, and 3) decreased with temperature at D29-9°C, D14-11°C, and D2-13°C, respectively.

Upregulated genes at D14-13°C, D29-11°C, and D29-13°C (i.e., time points following the peak of the response at each temperature) were primarily enriched for developmental and immune-related processes (Supplementary data 1, 2). At day 29, these included BinGO-enriched terms related to heart development (e.g., GO: 55009), the acute inflammatory response (GO: 2541), and the regulation of a suite of interleukins (GO: 32653, 32673, 32674, 32693, 32714, 32753). ClueGO-enriched terms were mainly associated with brain (GO: 21762, 30901) and heart (11°C only) development.

Downregulated genes at D2-11°C and D2-13°C were largely enriched for light perception, while at D14-9°C they were primarily enriched for cardiac development and muscle contraction (Supplementary data 3). Processes related to development and visual perception continued to be the most commonly enriched processes among downregulated genes in all treatments for the duration of the experiment (Supplementary data 3, 4).

3.3.6 Minimum Stress Proteome

Of the 44 genes that comprise the minimum stress proteome (Kültz 2005), 40 were detected in our *de novo* transcriptome annotation database. Thirty-three of these were differentially expressed in at least two of the three temperature treatments (at D2-13°C, D14-11°C, and/or D29-9°C), with the fewest detected at D29-9°C (Table 3.1). Many genes were represented by multiple transcripts and most were upregulated across treatments.

3.3.7 Growth and Survival Reaction Norms

Thermal reaction norms at 29 dph show that growth increased with temperature ($F_{2,87}$=12.7, P<0.001; Figure 3.5a) while survival decreased (P<0.001; Figure 3.5b). The magnitudes of these effects were substantial: a 117% increase in growth and a 75% reduction in survival from 9°C to 13°C. The negative effect of increased temperature on survival was also apparent at 43 dph (79% reduction from 9°C to 13°C; P<0.001; Figure S3).

3.4 Discussion

Here we show that warmer temperatures accelerate the onset of a broad change in transcription in larval Atlantic cod while increasing growth and mortality. Aside from temporal differences, a similar pattern of gene transcription consistent with a severe cellular stress response was observed at all temperatures, including the local ambient temperature that has already risen an average of 1°C since the late 1980s (Barceló *et al.*

2016; Figure S4) and projected temperatures under future warming scenarios (+2°C and +4°C) (IPCC 2013).

3.4.1 Transcriptomic Response to Warming

Warming generally increases metabolic energy requirements and oxygen consumption (Fry & Hart 1948). Indeed, transcripts involved in cellular respiration were the earliest to be upregulated at all temperatures in our experiment and enrichment of this process increased with temperature at the peak of the common transcriptomic response. Sufficient warming causes a build-up of oxygen metabolism byproducts, reactive oxygen species, that damages complex molecules and cellular structures (Abele & Puntarulo 2004). Damage to macromolecules activates the highly conserved cellular stress response (CSR), the core components of which include 1) the protection of macromolecules (e.g., through chaperoning of misfolded or damaged proteins and DNA repair mechanisms), 2) regulation of the cell cycle to temporarily arrest cell proliferation, 3) metabolic shifts and, if the stress is sufficiently severe, 4) programmed death (apoptosis) and removal of terminally damaged cells (Kültz 2005). Overall, these processes dominate the common transcriptome we observed. The enrichment of GO terms specific to stress in general and the response to heat are consistent with a broad and severe thermal stress response at all temperatures in the present study. The enrichment of GO terms related to hypoxia (oxygen deficiency) is also consistent with warming-related stress, as the decreased oxygen solubility with temperature coupled with increased oxygen consumption widens the gap between supply and demand. Our inference of a stress response is further supported by the upregulation of 33 of the 44 genes comprising the minimum stress proteome of all organisms (Kültz 2005). A similar number (31 of 44) of these stress genes were upregulated in yeast exposed to diverse stressors (Gasch *et al.* 2000). The lack of the full set in our experiment might be attributable to incomplete assembly, constitutive expression, or regulation by processes other than transcription (e.g., post-translational modification or protein turnover).

The majority of differentially expressed transcripts in our experiment were upregulated relative to the baseline, similar to that observed in larval zebrafish following acute exposure to heat (Long *et al.* 2012). High enrichment for upregulation of protein biosynthesis, regulation of transcription and translation, and RNA processing likewise suggest activation of a large suite of cellular machinery that is likely costly to maintain (Wagner 2005). Accordingly, this response was not consistently maintained beyond a single time point at either temperature (11°C and 13°C) for which data were available.

In addition to earlier onset of the stress response at higher temperatures, there is some evidence that the severity of the stress response increased with temperature. Greater enrichment for upregulated genes involved in oxidative stress and protein metabolism, particularly the endoplasmic-reticulum-associated protein degradation (ERAD) pathway, suggests a greater build-up of reactive oxygen species and damaged proteins at higher temperatures (Slimen *et al.* 2014). The associated increase in apoptotic signalling pathways (including those specifically induced by endoplasmic reticulum stress) is consistent with more prevalent terminal cell damage at higher temperatures. Similarly, genes involved in oxidative stress-induced neuron death were upregulated only at the warmer temperatures. Greater enrichment of upregulated genes related to carbohydrate metabolism and energy production at 11°C and 13°C might represent a larger metabolic shift in response to stress, a thermodynamic consequence related to the positive relationship between temperature and metabolism, or both.

Developmental transcription also differed markedly between temperatures. Many processes related to visual perception and development were commonly downregulated over time, consistent with the completion of some organ development and optical system formation. However, the lack of processes related to nervous system and heart development among genes upregulated at warmer temperatures suggests a disruption of neural and cardiac development. The reduction in enrichment of upregulated genes involved in the Wnt signalling pathways at warmer temperatures is also consistent with altered developmental progress. These highly conserved and strictly controlled pathways perform critical functions in cell proliferation and differentiation in developing tissues

and the immune system, and their dysregulation is implicated in developmental abnormalities and malignancies (Staal *et al.* 2008). Coral (*A. palmata*; Polato *et al.* 2013) and zebrafish (Long *et al.* 2013) larvae upregulate genes involved in Wnt pathways in response to heat and cold stress, respectively, suggesting that Wnt-associated genes might be widely vulnerable to thermal disruptions.

3.4.2 Earlier Onset of the Transcriptomic Response

We found that the transcriptomic stress response occurred earlier at higher temperatures, to an even greater extent than can be accounted for by developmental time (i.e., growing degree days). The growing degree day metric is widely applied to developing ectotherms, based on the essentially linear relationship between acclimation temperature and metabolic rate across the majority of the thermal window (Neuheimer & Taggart 2007). Because the growing degree day relationship follows a normal developmental rate, temporal deviations in transcription from this trend are consistent with thermal effects on gene expression that are in addition to potential effects of temperature-mediated development. Further, the differences in growth rates among temperatures in our experiment are small compared to the differences in the timing of transcription. However, the relationships between thermal rates at different levels of biological organization are unclear and likely extremely complex, making comparisons difficult (Chaui-Berlinck *et al.* 2004). Nonetheless, acceleration of normal developmental transcription, such as that documented in coral larvae over 72h of exposure to just 2°C of warming (Polato *et al.* 2013), also has potential fitness consequences.

3.4.3 A Potential Mechanistic Link to Fitness

Thermal stress depletes energy reserves such as lipid stores (Klepsatel *et al.* 2016) and the molecular response to thermal stress is energetically costly in particular. For example, continued overexpression of HSPs is known to negatively impact growth rate and fertility (Tomanek 2010). Such exhausting expression might help to explain why performance and its upper thermal range decrease with increasing duration of exposure to even nonlethal temperatures (Schulte *et al.* 2011). This hypothesis is supported by models,

based on thermal performance curves for ingestion rate, that incorporate the energetic costs associated with producing heat shock proteins in Tobacco hornworm (*Manduca sexta*) larvae (Kingsolver & Woods 2016). It is reasonable to infer that the upregulation of thousands of transcripts that we observed in response to warming in larval cod might act as a similar energetic drain, as gene expression is costly in general (Wagner 2005).

Faster growth, as observed at higher temperatures in the present study and in marine fish larvae generally (Pepin 1991), can improve fitness by reducing the duration of the vulnerable larval stage (Anderson 1988). Yet, fast growth can be suboptimal due to conflicts in energy allocation (Billerbeck *et al.* 2001). If fast-growing fish are unable to sufficiently reallocate energy away from growth in response to stress, the high energetic demands of the molecular stress response might exceed energy availability. Accordingly, mortality increased with temperature in our experiment. Thus, we hypothesize that the energetically costly stress response, coupled with increased growth rate at warmer temperatures, leads to faster depletion of energy reserves and increased risk of mortality in larval cod. Such energetic limitations are likely to be exacerbated in the wild, where food is limited compared to the laboratory environment, especially at warmer temperatures (Rogers *et al.* 2011).

3.4.4 Future Research Directions

The ambient temperature in our experiment is likely to be experienced during the latter, warmer part of the regional spawning period (January to May) in a relatively southern part of the distribution of this cold-water adapted species. Additional experiments are needed to characterize larval developmental expression at colder temperatures that are likely to be experienced earlier in the spawning season and farther North. Further, thermal responses can vary among populations adapted to different thermal regimes (Oomen & Hutchings 2015a). Genetic variation in thermal plasticity has been shown for growth and survival of cod larvae in the Northeast Atlantic (Oomen & Hutchings 2015b, 2016). Therefore, further research is needed to determine how the transcriptomic response observed in our study might differ between cod populations. Measures of

protein levels would help to further elucidate the mechanistic link between gene transcription and fitness in thermal responses, as would measures of energy usage (e.g., oxygen consumption, lipid storage levels).

3.4.5 Potential Implications

As sea surface temperatures continue to rise over the next century, reduced fitness of Atlantic cod larvae might lead to population declines in this ecologically and socioeconomically important species. Indeed, the physiological consequences of 2-4°C of warming observed in the present study contribute to a mechanistic understanding of the negative association between temperature and recruitment for relatively warm-water cod populations inhabiting regions such as coastal Skagerrak (Rogers & Stenseth 2017) and the North Sea (O'Brien *et al.* 2000). Accelerated development at warmer temperatures might lead to reduced population connectivity by shortening the duration of the pelagic larval phase, thereby limiting dispersal distance. Rapid adaptation to warmer temperatures might also occur given the apparently strong selection pressure observed in the present study, but only if heritable variation in thermal responses exists (Nussey *et al.* 2005).

3.5 Materials and Methods

3.5.1 Experimental Design

We conducted RNA sequencing of larval Atlantic cod that were reared at three temperatures in the laboratory to assess variation in gene expression, growth, and survival with temperature over time. Sixty-six adult Atlantic cod were collected near the *Institute of Marine Research, Flødevigen* on the Norwegian Skagerrak coast (58.39603 N, 8.73322 E) in December 2012. All cod were allowed to spawn undisturbed in a 45 m^3 spawning basin at the *Institute of Marine Research, Flødevigen* from February to May 2013. Cod were held at ambient temperature and photoperiod and fed shrimp daily until the end of the spawning period, when they were sacrificed by a blow to the head prior to dissection for sex identification and fin tissue collection.

Midway through the spawning season, fertilized eggs were collected and incubated at 9°C in a 900 L flow-through seawater tank until hatch, when they were randomly distributed among 40 L rearing tanks with flow-rates of 0.35 L/min (i.e., approximately 2 h turnover rate). Larvae were reared at three temperatures (9 °C, 11°C, and 13°C) with three replicate tanks per temperature initially containing 1600 larvae each. These temperatures represent the ambient seawater temperature outside the Flødevigen facility, in the vicinity where the adult cod were collected, and a 2 °C and 4°C increase representing projected climate scenarios by the year 2100 (IPCC 2013). The temperatures in the rearing tanks were 9°C upon transfer from the incubation tank and then gradually changed to the experimental temperatures over the course of 24 h. Larvae were reared under a constant light intensity of 2000 lux and fed *Brachionus plicatilis* rotifers enriched with RotiGrow *Plus*™ (Reed Mariculture, USA) in excess (4500 prey/litre three times daily, at approximately 10:00 am, 2:00 pm, and 6:00 pm). Water temperatures were recorded daily and water quality parameters (oxygen, pH, and ammonia concentration) were monitored with no notable deviations.

Ten larvae from each of the nine tanks were randomly sampled at 2, 14, and 29 days post hatch (dph), and an additional 30 larvae were sampled from the hatching tank at 0 dph. Larvae were individually placed in RNAlater™ (an ammonium sulphate solution) on a glass slide and immediately photographed, using a stereoscope with a Leica DFC 425 C Camera. Samples were preserved in RNAlater™ at -20 °C prior to DNA and RNA extraction.

Standard length at 29 dph was measured from the photographs, using ImageJ (Abràmoff *et al.* 2004), and considered a proxy for growth rate, following Hutchings et al. (2007). Survival was quantified as the number of larvae alive in each tank at 29 dph relative to the number initially in each tank. This count was obtained prior to that day's sampling, but was not otherwise adjusted for sampling mortality.

After 29 dph, the larvae continued to be reared with a change in feed: a 1:1 mixture of rotifers and *Artemia* from 32-39 dph and *Artemia* only from 40-43 dph. Survival was measured again at 43 dph to assess the consistency of temperature effects over time, beyond the end of the larval stage. Gene expression was not measured beyond 29 dph due to the confounding effect of different feed types with size and temperature; therefore, we refer to day 29 as the end of the experiment.

3.5.2 DNA/RNA Isolation

Of the sampled larvae, 30 were selected for RNA-seq: three from each of the three temperature treatments and three time points, plus three samples from the hatching tank (0 dph) to serve as a baseline (see Table S3 for details). Samples were selected from two of the tank replicates, which were considered to be biological replicates given the lack of phenotypic variation among tanks (random effect $\sigma^2=0$ in the growth model). Larvae were dissected into proximal (including the head, organs and part of the tail) and distal (the remainder of the tail) sections, which were used for RNA and DNA isolations, respectively. DNA was extracted from adult and larval tissue, using the E-Z 96 Tissue DNA Kit (Omega Bio-tek) in accordance with the manufacturer's instructions. Parentage analysis using methods described by Roney et al. (2018a) identified three full-sib/two half-sib families derived from two fathers and three mothers, with 90% of offspring coming from the same parent pair (Table S3).

3.5.3 RNA Sequencing and Assembly

For each larva, total RNA was isolated using the RNeasy Mini Kit (Qiagen) and a single paired-end library was created using the TruSeq™ RNA low-throughput protocol (Illumina)(Supplementary Materials and Methods). Libraries were sequenced with a 100bp paired-end (PE) protocol on the Illumina HiSeq 2500 platform at the Norwegian Sequencing Centre (www.sequencing.uio.no), producing a total of 798 million read pairs. Trimming and adapter removal was performed on all sequences (Appendix B), reducing the dataset to 740 million read pairs. Transcriptome assembly was performed *de novo* using the Trinity software suite v.2014-07-17 (http://trinityrnaseq.github.io) and

annotated using Trinotate v.2.0.1 (https://trinotate.github.io). See Appendix B for assembly details and comparisons of the *de novo* assembly and reference genome-based assemblies.

3.5.4 Differential Expression Statistical Analysis

Differential expression analysis was carried out using edgeR v.3.16.5 (Chen *et al.* 2014) in R v.3.3.2. We filtered transcripts that did not have a count per million (CPM) >1 in at least three samples. Pairwise comparisons were then carried out between all samples compared to the baseline sample, as well as across time within temperatures, and across temperatures within times, using a false discovery rate (FDR)-corrected P-value of 0.05. Venn diagrams were constructed using BioVenn (Hulsen *et al.* 2008) and Venny (http://bioinfogp.cnb.csic.es/tools/venny/) to compare differentially expressed gene lists among pairwise comparisons.

3.5.5 Gene Ontology Enrichment Analysis

Gene ontology (GO) enrichment analysis and network construction was performed using ClueGO v.2.3.2 (Bindea *et al.* 2009) and BiNGO v.3.0.3 (Maere *et al.* 2005) in Cytoscape v.3.2.1 (Shannon *et al.* 2003) to identify significantly enriched biological processes involved in the thermal response (Supplementary Materials and Methods). Annotations were compared to a human (in ClueGO) or custom (i.e., constructed from the Blastx hits from Trinotate; in BiNGO) gene ontology database. Up- and down-regulated genes were analyzed separately for both analyses and only the GO category 'Biological Processes' was analyzed as we considered it to be the most phenotypically informative. The Gene Fusion option was used in ClueGO to enhance clustering. An FDR-corrected P-value of 0.05 and otherwise default parameters were used for both analyses.

3.5.6 Downstream Analysis of De Novo-*Assembled Transcripts*

Due to the ability to annotate novel loci and an apparently greater sensitivity for detecting likely biologically meaningful differential expression in our experiment (e.g., greater average GO enrichment relative to the numbers of differentially expressed genes), we chose a *de novo* assembly approach (Appendix B). The numbers and log-fold changes of genes that were differentially expressed when compared to the baseline were evaluated relative to developmental time using the growing degree day metric, which is the sum of daily temperatures measured above a temperature threshold (in this case 0°C) that accounts for the relationship between temperature and rates of enzymatic reactions (Neuheimer & Taggart 2007). We performed a post-hoc evaluation for the presence of the minimum stress proteome (a set of 44 universally conserved stress proteins; Kültz 2005) in our experiment by manually searching the transcriptome annotations for gene descriptions corresponding to those contained in Kültz (2005) Table 1 and observing whether these transcripts were differentially expressed relative to the baseline.

3.5.7 Growth and Survival Statistical Analysis

The effect of temperature on growth was evaluated in R v.3.3.2 (R Development Core Team), using a linear mixed-effects model with temperature as a fixed effect and tank nested within temperature as a random effect. Survival was modeled in relation to temperature as a fixed effect, using a generalized linear model with a quasi-binomial distribution to account for overdispersion (i.e., dispersion parameter >1; in this case 3.54 and 2.00 for days 29 and 43, respectively). Back-transformed model estimates were used for plotting survival reaction norms. The assumptions of normality and homogeneity of variances were not violated except for a single datum from the low temperature treatment in the survival analyses, which we chose to retain.

3.6 Tables

Table 3.1: Transcripts annotated to genes that comprise part of the minimum stress proteome that were differentially expressed (FDR>0.05) relative to the baseline in larval Atlantic cod reared at three temperatures. Only contrasts in which differential expression was detected are included.

Transcript ID	Gene name	Description	min. Evalue	D2-13°C	D14-9°C	D14-11°C	D14-13°C	D29-9°C	D29-11°C	D29-13°C
DNA damage sensing/repair										
c79008_g1	MLH1	DNA mismatch repair protein MLH1	1.00E-126			6.62		5.07		
c139074_g1	MSH6	DNA mismatch repair protein Msh6	0	5.96		8.08		6.47		
c143511_g1	MSH2	DNA mismatch repair protein Msh2	0	6.28		8.18		7.15		
c79247_g1	RA51A	DNA repair protein RAD51 homolog A	0	5.54		8.31		6.53		
c141131_g1	TOP1	DNA topoisomerase 1	0	6.67		9.58		9.07		
c185971_g1	TOP3A	DNA topoisomerase 3-alpha	0	4.75		6.21		4.93		
Energy metabolism										
c136064_g1	AT2C1	Calcium-transporting ATPase type 2C member 1	0	5.58		6.72		5.42		
c145796_g2	AT2B1	Plasma membrane calcium-transporting ATPase 1	6.00E-42						-1.47	
c150107_g1	AT2B3	Plasma membrane calcium-transporting ATPase 3	0	6.98		8.17		7.01		
c153430_g1	AT2A1	Sarcoplasmic/endoplasmic reticulum calcium ATPase 1	2.00E-54			-1.18				
c153430_g4	ATC	Calcium-transporting ATPase sarcoplasmic/endoplasmic reticulum type	3.00E-54	6.48		6.72		5.70		
c153660_g13	AT2B3	Plasma membrane calcium-transporting ATPase 3	1.00E-147						-1.36	
c155386_g2	AT2B1	Plasma membrane calcium-transporting ATPase 1	0	7.47		8.61		7.73		
c157062_g2	AT2A1	Sarcoplasmic/endoplasmic reticulum calcium ATPase 1	2.00E-98			-0.98				
c158484_g6	AT2A1	Sarcoplasmic/endoplasmic reticulum calcium ATPase 1	4.00E-174			-1.18				
c160449_g5	AT2A1	Sarcoplasmic/endoplasmic reticulum calcium ATPase 1	6.00E-64			-1.25				
c130005_g1	CISY	Citrate synthase	0	8.57		9.89		7.85		
c149079_g1	ACLY	ATP-citrate synthase	0	7.83		9.41		6.47		
c159927_g2	ACLY	ATP-citrate synthase	0					-0.96	-1.17	
c141763_g1	ENOA	Alpha-enolase	0	9.59		10.59		9.19		
c140798_g1	PGM2	Phosphoglucomutase-2	0	5.85		7.94		6.00		
c141603_g1	PGM5	Phosphoglucomutase-like protein 5	9.00E-61					-1.64		
c263700_g1	PGM1	Phosphoglucomutase-1	0	7.64		8.28				
Fatty acid/lipid metabolism										

Transcript ID	Gene name	Description	min. Evalue	D2-13°C	D14-9°C	D14-11°C	D14-13°C	D29-9°C	D29-11°C	D29-13°C
c133422_g2	PATL1	Protein PAT1 homolog 1	5.00E-24	4.97		7.13		5.44		
c110543_g1	ACSL4	Long-chain-fatty-acid--CoA ligase 4	4.00E-142			6.59		5.30		
c129849_g1	ACSL5	Long-chain-fatty-acid--CoA ligase 5	0	5.68		6.68				
c134376_g1	ACSL1	Long-chain-fatty-acid--CoA ligase 1	0	5.61		6.99				
c143921_g1	ACSL3	Long-chain-fatty-acid--CoA ligase 3	0	6.99		8.46		6.98		
c79025_g1	DHB4	Peroxisomal multifunctional enzyme type 2	0	6.74		8.04		6.19		
Molecular chaperones										
c101741_g1	DJC11	DnaJ homolog subfamily C member 11	4.00E-115	5.58		6.75				
c106402_g1	DNJB2	DnaJ homolog subfamily B member 2	4.00E-34	5.73		7.06		5.32		
c111354_g1	DNJC5	DnaJ homolog subfamily C member 5	1.00E-27	5.27		6.16				
c116500_g1	DNJC2	DnaJ homolog subfamily C member 2	2.00E-64	6.08		7.61		5.89		
c118111_g1	DNAJ1	DnaJ protein homolog 1	4.00E-103	6.80		8.79		6.93		
c118596_g1	DJB11	DnaJ homolog subfamily B member 11	1.00E-151	6.08		8.17		7.07		
c120618_g1	DNJC7	DnaJ homolog subfamily C member 7	6.00E-136	6.28		7.94		6.01		
c122274_g1	DNJA1	DnaJ homolog subfamily A member 1	6.00E-150	7.35		8.70		7.46		
c123966_g1	DNJC3	DnaJ homolog subfamily C member 3	2.00E-121	5.62		7.76		5.80		
c125071_g1	DNJC9	DnaJ homolog subfamily C member 9	1.00E-46	5.43		8.83		7.22		
c136250_g1	DJB12	DnaJ homolog subfamily B member 12	1.00E-72	5.68		7.07		6.02		
c137180_g1	DJC16	DnaJ homolog subfamily C member 16	1.00E-54	5.36		6.99		5.04		
c141320_g1	DJC10	DnaJ homolog subfamily C member 10	0	5.33		6.87		6.60		
c144998_g2	DJC27	DnaJ homolog subfamily C member 27	0					-0.81		
c149091_g2	DNJC4	DnaJ homolog subfamily C member 4	6.00E-53			1.08				
c149153_g5	DNJC5	DnaJ homolog subfamily C member 5	2.00E-98			-0.71				
c53913_g1	DNJA2	DnaJ homolog subfamily A member 2	5.00E-104	7.17		9.01		6.71		
c79127_g1	DNJB2	DnaJ homolog subfamily B member 2	4.00E-41	4.87		7.99		6.39		
c138398_g2	HSP70	Heat shock 70 kDa protein	6.00E-101						2.02	
c158105_g1	HSP70	Heat shock 70 kDa protein	8.00E-50			3.90	3.91	3.38		
c159822_g1	HSP70	Heat shock 70 kDa protein	3.00E-70			3.33				
c160682_g2	HSP70	Heat shock 70 kDa protein	1.00E-142			3.17				
c237034_g1	GRPE1	GrpE protein homolog 1	2.00E-44	5.87		6.79				
c144731_g1	PPWD1	Peptidylprolyl isomerase domain and WD repeat-containing protein 1	0			7.14		6.24		

Transcript ID	Gene name	Description	min. Evalue	D2-13°C	D14-9°C	D14-11°C	D14-13°C	D29-9°C	D29-11°C	D29-13°C
Other functions										
c128565_g1	IMPA1	Inositol monophosphatase 1	1.00E-123			-2.01				-1.84
c138690_g1	IMPA3	Inositol monophosphatase 3	3.00E-47	4.94		6.94		5.96		
c143207_g1	IMPA1	Inositol monophosphatase 1	5.00E-143		2.32	2.96	2.32	2.90	3.10	2.94
c171140_g1	IMPA2	Inositol monophosphatase 2	2.00E-81	5.44		6.62				
c114902_g1	NDK7	Nucleoside diphosphate kinase 7	1.00E-110	5.49		6.92		6.21		
Protein degradation										
c131456_g1	GABT	4-aminobutyrate aminotransferase	5.00E-172	4.74		6.70		5.88		
c17068_g1	YME1	ATP-dependent zinc metalloprotease YME1 homolog	0	6.19		8.30		5.16		
c285460_g1	LONM	Lon protease homolog	0	6.29		8.21		5.73		
c143333_g1	PPCE	Prolyl endopeptidase	0	4.32		6.83		5.26		
c139221_g3	MASP1	Mannan-binding lectin serine protease 1	7.00E-131					-1.13		
c141329_g1	YM67	Putative serine protease K12H4.7	3.00E-97	6.38		7.62				
c157193_g1	MASP1	Mannan-binding lectin serine protease 1	2.00E-33						2.39	
Redox regulation										
c119300_g1	DDH1	2-hydroxyacid dehydrogenase homolog 1	3.00E-77	8.18		8.65		7.09		
c55314_g1	6PGD	6-phosphogluconate dehydrogenase, decarboxylating	0	7.49		8.50				
c131734_g1	ALDH2	Aldehyde dehydrogenase	0	8.28		8.66		6.36		
c146004_g1	AL7A1	Alpha-aminoadipic semialdehyde dehydrogenase	0	7.65		8.61				
c147930_g3	AL8A1	Aldehyde dehydrogenase family 8 member A1	8.00E-69	-1.75						-1.90
c147930_g5	AL8A1	Aldehyde dehydrogenase family 8 member A1	0	-1.88						
c160121_g1	A16A1	Aldehyde dehydrogenase family 16 member A1	5.00E-43	7.46		8.91		6.08		
c160121_g3	BETB	NAD/NADP-dependent betaine aldehyde dehydrogenase	3.00E-25	4.97		6.14				
c84031_g1	MMSA	Methylmalonate-semialdehyde dehydrogenase [acylating]	0	7.66		8.50				
c85116_g1	AL3A2	Fatty aldehyde dehydrogenase	2.00E-157	7.05		7.33				
c127863_g1	GPDA	Glycerol-3-phosphate dehydrogenase [NAD(+)]	1.00E-139	6.51		7.63				
c152592_g5	GPDA	Glycerol-3-phosphate dehydrogenase [NAD(+)]	5.00E-52			-0.99	-1.22			
c80177_g1	GPDM	Glycerol-3-phosphate dehydrogenase	0	6.22		7.43		5.87		
c142412_g1	IDH3B	Probable isocitrate dehydrogenase [NAD] subunit beta	2.00E-124	6.77		7.69		6.52		
c142481_g1	IDHP	Isocitrate dehydrogenase [NADP]	0	9.19		10.51		9.13		
c31815_g1	IDH3A	Probable isocitrate dehydrogenase [NAD] subunit alpha	0	7.10		8.40		7.00		

Transcript ID	Gene name	Description	min. Evalue	D2-13°C	D14-9°C	D14-11°C	D14-13°C	D29-9°C	D29-11°C	D29-13°C
c41378_g1	IDH3G	Isocitrate dehydrogenase [NAD] subunit gamma	1.00E-135	7.48		9.16		7.36		
c87013_g1	IDHC	Isocitrate dehydrogenase [NADP] cytoplasmic	3.00E-74	6.94		8.41		6.34		
c87013_g2	IDHC	Isocitrate dehydrogenase [NADP] cytoplasmic	5.00E-142	8.38		9.56		7.62		
c82288_g1	MSRA	Peptide methionine sulfoxide reductase MsrA	2.00E-67	5.97		6.18				
c101226_g1	PRDX6	Peroxiredoxin-6	1.00E-98	5.61		6.72				
c129981_g1	PRDX1	Peroxiredoxin 1	3.00E-105	7.52		7.77		5.67		
c290185_g1	PRDX4	Peroxiredoxin-4	2.00E-106	5.94		6.43				
c60400_g1	PRDX5	Peroxiredoxin-5	3.00E-51	8.03		8.25		6.07		
c142815_g1	PROD	Proline dehydrogenase 1	2.00E-146	7.00		7.06				
c100326_g1	NU1M	NADH-ubiquinone oxidoreductase chain 1	5.00E-52	11.08	10.43	13.11	9.69	11.44	9.37	9.49
c104850_g1	QOR	Quinone oxidoreductase	5.00E-118	5.24		6.71				
c126329_g1	NDUS1	NADH-ubiquinone oxidoreductase 75 kDa subunit	0	7.67		8.83		7.82		
c129954_g1	NU5M	NADH-ubiquinone oxidoreductase chain 5	1.00E-56	10.32	9.45	12.17	8.57	10.42	7.88	8.23
c136868_g1	ETFD	Electron transfer flavoprotein-ubiquinone oxidoreductase	0	6.62		8.52		7.18		
c154835_g7	SQRD	Sulfide:quinone oxidoreductase	0					0.91	1.11	
c133346_g1	SODC	Superoxide dismutase [Cu-Zn]	1.00E-31	7.59		9.54				
c23313_g1	SODM	Superoxide dismutase [Mn]	1.00E-100	6.70		8.13		5.83		
c236807_g1	SODM	Superoxide dismutase [Mn]	3.00E-81	8.80		9.41				
c238857_g1	SODC	Superoxide dismutase [Cu-Zn]	4.00E-30	7.51		9.09				
c106726_g1	TRX1	Thioredoxin-1	9.00E-36	7.33		8.32		6.36		
c108197_g1	THIOM	Thioredoxin	5.00E-39	5.80		7.60		5.84		
c109589_g1	TRX1	Thioredoxin-1	3.00E-28	8.36		7.07		5.49		
c124927_g1	TMX1	Thioredoxin-related transmembrane protein 1	6.00E-37	6.66		7.74		5.66		
c125785_g1	TXND9	Thioredoxin domain-containing protein 9	1.00E-65	5.83		7.87		6.71		
c133642_g1	PLP3B	Thioredoxin domain-containing protein PLP3B	2.00E-27			6.35		5.05		
c133860_g1	TXNL1	Thioredoxin-like protein 1	5.00E-87	5.25		6.76		4.44		
c286827_g1	TXND5	Thioredoxin domain-containing protein 5	3.00E-94	4.88		6.59				
c7693_g1	TMX2B	Thioredoxin-related transmembrane protein 2-B	1.00E-57	5.04		6.77		5.33		

3.7 Figures

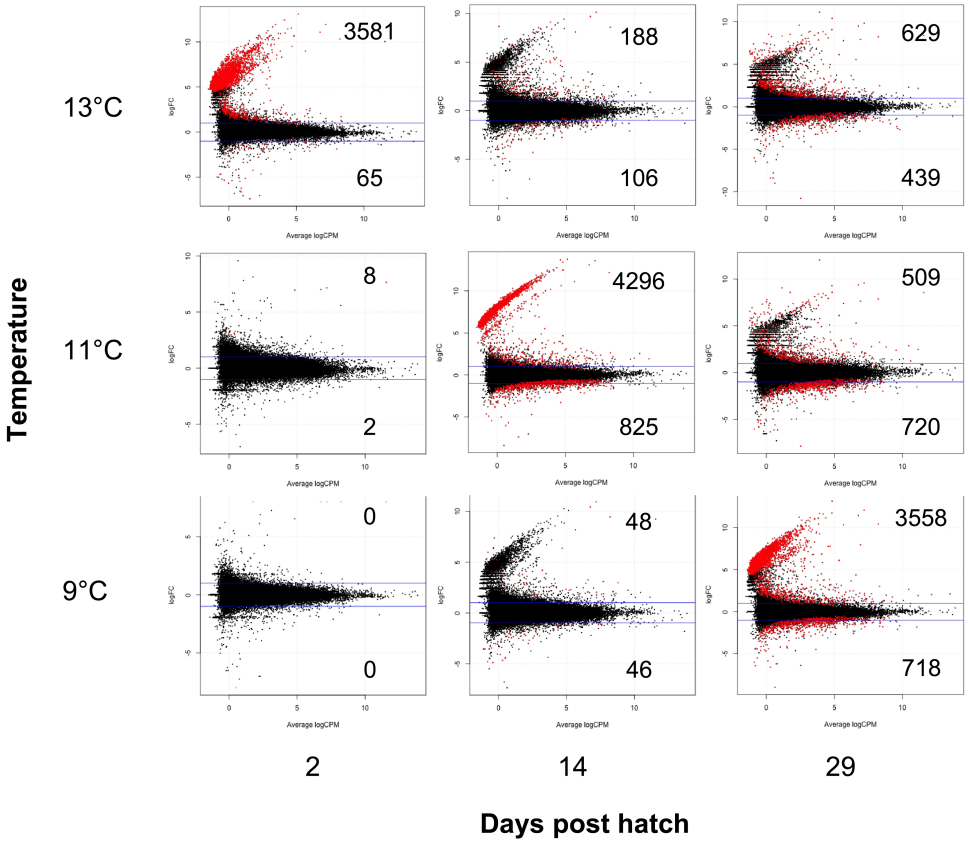

Figure 3.1: Differential gene expression of larval Atlantic cod (*Gadus morhua*) at ambient temperature, +2°C and +4°C. Log fold-change *vs.* average log counts-per-million of transcripts compared between each sample group (temperature X time) and the baseline sample (0 dph). The number of significantly up- and down-regulated transcripts are given in the upper and lower right-hand corners, respectively, and indicated in red (FDR<0.05). Blue lines represent positive and negative 2-fold differences in expression.

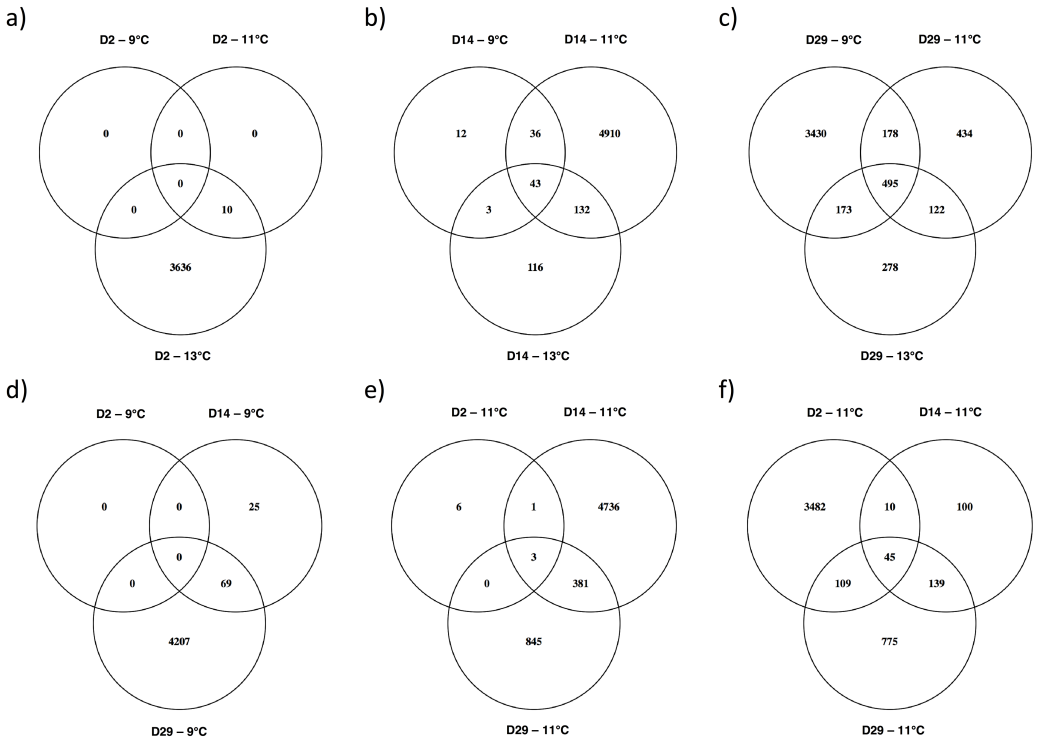

Figure 3.2: Overlap of differentially expressed genes. Venn diagrams depicting the overlap of differentially expressed (FDR<0.05) genes among temperature treatments at (a) 2 dph, (b) 14 dph, and (c) 29 dph, and among time points at (d) 9°C, (e) 11°C, and (f) 13°C.

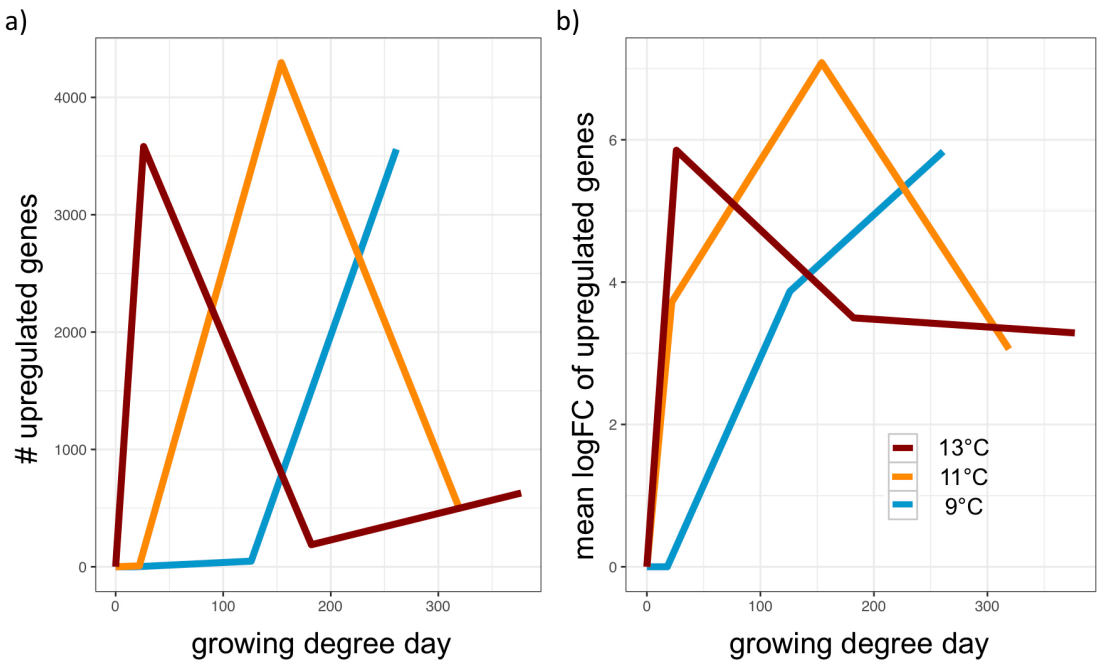

Figure 3.3: Gene upregulation by growing degree day. (a) Number of upregulated genes and (b) mean logFC of upregulated genes relative to the baseline sample (0 dph), plotted according to the growing degree day (i.e. 1 degree x 1 day) at which the sample was collected.

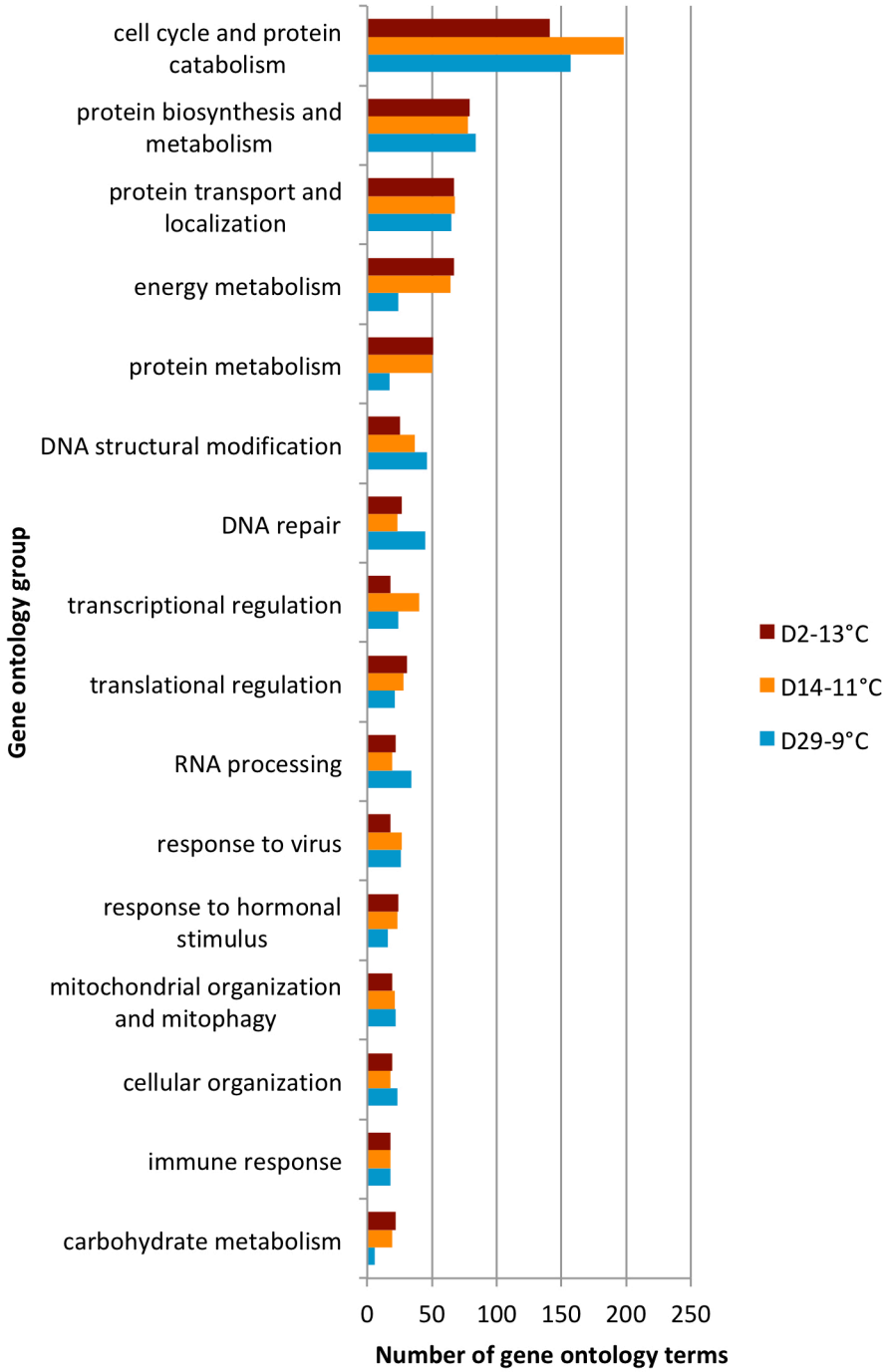

Figure 3.4: Biological processes represented by the gene ontology (GO) groups collectively containing the greatest number of enriched (FDR<0.05) GO terms based on ClueGO analysis of the Trinity transcripts upregulated (FDR<0.05) at D2-13°C, D14-11°C, and D29-9°C. The GO groups are manually defined across separate analyses for each sample based on a high degree of overlap among terms (see Figure S2).

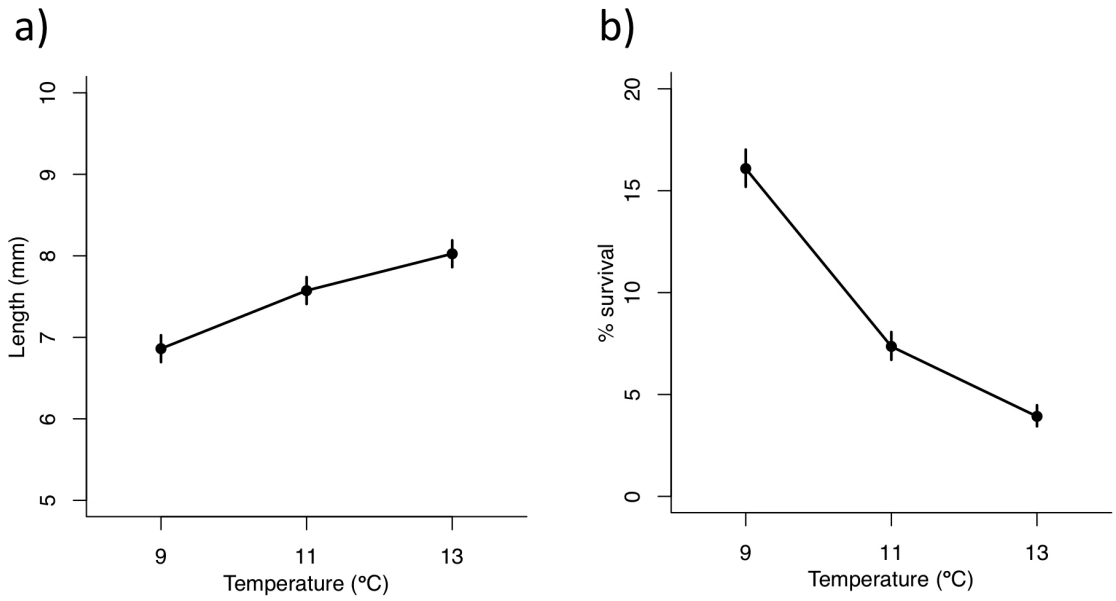

Figure 3.5: Thermal reaction norms for larval Skagerrak Atlantic cod. (a) Length and (b) survival at 29 days post hatch.

Chapter 4: Genetic Variation in Thermal Reactions Norms of Larval Atlantic Cod at a Microgeographic Scale

Supplementary materials for this chapter are located in Appendix C.

4.1 Abstract

Adaptation to local thermal regimes can result in genetically based variation in how populations respond to temperature. Although differential thermal responses influence fitness, thus driving population dynamics and species distributions, the spatial scales at which adaptation occurs are poorly understood, particularly for marine species. Here, a common-garden rearing experiment of Atlantic cod (*Gadus morhua*) larvae at 6°C, 9.5°C, and 13°C reveals cryptic genetic variation in thermal responses of growth and survival at a microgeographic scale within a single fjord system <20 km^2. Among six genetic crosses, characterized by maternal and paternal pre-spawning location (inner or outer part of the fjord) and ecotype (fjord or North Sea, as determined by a set of genomic markers), little or no plasticity was observed for the lower temperatures (6°C and 9.5°C) that are more typical of their native environments. However, substantial divergence in growth plasticity at higher temperatures resulted in 2/3 hybrid crosses between fjord and North Sea ecotypes exhibiting substantial (potentially maladaptive) plasticity that resulted in up to 1.2 mm (21%) smaller sizes at the highest temperature. All crosses experienced severe (75-93%) reductions in survival from 9.5°C to 13°C. Yet, significant variation in survival plasticity suggests a genetically variable basis for the severity with which survival declines with temperature and, consequently, the potential for an adaptive response to warming. However, a lack of clear and consistent differences between locations and ecotypes suggests that they are not primary determinants of thermal plasticity in coastal cod. Rather, these findings suggest the presence of intraspecific genetic variation not accounted for in the present study. Nonetheless, the spatial scale at which we detected potentially adaptive variation in thermal responses

(<20 km) is the smallest recorded for a marine species with high dispersal capabilities. Fine-scale, genetically based differences in larval growth and survival at warm yet ecologically relevant temperatures must be considered in an effective management strategy for coastal cod, especially in the context of global climate warming.

4.2 Introduction

In the face of environmental change, the persistence of a species depends on the extent to which individuals and populations differ in their responses and the spatial correspondence between the scale of adaptation in these responses and the scale of the disturbance (Hutchings *et al.* 2007). Phenotypic plasticity is a primary mechanism by which populations might respond to environmental change by serving as a buffer against environmental variability (Canale & Henry 2010) and facilitating evolutionary adaptation to new environments (Lande 2009; Chevin *et al.* 2010). Species can also respond to environmental change through adaptation if sufficient heritable phenotypic variation exists for selection to act on (Franks & Hoffman 2012), or some combination of these mechanisms may occur (Aitken *et al.* 2008). Genetic variation in reaction norms (the range of phenotypes expressed by a genotype along an environmental gradient; Woltereck 1909; Schmalhausen 1949) is evidence that plasticity itself can evolve in response to local environmental regimes (e.g. Conover & Present 1990; McCairns & Bernatchez 2010; Baumann & Conover 2011). Therefore, population variation in plasticity represents differences in the responses of populations to directional environmental change, such as the forecasted increase in temperature due to global climate change, and the adaptive potential of the species as a whole. Understanding the mechanisms responsible for shaping population variation in environmental responses, and the spatial scales at which adaptive differences in plasticity occur, are critical for predicting the persistence of a species in the face of environmental change and managing populations effectively to mitigate the potential for population collapse and biodiversity loss.

The marine environment was traditionally assumed to be genetically homogenous, due to the high potential for dispersal (Levin 2006) and limited apparent physical barriers to gene flow (Hilbish 1996). There is now widespread evidence of local adaptation associated with broad-scale spatial variation in selection pressures, even in species with high connectivity (e.g., Limborg *et al.* 2012, Pespeni & Palumbi 2013, but see Pujolar *et al.* 2014). In marine fishes, divergence in plasticity has been quantified at relatively broad

spatial scales across open waters (reviewed by Hutchings 2011; Oomen & Hutchings 2015a). The smallest scale at which genetic variation in an adaptive trait (i.e., clearly fitness-linked, in this case survival plasticity) has been found across open waters in a marine fish is ~200 km, in Atlantic cod off the coast of Nova Scotia, Canada (Oomen & Hutchings 2015b). Although this variation was attributed to temporally variable selection on different spawning components, spatial variability in selection pressures could also drive local adaptation at small scales in the marine environment. For example, highly localized hydrography and the influence of environmental variation on nearby land can generate fine-scale environmental heterogeneity in coastal waters (Albretsen *et al.* 2012; Knutsen *et al.* 2018). Unlike broad-scale population differentiation, it is not well understood whether the migration-selection balance (Felsenstein 1976) can skew in favour of local adaptation under the high gene flow potential of shorter distances.

Norway has a heterogeneous coast with fjords, inlets, islets, skerries and variable depths. As a result, water temperatures, ocean current patterns, salinities and several other biotic and abiotic factors are spatially structured on a fine scale (Johannessen & Dahl 1996). This environment provides opportunities for species to adapt to local conditions at smaller spatial scales than the open ocean, although examples are rare. Imsland et al. (2001) found genetically-based differences in juvenile growth rates between fjord and off-shore turbot (*Scophthalmus maximus*) at a small spatial scale on the Southwest coast of Norway. Atlantic cod (*Gadus morhua*) exhibit genetic variation in maturation reaction norms among neighbouring fjords, where the scale of variation is comparable to that of population connectivity inferred from neutral genetic markers (Olsen *et al.* 2008). Thus, coastal Norway presents an ideal system for testing for small-scale variation in plasticity of adaptive traits in marine fishes.

The fjord system around Risør in the southern part of Norway covers an area of 20 km^2 and is shaped like a 'U' (Figure 4.1). The outer part of the fjord (Østerfjorden, hereby referred to as 'outer Risør') is dominated by skerries and exposed to the Skagerrak and the North Sea. The inner part of the fjord (Sørfjorden, hereby referred to as 'inner Risør') is a more sheltered area, characterized by numerous sills with depths ranging from 20 to

40 m (Bergstad *et al.* 1996; Knutsen *et al.* 2007, 2011). Neutral microsatellite markers have previously revealed a low but significant and temporally stable level of genetic differentiation between juvenile Atlantic cod from inner and outer Risør (Knutsen *et al.* 2011). It was later discovered, using a much larger set of markers, that this fine-scale spatial divergence is, at least in part, a reflection of the coexistence of two genetically distinct ecotypes of cod that vary in proportion inside and outside the fjord (Jorde *et al.* 2018; Knutsen *et al.* 2018; Barth *et al.* 2019; Sodeland *et al.* in review). The 'fjord' ecotype is more common inside than outside the fjord, is associated with lower juvenile growth rates (Knutsen *et al.* 2018), and is more likely to be targeted by the local recreational hook-and-line fishery (Jorde *et al.* 2018). The 'North Sea' ecotype is genetically indistinguishable from the offshore North Sea cod stock. It is not yet known whether the North Sea ecotype disperses through ocean currents as pelagic eggs and larvae from the North Sea to the coastal Skagerrak area, were spawned in coastal Skagerrak, or both (André *et al.* 2016). The North Sea ecotype has a higher juvenile growth rate (Knutsen *et al.* 2018) and is more likely to be caught by commercial trawlers compared to the fjord ecotype (Jorde *et al.* 2018). How these divergent ecotypes persist in sympatry is unknown. The fjord ecotype might be locally adapted to the sheltered inner fjord environment and, if the North Sea ecotype spawns in coastal Skagerrak, variation in spawning behaviours could contribute to reproductive isolation. To what extent there might be subtle genetic divergence between cod from inner and outer Risør within ecotypes is unknown.

Here, we conduct a common garden experiment to quantify genetic variation in thermal plasticity for larval cod growth and survival in the Risør fjord. The larval stage represents a critical period for survival and development that is especially sensitive to temperature (Pörtner *et al.* 2008) and for which thermotolerance often most accurately reflects the species climatic boundaries for colonization (Abele 2012). We disentangle the effects of fine-scale environmental heterogeneity between the inner and outer fjord areas (termed 'location') and genetic divergence between fjord and North Sea ecotypes using a set of genomic markers to better understand the genetic basis of variable thermal responses in cod and the minimum spatial scale at which such variation exists. Delineating spatial

scales sufficient for promoting/constraining local adaptation is of critical importance for conservation, as management policies are currently implemented geographically (ICES 2018). Therefore, we discuss potential implications of genetic variation in thermal plasticity for the conservation and management of coastal cod in Norway.

4.3 Methods

4.3.1 Temperature Data Collection

From February to May 2014, we had temperature loggers deposited in the fjord. Originally there were a total of 12 loggers distributed at three depths (5, 10 and 15 m) in four locations; two each in inner and outer Risør (Figure 4.1). Temperature data were successfully recovered from two depths at one location inside the fjord and from three depths at one location outside the fjord. In February, at the time when spawning initiated in the lab, the mean temperature at 5 metres was 2.95°C (SD±1.21) inside the fjord and 2.78°C (SD±0.84) outside the fjord. Throughout the spawning season, temperatures rose from 2°C to above 8°C at both locations. However, temperatures outside the fjord were more stable and exhibited a smoother increase than temperatures inside the fjord (Figure 4.1b, Table 4.1).

4.3.2 Broodstock

A common-garden experiment was conducted in spring 2014 with cod from the Risør area. Cod were caught, using non-baited fyke nets (mesh size: 20 mm), from late November 2013 to early January 2014. Individuals larger than 65 cm and smaller than 40 cm were not included in the experiment to ensure that the fish were mature and enhance mating prospects through similar size distributions (Rowe *et al.* 2007). This left a total of 73 potentially mature cod for the experiment: 21 females and 16 males from inner Risør and 24 females and 12 males from the outer Risør (Figure 4.1). Sampling of these adult cod is also described in a related study by Kuparinen et al. (2015). Cod were individually marked upon capture, using T-bar anchor tags (Hallprint Pty. Ltd., South Australia) and a

standard tag applicator. Immediately after capture the cod were transported to the research facility of the *Institute of Marine Research, Flødevigen*, approximately 60 km from Risør. Adults were held together in a 45 m^3 spawning basin and allowed to spawn undisturbed. Daily observations of egg production (from a collection box located at the surface outflow of the basin) showed that the fish started spawning in February and continued spawning until mid-April. The spawning basin and the surrounding environment reflected ambient temperature and photoperiod.

4.3.3 Experimental Design

Eggs for the experiment were collected at the peak of spawning (i.e., day 45 out of a 94-day spawning season, on which day the greatest number of eggs were observed; Figure S1). A mesh collector situated at the surface outflow of the spawning basin was used to collect the fertilized eggs. The eggs were held in a 900 L flow-through seawater incubation tank at 6°C until hatch, when they were randomly sampled and transferred to 40 L flow-through seawater experimental tanks. There were 12 tanks in total, each containing 2000 larvae. The larvae were reared at three temperatures with four replicate tanks per temperature. The target temperatures were 6°C, 9.5°C and 13°C, representing: 1) the average temperature outside the research facility in March/April (i.e., during and immediately after peak spawning), 2) a 3.5°C increase consistent with the projected increase of 2-4°C by the year 2100 (IPCC 2013) or the average temperature outside the research facility in April/May (i.e., ecologically relevant temperatures for offspring of late spawners), and 3) a 7°C increase consistent with the projected increase of 2-4°C by the year 2100 (IPCC 2013) to the average temperature outside the research facility in April/May (i.e., projected temperatures for offspring of late spawners)(Table 4.1). Temperatures were measured daily, with average (±SD) temperatures of, 6.3 ± 0.2°C, 9.7 ± 0.2°C, and 13.3 ± 0.3°C in the low, intermediate and high temperature tanks, respectively. Water quality parameters (oxygen, pH, and ammonia concentration) were monitored with no notable deviations. The larvae were fed rotifers (*Brachionus plicatilis*) in excess (4500 prey/L three times daily) (Hutchings et al., 2007). The experiment was

terminated at 28 days post hatch (dph), at which time the remaining larvae were counted prior to sampling.

4.3.4 Sample Collection

Forty larvae were sampled randomly from each experimental tank at 2, 14, 21, and 28 dph, as well as forty larvae from the incubation tank at 0 dph (n=1960). Samples collected at 0 and 2 dph were used to assess initial lengths. The growth analysis in this study uses length at 28 dph as a proxy for growth, following Hutchings et al. (2007). To avoid sampling bias due to potential differences in behaviour, a plastic rod was used to redistribute the larvae in the tank by gently mixing the water prior to sampling. All sampled larvae were put on a glass slide containing RNAlater (Ambion), immediately photographed using a stereoscope and a Leica DFC 425 C camera, and then submerged in a 1.5 ml microtube containing 250 µl RNAlater. The photographs were used to measure standard larval length (from the tip of the longest jaw to the end of the notochord; Kahn *et al.* 2004), using the software ImageJ (Abràmoff *et al.* 2004). A 1 mm scale bar photographed at the same time as the larvae was used for calibration. Four larvae were excluded due to missing or poor quality photographs. Some larvae were photographed in curved positions, therefore larval curvature was defined as 0=not curved, 1=slightly curved, and 2=very curved. A subset of larvae (three tanks with a total of 120 larvae) was measured twice and the correlation coefficient was used to infer that measurement error was extremely low (slope = 1.0054, $R^2 = 0.99$).

4.3.5 DNA Isolation

Of the 1960 larvae sampled, 1524 were selected for genotyping. DNA was individually extracted from whole larvae using the E-Z 96 DNA/RNA Isolation Kit (Omega Bio-Tek, USA) and from parental fin clips using E.Z.N.A. Tissue DNA Kit according to the manufacturer's protocol for tissue samples with elution buffer preheating. One well on every plate was used as a negative control, to be able to exclude possible errors due to contamination and wrong plate orientation.

4.3.6 Microsatellite Genotyping

Polymerase chain reaction (PCR) amplification was performed in two multiplexes containing four loci each (Table S1). The multiplexes were modified from Delghandi et.al. (2003) (Multiplex 1) and Dahle et al. (2006) and Glover et al. (2010) (Multiplex 2) and were previously used for parental assignment of offspring from the same broodstock used in the present study (Roney *et al.* 2018a).

The first multiplex consisted of 1.50 mM buffer, 0.30 mM dNTP, 0.80 U QiagenTaq pol, 0.12 µM GMO19, 0.32 µM TCH11, 0.04 µM GMO8, 0.20 µM GMO35 (all primers one forward and one reverse) and distilled H2O. The second multiplex consisted of 1.50 mM buffer, 0.3 mM dNTP, 0.80 U QiagenTaq pol, 0.12 µM GMO34, 0.23 µM GMO132, 0.18 µM GMO2, 0.35 µM TCH13 (forward and reverse) and distilled H2O. The total volume of each PCR was 10 µl, of which 1 µl was DNA extract of unknown concentration.

The PCR cycling conditions for both multiplexes consisted of an initial 5 min denaturation at 95°C followed by 30 cycles of denaturation (30 s at 90°), annealing (90 s at 56°C), and extension (60 s at 72°C). A final step of 10 min extension completed the amplification. PCR products were held at 4°C before being visualized using an ABI PRISM 3130xl Genetic Analyzer (Applied Biosystems). Genotypes were scored using Genemapper software v.4.0 (Life Technologies). To ensure accuracy of parental genotypes, all adults were amplified three times (for details see Roney *et al.* 2017), as were individuals with 3 or more missing loci or ambiguous genotypes. Individuals were independently genotyped by two (larvae) or three (adults) researchers. In Genemapper, default analysis settings were applied (minimum peak height 50 and size standard GS500LIZ). All 73 adults and 1519/1524 larvae were successfully genotyped at 5 or more microsatellite loci.

4.3.7 Parentage Analyses

Heterozygosities at each locus (H_o=observed heterozygosity within samples, H_e=expected heterozygosity total loci (Nei & Chesser 1983)) were estimated for the adults, using Genetic Data Analysis software (Lewis & Zaykin 2001) (Table S1). F_{IS}-values were estimated for the adults in GENEPOP v.4.2 (Rousset 2008). Tests for deviations from Hardy-Weinberg equilibrium (Weir & Cockerham 1984), conducted using the exact probability test with false discovery rate (FDR; α=0.05) correction for multiple testing (Benjamini & Hochberg 1995), showed no deviations (Table S2). These statistics were performed on adult genotypes only, as they are more representative of the wild populations given that reproductive success in cod is skewed (e.g., Rowe *et al.* 2008; Roney *et al.* 2017). CERVUS v3.0 (Kalinowski *et al.* 2007) was used to assign parents to offspring, using allele frequencies based on the adults. To estimate genotyping error, 78 larvae were amplified twice, genotyped and the genotypes were compared. This gave an error rate of 0.006536 (Juliussen 2016). For a subset of individuals from 2 and 28 dph, assignment was run with both the estimated error rate and a global error rate of 0.01 and the resulting assignments were identical (Juliussen 2016). Therefore, a global error rate of 0.01 was used to analyze the complete data set. The proportion of loci typed was 0.9943, and the minimum number of typed loci was four. For all other parameters, default settings were used. Parental assignments were made based on two criteria: 1) a confidence level of >95%, estimated from a simulated analysis of 10,000 offspring, and 2) a maximum of 1 mismatched locus per trio or two mismatched loci if both were only one repeat away from a putative parent allele (n=14). The second criterion was implemented because CERVUS forces an assignment if all parent genotypes are known. Parental assignment identified 10 mothers and 14 fathers (Table 4.2).

4.3.8 Parental Origin Assignments

To discriminate the parental origin – i.e. assigned to either fjord or North Sea ecotype – all adults were genotyped with a Sequenom MassARRAY multiplex of 40 single nucleotide polymorphisms (SNPs) specially developed to distinguish between these ecotypes (Jorde *et al.* 2018; Knutsen *et al.* 2018). The SNP panel was developed based on

reference samples from 1) mature adult cod in the North Sea (n=91), and 2) juvenile (0+) cod from the innermost areas of three Skagerrak fjords, including Risør (n=143) (for details see Jorde *et al.* 2018). Briefly, 9,187 SNPs from a 12k SNP array were scored in the reference samples as well as in cod caught by commercial trawls outside of the aforementioned Skagerrak fjords (n=118) (Sodeland *et al.* 2016; Jorde *et al.* 2018). SNPs were ranked by Nei's (1973) *G*ST between fjord and North Sea samples and filtered to exclude SNPs that were highly linked. A composite linkage disequilibrium (CLD; Gao *et al.* 2008) >0.5 to a higher ranked SNP resulted in exclusion. After filtering, 40 high-*G*ST-ranked SNPs were selected for genotyping in the multiplex. In our study and that of Knutsen et al. (2018), 26 of these SNPs were scored successfully. Assignments of the adult cod in our experiment to the two reference samples were performed with Geneclass II v.2.0 (Piry *et al.* 2004).

Individuals with fewer than 20 scored SNPs (n=2) were excluded from further consideration. Assignments with a score <80% (n=3) were considered to be ambiguous and the remaining assignments scored >90%. The offspring of fertilizations between one individual with ambiguous assignment (RIC5100) and unambiguously fjord type cod was later found to cluster with fjord x North Sea hybrid offspring based on a genome-wide SNP analysis (Figure S2; see Chapter 5 for details). Therefore, RIC5100 was classified as North Sea type. The remaining individuals with ambiguous assignment did not produce offspring. In sum, ecotype assignments were obtained for 69 of 73 adults present in the spawning basin, including all of those identified as parents in the present study (Table 4.2).

4.3.9 Genetic Cross Assignments

Larvae were classified into genetic crosses, depending on whether their mother and father were collected from Inner Risør (I) or Outer Risør (O) and of Fjord (F) or North Sea (N) ecotype. Of 16 possible crosses, 8 were detected in our experiment and 6 had sufficient sampling across treatments (n≥88) while 3 had insufficient sample sizes (n≤5) (Table S3). Thus, 1508 larvae were retained for further growth analysis, assigned to (mother×father)

IF×IF, IF×OF, OF×IF, IF×ON, ON×IF, and OF×ON. The same six crosses were included in the survival analysis.

4.3.10 Growth Reaction Norms

All statistical analysis on growth and survival reaction norms were conducted in R v.3.2.3 (R Development Core team 2015). A linear mixed effects model was used to test for differences in length between crosses at the beginning of the experiment (0 and 2 dph combined), with cross as a fixed effect, larval curvature as a covariate, and mother and father as random effects [1].

[1] length = cross + curvature + mother + father

Differences in thermal growth reaction norms between crosses were tested using a mixed effects linear model on length at 28 dph, with cross, temperature, and their interaction as fixed effects, larval curvature as a covariate, tank as a random effect nested within temperature, and mother and father as random effects [2].

[2] length = cross + temperature + cross×temperature + curvature + tank(temperature) + mother + father

A significant cross×temperature interaction indicates a significant difference in the slopes of the reaction norms, and suggests that there are genetic differences in thermal responses between populations. Post-hoc contrasts were used to identify the differences in slopes and test for temperature effects (i.e., plasticity) within populations. P-values were considered significant at α=0.05 and marginally significant at α=0.1.

Length at 28 dph followed a normal distribution (Figure S3) and variances were fairly homogenous among treatments, as assessed by visual inspection of the model residuals (Figure S4, S5).

4.3.11 Survival Reaction Norms

Cross-specific survival was quantified for each tank at 28 dph. First, proportional survival was calculated as the number of larvae assigned to each cross out of the number of larvae sampled. Survival was then estimated as the proportional survival multiplied by the total number of larvae counted at the end of the experiment. We did not correct for sampling mortality ($[n_{2dph}+n_{14dph}+n_{21\ dph}]$/initial n = [40+40+40]/2000 = 6%). We increased survival for all crosses by 1 larva to eliminate zeroes in the data set (n=2/54).

We tested for differences in survival reaction norms between crosses using a generalized linear model with a quasi-poisson distribution (dispersion parameter = 12.1 >1) and identity link. Cross, temperature, and their interaction were included as fixed effects [3].

[3] survival = cross + temperature + cross×temperature

Deviances were evaluated with Chi square tests and the forward stepwise method. Post-hoc contrasts were used to identify the differences. P-values were considered significant at α=0.05 and marginally significant at α =0.1.

The model residuals were normally distributed, as assessed by visual inspection (Figure S6). The variance was slightly lower at 13°C but all variances were evenly distributed around zero (Figure S7, S8).

4.4 Results

4.4.1 Genetic Assignments

Consistent with a long-term survey of juvenile cod ecotype composition in the Risør fjord system (Knutsen et al. 2018), adult cod collected from Inner Risør were dominated by the fjord genotype (91.2%) and Outer Risør cod were dominated by the North Sea genotype

(80.0%). Of those identified as parents in our study, the North Sea genotype was only present in Outer Risør individuals.

4.4.2 Growth Reaction Norms

There was no effect of cross on initial length ($F_{6,382}$=1.13, P=0.35; Table 4.3a). Mother and father explained 1% and <0.1% of the variance in initial length, respectively. However, there was a significant cross×temperature interaction for length at 28 dph ($F_{21,333}$=3.41, P<0.0001), indicative of variation in thermal plasticity for growth between crosses (Figure 4.2, Table 4.3b). The pure fjord crosses displayed little or no thermal plasticity in growth across a range of 7°C (Table 4.4), although OF×IF had a marginal increase in growth from 9.5°C to 13°C (t=1.54, P=0.066) and a significantly more positive growth reaction norm slope than IF×IF (P=0.007). In contrast, 2 of the 3 hybrid ecotype crosses experienced a significant decrease in growth from 9.5°C to 13°C (12.34% and 11.89% for IF×ON and OF×ON, respectively; Table 4.4). One of these hybrid crosses (IF×ON) achieved maximum length at the intermediate temperature. All other crosses showed little or no plasticity or variation in plasticity across the lower temperature range that encompasses typical temperatures experienced during the spawning season (Table 4.5). In contrast, growth reaction norms across the upper temperature range were highly divergent, displaying at least three qualitatively different responses to the warmest temperature (slight increase, no difference, large decrease; Table 4.5). Notably, there was no variation in length at the lowest temperature and up to a 1.2 mm (21%) length difference at the highest temperature (from 5.8±0.4 [mean±SD] mm in OF×ON to 7.0±0.3 mm in ON×IF). Mother and father explained 5% and 3% of the variance in growth, respectively (Table 4.3b).

Specific contrasts enabled explicit tests of independent effects of maternal and paternal location and ecotype. Maternal location had significant effects on the lower (IF×ON vs. OF×ON; P=0.029) and upper (IF×IF vs. OF×IF; P=0.007) thermal reaction norms. Maternal ecotype (ON×IF vs. OF×IF) and paternal location (IF×IF vs. IF×OF) had no significant effects (Table 4.5). Paternal ecotype (IF×OF vs. IF×ON) had a significant

effect on the lower thermal reaction norm (P=0.049). When comparing maternal and paternal location crosses of pure fjord cod (IF×OF vs. OF×IF), there was no significant effect on thermal plasticity (P=0.402 and P=0.149 for the lower and upper thermal ranges, respectively). However, maternal and paternal crosses of location and ecotype hybrids (ON×IF vs. IF×ON) differed in plasticity across both the lower (marginally; P=0.082) and upper (P=0.006) thermal ranges.

4.4.3 Survival Reaction Norms

There was a significant cross×temperature interaction for survival (P<0.0001), indicative of variation in thermal plasticity between crosses (Figure 4.3, Table 4.6). A lack of significant plasticity across the lower temperature range was evident in all but one cross (Table 4.7). The exception was IF×ON, which showed an increase in survival from 6°C to 9.5°C (t=2.45, P=0.019). This response was significantly different from IF×OF (P=0.011) and marginally different from OF×ON (P=0.093) (Table 4.8). All crosses showed a decrease in survival at the highest temperature, with reductions of 75-93% from 9.5°C to 13°C (Figure 4.3, Table 4.7). There were significant differences in the magnitudes of these reductions. In absolute terms, IF×IF and OF×IF exhibited a steeper decline than IF×OF, ON×IF, and OF×ON, whereas IF×ON exhibited an intermediate response (Table 4.8). In relative terms, the smallest reduction in survival was observed in OF×IF and ON×IF (both 75%), the latter of which only showed marginally significant plasticity (t=1.98, P=0.056; Table 4.7).

Maternal location alone had relatively little effect on plasticity (IF×IF vs. OF×IF and IF×ON vs. OF×ON, Table 4.8). Maternal ecotype (ON×IF vs. OF×IF) and paternal location (IF×IF vs. IF×OF) had significant effects of plasticity in the upper thermal range only (P=0.002 and P<0.001, respectively; Table 4.8). Paternal ecotype (IF×OF vs. IF×ON) affected plasticity in both the lower (P=0.011) and upper (P=0.024) thermal ranges. When comparing maternal and paternal location crosses of pure fjord cod (IF×OF vs. OF×IF), there were significant differences in thermal plasticity (P=0.044 and P=0.002 for the lower and upper thermal ranges, respectively). Maternal and paternal crosses of

location and ecotype hybrids (ON×IF vs. IF×ON) differed in plasticity only in the upper thermal range (P=0.022).

4.5 Discussion

4.5.1 Growth and Survival Plasticity

Here, we show that thermal plasticity for larval growth and survival varies genetically within a single fjord system and that this divergence in thermal responses is greater at warmer temperatures. Most crosses between parental pre-spawning locations (inner and outer Risør) and ecotypes (fjord and North Sea) exhibited little or no plasticity at the lower temperatures they are most likely to encounter in their native environment. However, divergence in growth plasticity across the upper thermal range resulted in two out of three hybrid ecotype crosses experiencing a significant reduction in growth from 9.5°C to 13°C. Such plasticity might be maladaptive, as slower growth can extend the duration of the vulnerable larval phase (Anderson 1988). Conversely, slower growth can confer energy savings, which could be beneficial under stressful conditions (Conover & Present 1990; Billerbeck *et al.* 2001).

We previously showed that temperatures of 9°C to 13°C elicit a stress response in cod larvae originating from nearby Flødevigen, Norway when reared under similar conditions (Chapter 2), supporting the possibility that these temperatures could be stressful for Risør cod larvae. In the present study, the two hybrid ecotype crosses that were plastic for growth experienced severe declines in survival across the same temperatures, suggesting that any potential energy savings from slow growth had a minimal impact on fitness. The reduced growth plasticity in the pure Fjord ecotype, even at higher temperatures, might represent phenotypic buffering of this trait against the greater thermal variability that characterizes the inner fjord environment for most of the spawning season (Figure 4.1; Table 4.1). However, there is no evidence that such buffering improved survival and therefore might be adaptive (Reusch 2014). Conversely, the Fjord ecotype cross with the

smallest reduction in survival at warm temperatures also experienced marginally higher growth at 13°C (OF×IF; Table 4.4, Table 4.7).

Regardless of growth plasticity, all crosses experienced a large (75-93%) reduction in survival from 9.5°C to 13°C, indicative of lower fitness at 13°C. While lower temperatures currently characterize the bulk of the spawning and subsequent larval seasons (Table 4.1), temperatures can increase rapidly in late spring, with high year-to-year variability (Chapter 3 Figure S12). In May 2014, shortly after termination of the present study, temperatures in the Risør fjord area were an average of 10-12°C with maximums of 12-16°C at 5 m and 10 m depths (Table 4.1). Therefore, it is probable for the offspring of late (i.e., late April-May) spawners to encounter warm enough temperatures to experience severe reductions in survival. Further, an increase in sea temperature of 2-4°C, as is projected to occur before the year 2100 (IPCC 2013), would increase exposure of the offspring of peak-season (i.e. March-early April) spawners to such warm temperatures. The decreased larval fitness associated with warmer temperatures documented in the present study might be predicted to reduce population productivity and connectivity of Skagerrak coastal cod.

High larval mortality is common in the wild (Sundby *et al.* 1989; Houde & Zastrow 1993) and in the laboratory (Gamble & Houde 1984; Otterlei *et al.* 1999; Steinarsson & Björnsson 1999; Oomen & Hutchings 2015b, 2016). If size-selective mortality was responsible for the variation in growth plasticity observed, we would expect to see a consistent correlation between changes in length and survival. The two crosses with the smallest reduction in survival from 9.5°C to 13°C (OF×IF and ON×IF) had more positive growth slopes than some crosses that experienced higher mortality (IF×IF, IF×ON, and OF×ON, although IF×IF *vs.* ON×IF was marginally significant), but not all (IF×OF) (Table 4.5). If it were not for the exception, this pattern would have supported higher mortality of larger individuals at higher temperatures. However, IF×ON experienced a significantly negative difference in growth and marginally positive difference in survival relative to IF×IF across the same thermal interval (Table 4.5, Table 4.8). Therefore, while variation in growth is not fully explained by variation in survival in our experiment, the

hypothesis of temperature-dependent size-selective mortality warrants further investigation.

4.5.2 Evolutionary Potential

Greater divergence in reaction norms at the highest temperature is consistent with the hypothesis that extreme environments reveal cryptic genetic variation (Ghalambor *et al.* 2007; Murren *et al.* 2014). Importantly, significant genetic variation in survival plasticity suggests that some larvae are more vulnerable to mortality at higher temperatures than others and that this trait has a genetic basis. Therefore, standing genetic variation exists for selection to act upon to produce an adaptive response to ocean warming, provided that evolutionary change can keep pace with the environment to avoid extinction (Maynard Smith 1989; Merilä & Hendry 2014).

The severe and ubiquitous increase in mortality we observed at 13 °C is likely to increase the probability of extinction under ocean warming. The probability of persistence will depend on the abundance of well-suited genotypes (Orr & Unckless 2008) and the potential for gene flow of beneficial alleles into local coastal areas that could effect a 'genetic rescue' (Tallmon *et al.* 2004). Norwegian Coastal Cod (NCC) is at historically low levels (ICES 2018), reducing the copy number of potentially beneficial alleles. Spawning site fidelity (Espeland *et al.* 2007), natal homing (Svedäng *et al.* 2007; André *et al.* 2016), limited migratory behaviour (Espeland *et al.* 2008; Rogers *et al.* 2014; Villegas-Ríos *et al.* 2017, 2018), and the retention of pelagic larval stages inside fjords (Ciannelli *et al.* 2010) reduce gene flow among coastal areas. While there is a large influx of larvae from the North Sea to coastal Skagerrak (Knutsen *et al.* 2004; Stenseth *et al.* 2006), the maintenance of divergent Fjord and North Sea ecotypes suggests low levels of gene flow between them and reduced fitness of the North Sea ecotype in the inner fjord environment (Knutsen *et al.* 2018), although the extent of these forces is unclear. Further, Skagerrak coastal cod are already near the upper thermal limit of the species distribution (Björnsson & Steinarsson 2002; Righton *et al.* 2010). Therefore, it is unlikely that nearby populations will harbour unique, locally adapted alleles conferring tolerance to higher

temperatures. Conversely, the flow of alleles that are poorly suited to the local coastal environments could lead to outbreeding depression (Tallmon *et al.* 2004). Under these conditions, it will be important for local populations to possess sufficient abundances of adaptive alleles in order to adapt to rising water temperatures, through a greater abundance of individuals and conservation of genetic diversity.

4.5.3 Genetic Basis of Variation in Thermal Plasticity

Surprisingly, we find no clear and consistent differences in larval size-at-hatch, growth, growth plasticity or survival plasticity between locations or ecotypes. This suggests that adaptation to fine-scale environmental heterogeneity between inner and outer fjord areas and overall genetic background are not primary determinants of thermal plasticity in coastal cod. Our ability to detect consistent differences between ecotypes might have been limited by a lack of pure North Sea crosses. It is reasonable to conclude that their inclusion might have increased reaction norm variability in our experiment. Representation from a greater number of families in some crosses at 28 dph (mean±SE = 4±1, range = 1-11) might also improve our ability to detect consistent differences in growth plasticity between locations and ecotypes, while likely further increasing overall reaction norm variability. Nonetheless, the observed variation of thermal plasticity in common environments suggests the presence of intraspecific genetic differences not accounted for in the present study.

One alternative hypothesis is that chromosomal inversions (Sodeland *et al.* 2016; Berg *et al.* 2017) are responsible for the variation in thermal plasticity we observed. Chromosomal inversions enable co-inheritance of a set of physically linked genes due to recombination suppression between inverted alleles (Sturtevant 1921; Cooper 1945; Kirkpatrick 2010). Empirical and simulation studies suggest that such linked gene complexes are favoured in systems with adaptation and high gene flow (reviewed by Tigano & Friesen 2016). The inversions in cod have been linked to different migratory ecotypes (LG1; Berg *et al.* 2016; Kirubakaran *et al.* 2016) and salinity adaptation (LG2; Barth *et al.* 2017) at small spatial scales, temperature at broad spatial scales (e.g., LG12;

Bradbury *et al.* 2010; Berg *et al.* 2015) and inner and outer fjord environments (Sodeland *et al.* 2016). However, inversion alleles are not alternately fixed in Fjord and North Sea ecotypes and their specific functions and key environmental drivers remain unclear (Barth *et al.* 2019). Notably, 5 out of the 26 SNPs used to distinguish between Fjord and North Sea ecotypes were located inside inversions (Sodeland *et al.* 2016; Knutsen *et al.* 2018) and their lack of alternate fixation may have contributed to ambiguous population assignments of the parental fish in the present study. We do not know the inversion genotype of the larvae, but further research is needed to determine whether these inversions play a role in thermal adaptation and plasticity in Atlantic cod.

Epigenetic effects are another potential source of variation in thermal plasticity, as has been found in several fishes (reviewed by Donelson *et al.* 2018). We found no differences in initial length among crosses, which suggests a lack of variation in maternal effects on egg size among crosses (Marshall 2008). Although the parents were held for 2-3 months in a common environment, epigenetic effects could contribute to differences between pre-spawning locations. However, no clear and consistent differences attributable to location were detected. For example, we found survival differences between crosses from the same locations that were characterized by different ecotypes (e.g., OF×IF and ON×IF; Table 4.7). Because epigenetic and maternal effects do not explain the patterns of variation in thermal responses observed in the present study, as was the case in previous studies of larval cod plasticity (Oomen & Hutchings 2015b, 2016), we interpret the variation to be largely of genetic origin. However, the potential contribution of epigenetic effects cannot be ruled out.

4.5.4 Spatial Scale of Adaptive Variation

Risør fjord, which encompasses ~20 km^2, represents the smallest spatial scale at which genetic variation in plasticity and fitness traits (i.e. survival or reproduction) have been detected in a marine fish apparently lacking physical barriers to dispersal. Previous studies in coastal Norway have found genetic divergence in growth rates of juvenile turbot (Imsland *et al.* 2001) and Atlantic cod maturation reaction norms (Olsen *et al.*

2008) at scales of ~60 km and ~40 km, respectively. In the Northwest Atlantic, Hice et al. (2012) detected variation in several putatively adaptive traits in Atlantic silverside (*Menidia menidia*) at distances as little as 58 km. Such fine-scale biocomplexity in a species that is widely distributed and has high potential for dispersal contradicts traditional notions of genetic homogeneity in marine systems (reviewed by Hilbish 1996) and raises questions about the mechanisms promoting and maintaining adaptive variation among sympatric conspecifics.

Our findings add to a growing body of work suggesting the presence of adaptive variation within fjord systems in Atlantic cod (Kuparinen *et al.* 2015; Sodeland *et al.* 2016; Barth *et al.* 2017; Jorde *et al.* 2018; Knutsen *et al.* 2018; Roney *et al.* 2018b), but is the first to examine the influences of environmental background (location) and genetic origin (ecotype) separately. We also provide rare evidence of genetic variation in a fitness trait in Atlantic cod, along with Jorde et al. (2018) who associated ecotype with fishing mortality. Knutsen et al. (2018) found differences in juvenile growth rates between ecotypes within similar habitats in the wild and showed that the frequency of the Fjord ecotype increases farther into the fjords and the North Sea ecotype is more common in the exposed outer areas. Using the same parental fish as the present study, Kuparinen et al. (2015) determined that cod from Outer Risør had higher adult growth rates than cod from Inner Risør. However the extent to which differences in ecotype frequencies between locations might have contributed to this trend, and the relative contributions of genotype and environment to growth in the wild, are unknown. A related study demonstrated higher reproductive success in the cod from Inner Risør compared to Outer Risør, after accounting for differences in size and age (Roney *et al.* 2018b). Although ecotype was not explicitly considered, this finding suggests a potential reproductive barrier between cod from inner Risør, which are mostly Fjord ecotype, and outer Risør, which are mostly North Sea ecotype. Such a barrier could promote adaptive divergence within fjords, especially when combined with environmental differences between deep fjord and outer coastal areas.

4.5.5 Conservation and Management Implications

Choosing the correct spatial scale at which conservation, harvesting, and climate mitigation strategies should be implemented is a fundamental challenge of wildlife management. Failure to identify and account for genetic substructure can lead to a loss of subunits and a decrease in intraspecific biodiversity (Frank & Brickman 2000; Bonanomi *et al.* 2015; Cardinale *et al.* 2017). As biodiversity declines, so does the ability of a population to adapt to and recover from environmental stressors such as climate change and overfishing (Hilborn *et al.* 2003). When the genetic components of a population differ in abundance or adaptive traits, including responses to environmental variables, strategies that fail to account for this variation are at a higher risk of failure (Schindler *et al.* 2010). For example, a study on the interacting effects of climate change and fishing that led to the 1970s collapse of the West Greenland cod fishery showed the importance of managing fisheries at the level of genetic populations in the face of environmental disturbance (Bonanomi *et al.* 2015). Considering that the majority of marine fishes are overexploited (Worm *et al.* 2009; Costello *et al.* 2012) and that ocean warming is occurring rapidly (IPCC 2013), resolving the spatial genetic substructure of harvested fishes is urgent.

Coastal cod in Norway are currently managed as two units, divided north and south of 62° North. Depletion of coastal cod north of 62° (termed 'Norwegian Coastal Cod') has led the International Council for Exploration of the Sea (ICES) to recommend a new management plan aimed at rebuilding the stock (ICES 2018). South of 62° to the Skagerrak, where the study area is located, is considered part of the North Sea Cod management unit, whereby Norway is responsible for the management of >1000 km of coastline. Yet, significant neutral genetic structure was recently documented along the entire Norwegian coast, attributed to isolation by distance and introgression with the Northeast Arctic Cod (Dahle *et al.* 2018). Along with the discovery of divergent ecotypes in coastal waters (Knutsen *et al.* 2018), this evidence emphasizes the need for revision of the current management units. Further, population divergence can occur more quickly in adaptive traits than neutral markers (Hard 1995; Conover 1998; Conover *et al.* 2006) and adaptive variation is likely to be relevant to population productivity and persistence (Hard

1995; Conover & Munch 2002; Olsen *et al.* 2008). The presence of additional functional genetic variation in the Risør fjord, as documented in the present study, underscores the need for a management strategy that protects the intraspecific genetic diversity necessary for maintaining resilient local populations. Further work is needed to better understand the contributions of ecotypic and structural genomic variation to adaptive genetic diversity in this system.

4.6 Tables

Table 4.1: Temperatures (°C) in inner and outer Risør fjord at 5 and 10 m depths from January to May 2014.

	Inner Risør		Outer Risør	
Month	5 m	10 m	5 m	10 m
Mean				
January	6.27	7.38	2.33	2.22
February	2.96	4.09	2.78	2.95
March	4.48	5.69	4.82	4.86
April	7.22	6.95	7.39	6.67
May	12.04	9.93	11.57	10.12
Standard deviation				
January	0.08	0.08	0.08	0.06
February	1.31	1.93	0.84	0.84
March	1.57	1.41	0.68	0.65
April	1.65	0.81	1.48	0.87
May	1.54	1.62	2.10	2.32
Minimum				
January	6.06	7.28	2.09	2.09
February	1.76	1.98	1.76	1.66
March	2.30	2.94	3.68	3.79
April	5.76	5.86	5.66	5.55
May	7.48	7.08	7.28	6.88
Maximum				
January	6.37	7.48	2.41	2.30
February	6.37	7.38	5.04	4.93
March	7.78	7.88	6.06	5.86
April	11.53	9.47	11.63	9.08
May	15.95	11.72	16.43	15.09

Table 4.2: Identities, collection locations, and ecotype assignments of broodstock and the numbers of offspring contributed to the experiment.

Parent ID	Location	Ecotype	# of offspring in experiment
Mothers			
F03	Inner	Fjord	352
F15	Inner	Fjord	140
F25	Inner	Fjord	217
F31	Inner	Fjord	46
F32	Inner	Fjord	1
F34	Inner	Fjord	32
RIC5060	Outer	Fjord	408
RIC5068	Outer	North Sea	24
RIC5071	Outer	Fjord	218
RIC5078	Outer	North Sea	76
Fathers			
F06	Inner	Fjord	82
F13	Inner	Fjord	15
F14	Inner	Fjord	162
F19	Inner	Fjord	105
F20	Inner	Fjord	225
F21	Inner	Fjord	363
F29	Inner	Fjord	11
F30	Inner	Fjord	58
F33	Inner	Fjord	36
F35	Inner	Fjord	11
RIC5064	Outer	Fjord	93
RIC5076	Outer	North Sea	98
RIC5087	Outer	Fjord	4
RIC5100	Outer	North Sea	251
		Total	1514

Table 4.3: Results of linear mixed effects models for (a) initial larval length (0 and 2 dph) and (b) growth (28 dph) for 6 crosses of Atlantic cod. Asterisks denote significance at α=0.05.

(a) Initial length						
Model term	d.f.	Sum of squares	Mean of squares	*F*	*P*-value	
cross	6	0.29	0.05	1.13	0.346	
curvature	1	0.06	0.06	1.32	0.251	
Model term	Variance	SD				
father	0.00	0.03				
mother	0.01	0.12				
residual	0.04	0.21				
(b) Growth						
Model term	d.f.	Sum of squares	Mean of squares	*F*	*P*-value	
cross	5	0.90	0.18	0.51	0.797	
temperature	2	1.11	0.56	1.58	0.207	
cross×temperature	1	5.74	5.74	16.37	<0.001	*
curvature	10	11.95	1.19	3.41	<0.001	*
Model term	Variance	SD				
father	0.03	0.17				
mother	0.05	0.23				
tank	0.02	0.15				
temperature:tank	0.01	0.12				
residual	0.35	0.59				

Table 4.4: Effect of increasing temperature on larval growth for 6 crosses of Atlantic cod. Asterisks denote significance at the following levels of α: *0.10 and **0.05.

Cross	Estimate	SEM	%	*t*	*P*-value	
6-9.5°C						
IF×IF	0.31	0.19	4.47	1.65	0.054	*
IF×OF	0.20	0.30	2.97	0.67	0.261	
OF×IF	0.12	0.19	1.90	0.65	0.261	
IF×ON	0.88	0.27	12.08	3.30	0.004	**
ON×IF	0.12	0.40	1.85	0.31	0.385	
OF×ON	0.14	0.28	2.16	0.51	0.311	
9.5-13°C						
IF×IF	-0.27	0.21	-3.92	-1.26	0.110	
IF×OF	-0.26	0.43	-3.84	-0.60	0.296	
OF×IF	0.28	0.18	4.15	1.54	0.066	*
IF×ON	-0.90	0.27	-12.34	-3.32	0.004	**
ON×IF	0.28	0.31	4.04	0.93	0.190	
OF×ON	-0.79	0.35	-11.89	-2.23	0.038	**

Table 4.5: Pairwise contrasts of the effect of increasing temperature on larval growth for 6 crosses of Atlantic cod. Estimates (±SEM) are given above the diagonal and P-values below. The point of contrast for the estimates is the row header. Asterisks denote significance at the following levels of α: *0.10 and **0.05.

6-9.5°C	IF×IF	IF×OF	OF×IF	IF×ON	ON×IF	OF×ON
IF×IF	-	-0.11 (0.30)	-0.19 (0.20)	0.57 (0.27)	-0.18 (0.40)	-0.17 (0.29)
IF×OF	0.365	-	-0.08 (0.30)	0.68 (0.36)	-0.08 (0.46)	-0.06 (0.37)
OF×IF	0.175	0.402	-	0.76 (0.27)	0.00 (0.40)	0.02 (0.29)
IF×ON	**0.031****	**0.049****	**0.010****	-	-0.76 (0.44)	-0.74 (0.34)
ON×IF	0.336	0.438	0.497	0.082*	-	-0.02 (0.45)
OF×ON	0.288	0.441	0.472	**0.029****	0.485	-
9.5-13°C	IF×IF	IF×OF	OF×IF	IF×ON	ON×IF	OF×ON
IF×IF	-	0.01 (0.44)	0.55 (0.21)	-0.63 (0.29)	0.55 (0.32)	-0.52 (0.37)
IF×OF	0.490	-	0.54 (0.43)	-0.64 (0.47)	0.54 (0.49)	-0.53 (0.52)
OF×IF	**0.007****	0.149	-	-1.18 (0.27)	0.01 (0.30)	-1.06 (0.35)
IF×ON	**0.026****	0.134	**0.001****	-	1.18 (0.36)	0.11 (0.40)
ON×IF	0.061*	0.176	0.493	**0.006****	-	-1.07 (0.42)
OF×ON	0.108	0.194	**0.014****	0.395	**0.026****	-

Table 4.6: Deviance table from generalized linear models for the effects of cross and temperature on larval Atlantic cod survival. The P-values were obtained from $\chi 2$ tests of whether the model fit improved by sequentially adding population, temperature, and their interaction to the null model. Asterisks denote significance at $\alpha=0.05$.

Model term	d.f.	Deviance	Residual d.f.	Residual deviance	*P*-value	
null			53	3045.70		
cross	5	1251.90	48	1793.80	<0.001	*
temperature	2	804.01	46	989.79	<0.001	*
cross×temperature	10	533.40	36	456.39	<0.001	*

Table 4.7: Effect of increasing temperature on larval survival for 6 crosses of Atlantic cod. Asterisks denote significance at the following levels of α: *0.10 and **0.05.

Cross	Estimate	SEM	%	*t*	*P*-value	
6-9.5°C						
IF×IF	26.05	34.65	16.12	0.75	0.457	
IF×OF	-24.34	19.02	-42.73	-1.28	0.209	
OF×IF	58.17	34.67	32.70	1.68	0.102	
IF×ON	54.90	22.45	61.12	2.45	0.019	**
ON×IF	18.37	14.51	52.15	1.27	0.213	
OF×ON	4.52	18.68	9.94	0.24	0.810	
9.5-13°C						
IF×IF	-145.79	26.77	-90.21	-5.45	0.000	**
IF×OF	-29.07	12.09	-89.09	-2.41	0.021	**
OF×IF	-134.08	29.93	-75.36	-4.48	0.000	**
IF×ON	-83.43	19.71	-92.88	-4.23	0.000	**
ON×IF	-26.38	13.35	-74.86	-1.98	0.056	*
OF×ON	-40.26	14.30	-88.58	-2.82	0.008	**

Table 4.8: Pairwise contrasts for the effect of increasing temperature on larval survival for 6 crosses of Atlantic cod. Estimates (±SEM) are given above the diagonal and P-values below. The point of contrast for the estimates is the row header. Asterisks denote significance at the following levels of α: *0.10 and **0.05.

6-9.5°C	IF×IF	IF×OF	OF×IF	IF×ON	ON×IF	OF×ON
IF×IF	-	-50.39 (39.53)	32.12 (49.02)	28.85 (41.28)	-7.68 (37.56)	-21.53 (39.36)
IF×OF	0.210	-	82.51 (39.55)	79.24 (29.42)	42.72 (23.92)	28.86 (26.66)
OF×IF	0.516	**0.044****	-	-3.28 (41.31)	-39.80 (37.59)	-53.65 (39.39)
IF×ON	0.489	**0.011****	0.937	-	-36.52 (26.73)	-50.38 (29.20)
ON×IF	0.839	0.083*	0.297	0.180	-	-13.86 (23.65)
OF×ON	0.588	0.286	0.182	0.093*	0.562	-
9.5-13°C	IF×IF	IF×OF	OF×IF	IF×ON	ON×IF	OF×ON
IF×IF	-	116.72 (29.37)	11.71 (40.16)	62.36 (33.25)	119.42 (29.91)	105.53 (30.35)
IF×OF	**<0.001****	-	-105.01 (32.28)	-54.36 (23.13)	2.70 (18.01)	-11.19 (18.73)
OF×IF	0.772	**0.002****	-	50.65 (35.84)	107.70 (32.77)	93.82 (33.17)
IF×ON	0.069*	**0.024****	0.166	-	57.05 (23.81)	43.17 (24.36)
ON×IF	**<0.001****	0.882	**0.002****	**0.022****	-	-13.89 (19.56)
OF×ON	**0.001****	0.554	**0.008****	0.085*	0.482	-

4.7 Figures

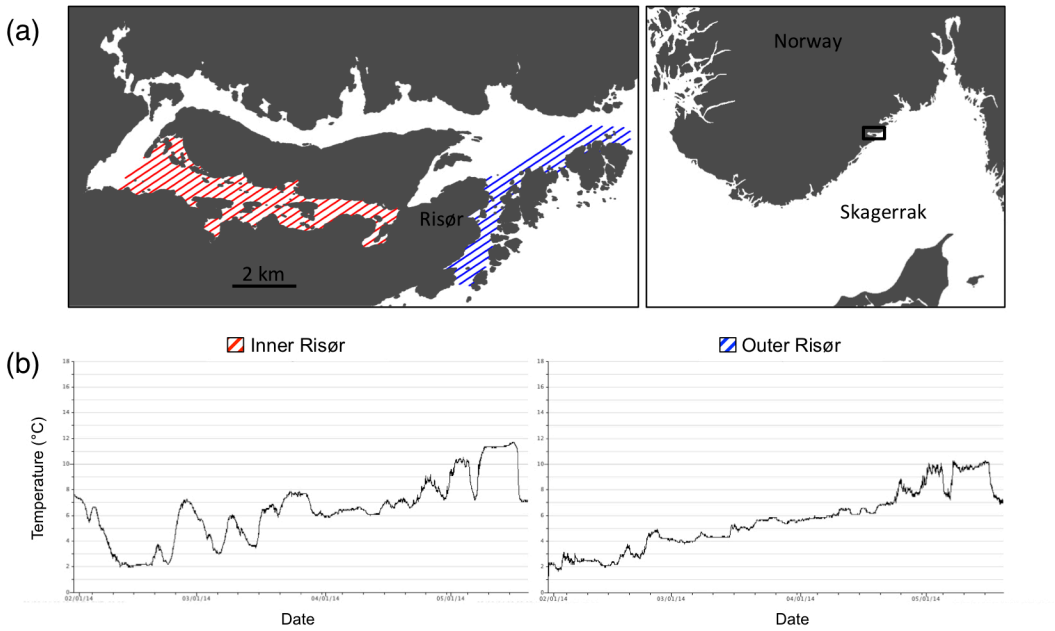

Figure 4.1: Risør fjord study system on the Norwegian Skagerrak coast. (a) Adult collection locations for inner and outer fjord areas (modified from Kuparinen *et al.* 2016) and (b) representative temperature profiles during the 2014 spawning season from data loggers positioned at 10 m depth in each study area.

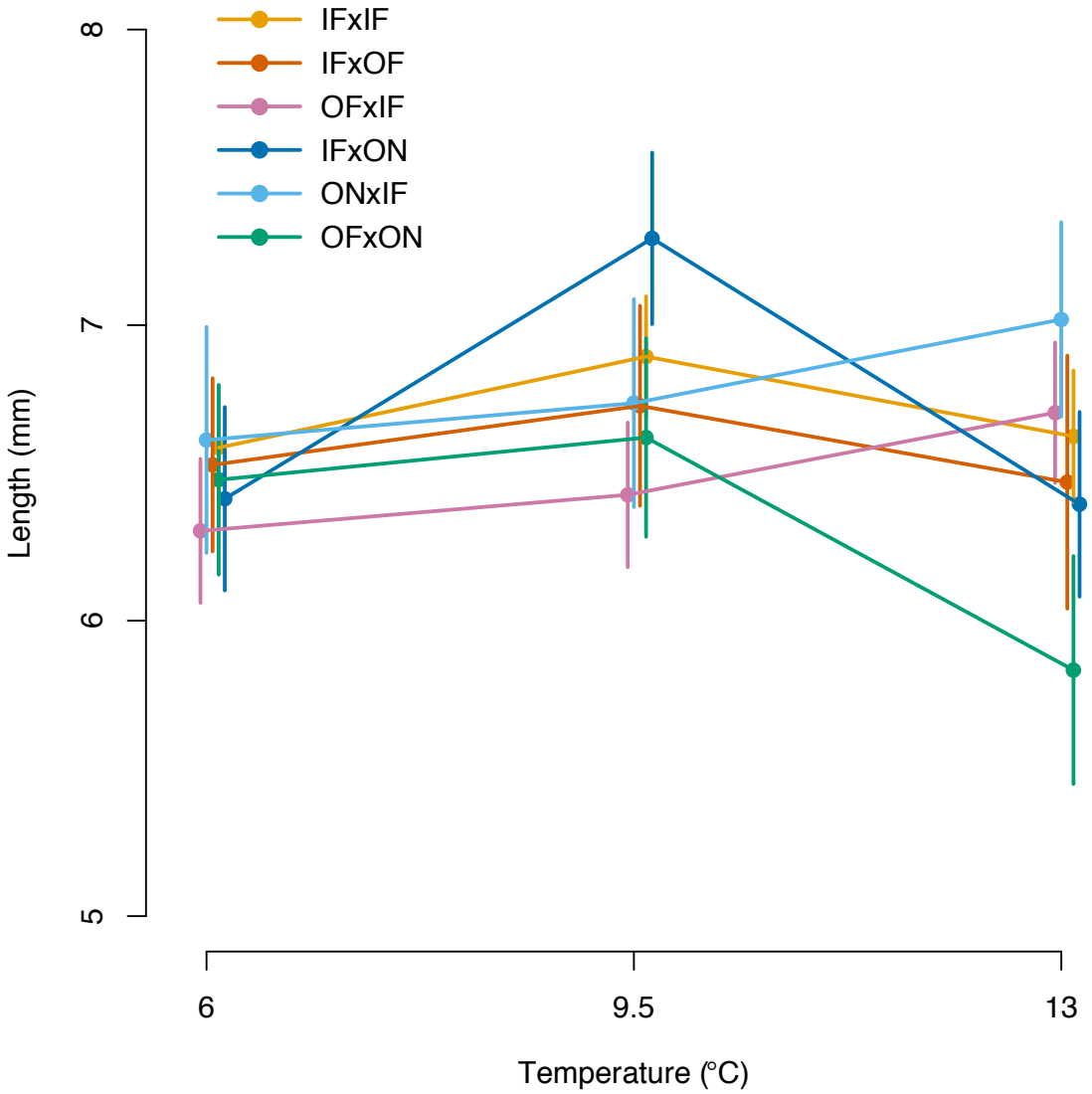

Figure 4.2: Thermal reaction norms for larval Atlantic cod growth (±1 SEM) for six crosses (mother×father: I = Inner Risør fjord, O = Outer Risør fjord, F = fjord ecotype, N = North Sea ecotype).

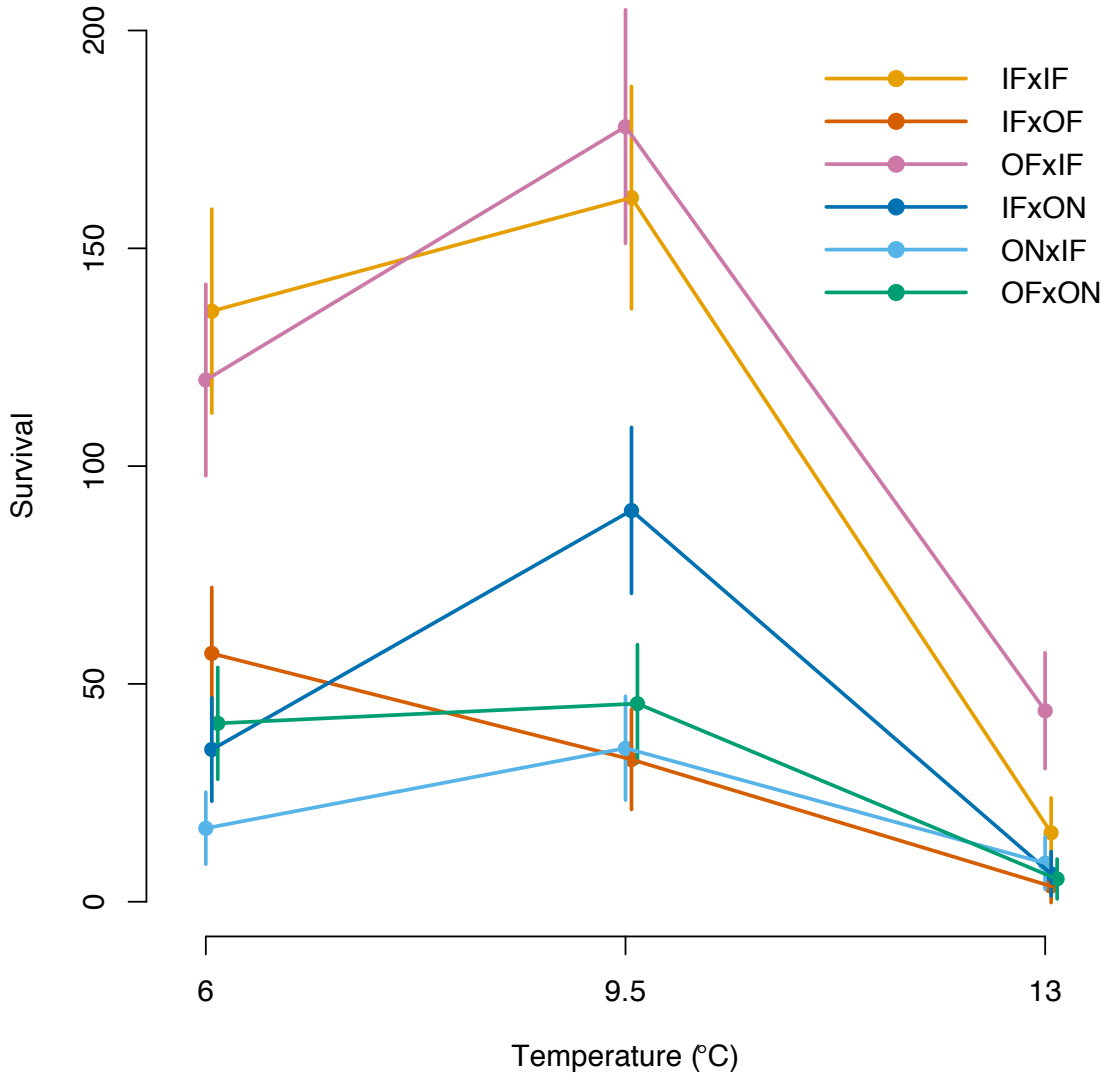

Figure 4.3: Thermal reaction norms for larval Atlantic cod survival (±1 SEM) for six crosses (mother×father: I = Inner Risør fjord, O = Outer Risør fjord, F = Fjord ecotype, N = North Sea ecotype).

Chapter 5: The Genomic Basis of Local Adaptation with Gene Flow at Multiple Spatial Scales

Supplementary materials for this chapter are located in Appendix D.

5.1 Abstract

Recent studies provide evidence of local adaptation in species with high connectivity and suggest that genetic architecture plays a key role in its origin and maintenance. However, the genomic basis of adaptation under gene flow remains poorly understood. The question of whether different genomic architectures underlie adaptation at different spatial scales with varying levels of gene flow has not been empirically explored. Here, using a common garden protocol combined with large-scale (n=462) RNA sequencing and SNP analysis of Atlantic cod (*Gadus morhua*) larvae of wild origin, we find variation in gene expression means and thermal plasticities, growth reaction norms, and survival consistent with adaptive divergence at macro- (~1300 km) and micro-geographic (<20 km^2) spatial scales along coastal Norway. Differences in gene expression and survival at warm yet ecologically relevant temperatures are consistent with the warm-adapted southern Skagerrak larvae having higher activity levels and enhanced development associated with higher fitness compared to the relatively cold-adapted northern Helgeland population. Differences between these populations in the magnitudes of the cellular stress response to warming suggest thermal adaptation at large spatial scales likely due to selection acting broadly across the genome. Within a Skagerrak fjord system, gene expression was uniquely impacted by: 1) parental pre-spawning environments, reflecting epigenetic effects, 2) coexisting ecotypes with low genome-wide divergence, and 3) three chromosomal inversion polymorphisms located on linkage groups (LGs) 02, 07, and 12. Putatively epigenetic effects had the greatest impact on thermally plastic variation in gene expression during early development. Paternal effects tended to be larger than maternal effects for gene expression. Ecotype affected initial length and mean expression of

transcripts involved in cell proliferation and growth, but had little effect on thermal plasticity. The LG02 inversion polymorphism had the greatest impact on mean gene expression at the microgeographic scale. LG02 affected an interaction between size and temperature associated with the regulation of oxygen transport, although within-generation experimental selection was consistent with adaptation to salinity as well. LG07 experienced strong selection in opposite directions at 6°C compared to warmer temperatures and affected thermally plastic gene expression related to DNA repair, circadian rhythm, and metabolic shifts. LG12 affected thermally plastic gene expression associated with energy metabolism and might, in a polygenic manner with LG02, confer adaptation to sea ice cover. This is the first experimental evidence for the putative adaptive functions of three large chromosomal inversions that are polymorphic throughout the Atlantic cod range. Overall, our findings suggest that, at a macrogeographic scale characterized by moderate gene flow, low-level differentiation located throughout the genome contributes most to local adaptation. At a microgeographic scale with high gene flow, blocks of tightly linked genes contribute most to local adaptation. This novel empirical investigation will aid our understanding of how climate change will affect population dynamics and distributions and enable effective management of harvested species with high gene flow.

5.2 Introduction

Adaptation of populations to local environmental conditions generates and maintains biological diversity (Fisher 1930; Dobzhansky 1940; Hoffmann *et al.* 2015). Due to the relatively higher fitness of native individuals compared to non-natives, local adaptation impacts population structure, dynamics, and resilience to environmental perturbations (Kawecki & Ebert 2004). Thus, identifying locally adapted populations and the ecological, evolutionary, and environmental circumstances under which they occur is necessary for understanding how species respond to environmental change and can contribute to effective conservation and management strategies (Andrew *et al.* 2013; Savolainen *et al.* 2013; Bernatchez 2016).

Gene flow works in opposition to directional selection on adaptive traits, homogenizing connected gene pools and leading to a loss of locally adapted alleles (Wright 1931; Bulmer 1972; Lenormand 2002). Consequently, the potential of local adaptation to promote population divergence and speciation in the face of gene flow has traditionally been perceived as low (reviewed by Hilbish 1996). However, recent studies reveal that local adaptation can occur even when gene flow is high and suggest that genetic architecture plays a key role in its origin and maintenance (reviewed by Tigano & Friesen 2016). Unraveling the mechanisms that enable adaptive divergence in the face of gene flow could be likened to describing a relatively unexplored form of evolution that is likely ubiquitous in the natural world: from vagile birds, bats, insects, and plants to the highly connected marine environment.

Theoretical work has implicated the genetic architecture of adaptive traits as the key element in determining whether they will be lost under high gene flow (Bürger & Akerman 2011; Yeaman & Whitlock 2011; Yeaman 2013; Akerman & Bürger 2014). Alleles with large effect sizes are less likely to be overwhelmed by gene flow (Yeaman & Otto 2011), but adaptive traits controlled by a single locus of large effect are considered to be rare (reviewed by Feder & Walser 2005). Polygenic architectures with many loci of small effect might be more common for adaptive traits (Savolainen *et al.* 2013; Palumbi

et al. 2014; Bay *et al.* 2017a), in which case linkage among loci, recombination rates, and epistatic interactions influence the migration-selection balance (Bürger & Akerman 2011; Yeaman & Whitlock 2011; Aeschbacher & Bürger 2014). In particular, tightly linked polygenic architectures are predicted to be favoured under adaptation with gene flow, as they effectively act as a single large-effect locus (Griswold 2006; Yeaman & Otto 2011). Regions of suppressed recombination, such as chromosomal rearrangements (e.g., inversions, fusions, and translocations), can theoretically act as 'supergenes' by capturing several locally adapted alleles, although there are few empirical tests of this (but see (Coughlan & Willis 2018). Chromosomal rearrangements can also disrupt the expression of genes located near the breakpoints, potentially affecting downstream phenotypes (Kirkpatrick 2010).

Although rearrangements are widely regarded for their role in speciation and evolution (Hoffmann & Rieseberg 2008; Schwander *et al.* 2014), experimental evidence of these and other linked genetic architectures facilitating adaptation in the face of gene flow is rare. Most evidence of local adaptation in general comes from studies that correlate variation in allele or haplotype frequencies with environmental clines and compare it to lower variation at neutral markers (reviewed by Pritchard & Di Rienzo 2010; Barrett & Hoekstra 2011; Savolainen *et al.* 2013). This is also the case for studies of the role of chromosomal inversions in environmental adaptation (reviewed by Wellenreuther & Bernatchez 2018). However, this approach usually sheds little light on the phenotypic consequences of observed genetic variation because the effects of adaptation and plasticity on phenotypic variation across different environments are indistinguishable. Exceptions include studies of contrasting ecotypes, for which phenotypic divergence observed among habitats is known to have a genetic basis (Feder *et al.* 2003; Jones *et al.* 2012; Joron *et al.* 2013; Roesti *et al.* 2015; Berg *et al.* 2016, 2017; Kirubakaran *et al.* 2016; Sinclair-Waters *et al.* 2018).

Potentially adaptive phenotypic variation among populations can be shown to have a genetic basis through common-garden or reciprocal transplant experiments (Conover & Baumann 2009). However, such experiments alone do not identify the specific genes

underlying the adaptations. Integrating experimental and genomic approaches can bridge the gap between genotypic and phenotypic variation and, when combined with measures of fitness, reveal the genomic basis of local adaptation (Lowry & Willis 2010; de Villemereuil *et al.* 2016; Oomen & Hutchings 2017).

Here, we integrate common-garden experiments with transcriptomics to investigate the genomic basis of adaptive divergence with gene flow in a widespread marine fish. Atlantic cod (*Gadus morhua*; hereafter, 'cod') is a demersal top predator inhabiting coastal waters throughout the North Atlantic. Signatures of adaptation to local environmental heterogeneity have been detected throughout their range despite widely dispersing pelagic egg and larval stages and few oceanographic barriers to adult dispersal (e.g., Hutchings *et al.* 2007; Olsen *et al.* 2008; Bradbury *et al.* 2010, 2014; Berg *et al.* 2015; Oomen & Hutchings 2015b, 2016; Berg *et al.* 2017). Cod also now appear to comprise several genetically diverged, yet partially overlapping, ecotypes that are associated to varying degrees with four large chromosomal inversions. Aside from the migratory ecotype distinguished by an inversion polymorphism on LG01 (Berg *et al.* 2016, 2017; Kirubakaran *et al.* 2016; Sinclair-Waters *et al.* 2018), there are non-migratory ecotypes with overlapping ranges that exhibit genome-wide differentiation as well as varying karyotype frequencies for three other inversions (Sodeland *et al.* 2016). These inversions are associated with oceanographic clines throughout the species range and have been linked to temperature, salinity, and/or oxygen adaptation at a variety of spatial scales (Bradbury *et al.* 2010, 2014; Berg *et al.* 2015; Sodeland *et al.* 2016; Barth *et al.* 2017). Yet, they are polymorphic within ecotypes and their specific adaptive functions and key environmental drivers are unknown (Barth *et al.* 2019).

The genomic mechanisms underlying adaptation with gene flow have implications for how natural populations will respond to environmental change (Razgour *et al.* 2018). The relative importance of genome-wide divergence between ecotypes and inversion frequency variation in local adaptation in cod is unclear. Importantly, in the absence of reproductive barriers, gene flow depends on geographic barriers, including the distance between populations relative to their dispersal capabilities. Therefore, because the extent

of gene flow usually varies across a species' range, different genomic architectures might underlie adaptation at different spatial scales (Nosil *et al.* 2009).

Temperature is a dominant factor shaping species distributions worldwide (Pörtner 2002; Pörtner & Peck 2010; Buckley *et al.* 2014). Among anthropogenic impacts on wildlife, changes in temperature associated with greenhouse gas emissions are the most concerning (Hoffmann *et al.* 2015). For marine fishes, the larval stage represents a fitness bottleneck that is especially sensitive to temperature (Pörtner *et al.* 2008). Yet, many fishes exhibit genetic variation in thermal plasticity at both the phenotypic (reviewed by Hutchings 2011; Oomen & Hutchings 2015a) and molecular (reviewed by Oomen & Hutchings 2017; Chapter 2) levels, reflecting differences in short- and long-term responses to environmental change.

We investigate the contributions of different genomic architectures of divergence to local adaptation in cod along the Norwegian coast by comparing body length, survival, and genome-wide expression patterns through larval development across a range of temperatures in a common-garden design. We first quantify adaptive variation at a broad spatial scale between Northern and Southern latitudes, then leverage the base-pair resolution of RNA sequencing to distinguish between ecotypes and inversion polymorphisms in facilitating local adaptation with gene flow at a microgeographic scale within a single fjord system. Using a reaction norm framework (see Chapter 1) we compare trait means and thermal plasticities to test for local adaptation among cod 1) collected in different environments, 2) assigned to historically-diverged coexisting ecotypes, and 3) possessing different arrangements for three chromosomal inversions. We provide evidence for the molecular basis of thermal plasticity and the adaptive basis of genomic variation through functional analyses of differential expression and tests for experimental selection on inversion polymorphisms in the F1 generation. In doing so, we provide new insights into the genomic mechanisms of local adaptation with gene flow and its implications for cod in the context of global environmental change.

5.3 Methods

5.3.1 Study System

Along the Norwegian coastline, non-migratory ('coastal') cod exhibit significant genetic structure consistent with a pattern of isolation by distance along a latitudinal gradient (Dahle *et al.* 2018). On the southerly Skagerrak coast, three non-migratory ecotypes with overlapping ranges coexist (Knutsen *et al.* 2018; Barth *et al.* 2019). Among these, the present study focuses primarily on the 'fjord' ecotype, which is more common in sheltered inner fjord locations and displays a consistent decrease in frequency towards the open ocean, and the 'North Sea' ecotype, which is more frequent outside fjords and is genetically similar to offshore populations in the North Sea (Knutsen *et al.* 2018). Ecotypic divergence has been traced to the occupancy of separate glacial refugia during the last ice age (Sodeland *et al.* in review). Their genetic distinctiveness is cryptic due to a lack of obvious phenotypic differences, yet now it appears that they might differ in juvenile growth rate (Knutsen *et al.* 2018), behaviour (Barth *et al.* 2019), and reproductive success (Roney *et al.* 2018b). While they have generally low but significant levels of genome-wide divergence (Sodeland *et al.* in review), they display varying frequencies for inversion polymorphisms in LG02, LG07, and LG12 that are associated with environmental variables throughout the North Atlantic range (Bradbury *et al.* 2010, 2014; Berg *et al.* 2015; Sodeland *et al.* 2016; Barth *et al.* 2017). It is not known how far the range of the North Sea ecotype extends northward along the western coast of Norway.

5.3.2 Experimental Design

Two similar rearing experiments were carried out in two consecutive years on cod from three locations across two regions of the Norwegian coast (Figure 5.1). In 2014, we carried out a common-garden experiment on cod from two locations in the Risør fjord system on the Norwegian Skagerrak coast (Chapter 4). From December 2013 to January 2014, cod were collected from deep inside Risør fjord and from the small islands outside the mouth of the Risør fjord (hereby referred to as 'inner Risør' and 'outer Risør', respectively). All Risør cod were treated as a single broodstock for which the offspring

occupied the same experimental tanks (for details see Chapter 4). In January 2015, we collected cod for a near-identical experiment from outside a fjord in Helgeland, a relatively northerly region on the west coast of Norway (Figure 5.1a). Cod were also collected from Risør in 2015. However, they were in poor spawning condition (i.e., few batches of low-quality eggs were obtained). Therefore, Helgeland cod alone were treated as a single broodstock. Thus, comparisons between the two Risør locations are in the context of a true common-garden experiment on a micro-geographic (<20 km^2) scale and comparisons made between these and Helgeland are in the context of a common-garden-like experiment on a broad spatial scale (~1300 km by sea). Importantly, all 2014 and 2015 samples were processed the same way and comprised a single RNA-seq experiment.

Both the Risør and Helgeland experiments are also compared to a smaller experiment conducted in 2013 on cod collected near Flødevigen, Norway (an exposed area ~ 60 km southwest of Risør) (Figure 5.1a; see Chapter 3 for details), for the purpose of assessing the relative impacts of region (i.e., Skagerrak *vs.* Helgeland), RNA-seq experiment (i.e., A [Flødevigen] *vs.* B [Risør and Helgeland]) and rearing experiment (i.e., 2013 [Flødevigen] *vs.* 2014 [Risør] *vs.* 2015 [Helgeland]).

5.3.3 Broodstock Collection and Rearing Experiments

Details about the Flødevigen, Risør, and Helgeland experiments are in Chapters 2 and 3 and Appendix D.1, respectively. Differences between experiments are summarized in Table S1. Briefly, adult cod were collected prior to the start of the breeding season (approximately February-May), transported to the *Flødevigen Research Station, Institute of Marine Research*, individually tagged, and allowed to acclimate for 4-12 weeks in a 45 m^3 spawning basin with ambient flow-through seawater prior to the start of egg collection. Cod were held at ambient temperature and photoperiod and fed shrimp daily until the end of the spawning period, when they were sacrificed by a blow to the head prior to fin tissue collection and dissection for sex identification.

Eggs were incubated in a 900 L flow-through seawater tank at ambient temperature (9°C for Flødevigen, 6°C for Risør and Helgeland) until hatch. At 0 days post hatch (dph), larvae were randomly sampled and distributed among 40 L rearing tanks with flow-rates of 0.35 L/min. All tanks were initially stocked to a density of 40 to ~100 larvae/L, i.e., within the range for which variation in density has been shown to have no effect on larval growth or survival under unlimited food conditions (Baskerville-Bridges & Kling 2000; Oomen & Hutchings 2015b). The temperatures in the rearing tanks were the same as the incubation tank upon transfer and then gradually changed to the experimental temperatures over the course of 24 h. Larvae were reared at three temperatures with 3-5 replicate tanks per temperature. Flødevigen larvae were reared at 9 °C, 11 °C, and 13 °C, representing the ambient seawater temperature outside the research facility during the experiment and 2 °C and 4 °C increases consistent with projected climate scenarios by the year 2100 (IPCC 2013). Risør and Helgeland larvae were reared at 6 °C, 9.5 °C, and 13 °C, representing: 1) the average temperature near the research facility in March/April (i.e., during and immediately after peak spawning), 2) a 3.5 °C increase consistent with the projected increase of 2-4 °C by the year 2100 (IPCC 2013) and the average temperature near the research facility in April/May (i.e., during and immediately after late spawning), and 3) a 7 °C increase consistent with the projected increase of 2-4 °C by the year 2100 (IPCC 2013) to the average temperature near the research facility in April/May (i.e., projected temperatures for offspring of late spawners) (Figure 5.1b, also see Chapter 4 Table S1). These temperatures best represent ecologically relevant scenarios for the Skagerrak region, whereas Helgeland is typically colder (2.9-5.4 °C from March-May, although the mean March temperature during the experimental year was 1.2 °C above average; Figure S1).

Larvae were reared under a constant light intensity of 2000 lux and fed *Brachionus plicatilis* rotifers enriched with RotiGrow *Plus*™ (Reed Mariculture, USA) in excess (4500 prey/L three times daily). Water temperatures were recorded daily and water quality parameters (oxygen, pH, and ammonia concentration) were monitored with no notable deviations.

Twenty (Helgeland) or forty (Risør) larvae were randomly sampled from the incubation tank at 0 dph. These served as baseline samples prior to transfer and temperature treatment exposure. Ten (Helgeland) or forty (Risør) larvae per tank were randomly sampled at 2, 7 (Helgeland only), 14, 21 (Risør and Helgeland only), and 28-29 dph, whereby sampling was always equal across temperature treatments (Table S1). Larvae were individually placed in RNAlater™ on a glass slide and immediately photographed, using a stereoscope with a Leica DFC 425 C Camera. Samples were preserved in RNAlater™ at -20°C prior to DNA and RNA extraction. Standard length at 28 dph was measured from the photographs using ImageJ (Abràmoff *et al.* 2004) and considered a proxy for growth rate, following Hutchings et al. (2007).

5.3.4 Microsatellite Genotyping and RNA-Seq Sample Selection

Of the 300 sampled Flødevigen larvae, 30 were selected for genotyping and RNA-seq (3 larvae × 3 temperatures × 3 time points, plus 3 from the baseline sample (for details see Chapter 3 Table S1). Parentage analyses based on eight microsatellite loci and the full-likelihood method in COLONY v. 2.0.6.0 (Jones & Wang 2010) identified two fathers and three mothers, with 90% of offspring coming from the same parent pair (Chapter 3 Table S1).

Of the 1960 Risør larvae sampled, 1524 were selected for individual nucleic acid extraction using E-Z 96 DNA/RNA Isolation Kits (Omega Bio-Tek, USA) according to the manufacturer's instructions with the following specifications. First, tissue homogenization was performed in 1.5 ml tubes containing ceramic (zirconium oxide) beads (Precellys) and 250 µl 1x lysis buffer (Omega Bio-Tek, USA) using a MagNA Lyser Instrument (Roche). DNA was eluted in two steps using 50 µl of 70°C elution buffer each. RNA was eluted in two steps using 25 µl of RNase-free water each. Following PCR amplification of the same 8 microsatellite loci that were amplified in the previous chapters (see Chapter 3 and 3 for details), genotypes were obtained for 1519 larvae. Parentage analyses based on 4-8 loci and the likelihood method in CERVUS v3.0 (Kalinowski *et al.* 2007) identified 10 mothers and 14 fathers for 1514 larvae. Parental

ecotypes were determined using a panel of 26 SNPs developed for the purpose (Jorde *et al.* 2018), except for the individual RIC5100, which was classified in the present study (see methods section *SNP Calling and Chromosomal Inversion Genotyping* for details). Parents with North Sea genotypes were all from Outer Risør (Chapter 4 Table 4.2). Larvae were classified into genetic crosses, depending on whether their parents were collected from Inner Risør (I) or Outer Risør (O) and of Fjord (F) or North Sea (N) ecotype. Considering maternal and paternal effects separately, 8 crosses were detected and 6 had sufficient sampling across treatments ($n \geq 88$) while 2 had insufficient sample sizes ($n \leq 5$) (Chapter 4 Table S3). Thus, 1508 larvae were retained for further analysis and assigned to crosses (mother×father): IF×IF, IF×OF, OF×IF, IF×ON, ON×IF, and OF×ON.

Of the 786 Helgeland larvae sampled, 192 were selected for individual nucleic acid extraction using E-Z 96 DNA/RNA Isolation Kits (Omega Bio-Tek, USA) and 190 were successfully genotyped according to the same extraction and amplification protocols as the Risør larvae. Parentage analyses based on 4-8 microsatellite loci and the likelihood method in CERVUS v3.0 (Kalinowski *et al.* 2007) identified 3 mothers and 5 fathers for 190 larvae (see Chapter 4 for analysis details). Because the provenance of the Helgeland larvae is known, all 786 larvae were retained in the growth analysis.

RNA quality from 1185/1499 Risør larvae and 190/190 Helgeland larvae was assessed using a Fragment Analyzer with PROSize Data Analysis Software (Advanced Analytical Technologies, Inc.). Except for IF×ON, for which only 11 larvae were available across the whole experiment, at least five larval replicates (mean±SD = 5.5±0.8, range = 2-7) were selected for RNA-seq for each time point, temperature, and genetic cross combination (hereafter, "group"), as well as for each cross from the baseline sample, when available (total n=432). Larvae were selected from 2-4 tanks in such a way as to maximize family-level variation within a set of replicates, minimize tank- and family-level variation among groups, and maximize RNA quality (RQN range = 5.6-10, mean±SD = 8.9±0.7).

5.3.5 RNA Library Prep and Sequencing

RNA libraries were prepared with the Illumina TruSeq™ RNA low-throughput protocol (Flødevigen) or the Illumina TruSeq™ RNA high-throughput protocol (Risør and Helgeland) and a fragmentation time of 4 minutes. The 30 Flødevigen libraries were sequenced with a 100 bp paired-end protocol on the Illumina HiSeq 2500 platform, producing a total of 798 million read pairs (Chapter 3 Table S3). The 432 Risør and Helgeland libraries were sequenced with a 150 bp paired-end protocol on the Illumina HiSeq 4000 platform. Reads from three sequencing lanes were pooled for each sample, producing a total of 11.716 billion read pairs and bringing the total number of read pairs assessed in this study to 12.514 billion. All sequencing was carried out at the Norwegian Sequencing Centre, University of Oslo (www.sequencing.uio.no).

5.3.6 Sequence Trimming, Adapter Removal, and Quality Control

Trimming and adapter removal was performed on all sequences using Trimmomatic v.0.36 (Bolger *et al.* 2014) with a 5-bp sliding window mean quality threshold of 20 and a minimum length of 40 bp. Read quality was evaluated before and after trimming using FastQC v.0.11.2 (Andrews 2011). Transcriptome assembly was performed using the remaining 9.6 billion read pairs.

5.3.7 Transcriptome Assembly and Annotation

Transcriptome assembly was performed based on the reference genome (Star *et al.* 2011; Tørresen *et al.* 2017) as well as *de novo* with refinement based on the reference genome. We initially analyze both transcriptomes for comparison. Thereafter, we focus on the reference genome-based assembly.

5.3.8 Reference-Genome Based Transcriptome Assembly

We assembled the transcriptome using the reference genome (Star *et al.* 2011; Tørresen *et al.* 2017) and the 'new Tuxedo' pipeline (Pertea *et al.* 2016). Briefly, the low-memory aligner HISAT v.2.1.0 (Kim *et al.* 2015) was used to map reads to the reference genome. Samtools v.1.3.1 (Li *et al.* 2009) was used to sort and convert the resulting SAM files to BAM files for transcript assembly, quantification, and merging of assemblies using StringTie 1.3.1 (Pertea *et al.* 2015). We included a reference annotation containing known gene models in StringTie to improve reconstruction of low-abundance genes. Otherwise, default options were used.

The resulting assembly was compared to the reference genome using gffcompare v.0.9.8 (https://github.com/gpertea/gffcompare) to evaluate the proportion of novel transcripts. More than half (65.3%) of all loci in the merged assembly did not have corresponding gene models in the reference genome annotation. Therefore we annotated the assembly using Trinotate v.3.0.1 (http://trinotate.github.io/), after first converting the GTF file to a FASTA file with the cufflinks_gtf_genome_to_cdna_fasta.pl script in Transdecoder v.5.0.1 (http://transdecoder.sf.net) and manually creating a gene-to-transcript map of the StringTie gene identifiers using the grep function in unix (grep ">" stringtie_merged.gtf.fasta | awk -F '>' '{print $2}' | awk -F ' ' '{print $2 "\t" $1}' > stringtie_merged.gtf.fasta.gene_trans_map). A matrix of raw gene counts was generated from the StringTie output using the prepDE.py script (http://ccb.jhu.edu/software/stringtie/dl/prepDE.py).

5.3.9 De Novo *Transcriptome Assembly*

The *de novo* transcriptome was initially assembled using the Trinity software suite v.2.3.2 (http://trinityrnaseq.github.io), including bowtie v.2.2.9 (Langmead & Salzberg 2012) and samtools v.1.3.1 (Li *et al.* 2009), with built-in normalization. We then refined the transcriptome based on the reference genome using Program to Assemble Spliced Alignment (PASA; Haas *et al.* 2003). The final assembly was evaluated for quality by calculating the contig ExN50 statistic using contig_ExN50_statistic.pl. Assembly completeness was assessed using BUSCO v.3.0.1 (Simao *et al.* 2015) based on the

expected gene content from near-universal single-copy orthologs in the Actinopterygii lineage dataset. Reads were mapped back to the assembly using align_and_estimate_abundance.pl with RSEM estimation and the bowtie aligner to generate sample-specific transcript counts. The assembly was annotated using Trinotate v.2.0.1 (http://trinotate.github.io/) with Transdecoder v.5.0.1 (http://transdecoder.sf.net).

5.3.10 Assessing Global Variation in Gene Expression

We performed a series of analyses including both RNA-seq experiments to assess broad-scale population variation (i.e., region effect) and technical variation between sequencing experiments (i.e., method effect), while accounting for technical variation between rearing experiments.

For both the reference-based and *de novo* transcriptome data, we constructed multidimensional scaling (MDS) plots based on log2 fold change (logFC) distances between samples calculated using the top 500 pairwise differently expressed genes. The raw counts were first TMM-normalized using edgeR (Chen *et al.* 2014) and transformed using the voomWithQualityWeights() function with quantile normalization in limma (Law *et al.* 2014). The MDS analysis was performed using edgeR to obtain coordinates for the first eight dimensions and Glimma (Law *et al.* 2016) to estimate the variance explained by each dimension. One-way ANOVAs were used to test for associations between logFC dimensions and experimental variables.

Due to the complex nature of the experimental design, we also assessed the hierarchical structure of gene expression variation using Grade of Membership (GoM) models implemented in CountClust (Dey *et al.* 2017). Unlike typical clustering models that partition samples into groups based on similar expression patterns, GoM, or admixture models, allow partial membership of each sample to multiple gene expression clusters. We exploit this functionality to infer the relative influences of correlated variables and complex genetic structure. A GoM model was fitted to the full data set using both the reference-based and *de novo*-generated read counts for values of K (number of clusters)

from 2-20 with a tolerance value of 0.1 and 1000 iterations. Model fit was assessed using the Bayes Factor.

Given the apparently lower sensitivity of the reference-based analyses to technical sources of variation, the remaining analyses were conducted using the reference-based transcriptome.

5.3.11 SNP Calling and Chromosomal Inversion Genotyping

We extracted SNPs from a combined dataset consisting of the 432 Risør and Helgeland reference-based transcriptomes as well as genomic reads from 861 Atlantic cod from the global Aqua Genome Project (e.g., see Barth *et al.* 2019). We used these SNPs to verify the genetic structure of populations and ecotypes in the present study, as well as to determine the chromosomal inversion haplotype at linkage groups (LGs) 01, 02, 07, and 12.

The read data from the 861 Atlantic cod specimens were separately processed using PALEOMIX (Schubert *et al.* 2014). Adapters were removed using AdapterRemoval v.1.5 (Lindgreen 2012) and aligned to the reference genome (Star *et al.* 2011; Tørresen *et al.* 2017) using BWA *mem* v.0.7.5a-r405 (Li & Durbin 2010). Reads that aligned with a minimum quality score (MapQ) of 25 were used for subsequent analyses. SNP genotypes were obtained using GATK v.3.4.46 (McKenna *et al.* 2010) after duplicate removal (Picard Tools v.1.96) and indel realignment (*GATKs IndelRealigner*). Genotypes were jointly (GATKs *Genotypecaller*) called for the 432 transcriptomic and 861 genomic samples separately with default settings, allowing a maximum of three alternate alleles. The 861-genome dataset was filtered with BCFTOOLS v.1.3 (Li *et al.* 2009) using parameters -e “FS>60.0 || MQRankSum<-12.5 || ReadPosRankSum<-8.0 || QD<2.0 || MQ<40' --SnpGap 10” and VCFTOOLS v.0.1.14 (Danecek *et al.* 2011), keeping bi-allelic loci with a maximum average read depth of 30 and a minimum MAF of 0.05. The genomic and transcriptomic datasets were intersected (BCFTOOLS *isec*), after which genotypes with a genotype quality <15 and read depth <3 were declared missing.

For inferring genome-wide population structure, SNPs were pruned (*--indep-pairwise 100 10 0.5*) for linkage disequilibrium (LD) using PLINK v1.90p (Purcell *et al.* 2007) and LG01, 02, 07 and 12 were excluded, which resulted in 318,574 SNPs. PCAs for the inverted regions of interest (LG01; 9.1 – 26.2 Mbp, LG02; 18.5 - 24 Mbp, LG07; 13.6 - 23 Mbp and LG12; 1.3 -13.6 Mbp) were generated without LD pruning (Ma & Amos 2012), which resulted in 15,991, 8,133, 11,573, and 12,144 SNPs, respectively. PCA was performed with smartPCA, EIGENSOFT v.6.1.4 (Patterson *et al.* 2006).

The results of the LD-pruned PCA were plotted for the study samples as well as for the North Sea, Western Baltic, and Tvedestrand fjord samples described by Barth et al. (2019) for reference. Tvedestrand fjord is adjacent to Risør fjord, and likewise includes individuals of fjord and North Sea ecotype (Knutsen *et al.* 2018), as well as a few intermediary and Western Baltic genotypes (Barth *et al.* 2019). Note that this analysis led us to classify the previously ambiguous adult genotype RIC5100 (according to the 26 SNP panel) as North Sea ecotype (see Chapter 4 Figure S2).

The results of the inversion-specific PCAs were plotted for the study samples alone. Based on the first principal components, which clearly distinguish haplotypes according to a typical trimodal pattern for a biallelic locus (Star *et al.* 2017), individuals were classified as either homokaryotypic A (extreme negative value), homokaryotypic B (extreme positive value), or heterokaryotypic AB (intermediate value). Allelic state relative to previous literature was inferred by comparing karyotype frequencies with those described by Berg et al. (2016), Sodeland et al. (2016), and Berg et al. (2017). Those haplotypes with frequencies consistent with the Northeast Arctic cod population were referred to as 'reference' because the Atlantic cod reference genome is based on a Northeast Arctic cod that is homokaryotypic for all inversions (Star *et al.* 2011; Tørresen *et al.* 2017). The alternative haplotype is referred to as 'non-reference'. It is not known which haplotypes represent the ancestral and derived inversion states. LG01 was monomorphic and therefore excluded from further analyses. Fishers exact tests were used to test for differences in inversion karyotype frequencies between Helgeland and Risør

(α=0.05).

5.3.12 Broad-Scale Differential Expression

We tested for regional variation in transcriptomes and transcriptomic plasticity between Helgeland and Skagerrak using a reaction norm framework, in which the intercepts and slopes of expression reaction norms for each gene are compared. To do this, we applied a generalized linear model with the limma package (Ritchie *et al.* 2015) on the full data set. The counts were filtered with an expression cut-off of 1 count per million (CPM) in at least two samples, TMM-normalized using edgeR (Chen *et al.* 2014) and transformed using the voomWithQualityWeights() function with quantile normalization prior to analysis (Law *et al.* 2014; Liu *et al.* 2015). Biological main effects included region, dph, temperature, mother and father [1]. Two-way interactions included dph with region, temperature, mother and father, separately. Three-way interactions included dph and temperature with region, mother and father, separately. Thus, the coefficients of interest (indicated in bold for this model) were the main effect of region (i.e., the difference in mean expression levels, or reaction norm intercepts) and the three-way nested interaction of dph, temperature, and region, which represents the difference in temperature effects between regions at each day separately (i.e., the difference in expression plasticity, or reaction norm slopes, at each time point). Technical variables included sequencing method, batch, and reverse library index. All variables were modelled as categorical fixed effects. For simplicity, 9°C and 9.5°C were considered to be the same level of temperature and 28 and 29 dph were considered to be the same level of dph. The number of differentially expressed genes was >0 for at least one coefficient of all model terms, thus all terms were retained.

[1] gene expression ~ **region** + dph + temperature + mother + father +
region:dph + temperature:dph + mother:dph + father:dph +
temperature:region:dph + temperature:mother:dph + temperature:father:dph +
method + batch + index

We removed Flødevigen from further analyses due to the large degree of technical variation between sequencing experiments.

5.3.13 Visualizing Biological Variation in Gene Expression

We constructed a series of GoM models for the Risør and Helgeland reference-based transcriptome data using CountClust (Dey *et al.* 2017). First, we visually confirmed batch effects by running a model with K=5 and grouping the samples by plate (Figure S2a). We repeated this model with counts that were adjusted for batch only and both batch and reverse index (Figure S2b) using linear models in the BatchCorrectedCounts() function. Remaining analyses were then performed on the batch- and index- corrected counts. GoM models were run for K=2 to *i,* where *i* is such that n/K is at least ~3, to a maximum K of 20. Therefore, we ran K=2-20 on the full data set, K=2-10 on the baseline samples, and K=2-20 on 2, 14, and 28 dph separately to assess cross-by-temperature interactions.

5.3.14 Microgeographic Scale Differential Expression

We tested for variation in transcriptomes and transcriptomic plasticity within the Risør fjord system using a generalized linear model with filtered, TMM-normalized counts, voom transformation with quality weights, and quantile normalization, as for the regional model (Law *et al.* 2014; Liu *et al.* 2015). Biological main effects included dph, temperature, location cross (Inner Risør × Inner Risør [I×I], Inner Risør × Outer Risør [I×O], or Outer Risør × Inner Risør [O×I]), ecotype cross (Fjord × Fjord [F×F], Fjord × North Sea [F×N], or North Sea × Fjord [N×F]), LG02 genotype, LG07 genotype, LG12 genotype, mother and father [2]. Two-way interactions included dph with temperature, location, ecotype, LG02 genotype, LG07 genotype, LG12 genotype, mother and father, separately. Three-way interactions included dph and temperature with location, ecotype, LG02 genotype, LG07 genotype, LG12 genotype, mother, and father, separately. Technical variables included sequencing batch and reverse library index. Thus, the coefficients of interest (indicated in bold for this model) were the main effects of location, ecotype, and LG02, 07, and 12 genotypes, and the three-way nested interactions

of dph and temperature with location, ecotype, and LG02, 07, and 12 genotypes, separately. All variables were modelled as categorical fixed effects. The number of differentially expressed genes was >0 for at least one coefficient of all model terms, thus all terms were retained.

[2] gene expression ~ **location** + **ecotype** + **LG02** + **LG07** + **LG12** + dph + temperature + mother + father + location:dph + ecotype:dph + LG02:dph + LG07:dph + LG12:dph + temperature:dph + mother:dph + father:dph + **temperature:location:dph** + **temperature:ecotype:dph** + **temperature:LG02:dph** + **temperature:LG07:dph** + **temperature:LG12:dph** + temperature:mother:dph + temperature:father:dph + batch + index

Venn diagrams of differentially expressed gene lists were constructed using Venny v.2.1 (http://bioinfogp.cnb.csic.es/tools/venny/).

5.3.15 Gene Ontology Enrichment Analysis

Gene ontology (GO) enrichment analysis was performed using ClueGO v.2.3.2 (Bindea *et al.* 2009) and BiNGO v.3.0.3 (Maere *et al.* 2005) in Cytoscape v.3.2.1 (Shannon *et al.* 2003) to identify significantly enriched GO terms in the category "biological processes" for differentially expressed genes (see Chapter 3 for further methodological detail). Briefly, annotations were compared to a human (in ClueGO) or custom (i.e., constructed from the Blastx hits from Trinotate; in BiNGO) gene ontology database. Due to the relatively high number of differentially expressed genes in the regional comparison, up- and down- regulated genes were analyzed separately. For the remaining comparisons, all dysregulated genes were analyzed together. The Gene Fusion option was used in ClueGO to enhance clustering. An FDR-corrected P-value of 0.05 and otherwise default parameters were used.

5.3.16 Broad-Scale Growth Reaction Norm Analysis

Growth reaction norms for the Risør crosses are presented in Chapter 4. Here, we tested whether initial length and the growth reaction norm of Helgeland differed from the Risør crosses for a comparison on a broad spatial scale. A linear mixed-effects model was used to test for differences in length between crosses at the beginning of the experiment (0 and 2 dph combined), with cross as a fixed effect and mother and father as random effects [3]. Parentage information was only available for 54/200 Helgeland larvae in this sample. We repeated the analysis for 1) all larvae and 2) all larvae for which parentage information was available.

[3] length ~ cross + mother + father

Differences in thermal growth reaction norms between crosses were tested using a mixed effects linear model on length at 28 dph, with cross, temperature, and their interaction as fixed effects, and tank, mother and father as random effects [4]. Parentage information was only available for 45/158 Helgeland larvae in this analysis. We repeated the analysis for 1) all larvae and 2) all larvae for which parentage information was available.

[4] length ~ cross + temperature + cross×temperature + tank + mother + father

Post-hoc contrasts were used to identify the differences in slopes and test for temperature effects within populations. P-values were considered significant at α=0.05. Model residuals for both growth analyses followed a normal distribution (Figure S3-4). Variances were fairly homogenous among treatments when all larvae were included, as assessed by visual inspection (Figure S5-6). Variance was slightly lower for Helgeland when those larvae lacking parentage information were excluded, but all variances were evenly distributed around zero (Figure S7-8). All statistical analysis on growth reaction norms and survival were conducted in R v.3.4.0 (R Development Core team 2015).

5.3.17 Broad-Scale Survival Reaction Norm Analysis

Survival of Risør larvae (analyzed in Chapter 4) was previously measured as the proportion of larvae from each population sampled in each tank at the end of the experiment and estimated in absolute terms by multiplying this proportion by the total number of larvae alive in each tank at the end of the experiment. Due to higher mortality of Helgeland larvae, survival was quantified as the time (dph) to complete mortality in the low-density tanks, which had the same initial number of larvae as the Risør experiment. If complete tank mortality did not occur, survival was quantified as the last day of the experiment (28 dph). Due to different survival metrics between rearing experiments, survival responses between populations were not compared quantitatively, but rather qualitatively with regards to whether there was an effect of temperature on survival. To test the effect of temperature on survival of Helgeland, we performed a one-way ANOVA with temperature as a fixed factor. Post-hoc contrasts were used to identify the differences (α =0.05).

5.3.18 Microgeographic Scale Length-at-Day Reaction Norm Analysis

Using those samples from Risør for which the inversion karyotype is known (i.e., those that were RNA sequenced) and excluding those for which length data were unavailable (n=4), we tested for variation in initial length and length-at-day reaction norms over time among locations, ecotypes, and chromosomal inversion karyotypes. A linear mixed effects model and ANOVA with type III sums of squares was used to test for differences in initial length (0 and 2 dph combined), with location, ecotype, and LG02, 07, and 12 genotypes as fixed effects and mother and father as random effects [5].

[5] length ~ location + ecotype + LG02 + LG07 + LG12 + mother + father

Differences in thermal reaction norms for length-at-day over time (2, 14, 21, and 28 dph) were tested using a linear mixed effects model similar to that used in the microgeographic scale differential expression analysis, with Type III sums of squares used for ANOVA. Main effects included dph, temperature, location, ecotype, LG02 genotype, LG07 genotype, and LG12 genotype [6]. Two-way interactions included dph with temperature,

location, ecotype, LG02 genotype, LG07 genotype, and LG12 genotype, separately. Three-way interactions included dph and temperature with location, ecotype, LG02 genotype, LG07 genotype, and LG12 genotype, separately. All fixed effects were modeled as categorical variables. Mother and father were included as random effects. Individuals with the rare homozygote genotype for LG02 (AA; n=19) and LG12 (BB; n=6) were removed prior to analysis in order to better balance the experimental design (total n = 318), considering that sample sizes were insufficient for reliable inference of interactions for those genotypes.

[6] length-at-day ~ location + ecotype + LG02 + LG07 + LG12 + dph + temperature + location:dph + ecotype:dph + LG02:dph + LG07:dph + LG12:dph + temperature:dph + temperature:location:dph + temperature:ecotype:dph + temperature:LG02:dph + temperature:LG07:dph + temperature:LG12:dph + mother + father

Model residuals were normally distributed (Shapiro-Wilk normality test, W=0.99, *P*=0.11). Visual inspection of residuals revealed that variances were homogenous among treatments (Figures S9-15), except for 2 dph, which had less variance but the residuals were evenly distributed around 0 (Figure S14).

We tested for interactions between genetic factors by expanding the previous model [6] with additional two-way interactions between all combinations of location, ecotype, LG02 genotype, LG07 genotype, and LG12 genotype, three-way interactions with dph, and four-way interactions with dph and temperature. However, this model was singular for mother (the variance explained by mother was 0; Table S2), so we proceeded with the previous approach with no interactions between genetic factors.

To facilitate interpretation of the three-way interactions in the full length-at-day model [6], we ran a simplified model on each dph separately [7].

[7] length-at-day ~ location + ecotype + LG02 + LG07 + LG12 + temperature + temperature:location + temperature:ecotype + temperature:LG02 + temperature:LG07 + temperature:LG12 + mother + father

Model residuals were normally distributed for 2, 21, and 28 dph (Shapiro-Wilk normality test, W=0.99, *P*=0.99 [2 dph], W=0.99, *P*=0.73 [21 dph], W=0.98, *P*=0.36 [28 dph]), but deviated slightly for 14 dph (W=0.99, *P*= 0.045). As with the full model, variances were fairly homogenous among treatments, as assessed by visual inspection of the residuals (data not shown).

To further test for independent effects of genetic factors in the presence of potential interactions, we ran reduced versions of the full length-at-day model [6] on three subsets of data: 1) pure Fjord crosses (IF×IF, IF×OF, and OF×IF), to test for a location effect independent of ecotype [8], 2) OF×IF and ON×IF only, to test for an ecotype effect independent of location [9], and 3) IF×IF only, to test for effects of LGs independent of location or ecotype [10].

[8] length-at-day ~ location + LG02 + LG07 + LG12 + dph + temperature + location:dph + LG02:dph + LG07:dph + LG12:dph + temperature:dph + temperature:location:dph + temperature:LG02:dph + temperature:LG07:dph + temperature:LG12:dph + mother + father

[9] length-at-day ~ ecotype + LG02 + LG07 + LG12 + dph + temperature + ecotype:dph + LG02:dph + LG07:dph + LG12:dph + temperature:dph + temperature: ecotype:dph + temperature:LG02:dph + temperature:LG07:dph + temperature:LG12:dph + mother + father

[10] length-at-day ~ LG02 + LG07 + LG12 + dph + temperature + LG02:dph + LG07:dph + LG12:dph + temperature:dph + temperature:LG02:dph + temperature:LG07:dph + temperature:LG12:dph + mother + father

Model residuals followed a normal distribution for model [9] (Shapiro-Wilk normality test, W=0.98, *P*=0.05), but deviated for models [8] (W=0.98, *P*=0.004) and [10] (W=0.92, *P*=0.001). As with the full model, variances were fairly homogenous among treatments except for 2 dph, which had less variance but the residuals were evenly distributed around 0 (data not shown).

5.3.19 Experimental Selection on Chromosomal Inversion Karyotypes

We investigated experimental, within-generation selection on LGs by testing for changes in LG karyotype frequencies over the course of the experiment in the same samples as the length-at-day analyses [n=318] and on two subsets representing the largest families (F03×RIC5064 [n=63] and RIC5060×RIC5076 [n=63]). Each LG was modelled separately, whereby karyotypes were considered binomial (as only one of the homokaryotypes were present) and used in a generalized linear model with dph, temperature, and their interaction as fixed effects [11].

[11] (homokaryotype, heterokaryotype) ~ dph + temperature + dph:temperature

Model residuals were normally distributed (Shapiro-Wilk normality test, W≥0.89, *P*≥0.08; Table S3), except for LG12 for the F03×RIC5064 subset in which the rearrangement was monomorphic (W=0.82, *P*= 0.007).

5.4 Results

5.4.1 Transcriptome Assembly and Abundance Estimation

The reference-based transcriptome consisted of 60,577 loci corresponding to 143,890 transcripts, with 65.3% novel loci (Table S4). The *de novo* pipeline with PASA refinement assembled 875,142 Trinity ‘genes’ corresponding to 1,383,739 unique isoforms. A peak N50 value (3507) around E90 (6.98) suggests that sufficient sequencing

depth was achieved and that approximately 23,656 biologically relevant transcripts were assembled (Figure S16). The *de novo* assembly included 4294/4584 (93.7%) complete and 216/4584 (4.7%) partial benchmarking universal single-copy orthologs (BUSCOs). Higher mapping rates were achieved using the reference genome compared to the *de novo* assembly, with an average of 95.1±1.2% and 84.1±1.5% of read pairs, respectively, being successfully mapped (Table S5).

5.4.2 Global and Technical Variation in Gene Expression

The first dimension of the MDS plot based on the reference-based analysis explained 3% of the variation and was associated with dph ($F_{6,455} = 117.03$, $P < 0.001$; Figure 5.2a-b). The second dimension, also explaining 3% of the variation, was associated with method ($F_{1,460} = 732.23$, $P < 0.001$; Figure 5.2c-d). The third dimension explained 2% of the variation and appeared to be associated with genetic background (Figure 5.2c). The remaining dimensions explained 1% or less of the variation.

The first dimension of the MDS plot based on the *de novo* transcriptome explained 14% of the variation and was associated with method and sequencing batch ($F_{5,456} = 3524.9$, $P < 0.001$; Figure 5.3a-b). The second and third dimensions, explaining 5% and 2% of the variation, respectively, separate the two regions ($F_{2,459} = 5.81$, $P = 0.003$ and $F_{2,459} = 350.73$, $P < 0.001$ for the second and third dimensions, respectively; Figure 5.3c-d). Notably, all the Flødevigen samples fall in the centre of the Risør sample cluster once the technical variation incorporated in the first dimension is removed. The remaining dimensions explained 1% or less of the variation.

Bayes Factors were not returned for the reference-based GoM models based on the full data set, although this should not affect the structure plot (https://github.com/kkdey/CountClust/issues/36). The Bayes Factor for each of the *de novo*-based GoM models of varying K increased steadily with several small "elbows" indicating larger improvements of the model fit with certain values of K (e.g., 2, 3, 5, 9, and 18) and a peak at K=19 (Figure S17a). For brevity, we present results from K=2, 5,

10, and 20 for both the reference- and *de novo*- based models (Figures 4 and 5, respectively). The *de novo* analysis clearly distinguished between methods while the reference-based analysis instead showed some similarities between the Flødevigen experiment and the remaining experiments. These results mirror the structure observed in the first dimensions of the MDS plots, in which technical sources of variation drive the major patterns observed in the *de novo* data but not the reference-based data. The remaining results were obtained from the reference-based analysis.

5.4.3 Population Genomic Structure

Principal component analysis of linkage-disequilibrium-purged genome-wide SNPs revealed genomic structure among study and reference populations (Figure 5.6). A subset of the Tvedestrand fjord reference samples clusters with the North Sea reference genotypes, while a few individuals fall among the Western Baltic genotypes, and the remainder (apart from a few intermediary genotypes) form a putatively fjord-type cluster (Barth *et al.* 2019). All F×F larvae formed a distinct cluster that overlapped with the fjord component of Tvedestrand cod. The ecotype hybrids (F×N and N×F) formed two slightly overlapping clusters midway between the fjord and North Sea clusters. Helgeland individuals clustered adjacent to the ecotype hybrids, in the direction of the North Sea cluster.

5.4.4 Chromosomal Inversion Genotypes

All 432 Risør and Helgeland offspring were homozygous for the LG01 haplotype (Figure 5.7a), characteristic of non-migratory coastal cod (Berg *et al.* 2017). LG02, LG07, and LG12 were polymorphic with frequencies (AA:AB:BB) of 22:189:221, 285:147:0, and 253:162:17, respectively. ‘A’ represents the non-reference haplotype and ‘B’ represents the reference haplotype, except for LG02 for which the reverse is true (Figure 5.7b-d, Table 5.1). All inversion haplotypes were found in all location crosses and ecotype crosses, as well as in the Helgeland cross (Table 5.1). Inversion frequencies differed between regions for LG02 (P=0.006), with an excess of the BB karyotype in Risør

(adjusted P=0.007), and LG12 (P<0.001), with an excess of the AA karyotype in Risør (adjusted P<0.001). LG07 karyotype frequencies did not differ significantly between regions (P=0.57).

5.4.5 Population Genomic Expression Structure

As the Bayes Factors increased fairly steadily with K for the GoM models based on the full Risør and Helgeland data set and the dph subsets (Figure S17b-f), we present K=5, 10, and 20. As observed in the reference-based MDS, gene expression structure showed a clear effect of dph (Figure 5.8). For example, in the K=5 model there is a shift from cluster 2 to cluster 3 membership over time. At K=10, within-day temperature effects are observed. K=20, cross substructure becomes more apparent, as well as its interaction with dph. For example, Helgeland shows substantial membership to cluster 17 at 28 dph but not at 2 dph.

For the baseline samples, we present K=3 and 9 to illustrate hierarchical levels of structure among crosses (Figure 5.9). At K=3, the pure fjord crosses show similar membership proportions that tend to be dominated by cluster 2. The remaining crosses tend to be dominated by cluster 1 and Helgeland in particular shows little or no membership to cluster 2. At K=9, the similarities in expression profiles of the fjord crosses is further evident. The remaining crosses show little or no membership to cluster 2, and Helgeland tends to have greater membership to clusters 7 and 8.

For the dph subsets, we present the results from the K=20 models (Figure 5.10). As GoM models were fitted to each dph separately, cluster identities are not necessarily comparable between dph. Therefore, we interpret variation across temperatures and crosses within dph, but not between dph. At all dph, overall differences between crosses is evident, with the pure fjord crosses appearing more similar to each other than to MIR, and the ecotype hybrids displaying somewhat intermediary expression patterns. Further, each cross shows a combination of shared and unique patterns associated with temperature.

At 2 dph, cluster 8 is evident in many individuals at 9.5°C and 13°C, but not at 6°C. OF×IF shows a reduction in clusters 3 and 4 and an increase in cluster 2 with increasing temperature. A reduction in cluster 2 at the highest temperature is evident in some, but not all crosses. Notably, Helgeland consistently displays substantial membership to cluster 2 at all temperatures, while there are subtle reductions in clusters 4, 9, and 18 with increasing temperature. IF×OF shows an increase in cluster 10. Interestingly, at 2 dph the two ecotype hybrids ON×IF and OF×ON show a small but consistent membership proportion to clusters 16 and 19, respectively. These clusters are largely absent from the pure fjord crosses, except at 6°C.

Temperature effects are more evident at 14 dph, with a tendency for cluster 2 to decrease and cluster 4 to increase with temperature in all Risør crosses except perhaps OF×ON, which had variable membership to cluster 2 at the 6°C. In contrast, Helgeland displays very little membership to clusters 2 and 4 at all temperatures, but an increase in cluster 14 and decrease in cluster 17 with increasing temperature.

Expression profiles are generally more similar across temperatures in the pure fjord crosses at 28 dph compared to 14 dph. However, decreasing membership to cluster 5 with temperature is evident in all Risør crosses, as well as increasing membership to cluster 9 and/or 10. A 6°C, the expression profiles of all Risør crosses are similar in comparison with the distinct profile of MIR, which is dominated by cluster 4. Helgeland consistently has the most distinct expression profile, which is characterized by increasing membership to cluster 8 and decreasing membership to clusters 4 and 18 with temperature (although the latter decrease is only evident at the highest temperature).

5.4.6 Broad-Scale Variation in Transcriptomes

Overall, 2056 out of 26,338 transcripts tested (7.8%) were differentially expressed between regions, with 1071 transcripts showing greater expression in Helgeland and 985 transcripts showing greater expression in Skagerrak (Table 5.2). Due to the large number

of differentially expressed transcripts, we used the ClueGO enrichment analysis, which implements upper-level GO term clustering, for those transcripts expressed higher in Helgeland and Skagerrak separately.

Transcripts expressed more in Helgeland were enriched for 95 GO terms that clustered into 31 GO groups. The largest GO groups (with the number of constituent GO terms contained in parentheses) were associated with DNA replication and telomere maintenance (13), histone modification (10), corticosteroid secretion and lipid localization (8), cell division (8), and DNA metabolism (7) (Figure 5.11a). Transcripts expressed more in Skagerrak were enriched for 873 GO terms that clustered into 102 GO groups. The largest GO groups were associated with development and growth (especially of the cardiac and nervous systems) (77), neurotransmitter activity associated with exploratory behaviour (60), ion transport and blood circulation (46), heart development (46), brain development (37), glucose metabolism (34), and cardiovascular activity (32) (Figure 5.11b). In addition, there was a group of 21 GO terms associated with intracellular signalling via regulation of the MAPK cascade (e.g., stress-activated MAPK cascade [GO:0051403]) that also included processes related to heart development (e.g., cardiac muscle tissue growth [GO:0055017]). One term relating to cell death was enriched among the transcripts expressed more in each of Helgeland (apoptotic DNA fragmentation [GO:0006309]) and Skagerrak (epithelial cell apoptotic process [GO:1904019]), but no further terms specific to 'stress', 'cell death', or 'DNA damage/repair' were enriched (Supplementary data 1).

5.4.7 Broad-Scale Variation in Transcriptomic Plasticity

In addition to differences in mean expression levels, transcriptomic plasticity in response to temperature differed between regions (Table 5.2). At 2 dph, 41 and 29 transcripts differed in their response to 9.5°C and 13°C relative to 6°C, respectively, whereas this increased to 562 and 354 transcripts at 14 dph, and 1183 and 2942 transcripts at 28 dph (Figure 5.12). However, only 26 transcripts differed in response to 13°C at 21 dph (there was no Helgeland sample collected at 9.5°C at this time point). Thus, the greatest

numbers of differentially plastic transcripts were observed at the end of the experiment and there was a 2.5-fold greater divergence in genomic reaction norms across the upper temperature range at this time point compared to the lower temperature range (Figure 5.12).

Significant GO enrichment was only detected among transcripts that were differentially plastic in response to temperature at 14 and 28 dph. At 14 dph, transcripts that differed between regions in response to 9.5°C were enriched for 313 GO terms in 32 groups. The largest groups (with the number of constituent GO terms contained in parentheses) were associated with cell cycle regulation (56), DNA replication associated with a DNA damage response (20), histone modification and chromosome organization (19), and RNA processing (16) (Supplementary data 2). Three terms specific to apoptosis were also detected (e.g., epithelial cell apoptotic process [GO:1904019]). Less enrichment was detected among the differential 13°C responses (33 GO terms in 8 groups). The largest groups mainly contained terms relating to lipid digestion (12), smooth muscle cell proliferation (6), and oxidant detoxification (5). There were also 6 GO terms directly relating to the inflammatory response, such as cytokine secretion (e.g., GO:0050663) and interleukin-1 beta production (GO:0032611).

At 28 dph, transcripts that differed between regions in response to 9.5°C were enriched for 515 GO terms in 83 groups. The largest groups were associated with protein metabolism and cell cycle arrest (77), nervous system development (28), histone modification and chromosome organization (25), regulation of gene expression (24), and neuron death induced by oxidative stress via the cellular stress response (23). Another group was associated with oxidative stress (10). Sixteen and two additional terms were related to apoptosis (e.g., execution phase of apoptosis [GO:0097194]) and the cellular response to stress (e.g., GO:0033554), respectively. A greater difference was observed in response to 13°C, consisting of 1704 enriched GO terms in 190 groups. The largest groups were associated with nervous system and organ development (154), protein metabolism and DNA-damage-induced cell cycle regulation (104), regulation of gene expression (85), cell signaling and protein metabolism (75), nervous system development

(56), insulin secretion and intracellular localization (53), neurological regulation of respiratory gaseous exchange (39), and cardiac activity (39). An additional 13 groups contained 94 terms associated with stress-induced DNA damage response and cell death, while 3 groups contained 20 terms related to oxidative stress (Supplementary data 1).

5.4.8 Broad-Scale Variation in Growth and Survival Plasticity

There was no effect of cross on initial length, whether all larvae were included ($F_{7,588}$=1.33, P=0.23; Table 5.3a) or only those with parentage information ($F_{7,444}$=1.28, P=0.26; Table 5.3b). There was a significant cross×temperature interaction for length at 28 dph whether all larvae were included ($F_{12,500}$=3.66, P<0.001; Table 5.4a) or only those with parentage information ($F_{12,388}$=3.55, P<0.001; Table 5.4b). We focus on the results of the analysis including all larvae (Table 5.5) because the variance attributed to the parents was low in both analyses (Table 5.4) and the 3.5-fold greater sample size of Helgeland in the analysis including all larvae is likely to provide more reliable estimates of growth for this population (see Table S6 for the alternative set of contrasts). Helgeland exhibited an increase in growth of 1.27±0.27 mm (mean±SEM) from 6°C to 9.5°C (t=4.74, P<0.001; Figure 5.13), but no significant growth plasticity from 9.5°C to 13°C (t=0.96, P=0.172)(Table 5.5). The plasticity of Helgeland across the lower thermal range was significantly different from all Risør crosses except for IF×ON (Table 5.5). Across the upper thermal range, Helgeland did not exhibit a significantly different response compared to the Risør crosses (Table 5.5).

There was a significant effect of temperature on survival of Helgeland larvae ($F_{2,6}$=6.87, P=0.028; Figure 5.14). Survival was significantly lower at 13°C compared to 6°C (t=3.71, P=0.010) but not compared to 9.5°C (t=1.81, P=0.120), and there was no difference between 6°C and 9.5°C (t=1.90, P=0.107). The premature termination of 6 out of 9 low density Helgeland tanks and lack of premature termination of Risør tanks of equal starting density is indicative of Risør larvae experiencing higher survival overall under the experimental conditions. Risør crosses only exhibited decreases in survival from 9.5°C to 13°C (Chapter 4), whereas Helgeland exhibited a decrease from 6°C to

13°C but not 9.5°C to 13°C (survival at 9.5°C was highly variable; Figure 5.14). This indicates that Helgeland and Risør differ in their survival plasticity, although we were unable to quantify this directly.

5.4.9 Microgeographic-Scale Variation in Transcriptomes

Among all mean pairwise contrasts between location (i.e., parental pre-spawning environment) crosses and ecotype crosses, there were 37 and 132 instances of differentially expressed transcripts out of the 25,227 tested, respectively (Table 5.2). For LG02, LG07, and LG12, there were 135, 7, and 46 instances of differentially expressed transcripts, respectively (Table 5.2). Due to the detection of fewer differentially expressed transcripts compared with the previous broad-scale analysis, we present the results of the custom-annotation-based BinGO enrichment analysis of total dysregulated transcripts at the microgeographic scale (Table S7).

The effect of location on mean expression was minimal (Table 5.2). The greatest differences were between O×O and the two hybrids crosses, I×O and O×I, with 10 and 14 differentially expressed genes, respectively. Only the two hybrid crosses showed no differential expression when compared with each other. However, there was no significant enrichment of biological processes in any location contrast.

Differential expression among ecotype crosses was substantial (Table 5.2). The 63 transcripts that were differentially expressed overall between F×F and F×N, representing the effect of paternal ecotype, were enriched for 16 GO terms primarily related to cell proliferation (e.g., cell division [GO: 51301], mitosis [GO: 7067]) and growth (e.g., organ growth [GO: 35265], growth involved in heart morphogenesis [GO: 3241](Table S8). No enrichment was detected among the 32 transcripts differentially expressed between F×F and N×F, representing the effect of maternal ecotype, and there was no overlap between these transcripts and those affected by paternal ecotype (Figure 5.15a). Only one GO term (hemopoietic progenitor cell differentiation [GO: 2244]) was enriched among the 37 transcripts differentially expressed between F×N and N×F.

LG02 marginally had the greatest impact on mean expression at the microgeographic scale (Table 5.2). The two homokaryotypes differentially expressed 83 transcripts that were enriched for 24 GO terms primarily involved in the regulation of translation (GO: 6417), porphyrin biosynthesis (GO: 6779), and cellular iron ion homeostasis (GO: 6879) (Figure 5.16; Table S8). Although it did not contribute to any enrichment, the gene for dermatopontin (DPT) was expressed at higher levels in the homokaryotype AA. The heterokaryotype exhibited intermediary differential expression from the homokaryotype BB. The majority of differentially expressed transcripts overlapped with those that differed between the homokaryotypes (38/48; Figure 5.15b), as did the enriched GO terms (6/8), which were associated with translation (e.g., GO: 6412). Only 4 transcripts were differentially expressed between the heterokaryotype and the homokaryotype AA and they were not annotated.

Only 7 transcripts were differentially expressed overall between homokaryotypes and heterokaryotypes for LG07 (Table 5.2) and they were not enriched for any biological processes. The LG12 homokaryotype AA differed from the heterokaryotype in the mean expression of 42 transcripts (Table 5.2). However, many of these were not annotated and the remainder was not enriched for any biological processes. Although it did not contribute to any enrichment, DPT was expressed at higher levels in the homokaryotype AA. The same two transcripts were dysregulated between the homokaryotype BB and the two other karyotypes (Figure 5.15c). These were enriched for 3 GO terms involved in energy metabolism (e.g., mitochondrial citrate transport [GO: 6843]) (Table S8).

5.4.10 Microgeographic-Scale Variation in Transcriptomic Plasticity

Location had the greatest impact on transcriptomic plasticity at the microgeographic scale (Figure 5.17, Table 5.2). The greatest differences between responses of location crosses were observed at the earlier time points (2 and 14 dph) and between I×I compared to the two hybrid crosses, I×O and O×I (Figure 5.17a-b).

At 2 dph, transcripts that differed between locations in response to 9.5°C were enriched for varied GO terms related to early development, such as the regulation of determination of dorsal identity (GO: 2000015) and angiogenesis (GO: 45765) (Table S9). Large numbers of genes showing differences in transcriptomic plasticity to 13°C between I×I and the hybrid crosses I×O (99 GO terms) and O×I (50 GO terms) were enriched for processes relating to cellular respiration (e.g., ATP synthesis coupled proton transport [GO: 15986]), RNA synthesis (e.g., ribonucleotide biosynthetic process [GO: 9260]) and amino acid metabolism (e.g., cellular amino acid catabolic process [GO: 9063]). O×I also differed from I×O and O×O in response to 13°C for genes that were enriched for sugar metabolism (e.g., hexose transport [GO: 8645] and glycolysis [GO: 6096] for I×O and O×O, respectively).

At 14 dph, I×I differed from O×I and O×O in response to 9.5°C for genes enriched for growth factor receptor signaling (e.g., regulation of insulin-like growth factor receptor signaling pathway [GO: 43567]). Diverse processes were enriched among differential responses to 13°C (Table S9). These included the post-translational modification glycosylation (I×I vs. O×I and O×O; e.g., protein amino acid C-linked glycosylation [GO: 18103] and protein amino acid N-linked glycosylation [GO: 6487], respectively), growth factor receptor signaling (I×I vs. O×I; e.g., regulation of insulin-like growth factor receptor signaling pathway [GO: 43567]), neuron development (I×I vs. O×O; e.g., ganglioside biosynthetic process [GO: 1574]), and DNA replication (O×O vs. I×O and O×I; e.g., DNA unwinding involved in replication [GO: 6268]).

Diverse processes were also enriched among differential responses to 9.5°C at 21 dph, including cell signaling (I×O vs. I×I and O×I; e.g., negative regulation of nitric-oxide synthase activity [GO: 51001] and semaphorin-plexin signaling pathway [GO: 71526], respectively), post-translational modification (I×I vs I×O and O×I; e.g., protein geranylgeranylation [GO: 18344]), and rRNA modification (O×O vs. I×I and O×I [GO: 154]) (Table S9). At 13°C, only 2 GO terms involved in cell morphogenesis were enriched among genes that were differentially plastic between location crosses (I×I vs. I×O; e.g., regulation of cell shape [GO: 8360]).

At 28 dph, 50 GO terms primarily involved in brain and nervous system development were enriched among genes that were differentially plastic between I×I and the hybrid crosses in response to 9.5°C (e.g., hypothalamus cell differentiation [GO: 21979], nerve development [GO: 21675]) (Table S9). Energy metabolism (e.g., mitochondrial citrate transport [GO: 6843]) was widely enriched among differentially plastic genes in response to 13°C, while genes that differed in plasticity between I×I and I×O were also enriched for intracellular cAMP-mediated signalling (GO: 19933) associated with the dopamine receptor signaling pathway (GO: 7212).

Ecotype had comparatively little effect on transcriptomic plasticity (Table 5.2). An ecotype effect was essentially only detected early in development and there was no apparent association between the magnitude of plasticity differences and temperature (Figure 5.17g-i). The only enrichment detected was among genes that were differentially plastic in response to 9.5°C between the ecotype hybrids at 14 dph. These GO terms were involved in lipid metabolism (e.g., positive regulation of lipid catabolic process [GO: 50996]), nutrient transport (e.g., carnitine transport [GO: 15879]), and eating behaviour (GO: 42755) (Table S9).

Due to a limited distribution of LG02 AA karyotypes in the experiment, we were only able to test for differences in plasticity between the heterokaryotype and BB homokaryotypes across all temperatures and time points (Table 5.2). This revealed moderate levels of differentially plastic expression, particularly in the short-term responses to 13°C (Figure 5.17j), but limited enrichment. Notably, the gene for heat shock cognate 70 kDa protein (HSP70) was among those that were differentially plastic in response to 13°C at 2 dph, while many others lacked annotations (20/29 at 2 dph and 14/16 at 14 dph). Differential responses to 9.5°C at 21 dph had 4 enriched GO terms, mostly involved in MAPK cell signalling (e.g., regulation of stress-activated MAPK cascade [GO: 32872]) (Table S9). Interestingly, the one reaction norm for which it was possible to test for differences in transcriptomic plasticity between the AA homokaryotype and the alternate karyotypes (response to 9.5°C at 28 dph) resulted in the

enrichment of 33 (AA vs. AB) and 50 (AA vs. BB) GO terms associated with brain and nervous system development (e.g., forebrain neuron development [GO: 21884] and vestibulocochlear nerve development [GO: 21562]), energy metabolism (e.g., citrate transport [GO: 15746]), and heart development (e.g., outflow tract morphogenesis [GO: 3151]), the latter of which was more prevalent in the comparison between homokaryotypes.

Low levels of variation in transcriptomic plasticity were observed between LG07 AA and AB karyotypes (Figure 5.17k, Table 5.2). Enrichment was only detected among genes that were differentially plastic in response to 13°C at 14 dph. These 40 GO terms were associated with diverse processes including the circadian regulation of gene expression (GO: 32922), DNA damage response (e.g., DNA damage induced protein phosphorylation [GO: 6975]), chloride transport (GO: 6821), and several terms relating to various metabolic processes (e.g., carbohydrate biosynthetic process [GO:16051], gluconeogenesis [GO: 6094], lipid storage [GO:19915]) (Table S9).

Due to a limited distribution of LG12 BB karyotypes in the experiment, we were only able to test for differences in plasticity between AA and the heterokaryotype across all temperatures and time points (Table 5.2). Despite this, LG12 had a relatively large impact on differential responses to 9.5°C and 13°C at the microgeographic scale, affecting 18 and 74 genes at 2 dph and 62 and 13 genes at 14 dph, respectively (Figure 5.17l). Enrichment was detected at 2 dph in the differential response to 13°C and consisted of diverse processes associated with cellular respiration [GO: 45333], RNA synthesis (e.g., ribonucleotide biosynthetic process [GO: 9260]), gas transport (e.g., carbon dioxide transmembrane transport [GO: 35378]), and muscle development (e.g., striated muscle cell development [GO: 55002]) (Table S9). At 21 dph, only one GO term (rRNA modification [GO: 154]) was enriched among differential responses to 9.5°C. At 28 dph, 8 and 3 GO terms associated with energy metabolism (e.g., mitochondrial citrate transport [GO: 6843]) were differentially plastic among responses to 9.5°C and 13°C, respectively.

5.4.11 Microgeographic-Scale Variation in Growth Reaction Norms

There were significant effects of ecotype (χ^2=33.94, P<0.001) and location (χ^2=20.03, P<0.001), but not LG ($\chi^2 \leq 2.56$, $P \geq 0.110$) on initial length (Figure 5.18, Table 5.6). N×F was significantly larger than F×F and F×N, and O×I was significantly smaller than I×I and I×O (Table 5.7). Consequently, OF×IF and ON×IF were the smallest and largest cross, respectively (Figure 5.18).

Length increased over time (χ^2=15.29, P=0.002), although at 6°C and, to a lesser extent, 13°C, the lower length limit at 14 dph is lower than that at 2 dph (Figure S18). There was also a significant LG02×dph interaction (χ^2=12.73, P=0.005) and 3-way interaction with temperature (χ^2=15.63, P=0.048) for length-at-day (Table 5.8). Analysis of each dph separately revealed a LG02 karyotype×temperature interaction for length at 14 dph (Table 5.9). LG02 AB had a significantly more negative slope from 6°C to 9.5°C compared to BB (-1.4+0.59, t=-2.38, P=0.019; Figure 5.19). There was no difference between LG02 karyotypes in slopes from 9.5°C to 13°C at 15 dph (t=0.15, P=0.444). No other fixed effects were significant in the analysis of all dph (Table 5.8) or each dph separately (Table 5.9). Father explained 5% of the variance in length-at-day in the full model (Table 5.8) and 1-23% of the variance at each dph (Table 5.9). Mother explained <0.001% of the variance in the full model (Table 5.8) and 1% and 4% of the variance at 2 and 21 dph, respectively (the variance for mother was not estimable at 14 and 28 dph).

Notably, in the (computationally singular) model containing interactions among all genetic factors, there were significant effects of LG12 and an interaction effect with LG02 (Table S2), warranting further investigation into the relationship between these structural variants. The fjord ecotype-only model, though deviating from normality, did not detect an effect of location independent of ecotype (χ^2=2.93, P=0.23) (Table S10). The O×I-only model, though computationally singular for mother, did not detect an effect of ecotype independent of location (χ^2=2.7206, P=0.10) (Table S11). The IF×IF-only model, though deviating from normality, supported effects of LG02 and LG12 (Table S12).

5.4.12 Experimental Selection on Chromosomal Inversion Genotypes

The frequency of the LG02 BB karyotype increased over the course of the experiment (P=0.004; Figure 5.20a, Table 5.10a). There was also a significant dph×temperature interaction for LG07 karyotype frequency (P=0.020; Table 5.10a), whereby the frequency of the AA karyotype decreased over time at 6°C but increased over time at 9.5 and 13°C (Figure 5.20a). LG12 karyotype frequency did not vary by dph (P=0.987), temperature (P=0.734), or their interaction (P=0.644; Figure 5.20a, Table 5.10a).

The frequency shift observed in LG02 karyotypes was also observed when one of the largest families, F03×RIC5064, was examined separately (P<0.001; Figure 5.20b, Table 5.10b). This family was monomorphic for the LG12 A arrangement and had approximately even proportions of LG07 karyotypes that did not vary with dph (P=0.883), temperature (P=0.898), or their interaction (P=0.522) (Figure 5.20b, Table 5.10b). The other largest family, RIC5060×RIC5076, exhibited an increase in LG07 AA karyotype over time (P=0.016), but there was no significant dph×temperature interaction (P=0.135) despite an apparent trend (Figure 5.20c, Table 5.10c). All RIC5060×RIC5076 larvae were homokaryotypic BB at LG02 and heterokaryotypic at LG12.

5.5 Discussion

5.5.1 Genomic Basis of Adaptation at Multiple Spatial Scales

Using a common-garden-gradient experimental design, we revealed the relative contributions of different architectures of genomic divergence on local adaptation with gene flow at multiple spatial scales. Altogether, our findings suggest that, at a broad spatial scale characterized by moderate gene flow, differentiation located throughout the genome likely contributes most to local adaptation. However, at a microgeographic scale with relatively high gene flow, chromosomal inversions contribute most to local adaptation. While consistent with theoretical expectations (Yeaman & Otto 2011;

Yeaman & Whitlock 2011), these findings represent a novel empirical investigation of the mechanisms underlying adaptation with gene flow and provide insights into the genomic basis of functional variation in gene expression, phenotypes, and their thermal plasticities with direct links to fitness.

Overall, the greatest differences in genome-wide expression, thermal plasticity for gene expression, and survival occurred between larvae from Helgeland and Skagerrak, separated by ~1300 km of coast. These populations also differed in length-at-day reaction norms across the lower (6-9.5°C) thermal range at which little or no variation was detected within Skagerrak. Intriguingly, we found variation for genome-wide expression uniquely attributable to divergence between fjord and North Sea ecotypes and chromosomal inversion haplotypes, as well as effects of pre-spawning location and inversion haplotypes on thermal plasticity for gene expression. LG02 had the greatest impact on gene expression at the microgeographic scale (<20 km^2), while also affecting reaction norms for body length. LG02 and LG07 also displayed significant shifts in karyotype frequencies consistent with within-generation directional selection during the experiment, whereby the direction of selection on LG07 depended on temperature. Notably, differential expression and differentially plastic expression were one to three orders of magnitude greater (according to the numbers of differentially expressed genes) between regions than within the Skagerrak region.

5.5.2 Macrogeographic Scale Variation

5.5.2.1 Neutral and Adaptive Variation

There are several reasons to suggest that the functional variation observed between regions in the present study is largely adaptive in nature, as opposed to being purely the result of neutral processes. Generally, high effective population sizes, connectivity, and fecundity (Ward *et al.* 1994; Poulsen *et al.* 2006; Therkildsen *et al.* 2010) suggest that selection is the main driver of genomic differentiation in cod (Allendorf *et al.* 2010). Consistent with this hypothesis, F_{ST} is generally lower for neutral markers relative to the

rest of the genome (e.g., in the study system [neutral F_{ST} vs. genome-wide F_{ST}]: 0.00519<0.00839 for coastal cod *vs.* North Sea, Berg *et al.* 2016; 0.0037<0.0063 for inner Risør *vs.* outer Risør, Knutsen *et al.* 2011; Sodeland *et al.* 2016). Differentiation between Helgeland and Skagerrak at neutral markers is nevertheless estimated to be low but significant (F_{ST} = 0.0069-0.0093) and a weak pattern of isolation by distance is supported (Dahle *et al.* 2018). The regions also differ in the frequencies of LG02 and LG12 inversion karyotypes, which were not factored into the macrogeographic scale differential expression analysis due to a lack of inversion genotypes for Flødevigen larvae. However, given the relatively low impact of the inversions on gene expression in the microgeographic scale analysis, we infer that the majority of the differential expression between regions is not attributable to the inversions. Instead, differential selection is likely acting broadly across the genome, in addition to on the inversion polymorphisms, with divergence between regions enhanced by a small degree of isolation by distance. Comparing F_{ST} estimates from neutral and outlier (with and without the inversions) loci in the parental generation would shed further light on this theory. Including all factors in a differential expression model tested on the full data set would reveal the relative contributions of the inversions on local adaptation at the regional scale, but would need to be compared to the analyses herein in order to disentangle effects across multiple spatial scales.

5.5.2.2 Epigenetic Variation

We cannot rule out the possibility that regional differences are due in part to epigenetic variation stemming from environmental influences on the parental generation prior to collection (reviewed by Donelson *et al.* 2018), despite our efforts to minimize its influence (discussed in Chapter 4). Parental effects were not detected in the previous analysis of growth and survival plasticity in Risør (Chapter 4) or similar studies (Oomen & Hutchings 2015b, 2016) and there was no difference in initial larval size between regions that might indicate a region-specific maternal effect (Marshall 2008). Nonetheless, epigenetic effects can impact mRNA abundance directly and thus are likely more easily detectable through differential expression analysis. Therefore, epigenetic

effects likely contribute to the gene expression differences between regions, but are unlikely to be solely responsible for shaping the phenotypic and fitness outcomes we observe. This is supported by a lack of effect of location on mean gene expression at the microgeographic scale, as well as relatively little variation in expression plasticity compared to that observed at the regional scale (discussed below). Of course, epigenetic variation is expected to be greater on the macrogeographic scale. Further investigation, such as through bisulfite sequencing (Meissner *et al.* 2005) to map methylation patterns in the parents and offspring, is needed to evaluate this.

5.5.2.3 Growth and Survival Reaction Norms

The high overall mortality of Helgeland relative to Risør at all temperatures and increasing mortality with temperature is consistent with this more northerly population being poorly adapted to increases in temperature beyond those typically experienced in the wild. In contrast, Risør larvae overall experienced the highest survival at the intermediate temperature, although it did not differ significantly from the low temperature for most crosses (Chapter 4). Nevertheless, these mortality patterns are consistent with local adaptation resulting in decreased fitness as temperatures extend upwards beyond those typically experienced, and suggest that the critical temperature threshold is lower for the putatively cold-adapted Helgeland compared to Risør. It is unknown how either region would respond to the even colder temperatures that Helgeland might experience in the wild, thus preventing a complete test of 'strict' local adaptation (*sensu* Kawecki & Ebert 2004).

Despite increasing mortality, Helgeland larvae were ultimately larger at warmer temperatures relative to the coldest temperature. Increasing growth with temperature is typical of cod (Hutchings *et al.* 2007; Oomen & Hutchings 2015b, 2016) and marine fish larvae in general (Pepin 1991), but it might lead to faster depletion of energy reserves (Conover & Present 1990; Billerbeck *et al.* 2001, Chapter 3). A stable, cold-adapted population such as Helgeland might have experienced selection for energy savings at cold temperatures, which could explain the slower growth at the coldest temperature (Pörtner

et al. 2008). Energy savings was also suggested as a mechanism to explain non-plastic growth of a fall spawning component of Northwest Atlantic cod that experience cold, decreasing temperatures during the larval stage (Oomen & Hutchings 2015b, 2016). It is unlikely that the observed variation in length-at-day reaction norms is purely the result of size-selective mortality during the experiment, given their lack of correspondence with the survival responses, although it might be a contributing factor.

5.5.2.4 Genomic Reaction Norms

Mean expression differences in nearly 8% of the transcriptome suggest that Helgeland and Skagerrak larvae were in markedly different physiological states overall. Skagerrak larval expression is indicative of more active exploratory behavior and enhanced heart and nervous system development relative to Helgeland (Figure 5.11b). In general, activity levels are used as a larval performance indicator (Skiftesvik 1992), whereby higher activity suggests enhanced foraging capacity and greater energy store availability (O'Brien-Macdonald *et al.* 2006; Claireaux & Lefrançois 2007). Vital organ development is presumably a healthy sign of energy being allocated to growth. Concurrently, higher foraging rates would place increased demands on developing cardiovascular and nervous systems, perhaps further stimulating their development. A relative reduction of these processes in Helgeland larvae suggests a reduced energy budget and lower rates of feeding and development. Consistent with this, Helgeland larvae were smaller than those of Risør, though only at the coldest temperature most similar to that experienced in the wild. Energetic limitations will not necessarily be reflected in smaller sizes at higher temperatures, which can obscure the effects of reduced foraging on growth (Killen & Brown 2006). To a far lesser degree, Helgeland expression is indicative of higher rates of DNA replication, metabolism, modification, and maintenance, as well as cell division (Figure 5.11a). The functional significance of this is currently unclear.

Differentially plastic gene expression between regions is largely related to core components of the cellular stress response (Kultz et al. 2005, see Chapter 3), such as cell cycle regulation and arrest, DNA repair, protein metabolism, and apoptosis. This is in

contrast with the lack of evidence for differences in the mean expression of stress-related processes, despite differences in mortality rates. Divergence in genomic stress reaction norms increased over time, suggesting that responses to chronic thermal stress differ more than short-term responses and that acclimation capacities differ between regions. For example, differences in the amount of cell death, a last line of defense characteristic of severe stress (Kültz 2005), appear to increase from 2 to 14 to 28 dph at the intermediate temperature and were greatest at the highest temperature at the end of the experiment. Despite evidence of increasing stress differences with temperature, Helgeland larvae achieved similar lengths to most of the Risør crosses at the two warmer temperatures, perhaps representing a maximum size under the conditions or selective mortality of larger sizes.

All crosses experienced the lowest survival at the highest temperature and, at the end of the experiment, the regional difference in expression response to this temperature was 1.5-fold greater than the mean expression difference between regions. This suggests that environmental extremes can reveal cryptic diversity in expression plasticity. Further, it suggests that divergence in expression plasticity could have a greater impact on fitness than divergence in mean expression. Differences in expression plasticity at 28 dph suggest that the thermal sensitivity of development differed between regions. Differentially plastic expression also relates specifically to the neurological regulation of respiratory gas exchange, suggesting different degrees or mechanisms of compensation for increased metabolic rate and decreased oxygen availability at higher temperatures (Piiper 1982; Nilsson & Lefevre 2016). In addition to the core cellular stress response, these differences were associated with differential plasticity for genes involved in oxidative stress-induced neuron death, suggesting differing degrees of neurological impairment at high temperatures. Compromised neural function has been implicated in setting the lethal upper thermal limit in some ectotherms (e.g., Ern *et al.* 2015). However, we do not know which region, if any, experienced a more severe decline in survival with temperature because survival metrics differed between populations. Further, the directions of expression plasticity and its divergence need to be examined before drawing conclusions about the specific mechanisms of mortality at higher temperatures.

5.5.3 Microgeographic-Scale Variation

5.5.3.1 Parental Pre-spawning Location and Potential Epigenetic Effects

Within the high gene flow Risør fjord system, local adaptation to the sheltered inner fjord environment could manifest through multiple, non-exclusive genomic mechanisms: 1) higher frequency of fjord relative to North Sea ecotypes, as found by Knutsen et al. (2018); 2) higher frequencies of particular chromosomal inversion polymorphisms, as documented by Sodeland et al. (2016); and 3) other within-ecotype adaptive variation associated with subtle landscape genetic structure (for which there is currently no supporting evidence). The latter factor is represented in the present study by the parental pre-spawning location (i.e., inner and outer Risør). Given that the Risør larvae clustered by ecotype rather than location in the LG-purged genome-wide SNP analysis, we infer such landscape genetic structure to be negligible relative to the other genomic factors. Indeed, location had little or no impact on length-at-day reaction norms or mean gene expression. However, it had the greatest effect on transcriptomic plasticity at the microgeographic scale. As discussed previously, location is confounded by parental environmental influences on the F1 generation and gene expression can be a sensitive measurement of transgenerationally plastic effects (Shama *et al.* 2016).

Ecotypes and inversions exhibit clear genomic divergence, yet their effects on expression plasticity were smaller than or similar to the size of the location effects, supporting a negligible role of hypothetical landscape genetic structure on generating the differentially plastic expression observed. Therefore, epigenetic variation is most likely responsible in this case. A positive effect of inner Risør maternal origin on initial length suggests a possible maternal effect in particular (Marshall 2008). However, the limited differences in mean expression despite initial size variation suggest that the maternal effect might manifest largely through non-mRNA deposits, such as nutrients, as was proposed for brook charr (*Salvelinus fontinalis*; Bougas *et al.* 2013).

Most of the differentially plastic expression attributed to location was observed between the pure inner Risør cross and the reciprocal location hybrids and, consistent with parental effects, was stronger earlier in development (Lindholm *et al.* 2006; Bougas *et al.* 2013). At 2 dph, location modulated larval development differently in response to the intermediate temperature. Cellular respiration (the earliest physiological response to warming) was differentially plastic in response to the highest temperature. These responses did not differ functionally between reciprocal location hybrids, suggesting that maternal and paternal effects are of a similar nature in this case, but the paternal effect was ~3-fold larger than the maternal effect based on the numbers of differentially expressed transcripts. Paternal effects also influence thermal reaction norms for hatching success in Atlantic cod (Dahlke *et al.* 2016), suggesting they might play an underappreciated role in transgenerational thermal plasticity during very early life when the mother is considered to have a dominant influence (Mousseau & Fox 1998; Marshall 2008; Shama *et al.* 2016).

Parental effects on expression plasticity of insulin-like growth factor receptor signaling, which plays a crucial role in the neuroendocrine regulation of somatic growth in fishes (Wood *et al.* 2005), were observed in response to both warmer temperatures at 14 dph. Various parental effects persisted, though to a lesser degree, until 28 dph, at which time they appear to differentially modulate nervous system development in response to the intermediate temperature and energy metabolism in response to the highest temperature. We did not detect variation in length-at-day reaction norms specifically attributable to location. However, this analysis lacked the power of the previous reaction norm analyses, as we were limited to the samples for which we had transcriptome data in order to account for inversion genotypes. Therefore, epigenetic parental effects might influence transcriptomic plasticity in response to temperature during larval development. These effects might alter the relationship between developmental rate and temperature, but the resulting phenotypic and fitness consequences are not yet clear.

5.5.3.2 Coexisting Ecotypes

Variation in cod life history and reproductive traits has been documented along the Norwegian coast at fine spatial scales by comparing individuals from different locations (e.g., Olsen *et al.* 2004, 2008; Kuparinen *et al.* 2015; Roney *et al.* 2016). In general, Norwegian coastal cod have been assumed to have a homogeneous genetic background for local selection to act upon, which we now know not to be the case owing to historically diverged ecotypes coexisting in coastal waters (Jorde *et al.* 2018; Knutsen *et al.* 2018; Sodeland *et al.* in review) and spatial variations in the frequencies of large chromosomal inversions (e.g., (Berg *et al.* 2015; Sodeland *et al.* 2016; Barth *et al.* 2017). Yet, this phenotypic and genomic variation has yet to be linked, preventing our understanding of the genomic basis of adaptive variation in cod. We present the first study linking molecular and phenotypic variation at a fine spatial scale while controlling for environmental influences, thereby revealing the potential adaptive mechanisms underlying the maintenance of sympatric ecotypes and inversion polymorphisms in a high gene flow environment.

While the effect of ecotype on mean gene expression was substantial, it differed between reciprocal ecotype crosses, suggesting an ecotype-by-parent interaction effect. The paternal ecotype effect was twice that of the maternal effect and involved completely different genes, which were associated with cell proliferation, growth, and development. Knutsen et al. (2018) found differences in size-at-age between ecotypes in the wild, whereby North Sea juveniles tended to be larger than fjord juveniles. A failure of known environmental variables to fully account for such variation suggested at least a partial genetic basis. In the present study, larvae from the maternal North Sea ecotype cross had a larger initial size. The functional significance of the genes modulated by maternal ecotype requires more detailed investigation, as they were not enriched for any biological processes. Ecotype also had a relatively minor, yet specific, effect on expression plasticity in response to the intermediate temperature at 14 dph that is consistent with differential responses of feeding, digestion, and metabolism; processes tightly linked to growth. However, we did not detect variation in length-at-day reaction norms specifically attributable to ecotype in our limited investigation of these effects. Still, the probable role of differential gene expression in promoting divergent growth rates among ecotypes

warrants further investigation, especially in light of the potential for growth rate variation to contribute to maintaining ecological divergence in a shared environment (Hutchings 1993; Knutsen *et al.* 2018).

5.5.3.3 Chromosomal Inversions

The roles of the inversions on LG02, 07, and 12 in local adaptation have been difficult to disentangle from the ecotypes and from one another, because they often show parallel allele frequency clines and there is some evidence of inter-chromosomal linkage disequilibrium (Bradbury *et al.* 2014; Berg *et al.* 2015). The present study reveals unique roles and putative functions of each inversion polymorphism, while also providing the first limited evidence of functional interactions between them.

5.5.3.3.1 Inversion on LG02

The reference LG02 haplotype occurs at high frequencies in very cold environments and low salinity environments with deep, hypoxic basins (Bradbury *et al.* 2010, 2014, Berg *et al.* 2015, 2017). As such, it is nearly fixed in the Northeast Arctic and Baltic cod ecotypes (Berg *et al.* 2015, 2017). Yet, it also exhibits consistently higher frequencies within fjords in western Skagerrak compared to adjacent outer coastal areas and the North Sea (Sodeland *et al.* 2016), as well as in particularly sheltered fjords in eastern Skagerrak (Barth *et al.* 2017). The sheltered inner fjord environment shares similarities with the Baltic Sea, in terms of relatively low salinity, due to high freshwater input and partially restricted exchange with more saline oceanic water, and the presence of deep, largely hypoxic basins (Barth *et al.* 2017). This estuarine environment has been proposed to drive divergent selection for the reference haplotype through its role in osmoregulation (Sodeland *et al.* 2016; Barth *et al.* 2017). However, this does not explain its high frequency in Northeast Arctic cod, which are exposed to relatively high oceanic salinities, nor the temperature-associated clines observed throughout the North Atlantic (Bradbury *et al.* 2010, 2014; Berg *et al.* 2017).

The upper water layer beneath the freshwater surface layer in the Risør fjord, where pelagic larvae reside, is characterized by normoxia and a salinity of 32-33 ppt. (Bergstad *et al.* 1996). In the present study, which was conducted using normoxic full strength seawater from the Skagerrak (33.8-34.5 ppt.; Roney 2016), homozygotes for the reference haplotype on LG02 were rare and heterokaryotypes were strongly selected against at all temperatures. This is consistent with the reference haplotype conferring a fitness disadvantage at oceanic salinities. Intriguingly, mean gene expression differences between LG02 karyotypes implicate it in regulating oxygen delivery. Hemoglobin transports oxygen to tissues through the bloodstream. It is composed of four subunits surrounding a heme, which is a complex consisting of an iron ion and a porphyrin molecule (Perutz 1979). LG02 karyotypes differed in the expression of genes enriched for porphyrin biosynthesis and cellular iron ion homeostasis, as well as hemoglobin subunit alpha-2 (Hb-α2), consistent with an effect of the inversion on oxygen transport. The number of differentially expressed transcripts between homokaryotypes was nearly twice that between the heterokaryotype and the non-reference homokaryotype (BB), while the heterokaryotype and the reference homokaryotype (AA) showed very few differences, a pattern consistent with additive dominance of the inversion. In all three karyotypic comparisons, most transcripts (a ratio of 3-4:1) were expressed more in the karyotype containing more of the reference haplotype, indicating that it largely increases expression of genes involved in oxygen transport. Whether this reflects higher constituent expression of these pathways, which may be costly in the normoxic laboratory environment, or a state of oxygen limitation in LG02 reference haplotype-rich karyotypes is unclear.

Although we found no evidence from karyotype frequency shifts that the strength of selection on LG02 varied with temperature across a 7°C range, the inversion polymorphism was the only factor found to affect thermal plasticity for length-at-day. At 14 dph, the heterokaryotype exhibited little or no plasticity across the lower thermal range, while the non-reference homokaryotype displayed a positive change in length with temperature. There is evidence that this is, to some extent, the result of selective mortality against larger sizes at 6°C. The observation of several larvae at 14 dph that are smaller relative to the size distribution at 2 dph at this temperature indicates that the proportion of

small larvae (in addition to large larvae) increased during this time period. This period encompasses the highest mortality event during the larval stage: the initiation of exogenous feeding and subsequent starvation upon failure and depletion of energy reserves (O'Brien-Macdonald *et al.* 2006). The divergent LG02 reaction norms at 14 dph indicate that the smaller larvae were non-reference homokaryotypes. Selection against large sizes of this genotype, which exhibited transcriptomic signatures of lower oxygen delivery, is consistent with a failure to meet the higher aerobic demands of a larger body size (Gillooly *et al.* 2001). Why this difference is observed only at the coldest temperature is unclear, as oxygen limitation on body size generally increases with temperature (Bergmann 1847; Gillooly *et al.* 2001).

LG02 also modulated transcriptomic plasticity in response to temperature. This effect was greatest in the short-term response to the highest temperature, supporting a role for the inversion in the acute thermal stress response. Most of the genes that were differentially plastic between the heterokaryotype and non-reference homokaryotype lacked annotations. One exception is HSP70, a critical component of the heat shock response that can be activated by both warm and very cold temperatures (Tomanek 2010; Chen *et al.* 2018). Interestingly, HSP70 is located in the inversion on LG07 (Berg *et al.* 2017), suggesting possible interactions between LG02 and 07 inversion polymorphisms. Differentially plastic expression between the reference homokaryotype and karyotypes possessing the non-reference haplotype at 28 dph suggest that the inversion affects nervous and cardiovascular system development and energy metabolism in response to temperature at the end of the larval stage, but the fitness impacts are unclear.

Interestingly, one of the two hemoglobin gene clusters in Atlantic cod is located on LG02 near the inversion (MN; Bradbury *et al.* 2010; Berg *et al.* 2015; Hoff *et al.* 2018). It contains the gene for hemoglobin subunit beta-1 (Hb-β1), which is famously characterized by a polymorphism associated with oxygen binding affinity (Sick 1965). This polymorphism appears to show similar clines in haplotype frequencies as the inversion on LG02 in the Northeast Arctic, Baltic, and North Sea cod (Andersen *et al.* 2009; Berg *et al.* 2015, 2016), although it is not yet known to what extent they may be

linked and the Hb-β1 allele frequencies in the inner fjord environment are unknown. An interaction between the Hb-β1 and LG02 inversion polymorphisms, such as inversion-associated modulation of Hb-β1 expression or *vice versa*, could help explain the adaptive significance of the inversion in the inner fjord and Arctic environments in light of its association with osmoregulation (Berg *et al.* 2015, 2016; Barth *et al.* 2017). It might also explain the surprising results of a recent study that found no effect of temperature or Hb-β1 polymorphism on oxygen binding in cod from the warm-adapted Irish Sea (Barlow *et al.* 2017), where the non-reference haplotype is dominant (Bradbury *et al.* 2010; Berg *et al.* 2016; Sodeland *et al.* 2016). We found no evidence of differentially plastic expression levels of Hb-β1 associated with LG02 haplotype, although we did for Hb-α2, which is located in the other hemoglobin gene cluster on LG18 (LA; Hoff *et al.* 2018). Regardless of a potential interaction with the Hb-β1 polymorphism, which is purely speculative, evidence supports an interaction with one of the hemoglobin gene clusters and a major role for the LG02 inversion in oxygen regulation and fitness, thus warranting further investigation of its role in adaptation to diverse environments.

5.5.3.3.2 Inversion on LG07

The inversion polymorphism on LG07 has been associated with temperature at broad spatial scales throughout the North Atlantic (Bradbury *et al.* 2010). It has also been linked to migratory behaviour (Hemmer-Hansen *et al.* 2013; Berg *et al.* 2017), which is often associated with latitude/temperature (Berg *et al.* 2017). However, at small spatial scales, it is not associated with bottom temperature and salinity (Berg *et al.* 2015) or inner fjord and oceanic environments (Sodeland *et al.* 2016; Barth *et al.* 2017). Thus, the factors underlying its range-wide polymorphism remain perhaps the most mysterious of the four large chromosomal inversions.

We found evidence of divergent selection on LG07 during the larval stage with a thermal threshold between 6 and 9.5°C. The non-reference homokaryotype undergoes positive selection at the intermediate and high temperatures, but negative selection at the low temperature. This pattern is consistent with the higher prevalence of the non-reference

haplotype in warm-adapted/non-migratory wild populations (Berg *et al.* 2017). In contrast, the presence of a reference haplotype, which is more common in cold-adapted/migratory populations, appears to be advantageous at 6°C. We suggest that balancing selection acting through an LG07 inversion-based thermal threshold could be responsible for the range-wide patterns of allele frequencies observed. Such a threshold explains the maintenance of the polymorphism in the coastal environment, and through much of the species range, as seasonal and year-to-year thermal variability would likely span alternative selective states (Figure 5.1b, Righton *et al.* 2010).

While relatively few differences in expression were detected between LG07 karyotypes overall, there is evidence for a role in diverse processes in response to high temperature at 14 dph, including those related to DNA repair and circadian rhythm. DNA repair is a core component of the cellular and thermal stress response (Kültz 2005, Chapter 3). Circadian rhythm is closely tied to temperature, which, along with photoperiod, entrains daily metabolic and behavioural cycles through the actions of clock genes (Dunlap 1999; Vallone *et al.* 2007). Gene expression associated with circadian rhythm was altered by both heat and cold stress in pre-feeding zebrafish (*Danio rerio*) larvae (Long *et al.* 2012), suggesting a role in responding to general thermal stress. This might involve the potential of clock genes to enable metabolic shifts, another hallmark of the cellular stress response (Kültz 2005). Indeed, differential expression plasticity of several metabolic processes in the present study is consistent with a shift between lipid and carbohydrate metabolism, a mechanism that has been observed in response to thermal stress and cold adaptation in other fishes (reviewed by Logan & Buckley 2015). We note that oxygen concentration varied naturally with temperature in the experiment, as in the wild. Therefore, we are unable to separate their synergistic effects, but our findings are more ecologically relevant for it.

5.5.3.3.3 Inversion on LG12

The LG12 inversion polymorphism has largely been associated with thermal clines in the wild (Bradbury *et al.* 2010; Berg *et al.* 2015) and the reference haplotype is nearly fixed

in extreme cold-adapted Northeast Arctic cod (Berg *et al.* 2017). It also shows a shift in haplotype frequencies between the inner fjords of the western Skagerrak and the North Sea (Sodeland *et al.* 2016). Survival of homokaryotypic reference/North Sea adults was lower than that of fjord ecotypes in Tvedestrand fjord, indicating possible selection against the LG12 reference haplotype and/or North Sea ecotype in the fjord environment (Barth *et al.* 2019). In agreement with this, the non-reference arrangement was observed at a higher frequency in the fjord ecotype compared to the ecotype hybrids in the present study and the reference homokaryotype was rare.

We found no evidence of experimental selection on the LG12 inversion, as frequencies were consistent across times and temperatures. Yet, the inversion haplotype affected the expression of genes involved in cellular respiration, largely through differentially plastic expression in response to higher temperatures that, somewhat variably, persisted through the larval stage. Gene expression, carbon dioxide transport, and muscle development also appear to be differentially regulated between haplotypes in the short-term (2 dph) response to the highest temperature. Plasticity for these processes could represent different mechanisms of maintaining homeostasis across a wide range of temperatures, which could explain the apparent lack of impact on fitness at the experimental temperatures. The large number of genes differentially regulated in response to temperature coupled with the temperature-associated clines in the wild suggests an important role of LG12 in thermal regulation.

The inversion on LG12 contains the gene DPT (Berg *et al.* 2017), which encodes the extracellular matrix protein dermatopontin. Dermatopontin accelerates the formation of collagen fibrils and stabilizes them against dissociation at cold temperatures (Macbeath *et al.* 1993). Both LG02 and LG12 altered the mean expression of DPT, whereby homokaryotypes for the arrangement that is overrepresented in the fjord ecotype showed higher levels of expression. The inner Risør fjord is covered in sea ice during the winter, as are several other highly sheltered Skagerrak fjords (Bergstad *et al.* 1996) where strong frequency shifts have been observed in the LG02 and/or LG12 inversions (Sodeland *et al.* 2016; Barth *et al.* 2017). Under the ice, inner fjord larvae might be exposed to

temperatures well below 6°C, especially right after hatch when they are not yet able to swim to deeper, warmer waters. Our findings suggest that the LG02 and LG12 inversion polymorphisms have a polygenic effect on a gene involved in cold protection on LG12 that might contribute to adaptation to sea ice conditions. Fine-scale mapping of temperature, salinity, and ice between 0 and 5 m depths within fjords and a test for an association between sea ice cover and inversion haplotype frequencies would shed light on this theory.

5.5.4 Directions for Future Research

The lack of experimental selection on LG12 could be due to rearing temperatures above those that are relevant for its adaptive function or the result of the sample selection process for RNA sequencing, which aimed for equal numbers of location/ecotype crosses. Due to the relationship between the crosses and the inversions, this procedure is biased for selection of balanced inversion frequencies, making the tests for experimental selection on inversion haplotypes highly conservative. Thus, they may have obscured signatures of selection acting on LG12 or masked a temperature effect on LG02, neither of which should be ruled out. Obtaining inversion genotypes (e.g., using a set of diagnostic SNP markers) for the remaining ~1100 Risør larvae that were not sequenced would permit a robust test for selection on the inversions. It would also enable a stronger analysis of length-at-day reaction norms and assessment of size-selective mortality.

Due to the skewed frequencies of ecotypes and inversion haplotypes, we were unable to evaluate the pure North Sea ecotype or, to varying degrees, the rare homokaryotype for each chromosomal inversion. This limited our ability to quantify the full extent of divergence between haplotypes. We suggest that the true effects are likely greater than those documented in the present study. Some of the effects could result from non-additive genetic architectures, such as overdominance or underdominance. Nonetheless, the present study accurately reflects the genomic diversity in the coastal study area, in addition to having broader implications for cod throughout the North Atlantic.

We present limited evidence for interactions between the inversions, particularly between LG02 and LG07 (through the modulation of HSP70) and LG02 and LG12 (through a possible interaction effect on length-at-age in the full genetic interaction model, which we were unable to properly assess, and polygenic effects on DPT). Signatures of inter-chromosomal linkage disequilibrium in the wild further support investigating the potential for such interactions (Bradbury *et al.* 2014; Berg *et al.* 2015). Mapping the genomic locations of all genes that were differentially expressed between inversion karyotypes would illuminate this possibility.

Finally, because adults were held in a common spawning environment and all eggs were incubated at the lowest experimental temperature, we are unable to disentangle pure temperature effects from mismatches in thermal history between life stages or generations. A factorial design for spawning, incubation, and rearing temperatures would be informative in this regard (e.g., Shama *et al.* 2016), though would represent a substantial logistical challenge.

5.5.5 The Role of Chromosomal Inversions in Ecotype Divergence

We provide the first experimental evidence for the putative adaptive functions of three large chromosomal inversions that are polymorphic throughout the range of Atlantic cod. These inversions, especially the one located on LG02, have strong effects on gene expression and thermal plasticity. For LG02 and LG07, direct impacts on fitness are consistent with directional selection by salinity and temperature, respectively. Differential gene expression also supports divergent growth rates of fjord and North Sea ecotypes. However, LG02 appears to moderate an interaction between size and temperature, associated with the regulation of oxygen delivery and possibly related to the nearby hemoglobin gene complex. LG12 might interact with LG02 and confer adaptation to extreme cold. Chromosomal rearrangements can capture coadapted alleles or alter the expression of nearby genes (Coghlan *et al.* 2005; Wellenreuther & Bernatchez 2018). Distinguishing between these causes underlying the adaptive nature of a rearrangement, although not mutually exclusive, remains a major question in the quest to understand the

role of structural genomic variation in evolution (Wellenreuther & Bernatchez 2018) and should be investigated further in the context of the present study.

The relatively strong effects of the inversions likely underlie the ability of divergent ecotypes to inhabit overlapping ranges, while contributions of these inversions to life history or behavioural variation would help maintain ecological divergence among ecotypes (Barth *et al.* 2019). In insects, inversions maintain sympatric mimetic morphs of *Heliconius numata* butterflies (Joron *et al.* 2013) and sympatric host races of apple maggots (*Rhagoletis pomonella*; Feder *et al.* 2003). Genomic field investigations have shown that inversions facilitate adaptive divergence in hybrid zones of marine and freshwater threespine sticklebacks (*Gasterosteus aculeatus*; Jones *et al.* 2012; Roesti *et al.* 2015) and between migratory ecotypes of Atlantic cod (Berg *et al.* 2016, 2017; Kirubakaran *et al.* 2016; Sinclair-Waters *et al.* 2018). In a rare example of a test for local adaptation with gene flow, a combination of reciprocal transplants and quantitative trait loci mapping implicated chromosomal inversions in life-history divergence between connected populations of yellow monkeyflowers (*Mimulus guttatus*; Lowry & Willis 2010). Therefore, the potential for adaptation with gene flow, and the role of chromosomal inversions in it, should not be underestimated and will become increasingly understood as technological advances improve our ability to detect genomic structural variation in non-model species.

5.5.6 Conservation and Management Implications

Given the high levels of inversion polymorphism observed throughout the North Atlantic and the potential for linked gene complexes to confer rapid adaptation (Tigano & Friesen 2016; Kirkpatrick 2017), cod may be suited to readily adapt to a variety of environmental scenarios, so long as genomic diversity is maintained, populations are sufficiently large (Hoffmann *et al.* 2017), and depending on the degree to which the inversions may be linked. Importantly, non-inversion-associated adaptive variation is also evident at broader spatial scales (Helgeland *vs.* Skagerrak). Coastal cod in Norway are currently managed as two units defined as North and South of 62°N. The present study adds to a growing body

of research demonstrating that these management units have little basis in biological reality (e.g., Dahle *et al.* 2018; Jorde *et al.* 2018; Knutsen *et al.* 2018) and provides some explanation of why current management regulations are failing (ICES 2018). In particular, evidence of highly locally adapted fjord populations, which are preferentially targeted by the largely unregulated recreational fisheries (Jorde *et al.* 2018), is now abundantly clear (Roney *et al.* 2016, 2018b; Sodeland *et al.* 2016; Barth *et al.* 2017; Knutsen *et al.* 2018). A new fisheries management strategy is required that accounts for local adaptation at multiple spatial scales that is associated with multiple genomic architectures, especially in the face of rising sea temperatures.

5.6 Conclusion

The genomic mechanisms underlying adaptation with gene flow have implications for how natural populations will respond to environmental change (Razgour *et al.* 2018). Considering these genomic architectures when delineating units for conserving vulnerable species and managing harvested populations is likely to result in more effective actions (Bernatchez 2016; Pearse 2016; Bernatchez *et al.* 2017). Although inferring that particular genetic variants are adaptive based on genotype-phenotype and genotype-fitness associations is problematic (Barrett & Hoekstra 2011; Pearse 2016), such inferences provide testable hypotheses for determining the targets and agents of natural selection.

The present study sheds light on how cod populations have adapted in the face of gene flow and the potential for them to respond to environmental change. As dispersal is a common strategy for escaping unfavourable changes in environmental conditions, understanding this mode of evolution will be especially important for predicting the adaptive potential of vagile species and predicting their dynamics and distributions in the context of anthropogenic change (Tigano & Friesen 2016). The highly connected marine environment faces unprecedented threats from climate change, overharvesting, habitat alteration, and pollution. Failure to identify adaptive variation in marine species will

inhibit effective protection of biodiversity and sustainable use of biological resources in a changing world (Savolainen *et al.* 2013; Bernatchez 2016).

5.7 Tables

Table 5.1: Frequencies of chromosomal inversion genotypes for linkage groups 02, 07, and 12 in crosses in the present study and others, indicating the names used by each study to denote the reference (in bold) and non-reference arrangement according to the reference genome (Star *et al.* 2011; Tørresen *et al.* 2017). The key indicates which samples represent the same or similar populations.

		LG02			LG07			LG12			Reference
	Key	***AA***	*AB*	*BB*	*AA*	***AB***	***BB***	*AA*	***AB***	***BB***	
I×I	*a*	0.19	0.38	0.42	0.90	0.10	0.00	0.58	0.41	0.01	
I×O and O×I		0.02	0.53	0.45	0.64	0.36	0.00	0.90	0.08	0.02	
O×O	*b*	0.00	0.02	0.98	0.42	0.58	0.00	0.00	1.00	0.00	
F×F		0.09	0.39	0.53	0.63	0.37	0.00	0.85	0.15	0.00	
F×N and N×F		0.00	0.44	0.56	0.69	0.31	0.00	0.40	0.56	0.03	
Helgeland	*c*	0.05	0.62	0.34	0.69	0.31	0.00	0.12	0.71	0.17	
		AA	*AB*	*BB*	*AA*	***AB***	***BB***	*BB*	***AB***	***AA***	*Berg et al. 2016*
Northeast Arctic Cod	*d*	0.96	0.04	0.00	0.00	0.14	0.86	0.00	0.02	0.98	
Norwegian Coastal Cod	*c*	0.19	0.44	0.37	0.50	0.42	0.08	0.06	0.17	0.77	
North Sea	*e*	0.00	0.14	0.86	0.75	0.25	0.00	0.16	0.48	0.36	
		II/II	*I/**II***	*I/I*	*II/II*	***I**/II*	***I/I***	*II/II*	***I**/II*	***I/I***	*Sodeland et al. 2016*
Inner coastal	*a*	0.11	0.40	0.49	0.51	0.41	0.08	0.63	0.33	0.04	
Outer coastal	*b*	0.02	0.11	0.86	0.80	0.19	0.01	0.55	0.33	0.12	
Oceanic	*e*	0.00	0.08	0.92	0.56	0.36	0.08	0.14	0.50	0.36	
		I	*NI/**I***	*NI*	*NI*	*NI/**I***	***I***	*NI*	*NI/**I***	***I***	*Berg et al. 2017*
Migratory	*d*	0.91	0.09	0.00	0.00	0.11	0.89	0.00	0.04	0.96	
Non-migratory		0.37	0.37	0.25	0.26	0.50	0.24	0.25	0.28	0.46	

Table 5.2: Numbers of genes that differ in mean expression and transcriptomic plasticity to temperature in pairwise contrasts on regional and microgeographic spatial scales. Contrasts are denoted A - B where A is the point of contrast.

		Mean expression differences			Differences in transcriptomic plasticity							
		All dph			2 dph		14 dph		21 dph		28 dph	
Factor	Contrast	+	-	DE	6-9.5°C	6-13°C	6-9.5°C	6-13°C	6-9.5°C	6-13°C	6-9.5°C	6-13°C
region	N - S	1071	985	2056	41	29	562	354	0	26	1183	2942
location	I×I - I×O	1	1	2	16	250	31	15	8	3	8	8
	I×I - O×I	4	4	8	11	76	45	22	6	4	3	7
	I×I - O×O	3	0	3	2	5	11	11	5	4	2	0
	I×O - O×I	0	0	0	4	9	0	8	7	1	2	1
	I×O - O×O	3	7	10	2	2	6	4	5	10	1	5
	O×I - O×O	12	2	14	1	14	5	4	5	6	0	6
ecotype	F×F - F×N	22	41	63	6	0	10	9	1	1	0	0
	F×F - N×F	6	26	32	6	0	6	9	1	1	0	0
	F×N - N×F	17	20	37	0	0	10	0	0	0	0	0
LG02	AA - AB	1	3	4	-	-	-	-	-	-	4	-
	AA - BB	22	61	83	-	-	-	-	-	-	5	-
	AB - BB	10	38	48	1	29	4	16	9	3	0	4
LG07	AA - AB	4	3	7	6	3	3	5	0	3	9	0
LG12	AA - AB	11	31	42	18	74	62	13	4	3	3	4
	AA - BB*	2	0	2	-	-	-	-	-	-	-	-
	AB - BB*	2	0	2	-	-	-	-	-	-	-	-

*lg12BB n=6

- No differential expression test was performed.

Table 5.3: Results of a linear mixed effects model for initial larval length (0 dph and 2 dph combined) for 7 crosses of Atlantic cod from Risør and Helgeland for (a) all larvae and (b) all larvae for which parentage information is available. Asterisks denote significance at α=0.05.

(a) All larvae					
Model term	d.f.	Sum of squares	Mean of squares	*F*	*P*-value
cross	6	0.40	0.07	1.50	0.241
Model term	Variance	SD			
father	0.00	0.01			
mother	0.01	0.10			
residual	0.04	0.21			
(b) All larvae with parentage information					
Model term	d.f.	Sum of squares	Mean of squares	*F*	*P*-value
cross	6	0.35	0.06	1.44	0.197
Model term	Variance	SD			
father	0.00	0.02			
mother	0.01	0.11			
residual	0.04	0.20			

Table 5.4: Results of a linear mixed effects model for larval growth for 7 crosses of Atlantic cod from Risør and Helgeland for (a) all larvae and (b) all larvae for which parentage information is available. Asterisks denote significance at α=0.05.

(a) All larvae

Model term	d.f.	Sum of squares	Mean of squares	*F*	*P*-value	
cross	6	5.78	0.96	2.57	0.019	*
temperature	2	7.84	3.92	10.46	<0.001	*
cross×temperature	12	16.48	1.37	3.66	<0.001	*

Model term	Variance	SD
father	0.03	0.16
mother	0.08	0.29
tank	0.04	0.21
residual	0.38	0.61

(b) All larvae with parentage information

Model term	d.f.	Sum of squares	Mean of squares	*F*	*P*-value	
cross	6	5.10	0.85	2.52	0.021	*
temperature	2	2.86	1.43	4.23	0.015	*
cross×temperature	12	14.38	1.20	3.55	<0.001	*

Model term	Variance	SD
father	0.02	0.16
mother	0.05	0.22
tank	0.03	0.18
residual	0.34	0.58

Table 5.5: Effect of increasing temperature on larval growth of Atlantic cod from Helgeland and differences in thermal plasticity between Helgeland and 6 crosses from Risør fjord. All larvae were included in the analysis. Estimates of interaction effects represent differences in slopes relative to Helgeland. Asterisks denote significance at α=0.05.

Contrast	Estimate	SEM	*t*	*P*-value	
Temperature effect					
6-9.5°C	1.27	0.27	4.74	<0.001	*
9.5-13°C	-0.28	0.29	-0.96	0.172	
Cross-by-temperature interaction with Helgeland at 6-9.5°C					
IF×IF	-0.95	0.35	-2.74	0.005	*
IF×OF	-1.12	0.42	-2.66	0.016	*
OF×IF	-1.16	0.35	-3.34	0.001	*
IF×ON	-0.48	0.40	-1.21	0.127	
ON×IF	-1.18	0.50	-2.35	0.039	*
OF×ON	-1.11	0.41	-2.70	0.011	*
Cross-by-temperature interaction with Helgeland at 9.5-13°C					
IF×IF	-0.03	0.38	-0.07	0.472	
IF×OF	-0.02	0.54	-0.03	0.488	
OF×IF	0.54	0.36	1.52	0.068	
IF×ON	-0.61	0.41	-1.48	0.085	
ON×IF	0.57	0.44	1.29	0.116	
OF×ON	-0.55	0.48	-1.15	0.150	

Table 5.6: Results of a linear mixed effects model for initial length (0 dph and 2 dph combined) of larval Atlantic cod from Risør fjord. Asterisks denote significance at α=0.05.

Model term	χ2	d.f.	*P*-value	
ecotype	33.94	2	<0.001	*
location	20.03	2	<0.001	*
LG02	0.00	1	0.968	
LG07	2.56	1	0.110	
LG12	0.00	1	0.972	

Model term	Variance	SD
father	<0.001	<0.001
mother	<0.001	0.01
residual	0.04	0.20

Table 5.7: Results of post-hoc contrasts for a linear mixed effects model for initial length (0 dph and 2 dph combined) of larval Atlantic cod from Risør fjord. Asterisks denote significance at α=0.05. Estimates (±SEM) are given above the diagonal and P-values below. The point of contrast for the estimates is the row header. Asterisks denote significance at α=0.05.

Ecotype	F×F	F×N	N×F
F×F	-	-0.05 (0.09)	0.43 (0.07)
F×N	0.300	-	0.52 (0.12)
N×F	**<0.001***	**<0.001***	-
Location	I×I	I×O	O×I
I×I	-	0.04 (0.07)	-0.24 (0.08)
I×O	0.287	-	-0.28 (0.06)
O×I	**0.003***	**<0.001***	-

Table 5.8: Results of a linear mixed effects model for growth of larval Atlantic cod from Risør fjord from 2 to 28 dph. Asterisks denote significance at α=0.05.

Model term	$\chi 2$	d.f.	*P*-value	
ecotype	0.10	2	0.950	
location	0.34	3	0.953	
LG02	0.28	1	0.598	
LG07	0.10	1	0.755	
LG12	0.27	1	0.602	
dph	15.29	3	0.002	*
temperature	0.52	2	0.769	
ecotype×dph	4.65	6	0.590	
location×dph	11.35	8	0.183	
LG02×dph	12.73	3	0.005	*
LG07×dph	1.26	3	0.738	
LG12×dph	0.91	3	0.824	
temperature×dph	5.10	6	0.531	
ecotype×dph×temperature	10.54	16	0.837	
location×dph×temperature	21.66	17	0.198	
LG02×dph×temperature	15.63	8	0.048	*
LG07×dph×temperature	9.79	8	0.280	
LG12×dph×temperature	6.93	8	0.544	

Model term	Variance	SD
father	0.05	0.23
mother	<0.001	<0.001
residual	0.27	0.52

Table 5.9: Results of linear mixed effects models for length-at-day of larval Atlantic cod from Risør fjord at 2, 14, 21, and 28 dph. Asterisks denote significance at α=0.05.

2 dph				
Model term	χ2	d.f.	*P*-value	
ecotype	5.62	2	0.060	
location	2.29	2	0.318	
LG02	0.99	1	0.320	
LG07	2.14	1	0.143	
LG12	0.01	1	0.914	
temperature	2.05	2	0.359	
ecotype×temperature	6.33	4	0.176	
location×temperature	3.52	4	0.474	
LG02×temperature	0.26	2	0.879	
LG07×temperature	3.41	2	0.182	
LG12×temperature	2.06	2	0.356	
Model term	Variance	SD		
father	0.01	0.08		
mother	0.01	0.11		
residual	0.03	0.18		
14 dph				
Model term	χ2	d.f.	*P*-value	
ecotype	1.67	2	0.435	
location	4.44	3	0.217	
LG02	0.07	1	0.792	
LG07	2.65	1	0.103	
LG12	0.01	1	0.912	
temperature	2.54	2	0.280	
ecotype×temperature	6.77	4	0.149	
location×temperature	9.68	5	0.085	
LG02×temperature	6.44	2	0.040	*
LG07×temperature	0.10	2	0.953	
LG12×temperature	1.67	2	0.434	
Model term	Variance	SD		
father	0.03	0.18		
mother	0.00	0.00		
residual	0.46	0.68		
21 dph				
Model term	χ2	d.f.	*P*-value	
ecotype	0.23	2	0.892	
location	0.80	3	0.850	
LG02	1.47	1	0.226	
LG07	1.58	1	0.209	
LG12	2.40	1	0.122	
temperature	2.49	2	0.288	
ecotype×temperature	1.34	4	0.854	
location×temperature	0.89	4	0.926	
LG02×temperature	4.16	2	0.125	
LG07×temperature	2.82	2	0.245	
LG12×temperature	4.25	2	0.119	
Model term	Variance	SD		
father	0.07	0.26		
mother	0.04	0.19		
residual	0.18	0.42		

Continued on next page.

28 dph			
Model term	$\chi 2$	d.f.	*P*-value
ecotype	2.49	2	0.288
location	4.10	3	0.251
LG02	1.07	1	0.300
LG07	2.31	1	0.128
LG12	1.26	1	0.261
temperature	2.21	2	0.330
ecotype×temperature	5.94	4	0.204
location×temperature	3.80	4	0.434
LG02×temperature	0.98	2	0.613
LG07×temperature	4.53	2	0.104
LG12×temperature	2.26	2	0.323
Model term	Variance	SD	
father	0.23	0.48	
mother	0.00	0.00	
residual	0.34	0.59	

Table 5.10: Tests for experimental selection on chromosomal inversion haplotypes using a generalized linear model for haplotype frequencies for (a) all Risør larvae and (b-c) the two largest families. The P-values were obtained from $\chi 2$ tests of whether the model fit improved by sequentially adding population, temperature, and their interaction to the null model. Asterisks denote significance at $\alpha=0.05$.

Model term	d.f.	Deviance	Residual d.f.	Residual deviance	*P*-value	
(a) All Risør larvae						
LG02						
null			14	19.12		
dph	1	8.22	13	10.90	0.004	*
temperature	1	2.48	12	8.41	0.115	
dph×temperature	1	0.41	11	8.01	0.523	
LG07						
null			14	23.80		
dph	1	1.25	13	22.55	0.263	
temperature	1	2.92	12	19.62	0.087	
dph×temperature	1	5.42	11	14.21	0.020	*
LG12						
null			14	4.84		
dph	1	0.02	13	4.83	0.897	
temperature	1	0.12	12	4.71	0.734	
dph×temperature	1	0.21	11	4.50	0.644	
(b) F03×RIC5064 only						
LG02						
null			14	49.33		
dph	1	18.18	13	31.15	<0.001	***
temperature	1	0.00	12	31.15	0.995	
dph×temperature	1	2.41	11	28.74	0.121	
LG07						
null			14	5.93		
dph	1	0.02	13	5.91	0.883	
temperature	1	0.02	12	5.89	0.898	
dph×temperature	1	0.41	11	5.49	0.522	
LG12						
null			14	0.00		
dph	1	0.00	13	0.00	1.000	
temperature	1	0.00	12	0.00	1.000	
dph×temperature	1	0.00	11	0.00	1.000	
(c) RIC5060×RIC5076 only						
LG02						
null			14	0.00		
dph	1	0.00	13	0.00	1.000	
temperature	1	0.00	12	0.00	1.000	
dph×temperature	1	0.00	11	0.00	1.000	
LG07						
null			14	46.15		
dph	1	5.81	13	40.33	0.016	*
temperature	1	2.84	12	37.49	0.092	
dph×temperature	1	2.24	11	35.25	0.135	
LG12						
null			14	0.00		
dph	1	0.00	13	0.00	1.000	
temperature	1	0.00	12	0.00	1.000	
dph×temperature	1	0.00	11	0.00	1.000	

5.8 Figures

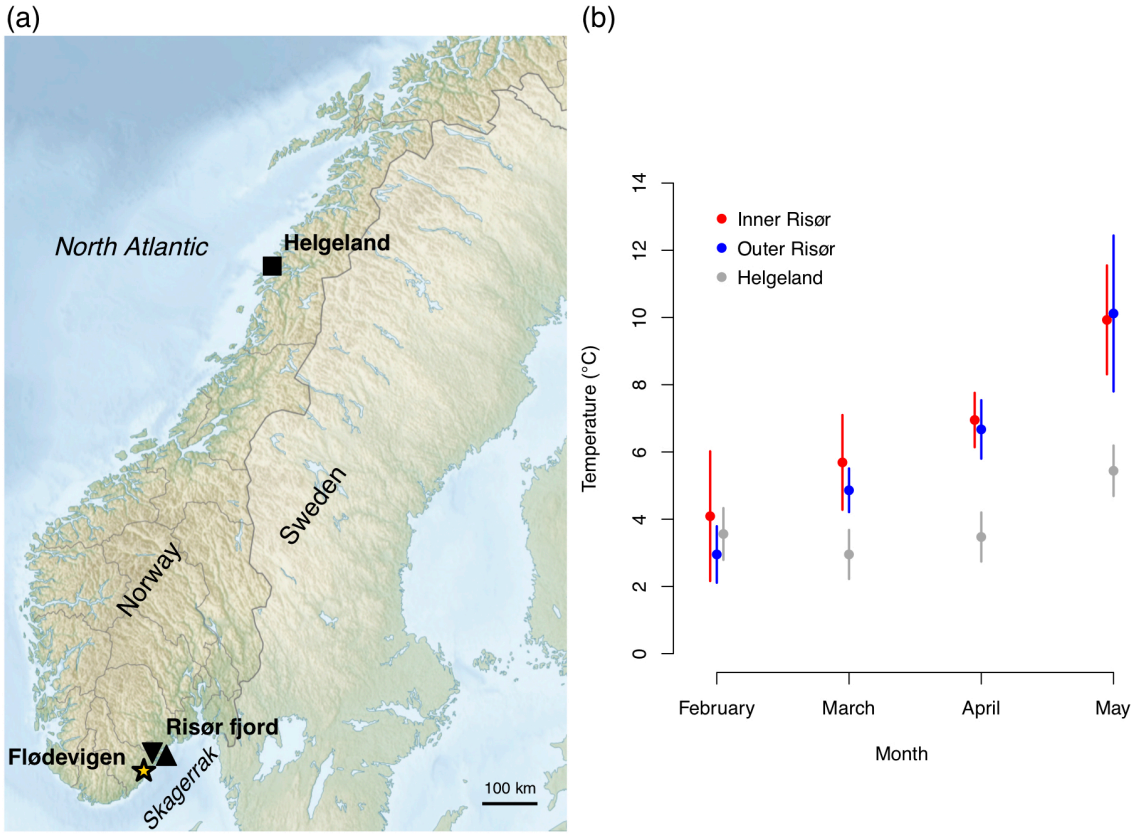

Figure 5.1: Study system. (a) Map of broodstock collection locations and (b) Mean temperatures (±SD) at 10 m depth during and shortly after spawning. Risør temperatures were measured in 2014 (see Chapter 3) and Helgeland temperatures are estimated based on data from 1980-2010 from the Skrova fixed hydrographical station of the Institute of Marine Research (available at http://www.imr.no/forskning/forskningsdata/stasjoner/view?station).

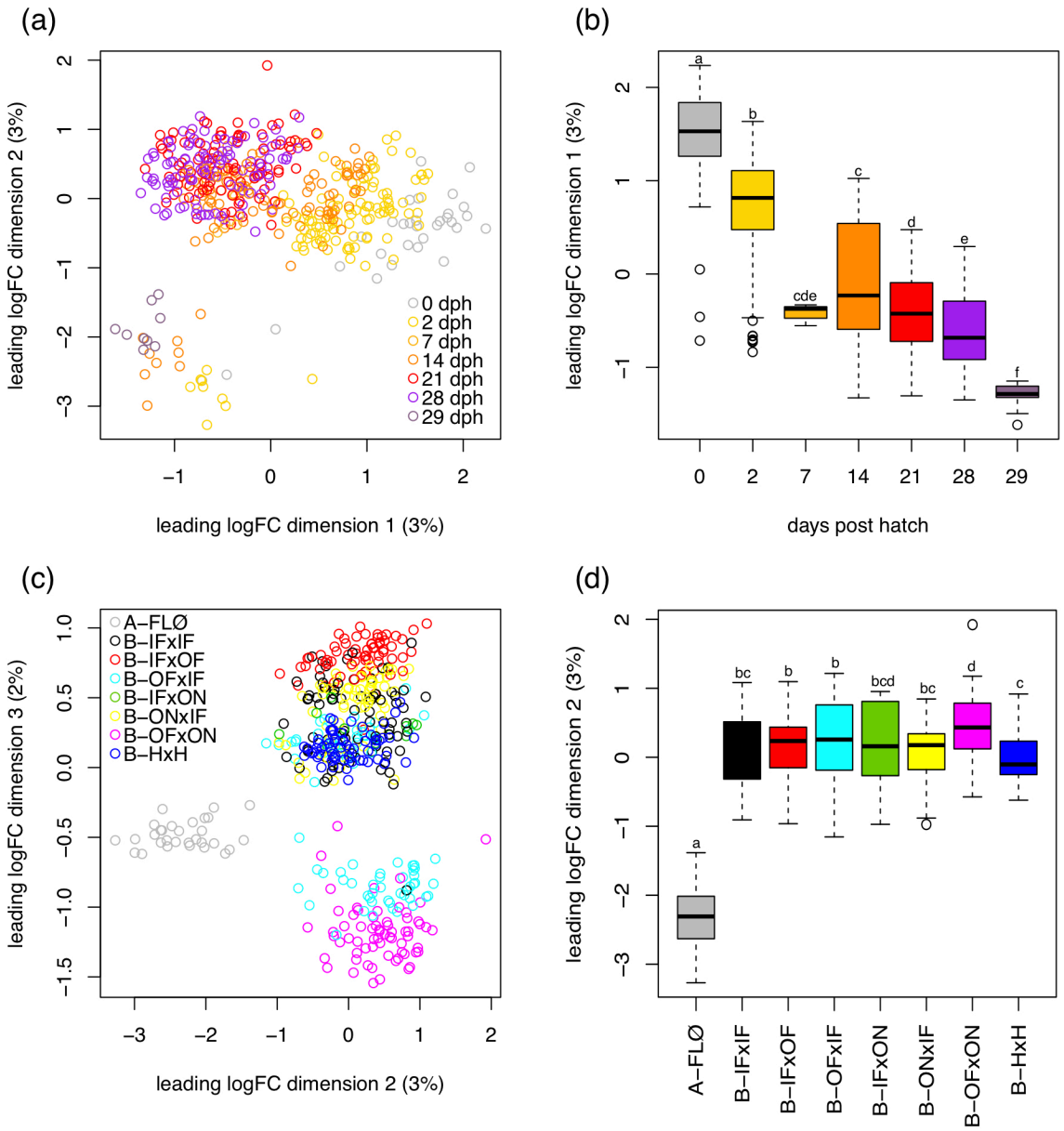

Figure 5.2: Multidimensional scaling (MDS) analysis of reference-based larval cod transcriptomes. (a) MDS plot of leading log2 fold change (logFC) dimensions 1 and 2; (b) effect of day post hatch on logFC dimension 1 based on a one-way ANOVA; (c) MDS plot of leading logFC dimensions 2 and 3; and (d) effect of cross on logFC dimension 2 based on a one-way ANOVA.

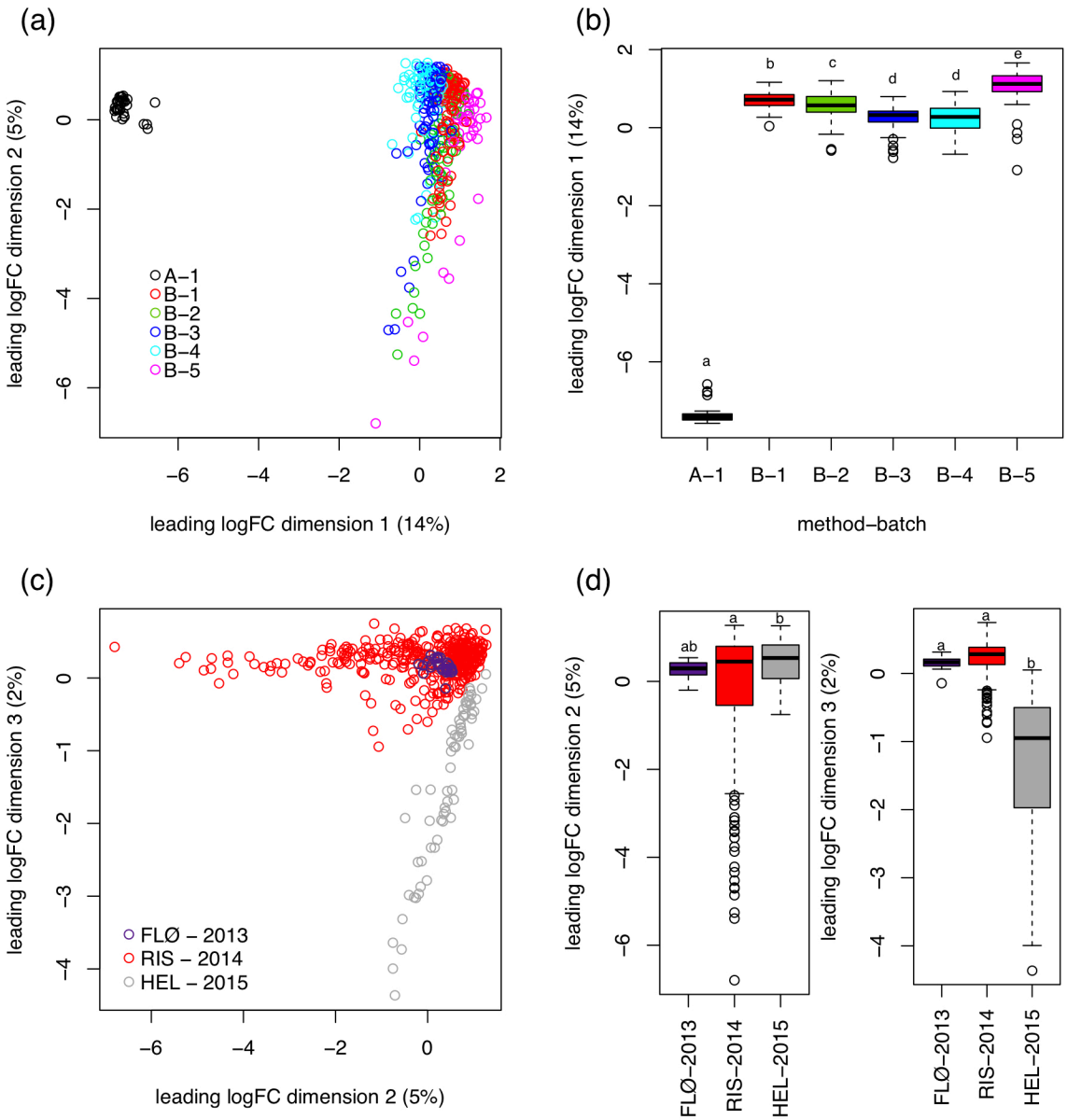

Figure 5.3: Multidimensional scaling (MDS) analysis of *de novo* larval cod transcriptomes. (a) MDS plot of leading log2 fold change (logFC) dimensions 1 and 2; (b) effect of sequencing batch on logFC dimension 1 based on a one-way ANOVA; (c) MDS plot of leading logFC dimensions 2 and 3; and (d) effect of rearing experiment or location on logFC dimensions 2 and 3 based on a one-way ANOVA.

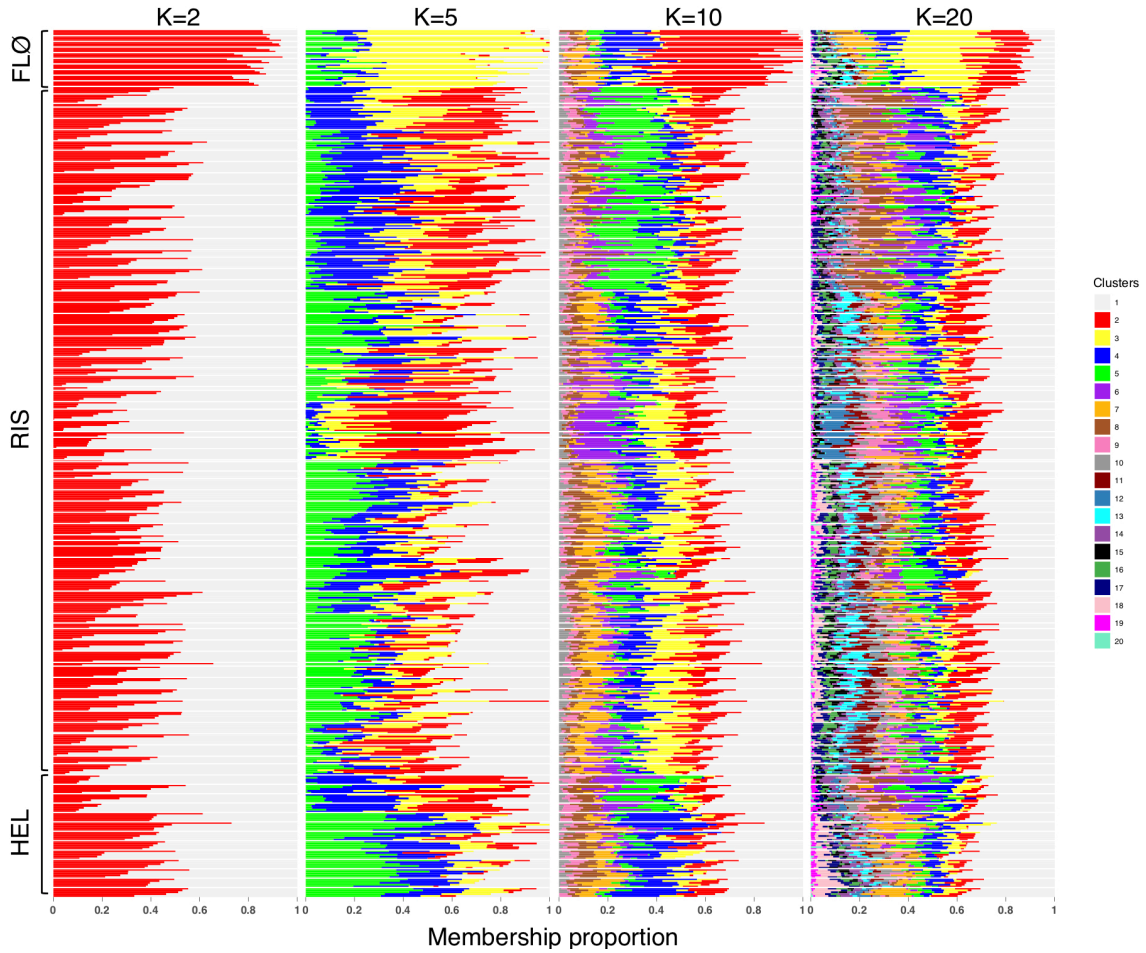

Figure 5.4: Grade of membership model proportions for all reference-based transcriptomes, sorted by location (FLØ = Flødevigen, RIS = Risør, HEL = Helgeland). Within locations, individuals are sorted consecutively by day post hatch, temperature, cross (if applicable), and cluster 1 membership proportion.

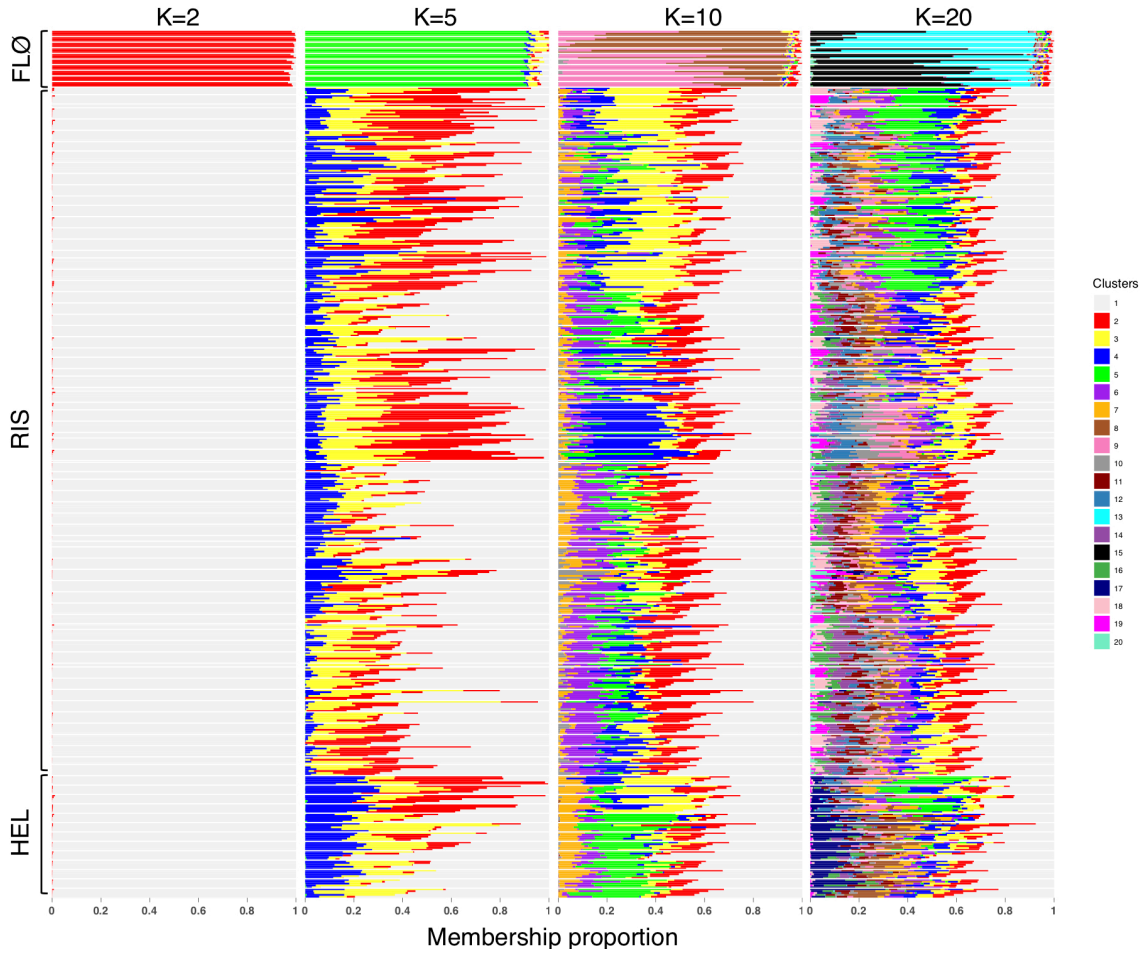

Figure 5.5: Grade of membership model proportions for all *de novo* transcriptomes, sorted by location (FLØ = Flødevigen, RIS = Risør, HEL = Helgeland). Within locations, individuals are sorted consecutively by day post hatch, temperature, cross (if applicable), and cluster 1 membership proportion.

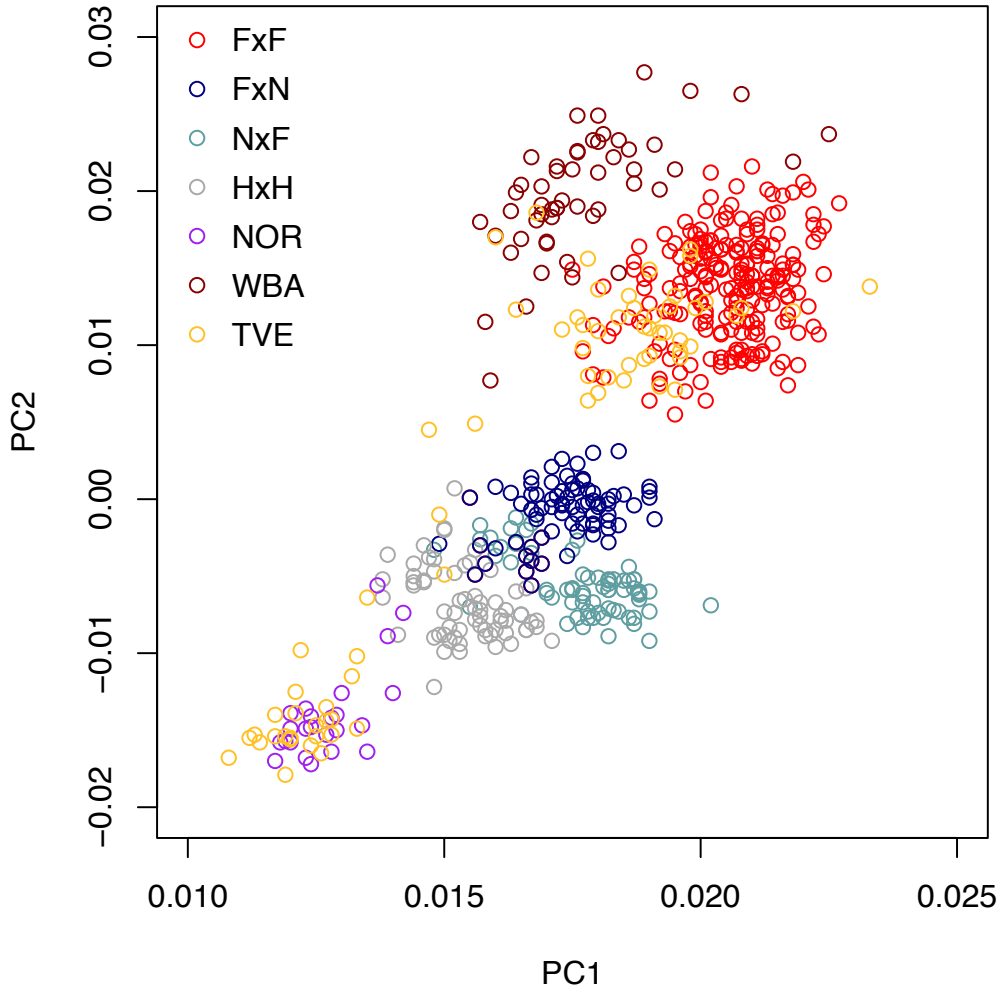

Figure 5.6: Projected results of a principal component analysis for linkage disequilibrium-purged genome-wide SNPs. Principal components were calculated based on a global dataset (n=861; Aqua Genome Project, e.g., see Barth *et al.* 2019) combined with the Risør and Helgeland samples in the present study (n=432), but only the study samples and select reference populations are plotted. The study samples include three ecotype crosses from Risør fjord (F×F = fjord mother x fjord father, N×F = North Sea mother x fjord father, F×N = fjord mother x North Sea father) and Helgeland (H×H). The reference samples include offshore North Sea (NOR), Western Baltic (WBA), and Tvedestrand fjord (TVE). Tvedestrand consists of both fjord and North Sea genotypes, as well as a few Western Baltic genotypes (Barth *et al.* 2019).

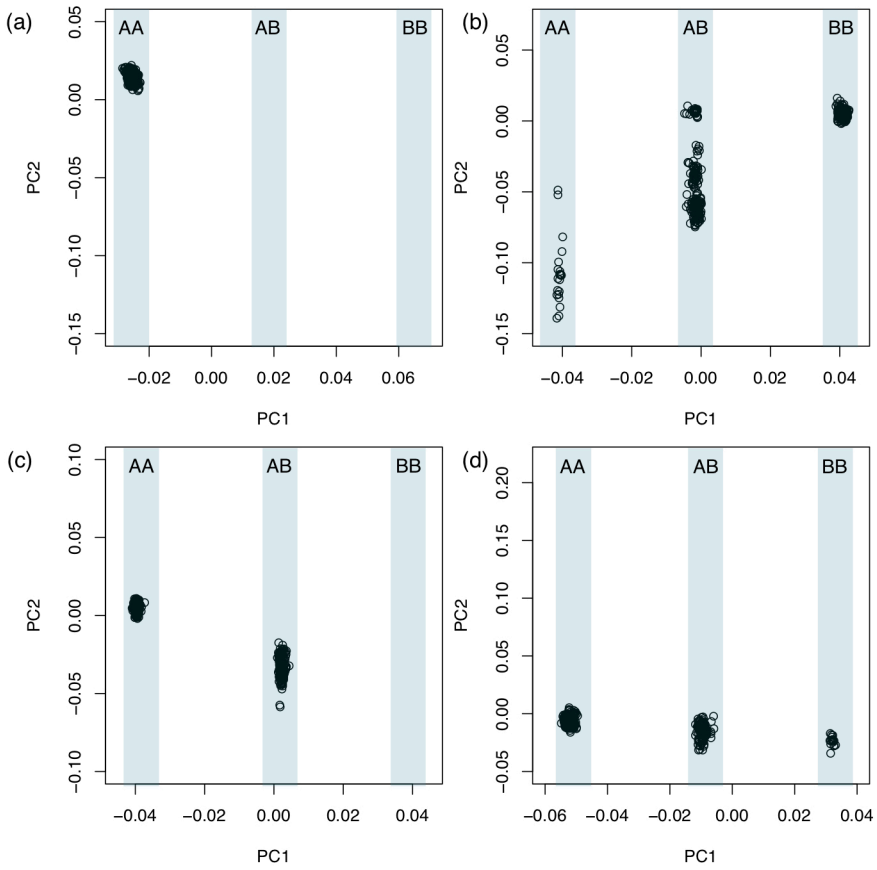

Figure 5.7: Projected results of principal component analyses for SNPs located in linkage groups (a) LG01, (b) LG02, (c) LG07, and (d) LG12. Principal components were calculated based on a global dataset (n=861; Aqua Genome Project, Barth *et al.* 2019) combined with the Risør and Helgeland samples in the present study (n=432), but only the study samples are plotted. Based on the first principal components, which clearly distinguish haplotypes according to a typical trimodal pattern for a biallelic locus (Star *et al.* 2017), individuals were classified as either homokaryotypic A (extreme negative value), homokaryotypic B (extreme positive value), or heterokaryotypic (intermediate value). 'A' represents the non-reference haplotype and 'B' represents the reference haplotype, according to the reference genome (Star *et al.* 2011; Tørresen *et al.* 2017), except for LG02 for which the reverse is true.

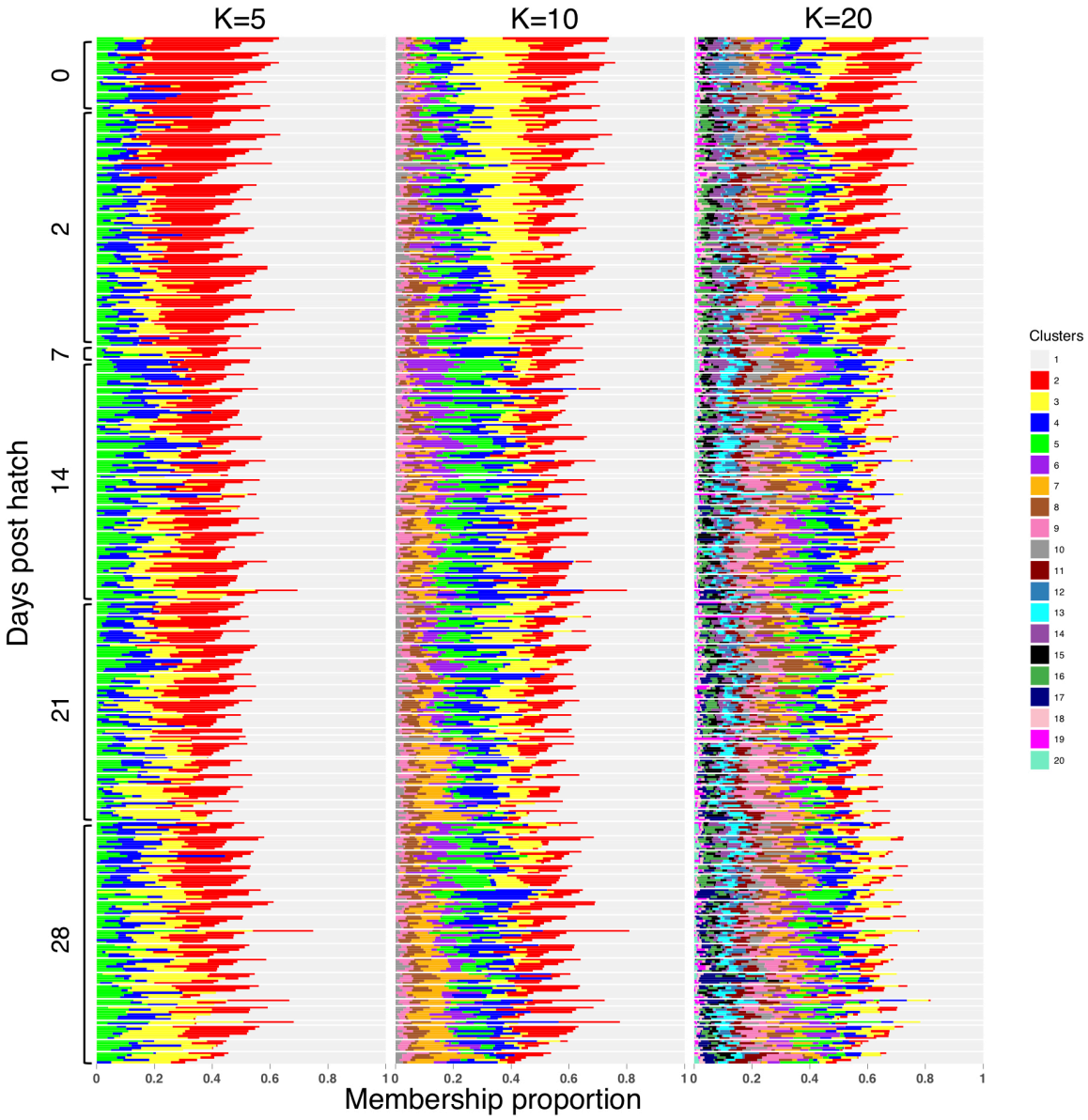

Figure 5.8: Grade of membership model proportions for Risør and Helgeland reference-based transcriptomes, sorted by day post hatch (dph). Within dph, individuals are sorted consecutively by temperature, cross (if applicable), and cluster 1 membership proportion.

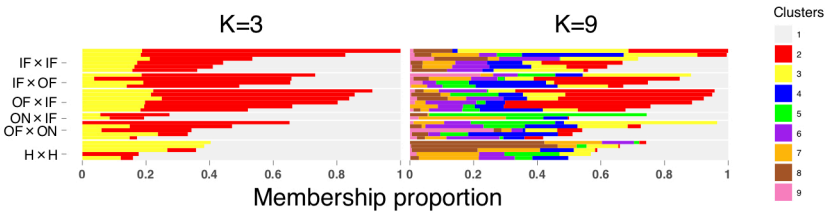

Figure 5.9: Grade of membership model proportions for Risør and Helgeland baseline (0 dph) reference-based transcriptomes, sorted by cross. Within crosses, individuals are sorted by cluster 1 membership proportion.

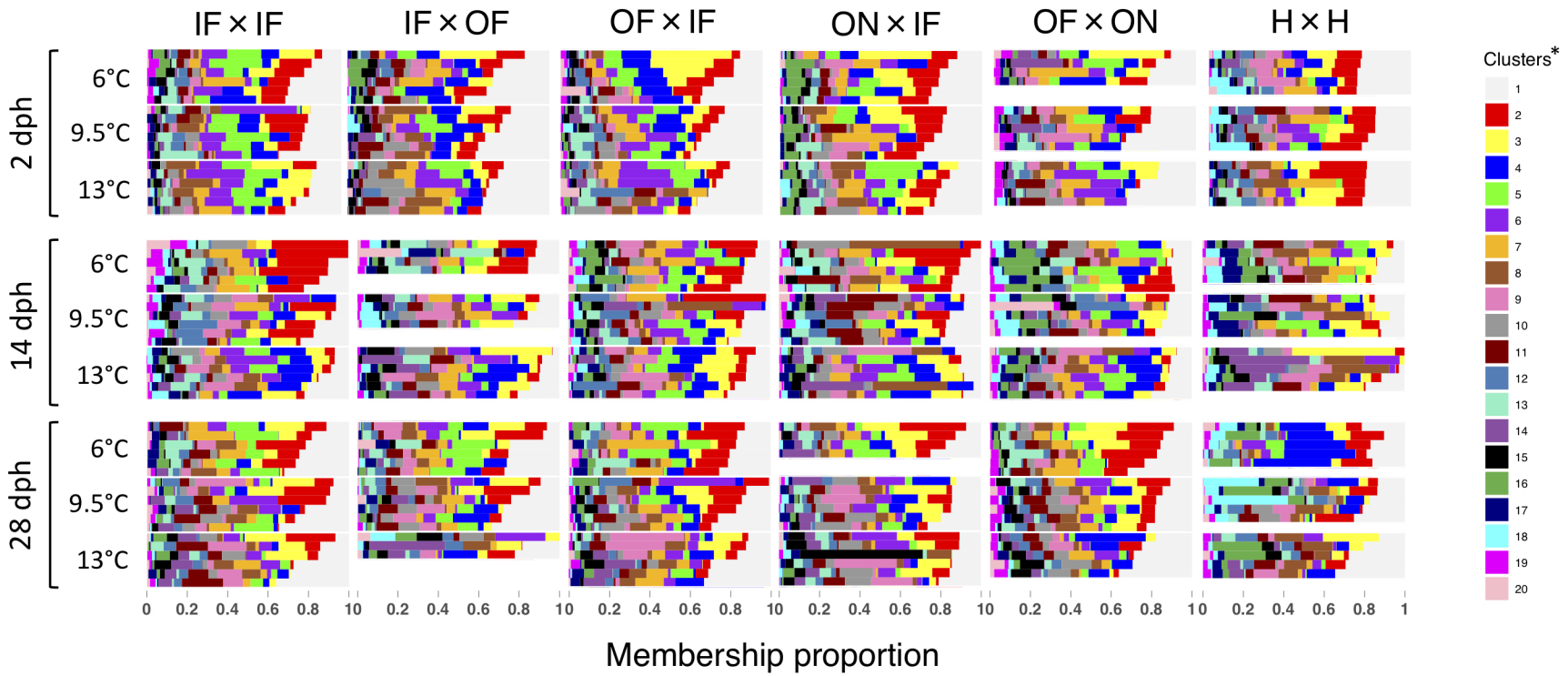

Figure 5.10: Grade of membership model proportions for Risør and Helgeland reference-based transcriptomes, sorted by cross and treatment. Within treatments, individuals are sorted by cluster 1 membership proportion. *Cluster identities are not necessarily comparable between dph as models were run for each dph separately.

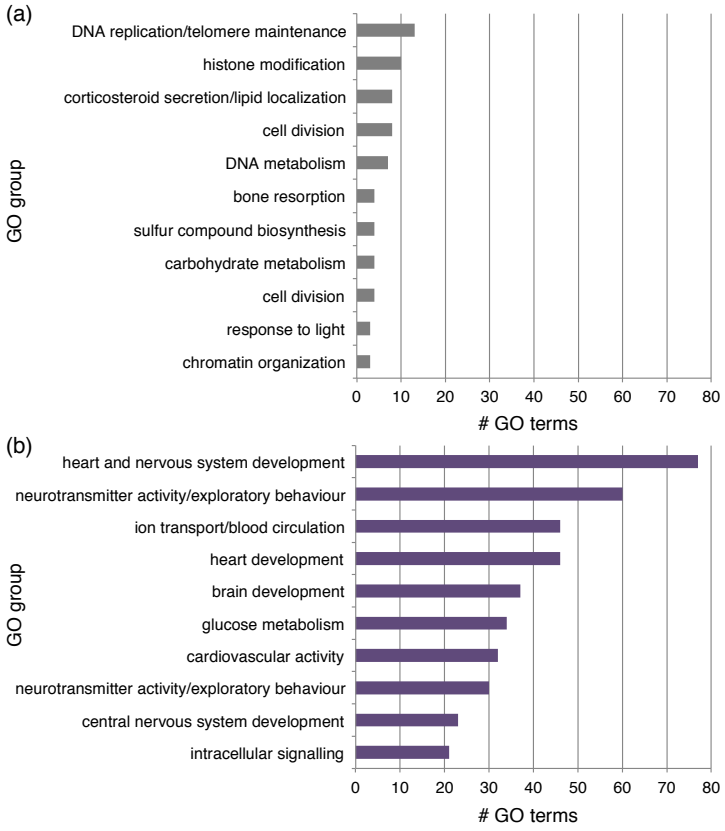

Figure 5.11: Biological processes represented by the gene ontology (GO) groups containing the greatest number of enriched (FDR<0.05) GO terms based on ClueGO analysis of the reference-based transcripts exhibiting greater expression (FDR<0.05) in (a) Helgeland and (b) Skagerrak.

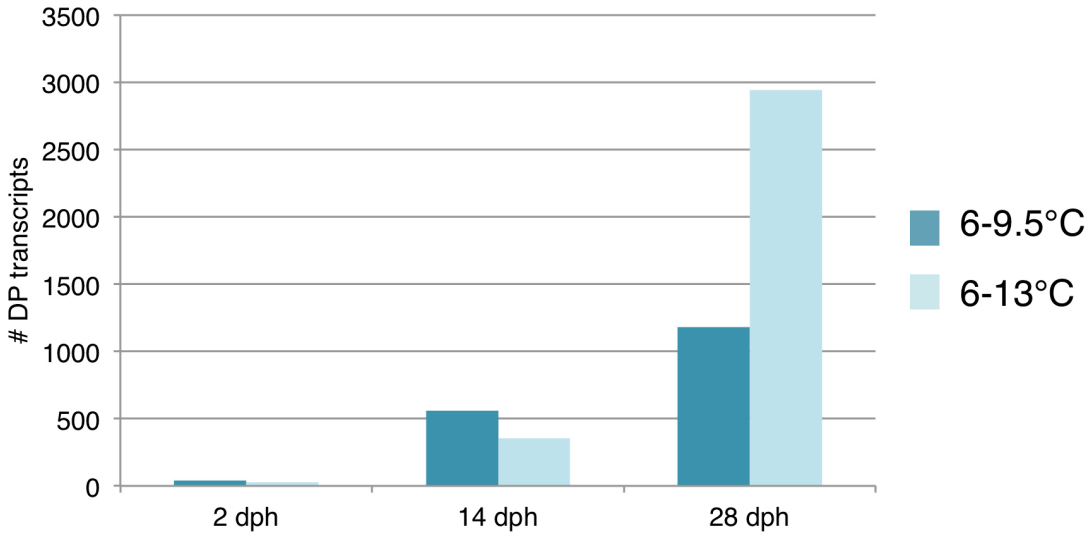

Figure 5.12: Number of transcripts that exhibit differentially plastic expression in response to temperature between Helgeland and Skagerrak larvae (dph = days post hatch).

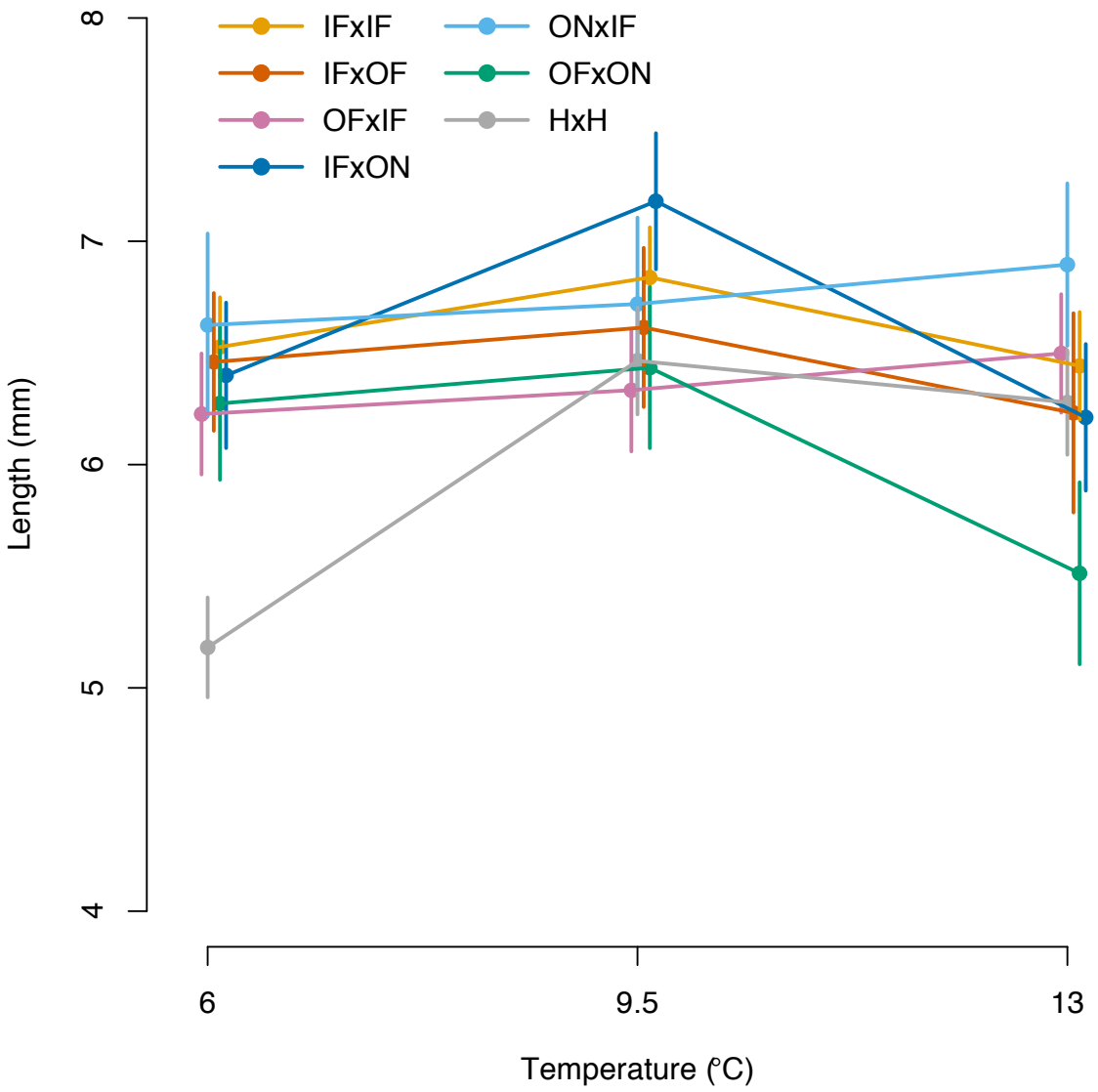

Figure 5.13: Thermal reaction norms for larval cod length at 28 days post hatch (±1 SEM) for seven crosses (mother×father: I = Inner Risør fjord, O = Outer Risør fjord, F = fjord ecotype, N = North Sea ecotype, H = Helgeland).

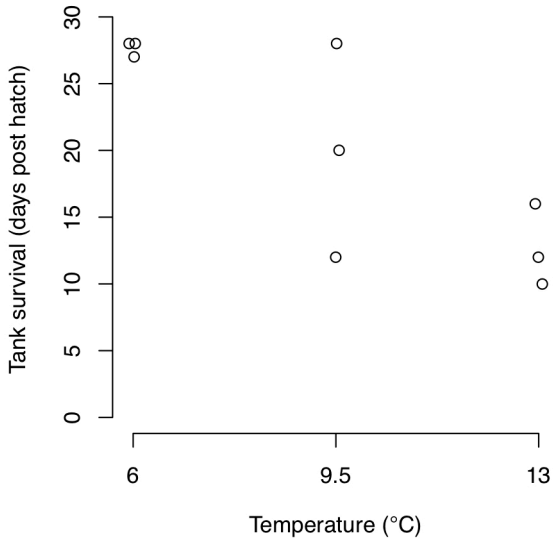

Figure 5.14: Effect of temperature on survival of Atlantic cod larvae from Helgeland, where survival is quantified as the number of days post hatch until complete mortality in each tank.

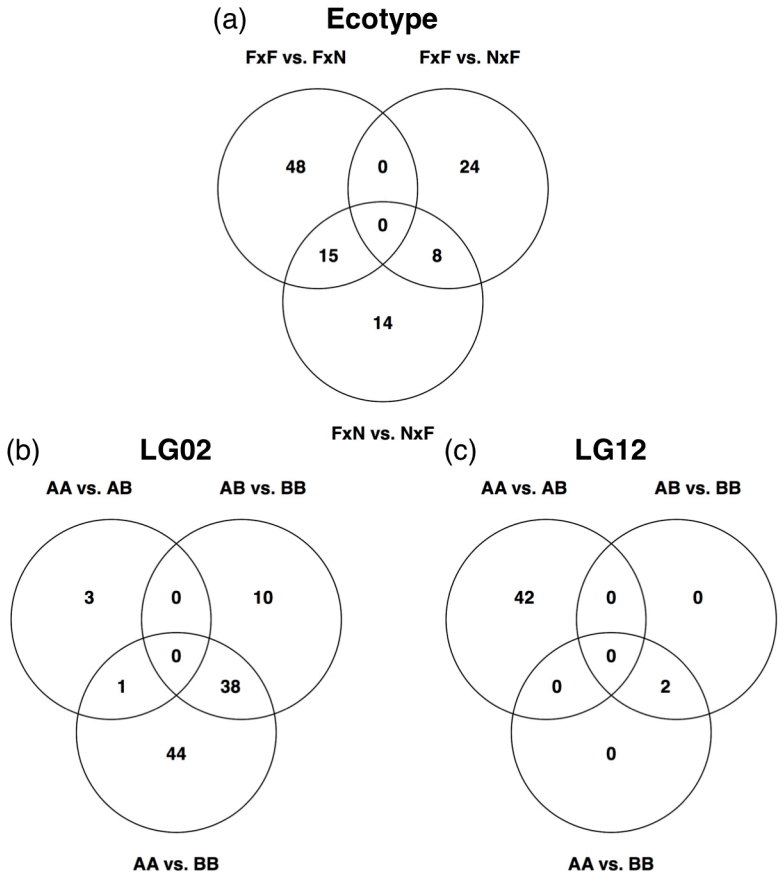

Figure 5.15: Venn diagrams depicting the overlap of differentially expressed (FDR<0.05) reference-based transcripts between genotypes for (a) ecotype, (b) LG02, and (c) LG12.

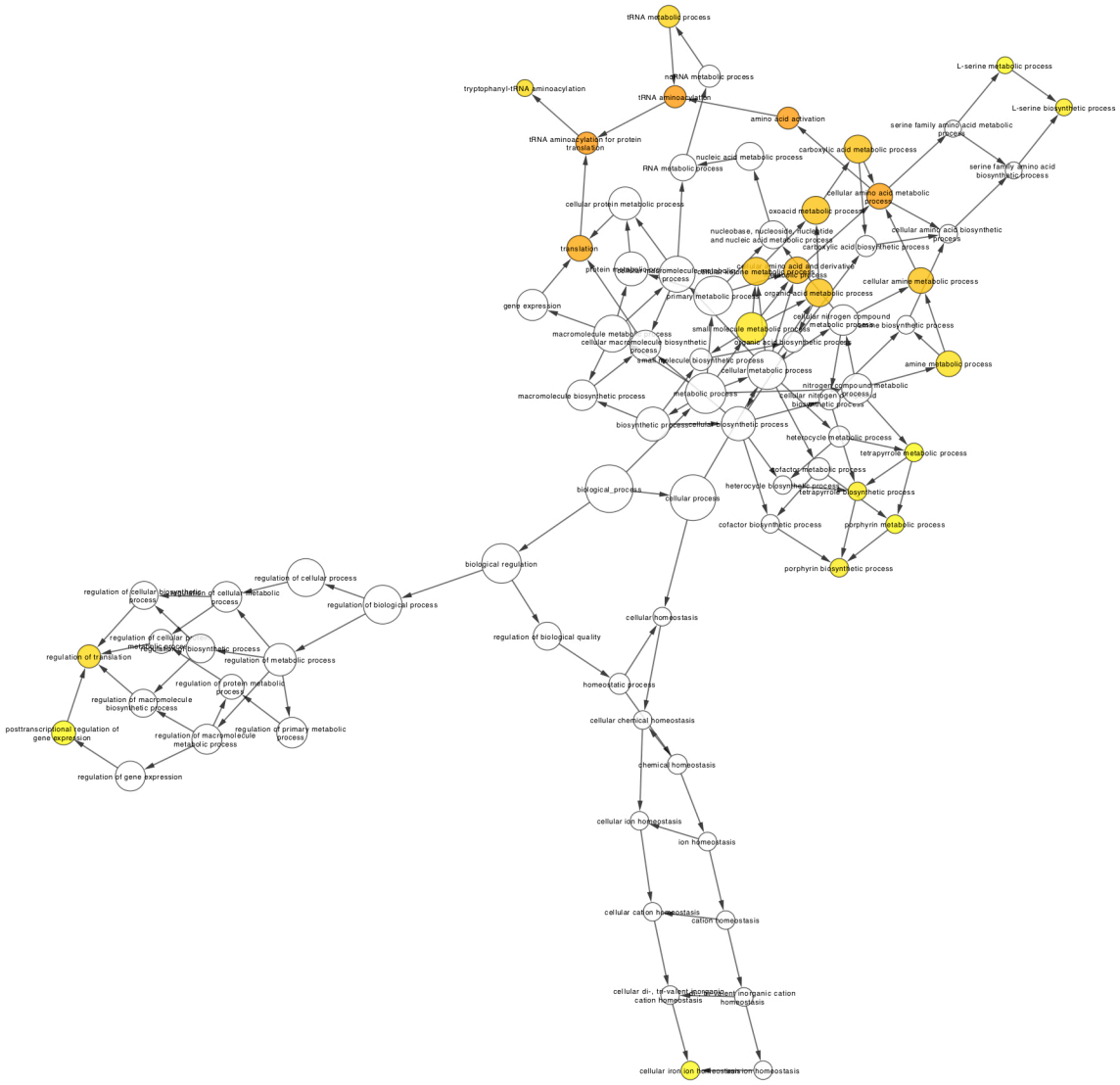

Figure 5.16: Gene expression network for transcripts differentially expressed between LG02 homokaryotypes based on a gene ontology (GO) enrichment analysis performed using BinGO. The size of the node (GO term) reflects the number of transcripts associated with that term. Coloured nodes are significantly enriched (FDR<0.05).

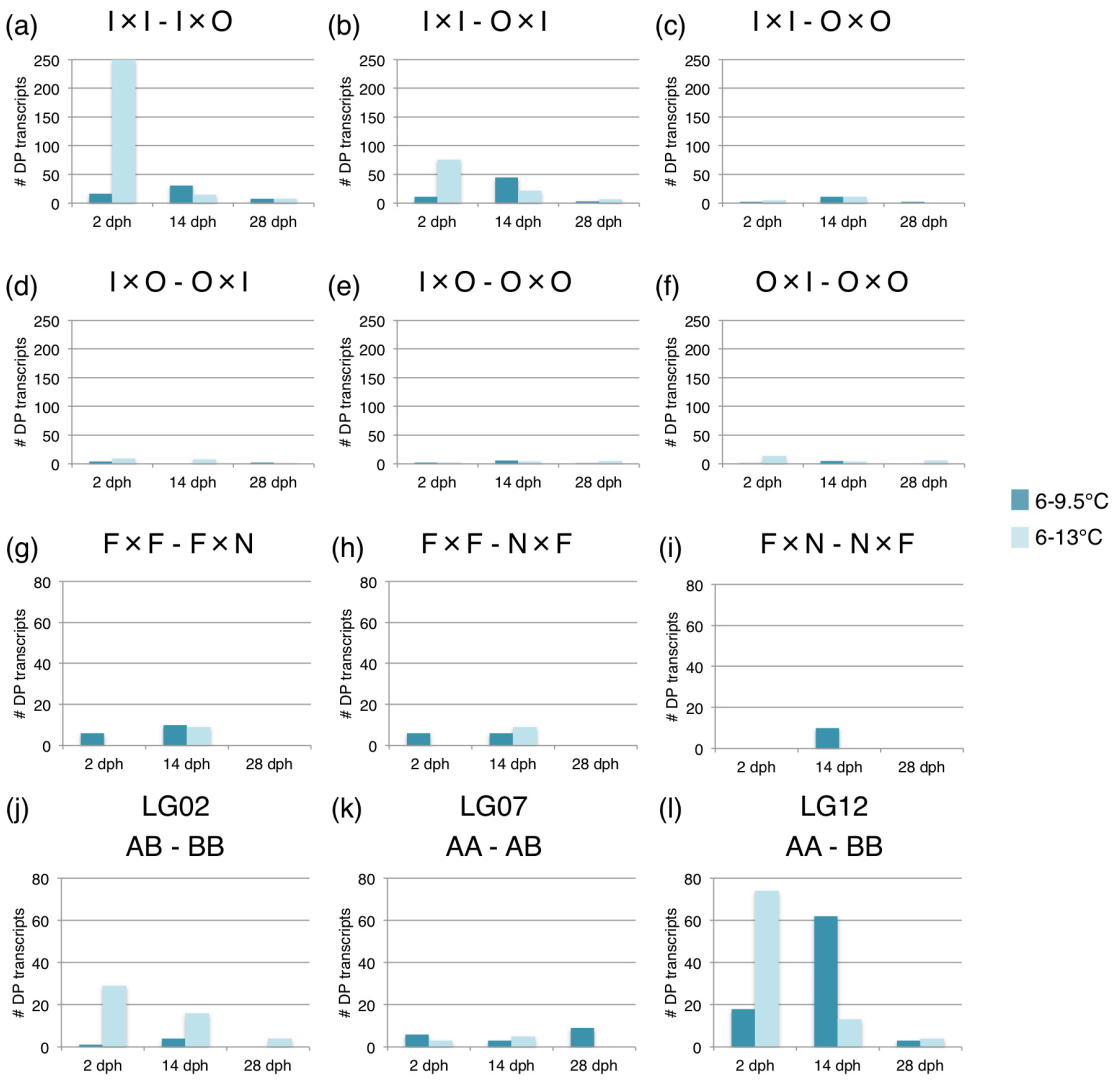

Figure 5.17: Number of transcripts that exhibit differentially plastic expression in response to temperature between (a-f) location crosses, (g-i) ecotype crosses, and (j-l) chromosomal inversion haplotype crosses (dph = days post hatch).

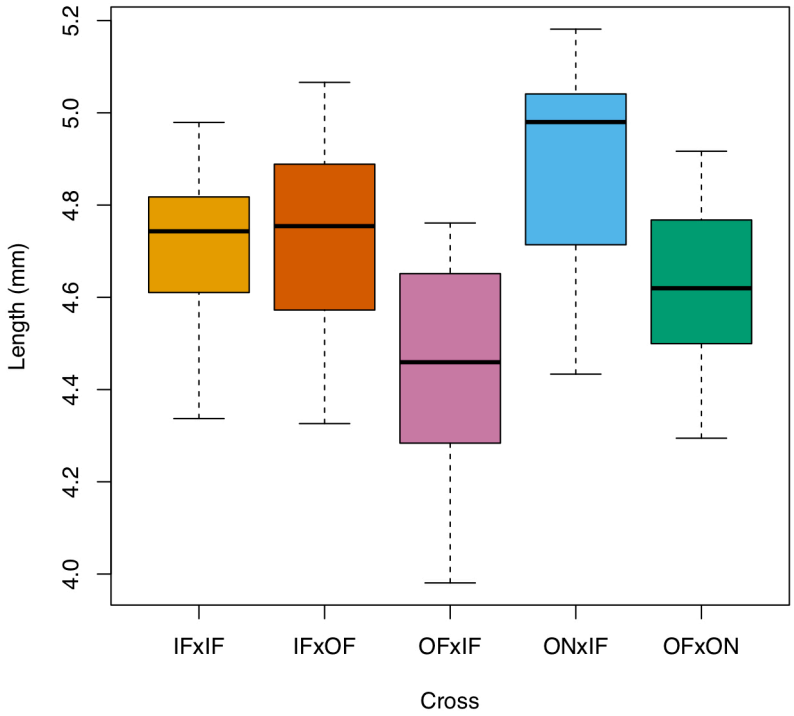

Figure 5.18: Boxplot of initial larval length for each Risør cross.

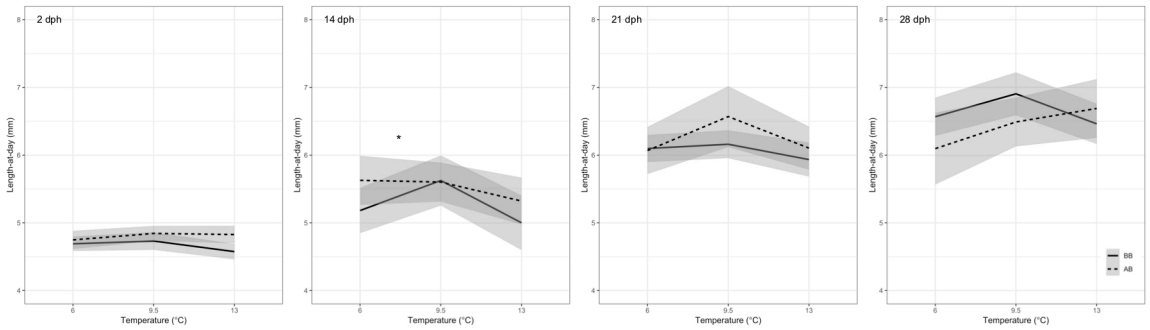

Figure 5.19: Thermal reaction norms for larval cod length-at-day for Risør larvae possessing different LG02 haplotypes, based on a linear mixed effects model with smoothed conditional means calculated from a loess regression on the model-fitted lengths. Shading represents 95% confidence intervals. Asterisks denote a significant difference (α =0.05) in reaction norm slopes (dph = days post hatch).

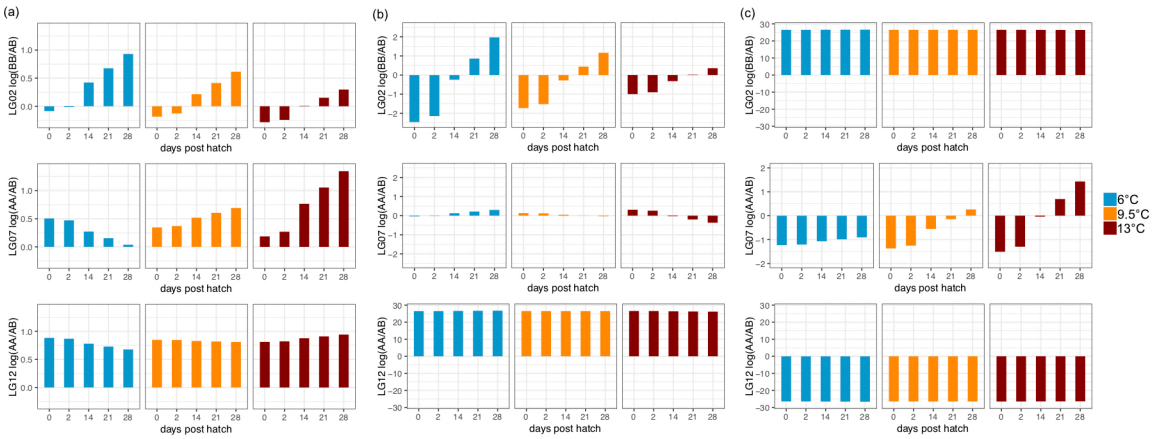

Figure 5.20: Karyotype frequencies for LG02, LG07, and LG12 over time at each temperature for (a) all Risør larvae, (b) F03×RIC5064 larvae, and (c) RIC5060×RIC5076 larvae, based on fitted coefficients from a binomial generalized linear model.

Chapter 6: General Discussion and Conclusion

The overarching aim of this thesis is to improve our understanding of plastic and evolutionary responses to environmental change in natural populations. This was achieved through four related studies on the molecular basis and spatial scale of genetic variation in thermal responses of Atlantic cod. Methodologically, we demonstrated that genomic common-garden-gradient experiments are powerful approaches for studying both plastic and adaptive responses to environmental change and that the reaction norm analytical framework facilitates interpretation of such experiments. Here, I will expand on the implications of our findings for cod populations in the context of their exploitation in a warming ocean. Then I will discuss the potential of a holistic approach, which combines genomic, phenotypic, and fitness data with eco-evolutionary modeling of population and ecosystem dynamics, for predicting changes in global biodiversity in response to anthropogenic change.

6.1 Implications of Ocean Warming for Cod

The literature review (Chapter 2) and subsequent experiments (Chapters 3-5) show that the immediate response of an organism to environmental change depends on historical, parental, and developmental environments, and can vary genetically both within and among species and populations. In Chapter 3, the plastic response to temperature in cod larvae is executed through modified expression of vast numbers of genes, primarily involved in the cellular stress response, and the magnitude and duration of thermal stress affected the severity of this response. If all cod experienced the severe declines in fitness at warmer temperatures that we observed in the Flødevigen larvae, the species would be in grave danger. However, in Chapters 4 and 5, we show that substantial variation in gene expression plasticity and downstream phenotypes exists at both macro- and micro-geographic scales. Such diversity is representative of a larger genomic toolbox for species coping with thermally stressful current and future climates. Chapter 5 further revealed that the genomic architecture of thermal plasticity is complex and highlighted the additional potential role of epigenetic mechanisms in its expression. Importantly, while

most phenotypic and fitness responses were relatively small between 6 and 9.5°C, larvae of all origins experienced severe declines in fitness at 13°C. Therefore, by keeping climate warming to a minimum, coastal cod in Norway probably have a much higher likelihood of persistence.

Of course, rising ocean temperatures are not occurring in a vacuum. The persistence of cod is dependent on selection from other sources being minimized as well, or else aligned in such a way as to accelerate an adaptive response to climate change. Of these, fishing pressure is the one that is perhaps most readily controlled. Others, such as changes in predator and prey distributions, will be extremely challenging to predict (Stenseth & Mysterud 2002). If the crux of larval survival under warming were maintenance of the larval energy budget, climate change-associated phenological shifts in larval prey abundance would likely have dire consequences. Further, the unavoidable rise in ocean acidification (IPCC 2013) might heighten thermal sensitivity of cod larvae, as it does for their embryos (Dahlke *et al.* 2017). More multifactorial experiments are needed to quantify the plastic effects of diverse environmental stressors and their interactions.

6.2 Adaptive Fisheries Management

Fishing represents a substantial selection pressure on cod in coastal Skagerrak. Annual fishing mortality is estimated to be at least 50% (Olsen & Moland 2011) and makes up as much as 100% of the total mortality of larger cod in some years (Fernández-Chacón *et al.* 2015). This thesis provides support for several fisheries management recommendations for coastal cod in Norway. First, the ubiquitous impact of temperature on larval cod fitness and its likely impact on recruitment suggest that regulations will need to be adjusted as the sea warms. Currently, commercial fisheries within 12 nautical miles of the Norwegian Skagerrak coast are only subject to technical regulations (e.g., minimum landing size, mesh size), not catch limits like those in place just outside of the coastal zone (Jorde *et al.* 2018). These regulations should be re-examined in the context of projected warming scenarios and rapid-response measures should be planned in case of an abrupt increase in temperature like that observed in the late 1980s (Olsen *et al.* 2009).

Likewise, management plans, which are currently updated on decadal timescales (ICES 2018), will probably need to be revised at a finer temporal scale given the rapid pace of global warming.

Second, the high, yet diverse, thermal sensitivities of all coastal cod in the present studies underscore the need for enhanced monitoring of local populations. Although recent decades have seen declines in populations along the Skagerrak coast (Svedäng & Bardon 2003; Olsen *et al.* 2009; Roney *et al.* 2016), relatively little is known about the productivity of the fjord components, as they have previously been assumed to be identical to those occupying the outer coastal areas. The phenotypic and fitness differences observed between the chromosomal inversion genotypes in Chapter 5 and their association with differentiation between fjord and North Sea ecotypes provide novel empirical support for the existence of locally adapted fjord populations, as suggested by several studies in the wild (e.g., Olsen *et al.* 2008; Kuparinen *et al.* 2015; Roney *et al.* 2016). The fjord ecotype is more likely to be targeted by the recreational fishery (for which neither catch nor effort data are collected) in this densely populated summer destination (Kleiven *et al.* 2016; Jorde *et al.* 2018). Genetic monitoring of fjord ecotype abundance and, if necessary, stricter regulations on the recreational fishery to reduce fishing mortality on the fjord ecotype could avert extirpation of cod in the fjords. The evidence of local adaptation described in Chapter 5 combined with the lower fitness of the adult North Sea ecotype in the fjord environment (Barth *et al.* 2019) suggest that extirpated fjord populations would be unlikely to be replaced by the North Sea ecotype. Further, there is no evidence that more than a century of stocking efforts along the Skagerrak coast produced any measurable benefit (Svåsand *et al.* 2000). Therefore, protection of locally adapted components remains the best strategy for ensuring healthy cod populations and coastal ecosystems.

Finally, poor documentation of both recreational and commercial cod fisheries along the coast (Kleiven *et al.* 2016; Jorde *et al.* 2018) fundamentally impedes the ability of fisheries management to respond in a changing environment. Improvements in

monitoring of both fishing activities and local population productivities represent, one would think, relatively agreeable actions for all stakeholders.

Although this thesis focuses on cod from coastal areas of Norway, the general phenotypic responses observed (i.e., increased growth and decreased survival with temperature) are consistent with spring-spawning Northwest Atlantic cod populations (Hutchings *et al.* 2007; Oomen & Hutchings 2015b, 2016). Yet, substantial variation in plasticity appears to exist on both sides of the Atlantic. In the Northeast, it is associated with spatially heterogeneous thermal environments and, in the Northwest, it is also associated with temporal variability in spawning and associated seasonal temperature variability (Oomen & Hutchings 2015b). Whether the genomic basis of variation in thermal plasticity is similar on both sides of the Atlantic or whether it involves unique local adaptations warrants further investigation, as does whether there exist similarly locally adapted populations within fjords in Newfoundland and Labrador.

6.3 Genomic Predictions of Responses to Environmental Change

The interplay between ecology, evolution, and genomics represents a nexus of research endeavours with tremendous potential to lead to paradigm shifts in long-standing hypotheses and theories of how organisms interact with and are adapted to their physical and biological environments. Notwithstanding tremendous strides that have been realized in understanding the functional genomic basis underlying traits of potential or known ecological or evolutionary importance (e.g., Jones *et al.* 2012; Barson *et al.* 2015; Wellenreuther & Bernatchez 2018), there remain major research gaps in linking ecology, evolution, and genomics across different scales of biological organization (Coulson *et al.* 2017; Kuparinen & Hutchings 2017; Oomen & Hutchings 2017). These scales or levels of organization range from the genome, transcriptome, proteome, and phenome through to individual fitness, population dynamics, and ecosystem structure and function (Figure 6.1). The environmental influence at every level – whether by stimuli integrated at the cellular level to influence downstream phenotypes, selection pressures acting on phenotypes to alter the genetic makeup of subsequent generations, or indirectly through

ecosystem interactions – necessitates considering the dynamics of the system as a whole in order to understand variability in its components.

While the need for a more holistic perspective on environmental responses has been realized for some time, a lack of sufficient data and analytical tools has, to some extent, hindered progress in this regard (reviewed by Pacifici *et al.* 2015, although without consideration for the role of genomics). Coulson et al. (2017) and Bay et al. (2017a) made particular conceptual progress for the integration of genomics into predictive modeling of evolutionary responses to environmental change. Bay et al. (2017a) laid out four components of the 'evolutionary response architecture': 1) population dynamics, 2) genetic architecture, 3) the spatial distribution and abundance of adaptive alleles, and 4) phenotypic plasticity. As implied by this list, understanding behavioural responses, such as dispersal, and other potential manifestations of plasticity, are key to predicting evolutionary responses. While an evolutionary perspective on environmental change is undoubtedly vital in the long term, a strategy that integrates predictions of these short-term, non-evolutionary responses will improve the accuracy of longer-term predictions while providing highly practical knowledge about tangible outcomes for policy makers. A more holistic 'response architecture', composed of behavioural, plastic, and evolutionary responses and their underlying, interconnected components, provides the best opportunity for successful wildlife management under climate change.

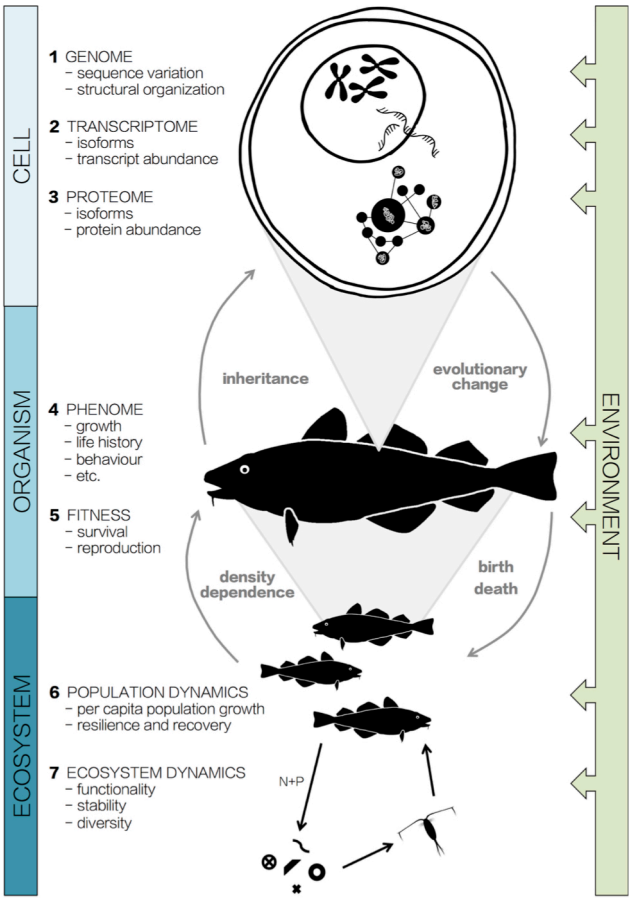

Figure 6.1: The complexity of biological systems and eco-evolutionary dynamics.

Genomics has a key role to play in informing such models. Population genomics reveals the dispersal potential of populations, their connectivity, and extent of local adaptation, which all serve to strengthen range-shift predictions. Identifying the genomic basis of plasticity (e.g., transcription factors, 'hub' genes; Costanzo *et al.* 2010) will improve quantitative predictions of its diversity and effects. Although metrics of genetic diversity (e.g., allelic richness, heterozygosity) have been used considerably for identifying vulnerable populations (Lande & Shannon 1996; Storfer 1996), the quantification of genetic diversity in plasticity lacks similar metrics. Quantifying plasticity, and its diversity, in natural populations is logistically challenging. Establishing explicit metrics for genetic variation in reaction norm slopes would represent a step towards detecting general patterns of plasticity and 'laws' surrounding its occurrence.

Recent advances in eco-evolutionary modeling are unlocking the potential for integrating species-specific genomic information into predictions of population responses to environmental change (Bay *et al.* 2017a). Particular advances have been made in understanding genomic architecture, as the structural characteristics and associated inheritance models of genes underlying particular traits are better characterized. Whether a trait is controlled primarily by a single locus or multiple loci will greatly influence its evolution in response to environmental stressors. Traditional evolutionary models have focused on the fixation dynamics of single-locus traits suddenly exposed to selection (Orr & Unckless 2014). As single-locus control of complex traits is thought to be rare (Feder & Walser 2005), eco-evolutionary models of complex non-model organisms often incorporate a standard 10-locus inheritance model. Recently, multi-locus (e.g., 100+ loci) models based on genomic SNP data were employed to predict the capacity of natural populations to evolve in pace with global climate change (Bay *et al.* 2017b, 2018; Ruegg *et al.* 2018). While acknowledging the polygenic architecture of many complex traits, these genomic studies, as well as the framework described by Bay et al. (2017a), focused on unlinked architectures involving many loci of small effect.

The assumption that single genetic variants accounting for large amounts of phenotypic variation are rare is being challenged as more refined statistical genomics enable their discovery (Hoban *et al.* 2016; Chandra *et al.* 2018). The implications of these variants for eco-evolutionary model predictions can be severe. For example, after the discovery that the VPL3 gene is responsible for 40% of the variation in age-at-maturity in salmon (*Salmo salar*; Barson *et al.* 2015), Kuparinen and Hutchings (2017) demonstrated that hypothetical single-locus control of this key life-history trait generates divergent and disruptive fisheries-induced evolution relative to that predicted by the *status quo* multi-locus model. Blocks of physically linked genes that undergo little or no recombination, such as those associated with chromosomal rearrangements, have emerged as taxonomically-widespread phenomena that can facilitate rapid adaptation (Hoffmann & Rieseberg 2008; Wellenreuther & Bernatchez 2018). This is even, and perhaps especially, the case in systems with high gene flow (Tigano & Friesen 2016; Barth *et al.* 2017; Wellband *et al.* 2019). Extreme cases of tightly linked co-adapted gene complexes associated with discrete complex phenotypes (i.e., supergenes, which includes sex chromosomes) underlie key life-history traits in a wide variety of species (Schwander *et al.* 2014). While the extent of recombination in linkage blocks can vary (and recombination suppression is likewise an active area of research; Charlesworth 2015), a tightly linked genomic architecture would enable single-locus-like modeling of polygenic adaptation to environmental change.

The disproportionate role of chromosomal inversions in local adaptation and thermal plasticity described in Chapter 5 suggests that these once-considered rare phenomena are more important to environmental adaptation than previously thought. Such findings highlight the potential of applying single-locus evolutionary theory to systems with fitness-associated traits largely controlled by multiple linked loci, such as linkage groups, chromosomal rearrangements, and supergenes. More broadly, the integration of genomic data into predictive modeling of responses to environmental change is a ripe field for future research. Beyond its academic utility, modeling demonstrates how abstract processes, such as local adaptation and human-mediated evolution, affect the food we eat, the resource-based economies on which we thrive, and the suite of ecosystem services

that the seas provide. Thus, such models would be of direct value for fisheries managers and conservation authorities, but would also translate eco-evolutionary dynamics of complex biological systems in a changing world into tangible outcomes for the public and policy-makers. The empirical approach undertaken in this thesis represents a foundation of data and systems knowledge on which to build such predictions.

Appendix A: Supplementary Materials for Chapter 3

A.1 Materials and Methods

A.1.1 RNA isolation and library prep

Total RNA was isolated using the RNeasy Mini Kit (Qiagen) according to the manufacturer's instructions with the following specifications. Tissue homogenization was carried out using a Fastprep-24 Instrument (MP Biomedicals) for 30 s at 4.0 M/S in 1.5 ml tubes containing ceramic beads and 250 µl 1x lysis buffer. RNA was eluted in two steps using 25 µl of RNase-free water each. Quality of RNA isolates was evaluated using an Agilent 2100 Bioanalyzer (BioRad) before and after library preparation with the TruSeq^{TM} RNA low-throughput protocol (Illumina) and a fragmentation time of 4 minutes.

A.1.2.2 Gene ontology enrichment analysis

GO terms identified by ClueGO were clustered into medium-specificity upper-level GO categories using a kappa-scoring algorithm based on gene membership similarity. Upper-level clustering in ClueGO facilitates interpretations of large numbers of enriched GO terms for those genes with annotations (in the form of gene names) that match the human database, while the custom GO database implemented in BiNGO identifies enriched processes using all available GO annotations (in the form of a numerical GO ID).

A.2 Supplementary Tables

Table S1: Numbers of transcripts differentially expressed in pairwise tests. Number of up- (+), down- (-), and dys- (+/-) regulated transcripts detected (A) at each temperature at each time point relative to the baseline sample, (B) between temperature treatments within time points, and (C) between time points within temperature treatments.

Day post hatch	Temperature (°C)	Direction	# DE transcripts
a) All vs. baseline (0 dph at 9°C)			
2	9	+	0
		-	0
		+/-	0
	11	+	8
		-	2
		+/-	10
	13	+	3581
		-	65
		+/-	3646
14	9	+	48
		-	46
		+/-	94
	11	+	4296
		-	825
		+/-	5121
	13	+	188
		-	106
		+/-	294
29	9	+	3558
		-	718
		+/-	4276
	11	+	509
		-	720
		+/-	1229
	13	+	629
		-	439
		+/-	1068
b) Temperature effects			
2	9-11	+	0
		-	0
		+/-	0
	11-13	+	3291
		-	64
		+/-	3355
	9-13	+	3556
		-	49
		+/-	3605
14	9-11	+	1507
		-	30
		+/-	1537
	11-13	+	156
		-	2324

Day post hatch	Temperature (°C)	Direction	# DE transcripts
		+/-	2480
	9-13	+	4
		-	0
		+/-	4
29	9-11	+	0
		-	0
		+/-	0
	11-13	+	1
		-	0
		+/-	1
	9-13	+	0
		-	0
		+/-	0
c) Time effects			
0*-2	9	+	0
		-	0
		+/-	0
2-14		+	50
		-	36
		+/-	86
14-29		+	206
		-	118
		+/-	324
2-29		+	3663
		-	835
		+/-	4498
0*-2	11	+	8
		-	2
		+/-	10
2-14		+	4580
		-	2447
		+/-	7027
14-29		+	546
		-	2946
		+/-	3492
2-29		+	1392
		-	2958
		+/-	4350
0*-2	13	+	3581
		-	65
		+/-	3646
2-14		+	167
		-	804
		+/-	971
14-29		+	22
		-	10
		+/-	32
2-29		+	375
		-	978
		+/-	1353
# of transcripts in analysis:			51075

Table S2: Numbers of enriched gene ontology terms detected through pairwise contrasts with the baseline. Numbers of enriched gene ontology (GO) terms among up- (+) and down- (-) regulated genes detected at each temperature at each time point relative to the baseline sample.

Day	Temperature	Direction	BinGO	ClueGO
2	9°C	+	0	0
		-	0	0
	11°C	+	10	0
		-	20	0
	13°C	+	305	1545
		-	10	0
14	9°C	+	4	0
		-	38	0
	11°C	+	334	1756
		-	195	80
	13°C	+	16	0
		-	40	1
29	9°C	+	307	1595
		-	69	90
	11°C	+	46	9
		-	117	199
	13°C	+	32	4
		-	47	28
# GO terms/DE gene (+)			0.20	0.15
# GO terms/DE gene (-)			1.33	0.06

Table S3: Sample information. Sample treatment, parentage, sequencing details for RNA-seq experiment, and number and percentage of read pairs per sample retained after trimming and mapping.

Sample ID	Day post hatch	Temperature (°C)	Tank	Father ID	Mother ID
D02-09-B5	2	9	B5	A35	A57
D02-09-B1	2	9	B1	A35	A57
D02-11-C2	2	11	C2	A35	A57
D02-09-C2	2	9	C2	A35	A57
D14-13-C4	14	13	C4	A35	A57
D14-09-B6	14	9	B6	A35	A57
D14-13-B2	14	13	B2	A35	A57
D14-09-C5	14	9	C5	A35	A57
D14-09-C6	14	9	C6	A35	A57
D14-11-B5	14	11	B5	A35	A57
C-5	0	9	n/a	A35	A57
D29-09-B2	29	9	B2	A35	A57
D29-09-C4	29	9	C4	A35	A57
D29-11-C3	29	11	C3	A35	A57
D29-13-B3	29	13	B3	A35	A57
D02-13-C4	2	13	C4	A35	A57
D02-11-B4	2	11	B4	A35	A57
D02-11-C4	2	11	C4	A35	A57
D02-13-B3	2	13	B3	A35	A57
D02-13-C3	2	13	C3	A35	A20
C-4	0	9	n/a	A35	A57
D14-11-B4	14	11	B4	A35	A57
D14-11-C3	14	11	C3	A35	A57
D14-13-C3	14	13	C3	A35	A57
D29-09-B4	29	9	B4	A35	A57
D29-11-B4	29	11	B4	A35	A57
D29-11-C4	29	11	C4	*1	A05
D29-13-B4	29	13	B4	A35	A57
D29-13-C4	29	13	C4	A35	A57
C-3	0	9	n/a	*1	A05

A.3 Supplementary Figures

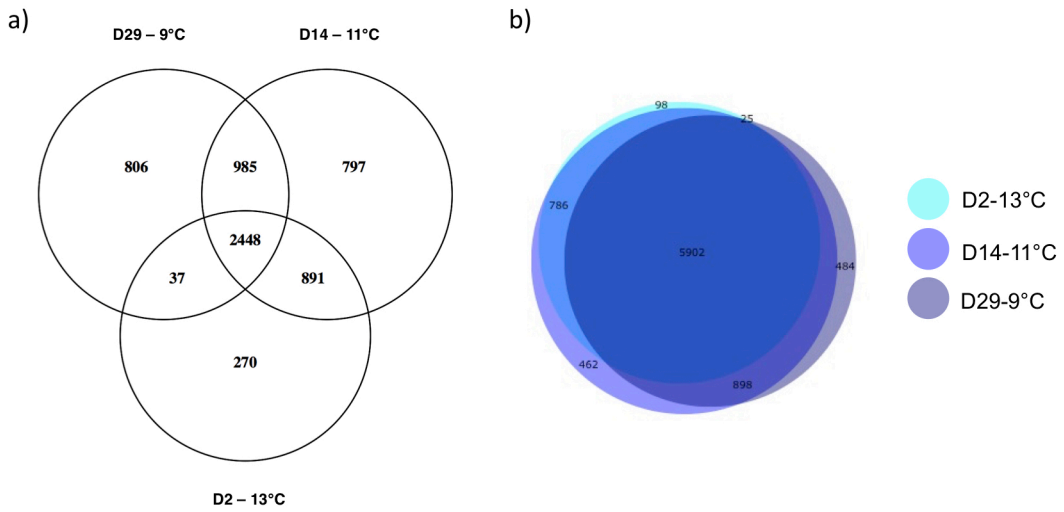

Figure S1: Overlap among peak transcriptomic responses. Numbers of differentially expressed (a) Trinity transcripts and (b) associated GO terms shared among D2-13°C, D14-11°C, and D29-9°C relative to the baseline.

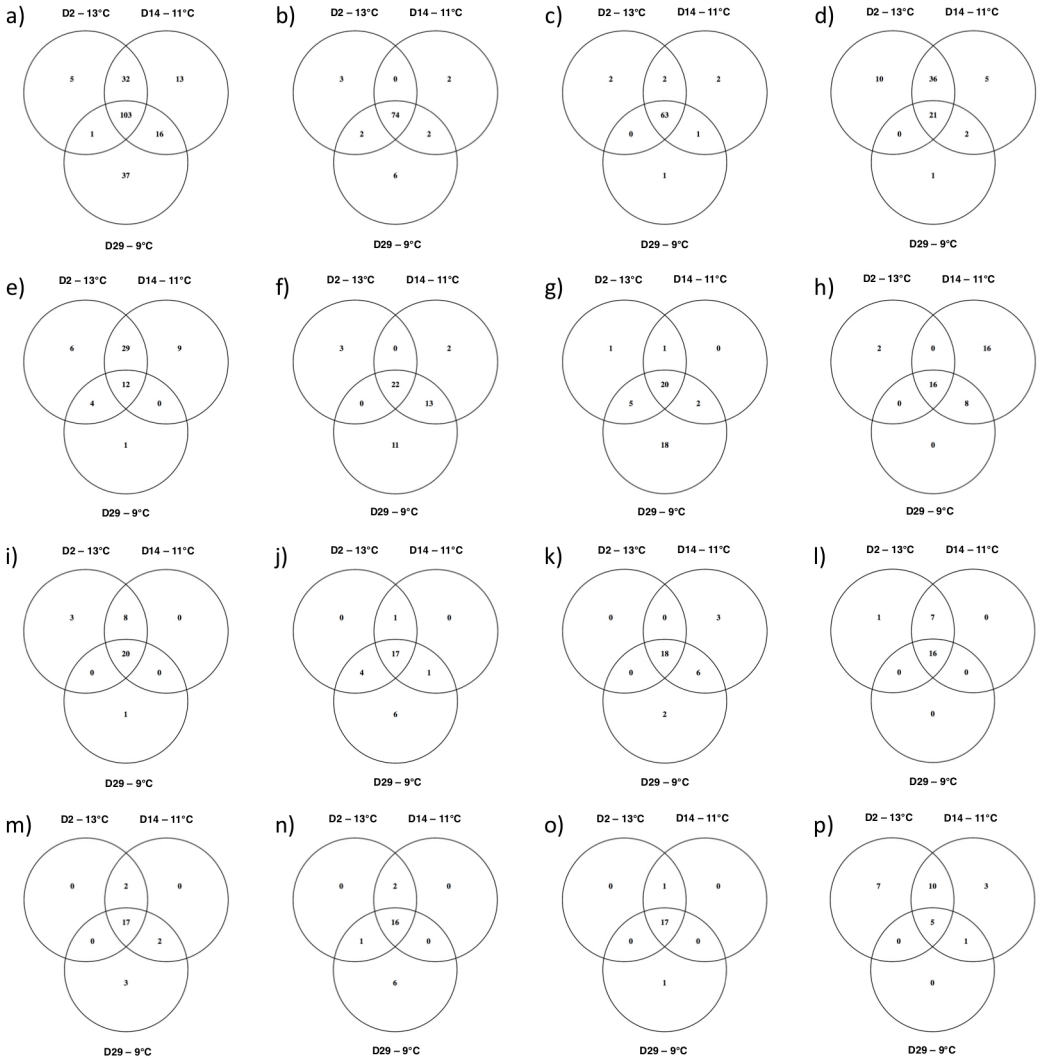

Figure S2: Overlap of gene ontology terms among peak transcriptomic responses for each gene ontology group. Venn diagrams depicting the overlap among gene ontology (GO) terms included within each manually defined GO group containing the greatest number of enriched (FDR<0.05) GO terms based on ClueGO analysis of the Trinity transcripts upregulated (FDR<0.05) at D2-13°C, D14-11°C, and D29-9°C. The GO groups are manually defined as follows, with group numbers corresponding to Supplementary data 2 given for D2-13°C, D14-11°C, and D29-9°C, respectively: (a) cell cycle and protein catabolism [210, 227+223+220, 203], (b) protein biosynthesis and metabolism [209, 226, 202], (c) protein transport and localization [208, 225, 201], (d) energy metabolism [207, 224, 193], (e) protein metabolism [206, 222, 185], (f) DNA structural modification [203, 219, 200], (g) DNA repair [204, 215, 199], (h) transcriptional regulation [192, 221, 192], (i) translational regulation [205, 218, 189], (j) RNA processing [199, 211, 196], (k) response to virus [194, 217, 195], (l) response to hormonal stimulus [202, 214, 182], (m) mitochondrial organization and mitophagy [198, 212, 190], (n) cellular organization [196, 206, 191], (o) immune response [195, 208, 187], and (p) carbohydrate metabolism [200, 209, 124].

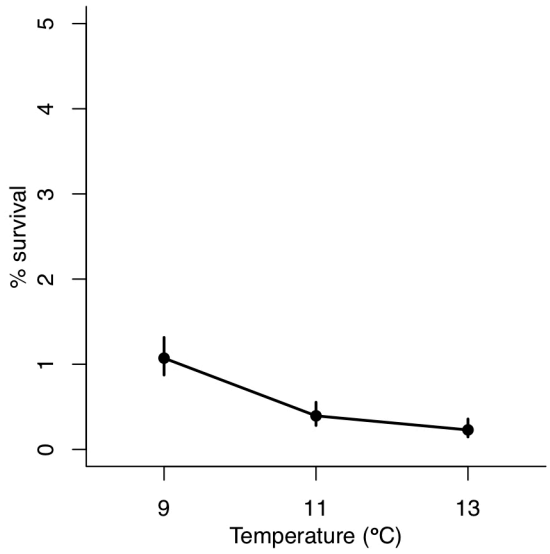

Figure S3: Thermal reaction norm for larval Skagerrak cod survival at 43 days post hatch.

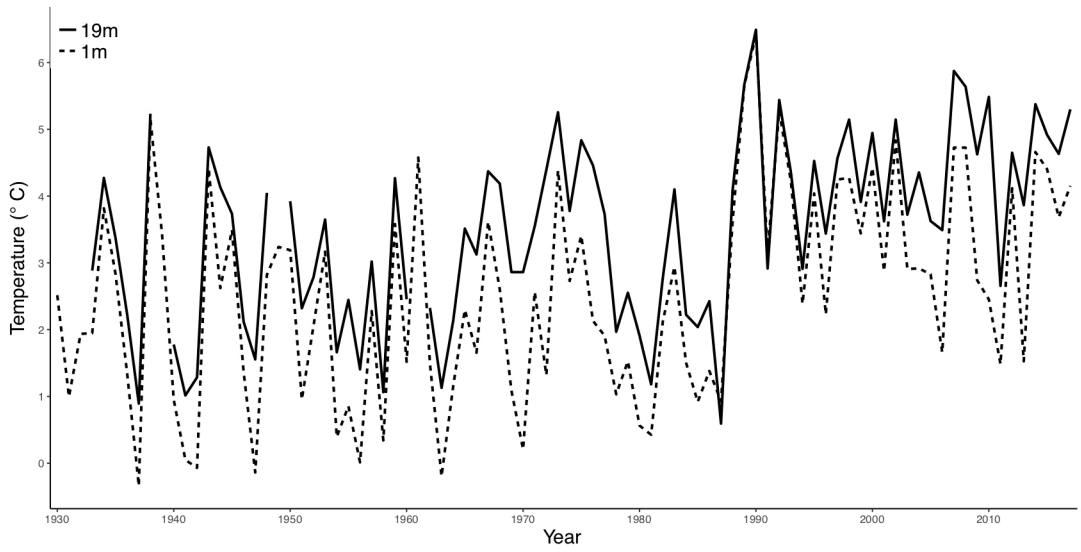

Figure 4: Sea temperature rise in study location. The average sea temperature during the peak spawning month (March) at 1m and 19m depth near the *Institute of Marine Research, Flødevigen*.

A.4 List of Supplementary Data Files

All files located at: https://github.com/rebekahoomen/PhD-thesis

Data S1: Enriched gene ontology terms based on genes upregulated relative to the baseline according to the Trinity pipeline and BinGO software.

<A_Data_S1_Trinity_BinGO_upregulated.xlsx>

Data S2: Enriched gene ontology terms based on genes upregulated relative to the baseline according to the Trinity pipeline and ClueGO software.

<A_Data_S2_Trinity_ClueGO_upregulated.xlsx>

Data S3: Enriched gene ontology terms based on genes downregulated relative to the baseline according to the Trinity pipeline and BinGO software.

<A_Data_S3_Trinity_BinGO_downregulated.xlsx>

Data S4: Enriched gene ontology terms based on genes downregulated relative to the baseline according to the Trinity pipeline and ClueGO software.

<A_Data_S4_Trinity_ClueGO_downregulated.xlsx>

Appendix B: Comparison of *De Novo* and Reference Genome-Based Transcriptome Assembly Pipelines for Differential Expression Analysis of RNA Sequencing Data

This appendix is based on a companion manuscript to Chapter 3.

B.1 Abstract

As sequencing technologies become more accessible and bioinformatic tools improve, genomic resources are increasingly available for non-model species. Using a draft genome to guide transcriptome assembly from RNA sequencing data, rather than performing assembly *de novo*, affects downstream analyses. Yet, direct comparisons of these approaches are rare. Here, we compare the results of the standard *de novo* assembly pipeline ('Trinity') and two reference genome-based pipelines ('Tuxedo' and the 'new Tuxedo') for differential expression and gene ontology enrichment analysis of a companion study on Atlantic cod (*Gadus morhua*). The new Tuxedo pipeline produced a higher quality assembly than the Tuxedo suite. However, greater enrichment of Trinity-identified differentially expressed genes suggests that a higher proportion of them represent biologically meaningful differences in transcription, as opposed to transcriptional noise or false positives. Coupled with the ability to annotate novel loci, the increased sensitivity of the Trinity pipeline might make it preferable over the reference genome-based approaches for studies aimed at broadly characterizing variation in the magnitude of expression differences and biological processes. However, the 'new Tuxedo' pipeline might be appropriate when a more conservative approach is warranted, such as for the identification of candidate genes.

B.2 Introduction

RNA sequencing (RNA-seq) revolutionized ecological genomics by enabling transcriptome assembly without *a priori* genomic information (Wang *et al.* 2009; Alvarez

et al. 2015). As sequencing technologies become more accessible and bioinformatic tools rapidly improve, genomic resources are increasingly available for non-model species (Oomen & Hutchings 2017). The choice of whether to use a draft genome to guide transcriptome assembly or perform assembly *de novo* is one that is best addressed early on in an RNA sequencing experiment and has the potential to substantially influence the results obtained from differential expression (DE) and enrichment analyses. Yet, studies are, by and large, reporting the outcome of a single analytical pipeline that produced perhaps the most comprehensible result. This is exacerbated by the fact that length restrictions on journal articles, and even supplementary materials, encourage unhelpful reductions in the reporting of technical details and alternative methods that had been evaluated during the course of data analysis. Here, we analyze a large set of RNA-seq data from a companion study on a widely distributed marine fish that exemplifies the increasingly common position of straddling the realms of model and non-model species, the Atlantic cod (*Gadus morhua*) (Oomen et al., submitted). Specifically, we compare *de novo* transcriptome assembly and two reference genome-based pipelines in the context of differential expression and gene ontology enrichment analysis in a larval rearing experiment. Our study will provide a useful resource for anyone planning or conducting transcriptomic analysis of non-model or semi-model species and will shed light on the issue of restrictive publication lengths in an age of rapidly expanding genomic tools and analytical pipelines.

B.3 Methods

B.3.1 Experimental Design

Briefly, we raised laboratory-hatched larvae of wild origin at three temperatures (9°C, 11°C, and 13°C). We sampled a total of three larvae from two tank replicates at each temperature at 2, 14, and 29 days post hatch (dph), and an additional three larvae from the hatching tank at 0 dph (prior to transfer to temperature treatments) to serve as a baseline sample (n=30). For details see Oomen et al. (submitted).

B.3.2 RNA Library Preparation and Quality Control

Total RNA was isolated from individual whole larvae, using the RNeasy Mini Kit (Qiagen) according to the manufacturer's instructions. Tissue homogenization was carried out using a Fastprep-24 Instrument (MP Biomedicals) for 30 s at 4.0 M/S in 1.5 ml tubes containing ceramic beads and 250 µl 1x lysis buffer. RNA was eluted in two steps, using 25 µl of RNase-free water each. Quality of RNA isolates was evaluated with an Agilent 2100 Bioanalyzer (BioRad) before and after library preparation with the TruSeq™ RNA low-throughput protocol (Illumina) and a fragmentation time of 4 minutes. Trimming and adapter removal was performed on all sequences, using Cutadapt v.1.8 (Martin 2011) with a quality threshold of 20, followed by a hard trim of 10 from the 5' end with a minimum remaining sequence length of 20 (Table 1). Sequence quality was evaluated before and after each trimming step, using FastQC v.0.11.2 (Andrews 2011). Transcriptome assembly was performed with the remaining 740 million read pairs. Default parameters were used unless otherwise stated.

B.3.3 De Novo *Transcriptome Assembly*

The transcriptome was assembled *de novo,* using the Trinity software suite v.2014-07-17 (http://trinityrnaseq.github.io), including bowtie v.1.0.0 (Langmead *et al.* 2009) and samtools v.0.1.19 (Li *et al.* 2009). Trinity was performed with built-in normalization, 50 GB maximum memory and 10 CPUs. Assembly statistics were generated with TrinityStats.pl. The assembly was further evaluated for quality by calculating the contig ExN50 statistic, using contig_ExN50_statistic.pl, evaluating the relationship between raw read counts and FPKM (Fragments Per Kilobase of transcript per Million mapped reads), using count_features_given_MIN_FPKM_threshold.pl, and by counting the number of full-length transcripts using blastx and blastp (https://blast.ncbi.nlm.nih.gov/Blast.cgi) with the analyze_blastPlus_topHit_coverage.pl script. Reads were mapped back to the assembly, using align_and_estimate_abundance.pl with RSEM estimation and the bowtie aligner, to generate sample-specific transcript counts. The assembly was annotated using Trinotate v.2.0.1 (http://trinotate.github.io/).

B.3.4 Reference Genome-Based Transcriptome Assembly

In the Tuxedo pipeline, sequences were mapped to the second version of the cod genome (Tørresen *et al.* 2017), using Tophat v. 2.1.1 (Kim *et al.* 2013) with a mate inner distance of 200±200 bp. Cufflinks v.2.2.1 (Trapnell *et al.* 2010) was used to assemble sample-specific transcriptomes in reference-annotation-based transcript assembly mode (Roberts *et al.* 2011a) with fragment bias correction (Roberts *et al.* 2011b), which were then combined into a single assembly with Cuffmerge. Global pairwise DE analysis was performed using Cuffdiff and cummeRbund v.2.8.2 in R v.3.3.2.

In the 'new Tuxedo' pipeline, the low-memory aligner HISAT v.2.1.0 (Kim *et al.* 2015) mapped reads to the reference genome (Tørresen *et al.* 2017). Samtools v.1.3.1 (Li *et al.* 2009) sorted and converted the resulting SAM files to BAM files for transcript assembly, quantification, and merging of assemblies, using StringTie 1.3.1 (Pertea *et al.* 2015). We included a reference annotation containing known gene models in StringTie to improve reconstruction of low-abundance genes. Otherwise, default options were used. A matrix of raw gene counts was generated from the StringTie output, using the prepDE.py script (http://ccb.jhu.edu/software/stringtie/dl/prepDE.py). The assemblies resulting from both reference-based pipelines were evaluated relative to the reference genome and to each other, using gffcompare (https://github.com/gpertea/gffcompare).

B.3.5 Differential Expression and Gene Ontology Enrichment Analysis

Differential expression analysis was conducted in edgeR v.3.16.5 (Chen *et al.* 2014) and included only those transcripts having a CPM (counts per million) >1 in at least three samples. We conducted pairwise comparisons between all samples compared to the baseline sample, using a false discovery rate (FDR)-corrected P-value of 0.05. Venn diagrams were constructed, using BioVenn (Hulsen *et al.* 2008) and Venny (http://bioinfogp.cnb.csic.es/tools/venny/). to compare differentially expressed gene lists.

Gene ontology (GO) enrichment analysis was performed, using ClueGO v.2.3.2 (Bindea *et al.* 2009) and BiNGO v.3.0.3 (Maere *et al.* 2005) in Cytoscape v.3.2.1 (Shannon *et al.*

2003), to identify significantly enriched biological processes. Up- and down-regulated genes were analyzed separately with an FDR-corrected P-value of 0.05 and otherwise default parameters. The Gene Fusion option was used in ClueGO.

B.4 Results

B.4.1 Assembly

The *de novo* pipeline assembled 386,872 trinity 'genes' (i.e., unique groups of isoforms) corresponding to 530,683 unique transcripts (Table 2). The peak N50 value of 2153 occurring at E90 suggests that sufficient sequencing depth was achieved and that approximately 41,413 biologically relevant transcripts were assembled (Figure 1, Table 3). This roughly corresponds with the number of transcripts with an expression level >1 FPKM (Fragments Per Kilobase Million) (39,767; Figure 2). Full-length transcript analysis, using blastx and blastp, detected 26,790 and 25,249 proteins, respectively, of which 9430 and 9774 were nearly full-length (≥90%) (Table 4). Overall mapping rates of 61-75% resulted in approximately 10-30 million reads (mean = 17 million) per sample being successfully mapped back to the transcriptome (Table 1), meeting or exceeding coverage guidelines for DE analysis in a complex eukaryote (Todd *et al.* 2016).

The 'new Tuxedo' aligner HISAT performed approximately 10x faster and used much less memory than the Tuxedo suite aligner Tophat (data not shown). StringTie assembled slightly more loci (34,132) compared to Cufflinks (31,830) and approximately half (55%) as many unique transcripts, with generally higher precision (i.e., a lower apparent false-positive rate), suggesting a higher quality assembly with fewer misassembled transcripts (Table 5). For both assemblies, approximately one-third of all loci (33.7% and 35.9% for Cufflinks and StringTie, respectively) were novel, meaning that there were no corresponding gene models in the reference genome annotation. Higher mapping rates were achieved by using the reference genome rather than the *de novo* assembly, with an average of 87.7%, 81.5%, and 69.3% of read pairs being successfully mapped by Tophat. HISAT, and Trinity, respectively (Table 1).

B.4.2 Differential Expression Analysis

All approaches detected changes in expression over time and differences between temperatures (Table 6). However, the amplitude of the transcriptomic response and, to a lesser extent, the general patterns of differential expression between sample groups differed. For example, the range in differentially expressed genes relative to the baseline is about 5X greater, according to Trinity (0-5121) compared to Cufflinks (147-1272) and StringTie (4-1001). Further, DE increases with temperature at 2 dph, peaks at the intermediate temperature at 14 dph, and is highest at the lower temperature at 29 dph, according to Trinity, whereas it always increases with temperature (StringTie) or varies (Cufflinks) according to the reference-based approaches.

B.4.3 Gene Ontology Enrichment Analysis

There was substantial overlap among ClueGO-enriched GO terms associated with differentially expressed genes detected by each pipeline (Figure 3). When more differentially expressed genes were detected by Trinity, the amount of overlap with the reference genome-based pipelines increased, resulting in near concordance between pipelines in those samples that were most different from the baseline (D2-13°C, D14-11°C, and D29-13°C). Conversely, when fewer differentially expressed genes were detected, the discrepancies between the *de novo* and reference-based pipelines were greater. The GO terms identified as being differentially expressed by Cufflinks and StringTie largely, though incompletely, overlapped, with Cufflinks detecting more than StringTie.

Notably, however, Trinity also tended to identify more enriched GO terms relative to the number of differentially expressed genes than the other pipelines, with an average of 0.20 (+/upregulated) and 1.33 (-/downregulated) BiNGO-enriched terms per gene for all samples relative to the baseline, compared to 0.07 (+) and 0.06 (-) for Cufflinks and 0.03 (+) and 0.42 (-) for StringTie (Table 7). The same pattern was true for upregulated, but not downregulated, ClueGO-enriched GO terms (Table 7).

Specifically, the numbers of ClueGO-enriched terms based on upregulated genes detected by Tuxedo/Cufflinks followed a similar pattern as those based on Trinity (despite different trends in the numbers of differentially expressed genes) except with a time lag: no enriched processes were detected at 2 dph, whereas the greatest response was observed at 14 dph at 13°C and 29 dph at 11°C.

B.5 Discussion

Overall, the three pipelines (Trinity, Tuxedo, and the 'new Tuxedo') produced different, yet complementary, results. The generally greater number of differentially expressed genes detected by Trinity could be due to *de novo* assembled transcripts that were unable to be mapped to the reference genome. This could be because they were located on genome fragments that were not assembled or filtered out of the reference, or because they were novel isoforms lacking corresponding gene models in the reference (Tørresen *et al.* 2017). The observation that approximately one-third of all transcripts assembled using the reference genome were novel supports the hypothesis that the reference genome and annotation are incomplete (Table 5). Indeed, genome assemblies and annotations are 'works-in-progress' (Denton *et al.* 2014; Francis & Wörheide 2017). Thus, draft genomes of non-model organisms are typically less complete and less accurate than their older, model counterparts. Further, although 10-15% (Cufflinks) and 12-28% (StringTie) of read pairs failed to map to the reference genome (Table 1), these reads might contribute to *de novo* transcripts constructed by Trinity.

The fragmented nature of the *de novo* transcriptome also likely contributed to the greater number of differentially expressed genes detected using Trinity, because fragmentation can result in a single gene being represented by multiple partial transcripts, which are identified as unique 'genes' according to Trinity. However, this alone does not explain the large number of unique GO terms relative to the reference genome-based pipelines (Figure 3; Table 7), as different fragments of a gene would have the same ontology.

B.6 Conclusion

Among the reference genome-based approaches, the 'new Tuxedo' pipeline (Pertea *et al.* 2016) outperformed the Tuxedo suite (Trapnell *et al.* 2012). This was expected, given that StringTie is known for improved reconstruction of low-abundance, multi-isoformic, and highly multi-exonic genes (Pertea *et al.* 2015). Greater enrichment by Trinity-identified differentially expressed genes suggests that a high proportion of them represent biologically meaningful differences in transcription, as opposed to transcriptional noise or false positives. Coupled with the ability to annotate novel loci, the increased sensitivity of the *de novo* pipeline for detecting likely biologically meaningful differential expression might make it preferable over the reference genome-based approaches for studies aimed at broadly characterizing variation in the magnitudes of expression differences and biological processes. However, the reference-based 'new Tuxedo' pipeline might be more appropriate when a more conservative approach is warranted, such as for the detection and identification of candidate genes.

The present methodological comparison is based on the genome and transcriptome assemblies of a single, non-model species. We do not know how common the discrepancies between pipelines we observed are; direct comparisons between *de novo* and reference genome-based pipelines are rarely reported. Indeed, the differences are likely to vary substantially between species depending on the quality of the genomic resources available. Overall, we suggest that the comparison and integration of multiple methods is highly informative. We also suggest that the annotation of the Atlantic cod genome could be improved by incorporating our transcriptome data (Denton *et al.* 2014; Francis & Wörheide 2017).

B.7 Tables

Table 1: Sample treatment, sequencing, trimming, and mapping details for RNA-seq experiment.

				Initial	Trimming		Trinity mapping		Tuxedo mapping		New tuxedo mapping	
Sample ID	Days post hatch	Temperature (°C)	Sequencing tag	# reads	# reads	%	# reads	%	# reads	%	# reads	%
D02-09-B5	2	9	2	27823421	26874862	96.6	19690676	73.3	24153483	88.8	23214510	86.4
D02-09-B1	2	9	2	25964999	25282323	97.4	18242550	72.2	22512386	87.8	21479112	85.0
D02-11-C2	2	11	2	27296151	26516131	97.1	18791272	70.9	23610006	87.9	22105973	83.4
D02-09-C2	2	9	2	23590062	23179774	98.3	17164878	74.1	20737259	88.3	20433461	88.2
D14-13-C4	14	13	2	28514132	27667225	97.0	19863808	71.8	24549905	86.8	23831459	86.1
D14-09-B6	14	9	4	26615216	26089673	98.0	19570646	75.0	23413709	88.7	22737326	87.2
D14-13-B2	14	13	4	26959597	26523970	98.4	19713728	74.3	23731125	88.4	23033205	86.8
D14-09-C5	14	9	4	24246261	23837204	98.3	17590759	73.8	21196567	87.5	20888582	87.6
D14-09-C6	14	9	4	43185802	41644107	96.4	30263857	72.7	36984287	87.6	36311682	87.2
D14-11-B5	14	11	4	38553914	37292970	96.7	27108508	72.7	32569953	86.2	31758439	85.2
C-5	0	9	5	24436259	23554855	96.4	17312196	73.5	21081254	88.3	20315968	86.2
D29-09-B2	29	9	5	22731753	22237928	97.8	16299695	73.3	19498950	85.8	18648770	83.9
D29-09-C4	29	9	5	38305770	37674511	98.4	27481656	72.9	32959477	86.0	32185501	85.4
D29-11-C3	29	11	5	23688649	19578742	82.7	12601656	64.4	17793862	90.0	14888808	76.0
D29-13-B3	29	13	5	18984226	15865267	83.6	10561119	66.6	14309502	89.3	12413088	78.2
D02-13-C4	2	13	6	26356040	25951703	98.5	19147849	73.8	22436687	85.1	21990632	84.7
D02-11-B4	2	11	6	29852805	26144539	87.6	17722401	67.8	23497551	88.8	21175848	81.0
D02-11-C4	2	11	6	23296670	20192870	86.7	13347849	66.1	18134805	88.7	15853243	78.5
D02-13-B3	2	13	6	25437794	22134148	87.0	14527953	65.6	19778042	88.4	17072652	77.1
D02-13-C3	2	13	6	25857421	22818682	88.2	14792406	64.8	20295344	87.9	17708744	77.6
C-4	0	9	7	24897254	24490957	98.4	18040441	73.7	21836098	87.8	21355613	87.2
D14-11-B4	14	11	7	24261730	21208187	87.4	14607743	68.9	18307126	85.3	16605460	78.3
D14-11-C3	14	11	7	26816730	23760318	88.6	15755187	66.3	20589428	85.8	17654605	74.3
D14-13-C3	14	13	7	25532209	22715662	89.0	15305220	67.4	20421338	88.8	18345345	80.8
D29-09-B4	29	9	7	22432697	20344481	90.7	13765241	67.7	17807769	86.5	16087401	79.1
D29-11-B4	29	11	12	26328524	23241618	88.3	14886144	64.1	20733793	88.1	17630079	75.9
D29-11-C4	29	11	12	24848859	22722112	91.4	14467330	63.7	20219418	87.7	17066530	75.1
D29-13-B4	29	13	12	22414790	18938416	84.5	11536863	60.9	16780344	87.5	13577095	71.7
D29-13-C4	29	13	12	24098850	20657148	85.7	13439165	65.1	18555480	88.7	15959289	77.3
C-3	0	9	12	24120921	20989004	87.0	13301248	63.4	18713208	88.0	15769774	75.1

Table 2: *De novo* transcriptome assembly statistics.

Statistic	Value
General	
Total trinity 'genes'	386872
Total trinity transcripts	530683
Percent GC	47.93
Based on all transcript contigs	
Contig N10	3949
Contig N20	2841
Contig N30	2180
Contig N40	1690
Contig N50	1278
Median contig length	431
Average contig	778.02
Total assembled bases	412883956
Based on only the longest isoform per 'gene'	
Contig N10	3484
Contig N20	2338
Contig N30	1648
Contig N40	1159
Contig N50	835
Median contig length	364
Average contig	612.59
Total assembled bases	236994575

Table 3: *De novo* transcriptome ExN50 statistics.

E	E-N50	# transcripts
E1	2710	2
E2	2343	4
E3	2343	6
E4	2343	9
E5	2343	11
E6	2343	14
E7	2710	17
E8	2343	21
E9	1523	24
E10	1523	28
E11	1292	31
E12	1292	35
E13	1282	39
E14	1117	43
E15	1039	48
E16	1039	52
E17	1021	57
E18	1262	63
E19	1282	68
E20	1292	74
E21	1282	81
E22	1262	88
E23	1282	95
E24	1248	103
E25	1248	112
E26	1220	123
E27	1292	134
E28	1389	147
E29	1389	161
E30	1404	178
E31	1371	197
E32	1523	218
E33	1404	242
E34	1428	269
E35	1488	298
E36	1523	331
E37	1488	367
E38	1535	407
E39	1561	453
E40	1628	504
E41	1599	561
E42	1615	625
E43	1650	698
E44	1661	780
E45	1680	872
E46	1713	973
E47	1721	1085
E48	1730	1208
E49	1741	1343
E50	1765	1491
E51	1775	1654
E52	1787	1833
E53	1812	2028
E54	1794	2243
E55	1797	2477
E56	1828	2732
E57	1851	3008
E58	1826	3304
E59	1836	3624
E60	1836	3970
E61	1868	4340
E62	1890	4737

E	E-N50	# transcripts
E63	1905	5162
E64	1917	5619
E65	1920	6107
E66	1943	6631
E67	1958	7191
E68	1967	7789
E69	1976	8427
E70	1976	9107
E71	1986	9833
E72	2007	10605
E73	2031	11426
E74	2034	12298
E75	2042	13227
E76	2048	14219
E77	2055	15279
E78	2068	16414
E79	2070	17631
E80	2079	18939
E81	2092	20348
E82	2105	21871
E83	2117	23524
E84	2119	25325
E85	2117	27303
E86	2129	29482
E87	2136	31915
E88	2142	34656
E89	2144	37789
E90	2153	41413
E91	2152	45701
E92	2143	50947
E93	2134	57639
E94	2122	66540
E95	2095	79086
E96	2053	97771
E97	1986	127442
E98	1871	177874
E99	1667	268326
E100	1318	488067

Table 4: De novo transcriptome blastx and blastp top hit statistics.

Percent length coverage bin	bin count	bin ≥ count
blastx		
100	6888	6888
90	2542	9430
80	2113	11543
70	2034	13577
60	2266	15843
50	2500	18343
40	2627	20970
30	2697	23667
20	2341	26008
10	782	26790
blastp		
100	7385	7385
90	2389	9774
80	2046	11820
70	1940	13760
60	2173	15933
50	2304	18237
40	2473	20710
30	2344	23054
20	1763	24817
10	432	25249

Table 5: Comparison of reference genome-based transcriptome assemblies with the reference genome annotation.

Statistic	Value(s)	Value(s)
	Cufflinks	Stringtie
mRNAs	167150	92033
Loci	31830	34132
Multi-exon transcripts	158926	83848
Multi-transcript loci	18066	17075
Mean transcripts per locus	5.3	2.7
	Reference	Reference
mRNAs	23243	23243
Loci	23243	23243
Multi-exon transcripts	22139	22139
	Cufflinks vs. Reference	Stringtie vs. Reference
Super-loci w/ reference transcripts	20333	20523
Base level sensitivity	100	100
Base level precision	52.8	56.7
Exon level sensitivity	100	100
Exon level precision	54.6	57.4
Intron level sensitivity	100	100
Intron level precision	61.2	64.4
Intron chain level sensitivity	100	100
Intron chain level precision	13.9	26.4
Transcript level sensitivity	100	100
Transcript level precision	13.9	25.3
Locus level sensitivity	100	100
Locus level precision	65.6	62.5
Matching intron chains	22139	22139
Matching transcripts	23243	23243
Matching loci	23243	23243
Missed exons	0/223454 (0.00%)	0/223454 (0.00%)
Novel exons	110161/427064 (25.80%)	94374/415948 (22.70%)
Missed introns	1/200211 (0.00%)	1/200211 (0.00%)
Novel introns	48063/327303 (14.70%)	43522/311125 (14.00%)
Missed loci	0/23243 (0.00%)	0/23243 (0.00%)
Novel loci	10720/31830 (33.70%)	12252/34132 (35.90%)
Total union super-loci across all input datasets	31830	34132

Table 6: Numbers of genes differentially expressed in pairwise tests. Number of up- (+), down- (-), and dys- (+/-) regulated transcripts detected a) at each temperature at each time point relative to the baseline sample, b) between temperature treatments within time points, and c) between time points within temperature treatments, using de novo (Trinity) and reference genome-based (Cufflinks and Stringtie) pipelines prior to differential expression analysis.

Day	Temperature	Direction	Trinity	Cufflinks	Stringtie
a) All vs. baseline (0 dph at 9°C)					
2	9°C	+	0	49	2
		-	0	98	2
		+/-	0	147	4
	11°C	+	8	97	29
		-	2	452	8
		+/-	10	549	37
	13°C	+	3581	70	67
		-	65	110	13
		+/-	3646	180	80
14	9°C	+	48	177	64
		-	46	179	41
		+/-	94	356	105
	11°C	+	4296	274	114
		-	825	278	61
		+/-	5121	552	175
	13°C	+	188	392	279
		-	106	372	110
		+/-	294	764	389
29	9°C	+	3558	366	318
		-	718	352	205
		+/-	4276	718	523
	11°C	+	509	465	499
		-	720	607	377
		+/-	1229	1072	876
	13°C	+	629	429	677
		-	439	630	324
		+/-	1068	1059	1001
b) Temperature effects					
2	9-11°C	+	0	16	5
		-	0	32	1
		+/-	0	48	6
	11-13°C	+	3291	114	7
		-	64	65	10
		+/-	3355	179	17
	9-13°C	+	3556	70	29
		-	49	78	8
		+/-	3605	148	37
14	9-11°C	+	1507	38	4
		-	30	18	2
		+/-	1537	56	6
	11-13°C	+	156	90	24
		-	2324	92	11
		+/-	2480	182	35
	9-13°C	+	4	103	19

Day	Temperature	Direction	Trinity	Cufflinks	Stringtie
		-	0	47	5
		+/-	4	150	24
29	9-11°C	+	0	80	13
		-	0	66	18
		+/-	0	146	31
	11-13°C	+	1	26	24
		-	0	59	8
		+/-	1	85	32
	9-13°C	+	0	46	11
		-	0	55	6
		+/-	0	101	17
c) Time effects					
9°C	0*-2	+	0	49	2
		-	0	98	2
		+/-	0	147	4
	2-14	+	50	470	33
		-	36	349	13
		+/-	86	819	46
	14-29	+	206	166	81
		-	118	168	27
		+/-	324	334	108
	2-29	+	3663	388	229
		-	835	387	109
		+/-	4498	775	338
11°C	0*-2	+	8	97	29
		-	2	452	8
		+/-	10	549	37
	2-14	+	4580	835	72
		-	2447	485	70
		+/-	7027	1320	142
	14-29	+	546	219	86
		-	2946	218	43
		+/-	3492	437	129
	2-29	+	1392	1261	816
		-	2958	1222	1319
		+/-	4350	2483	2135
13°C	0*-2	+	3581	70	67
		-	65	110	13
		+/-	3646	180	80
	2-14	+	167	456	134
		-	804	320	103
		+/-	971	776	237
	14-29	+	22	102	42
		-	10	219	20
		+/-	32	321	62
	2-29	+	375	399	417
		-	978	496	370
		+/-	1353	895	787
# of transcripts in analysis:			51075	31830	34064

Table 7: Numbers of enriched gene ontology terms detected through pairwise contrasts with the baseline.

			BinGO			ClueGO		
Day	Temperature	Direction	Trinity	Cufflinks	Stringtie	Trinity	Cufflinks	Stringtie
2	9°C	+	0	3	0	0	0	0
		-	0	22	0	0	1	0
	11°C	+	10	8	0	0	0	0
		-	20	73	21	0	40	0
	13°C	+	305	3	8	1545	0	0
		-	10	3	13	0	0	0
14	9°C	+	4	29	7	0	12	0
		-	38	0	0	0	5	0
	11°C	+	334	10	0	1756	23	0
		-	195	16	0	80	43	0
	13°C	+	16	30	6	0	44	3
		-	40	0	0	1	16	3
29	9°C	+	307	19	3	1595	25	1
		-	69	25	7	90	18	3
	11°C	+	46	11	0	9	35	2
		-	117	16	9	199	179	7
	13°C	+	32	44	4	4	20	1
		-	47	5	21	28	146	4
# GO terms/DE gene (+)			0.20	0.07	0.03	0.15	0.05	0.00
# GO terms/DE gene (-)			1.33	0.06	0.42	0.06	0.10	0.01

Numbers of enriched gene ontology (GO) terms among up- (+) and down- (-) regulated genes detected at each temperature at each time point relative to the baseline sample, using de novo(Trinity) and reference genome-based (Cufflinks and Stringtie) pipelines prior to differential expression analysis.

B.8 Figures

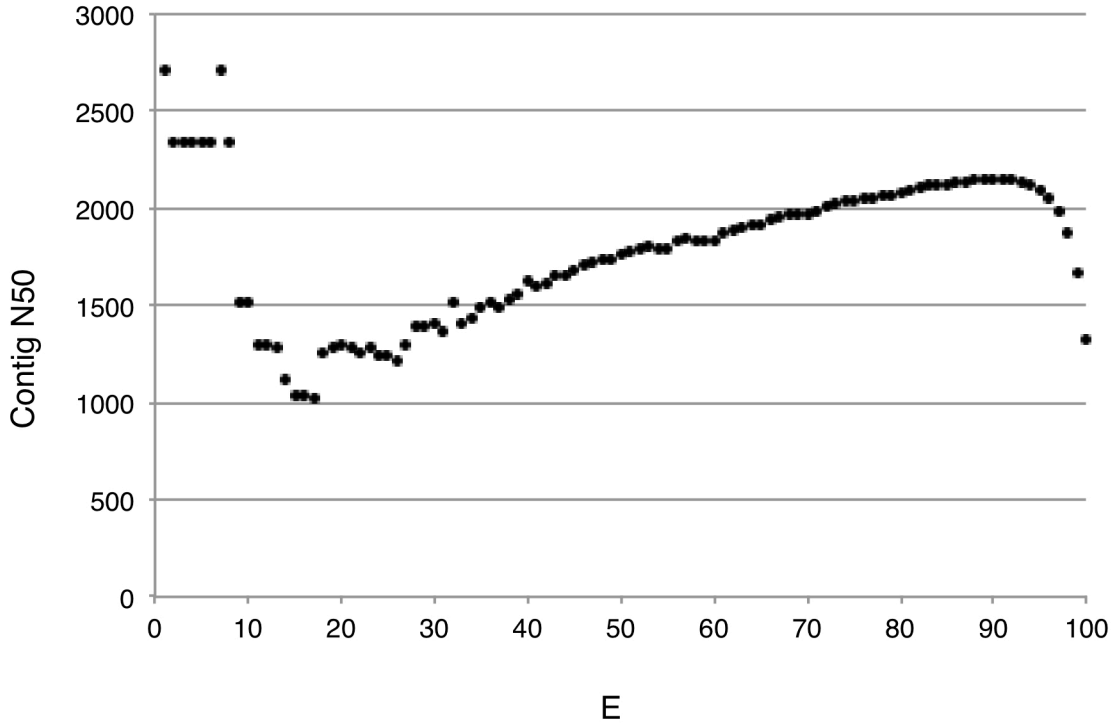

Figure 1: Expression contig N50 distribution of the *de novo* Trinity assembly. The minimum length of contig in which 50% of all assembled bases are contained as a function of the percentage of total normalized expression data represented by the most highly expressed trancripts in the *de novo* Trinity assembly.

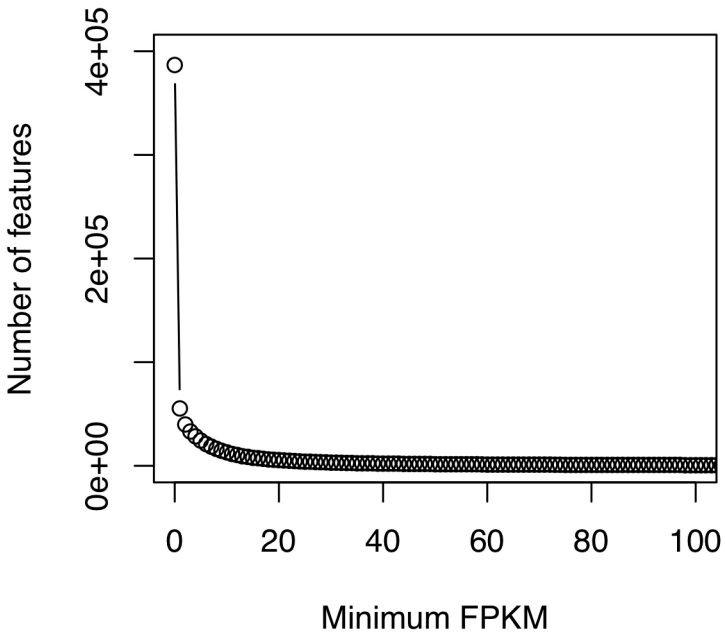

Figure 2: Minimum expression level gene count. The number of *de novo*-assembled Trinity 'genes' with a minimum expression level in FPKM (Fragments Per Kilobase of transcript per Million mapped reads).

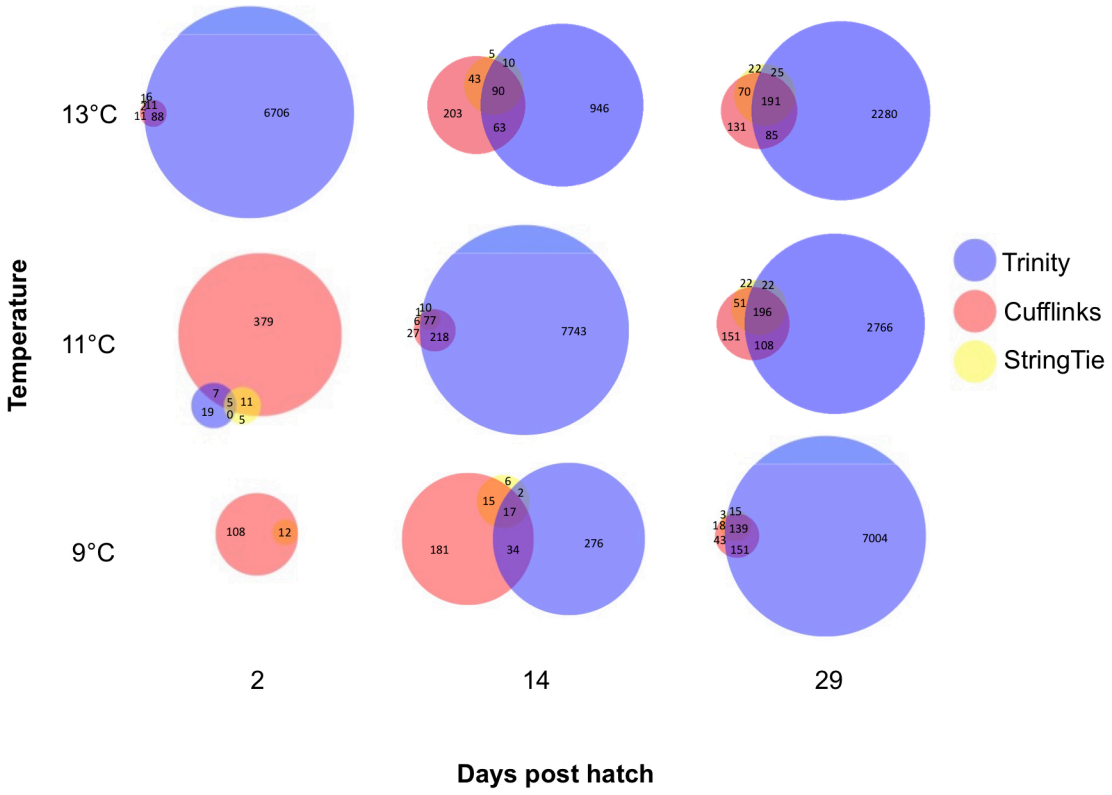

Figure 3: Overlap of gene ontology terms among bioinformatic pipelines. The number of unique gene ontology (GO) terms enriched among differentially expressed genes at each time and temperature in a larval Atlantic cod rearing experiment (Oomen et al. [submitted]), using the *de novo* Trinity pipeline, the reference-based Tuxedo pipeline (Cufflinks), and the 'new Tuxedo' pipeline (StringTie). Enrichment analysis was performed using ClueGO v.2.3.2 (Bindea *et al.* 2009) in Cytoscape v.3.2.1 (Shannon *et al.* 2003). The sizes of circles and overlaps are proportional to the number of GO terms within individual diagrams (i.e., time points × treatments), but not between them.

Appendix C: Supplementary materials for Chapter 4

C.1 Supplementary Tables

Table S1. Summary statistics of microsatellite loci used for parentage analysis of Risør cod: number of alleles ($N_{(a)}$), size range (bp), expected heterozygosity (H_e), observed heterozygosity (H_o), and inbreeding coefficient (F_{IS}).

Locus	$N_{(a)}$	Size (bp)	Reference	$He_{(Outer)}$	$Ho_{(Outer)}$	$F_{IS\ (Outer)}$	$He_{(Inner)}$	$Ho_{(Inner)}$	$F_{IS\ (Inner)}$
GMO8[1]	23	110-205	Miller et al. 2000	0.953	1.000	-0.050	0.881	0.865	0.018
GMO19[1]	24	120-220	Miller et al. 2000	0.930	0.833	0.106	0.919	0.784	0.149
GMO35[1]	12	110-145	Miller et al. 2000	0.826	0.750	0.093	0.827	0.865	-0.046
TCH11[1]	20	121-193	O'Reilly et al. 2000	0.917	0.806	0.123	0.937	0.946	-0.009
GMO2[2]	14	102-138	Brooker et al. 1994	0.887	0.833	0.061	0.838	0.784	0.065
GMO34[2]	8	80-120	Miller et al. 2000	0.659	0.667	-0.012	0.665	0.595	0.108
GMO132[2]	30	100-186	Brooker et al. 1994	0.923	0.944	-0.024	0.883	0.892	-0.011
TCH13[2]	7	74-86	O'Reilly et al. 2000	0.919	0.889	0.033	0.924	0.919	0.006

[1] Multiplex 1 (Delghandi et al. 2003)
[2] Multiplex 2 (Dahle et al. 2006; Glover et al. 2010)

Table S2. Tests for deviations from Hardy-Weinberg equilibrium for microsatellite loci used for parentage analysis of Risør cod, calculated separately for each population. No loci deviated significantly from Hardy-Weinberg equilibrium after correction for multiple testing (FDR; α=0.05).

Locus	P-value $_{(Outer)}$	P-value $_{(Inner)}$
GMO35	0.124	0.331
GMO19	0.163	0.038
GMO8	0.966	0.281
TCH11	0.196	0.444
TCH13	0.504	0.352
GMO34	0.900	0.301
GMO2	0.509	0.074
GMO132	0.876	0.177

Table S3: Genetic cross assignment of larval cod.

Experimental group			Genetic cross assignment of larvae								
dph	°C	Tank	IF×IF	IF×OF	OF×IF	IF×ON	ON×IF	OF×ON	ON×OF	ON×ON	Total
0	6	n/a	7	4	16	5	2	5		1	40
2	13	HT1	8	3	8	17	2	2			40
2	13	HT2	7	1	7	19	3	2			39
2	13	HT3	12	2	16	7	1	1			39
2	13	HT4	16		13	10	1				40
2	9.5	IT1	10	5	9	11	3	2			40
2	9.5	IT2	9	3	10	14	2	1			39
2	9.5	IT3	14	4	5	13	2	1			39
2	9.5	IT4	12	2	9	16		1			40
2	6	LT1	7	2	13	8	2	3			35
2	6	LT2	10	3	10	14	2	1			40
2	6	LT3	16	2	10	11	1				40
2	6	LT4	10	2	11	14	3				40
14	13	HT1	11		26	1	2				40
14	13	HT2	6	2	14	9	5	4			40
14	13	HT3	11	2	18	5	2	2			40
14	13	HT4	14	4	16	1	1	2			38
14	9.5	IT2	13	3	14	5	1	3			39
14	9.5	IT3	22		8	6	3	1			40
14	9.5	IT4	7	1	10		2	1			21
14	6	LT2	9	4	8	3	3	4	1		32
14	6	LT4	11	1	9	2	4	5			32
21	13	HT1	12	1	20	3	3	1			40
21	13	HT3	8		22	3	5	2			40
21	13	HT4	3		14	2	3	1			23
21	9.5	IT2	12	2	12	2	1	2			31
21	9.5	IT3	7	4	11	5	2	1	1		31
21	6	LT1	13	2	15	4	2	4			40
21	6	LT2	17	3	9	3	3	5			40
21	6	LT3	12	2	15	7	1	2			39
21	6	LT4	11	2	23	1	3				40
28	13	HT1	7	1	23	1	5	3			40
28	13	HT3	7	1	20	5	5	2			40
28	13	HT4	9	2	22	4	2	1			40
28	9.5	IT2	10	3	15	5	4	3			40
28	9.5	IT3	13	2	12	9		2	1		39
28	9.5	IT4	12	2	12	5	4	5			40
28	6	LT2	11	6	12	3	2	3	2		39
28	6	LT3	13	4	10	3	2	7			39
28	6	LT4	17	5	11	4		3			40
		Total	436	92	538	260	94	88	5	1	1514

C.2 Supplementary Figures

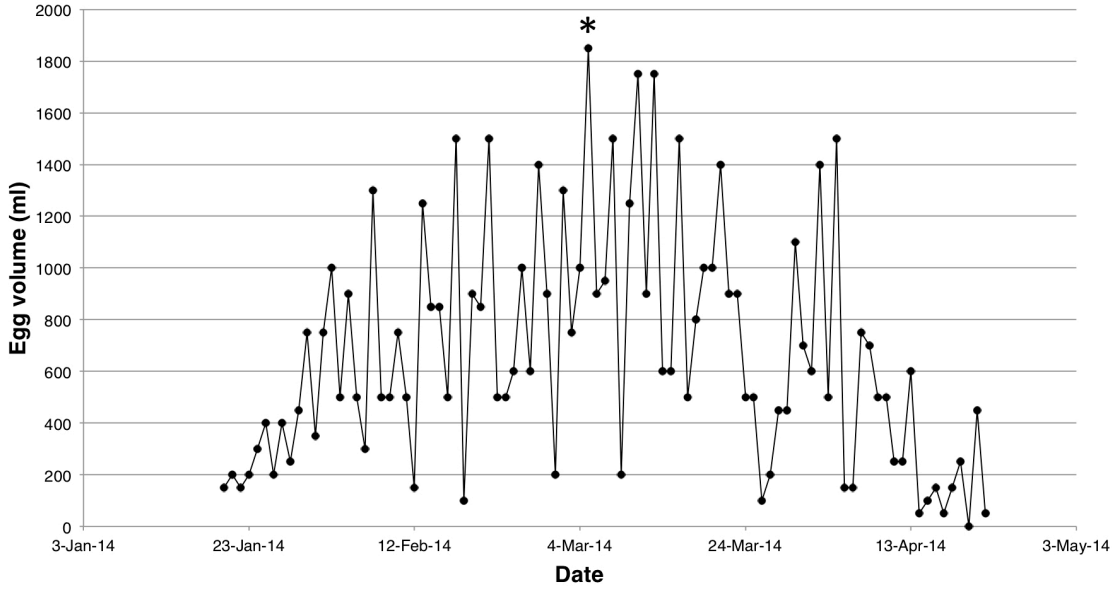

Figure S1: Daily volume of eggs collected throughout the spawning period. The asterisk indicates the eggs that were sampled for the present study.

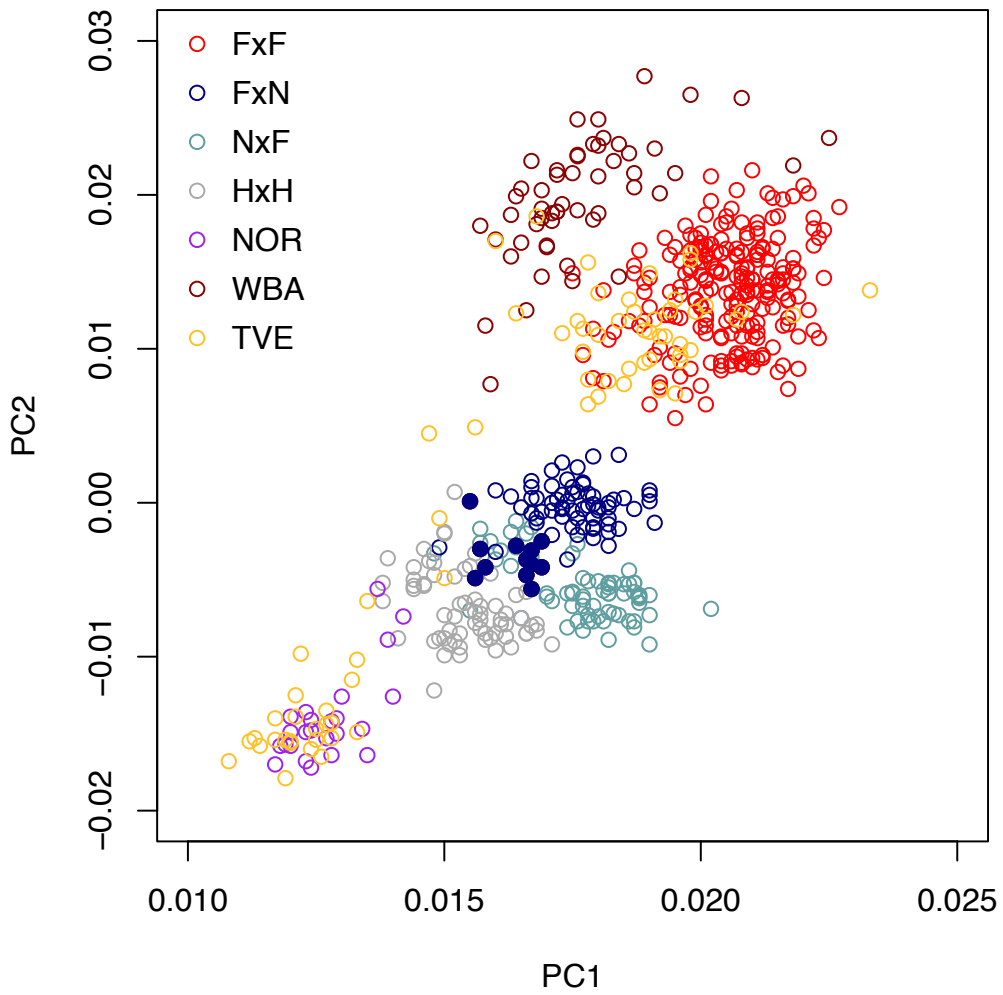

Figure S2: Projected results of a principal component analysis for linkage disequilibrium-purged genome-wide SNPs extracted from reference genome-based transcriptome assemblies (Chapter 5) and reference samples. Principal components were calculated based on a global dataset (n=861; Aqua Genome Project, e.g., see Barth et al. 2019) combined with the Risør and Helgeland samples in the present study (n=432), but only the study samples and select reference populations are plotted. The study samples include three ecotype crosses from Risør fjord (F×F = Fjord mother × Fjord father, N×F = North Sea mother × Fjord father, F×N = Fjord mother × North Sea father) and Helgeland (H×H). The reference samples include offshore North Sea (NOR), Western Baltic (WBA), and Tvedestrand fjord (TVE). Tvedestrand consists of both Fjord and North Sea genotypes, as well as a few Western Baltic genotypes (Barth et al. 2019). The filled circles represent the offspring of father RIC5100, which was classified as North Sea based on the clustering of offspring produced with Fjord females with the ecotype hybrids observed here.

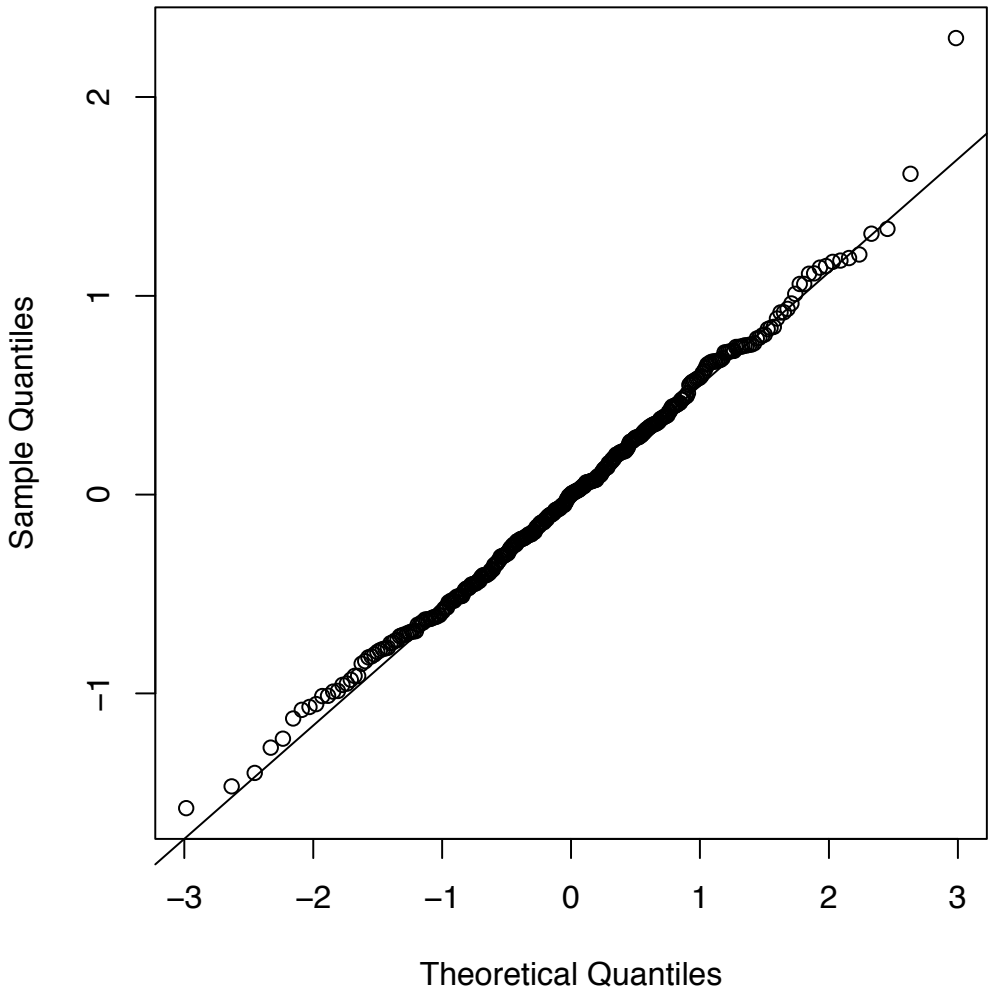

Figure S3: Q-Q norm plot of the residuals from the linear model used in the growth reaction norm analysis.

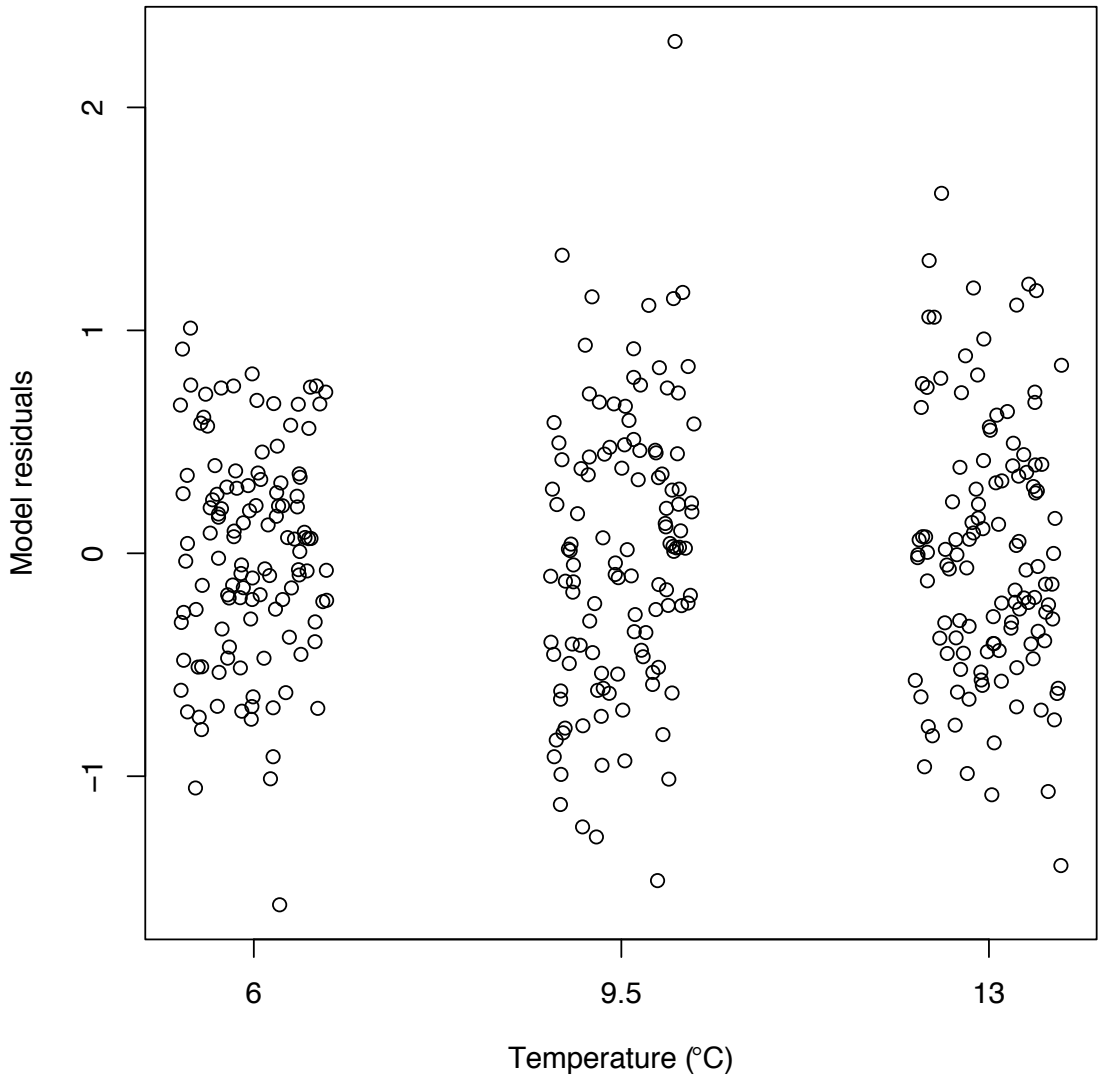

Figure S4: Linear model residuals for each temperature in the growth reaction norm analysis.

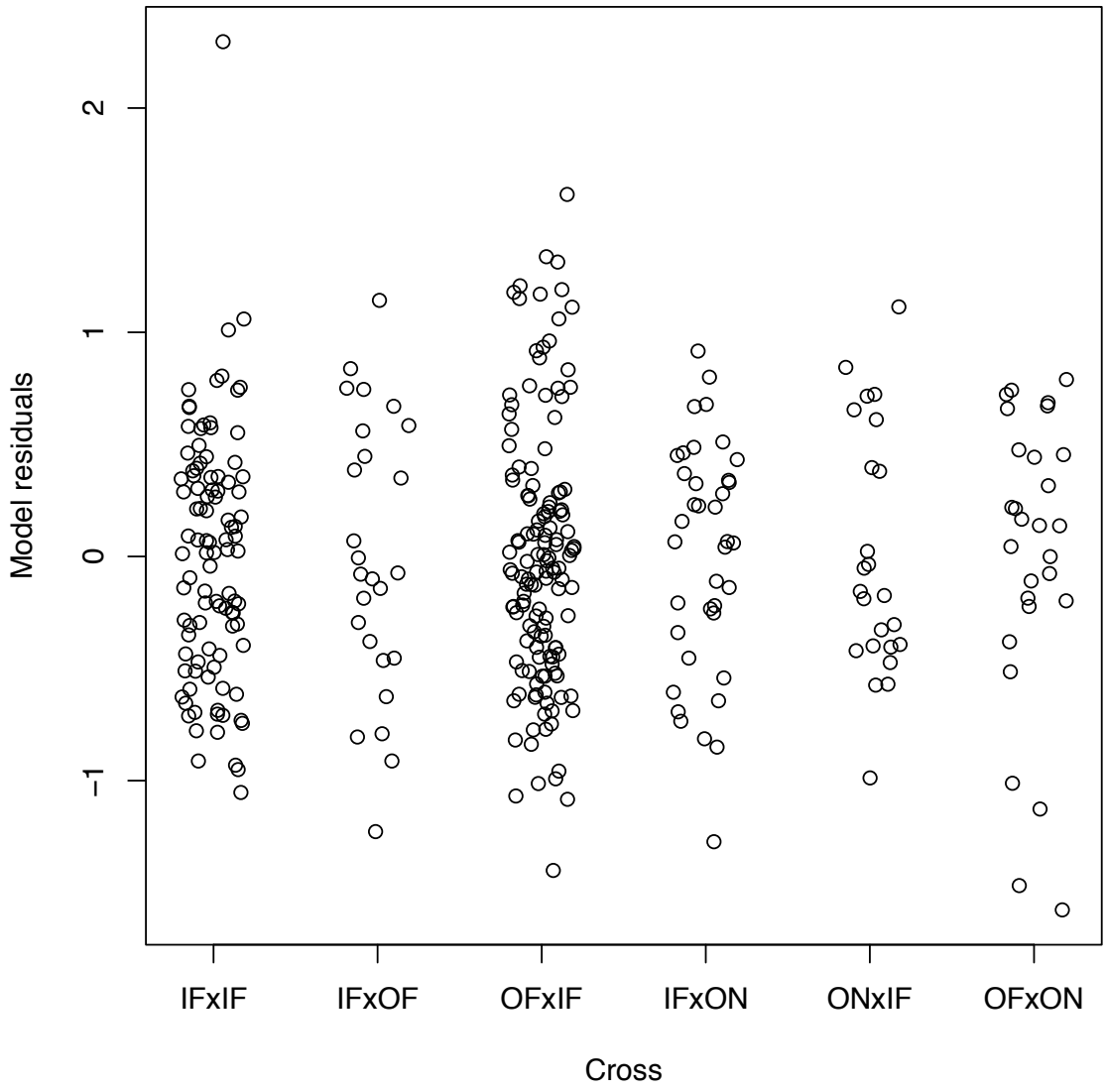

Figure S5: Linear model residuals for each cross in the length-at-day reaction norm analysis.

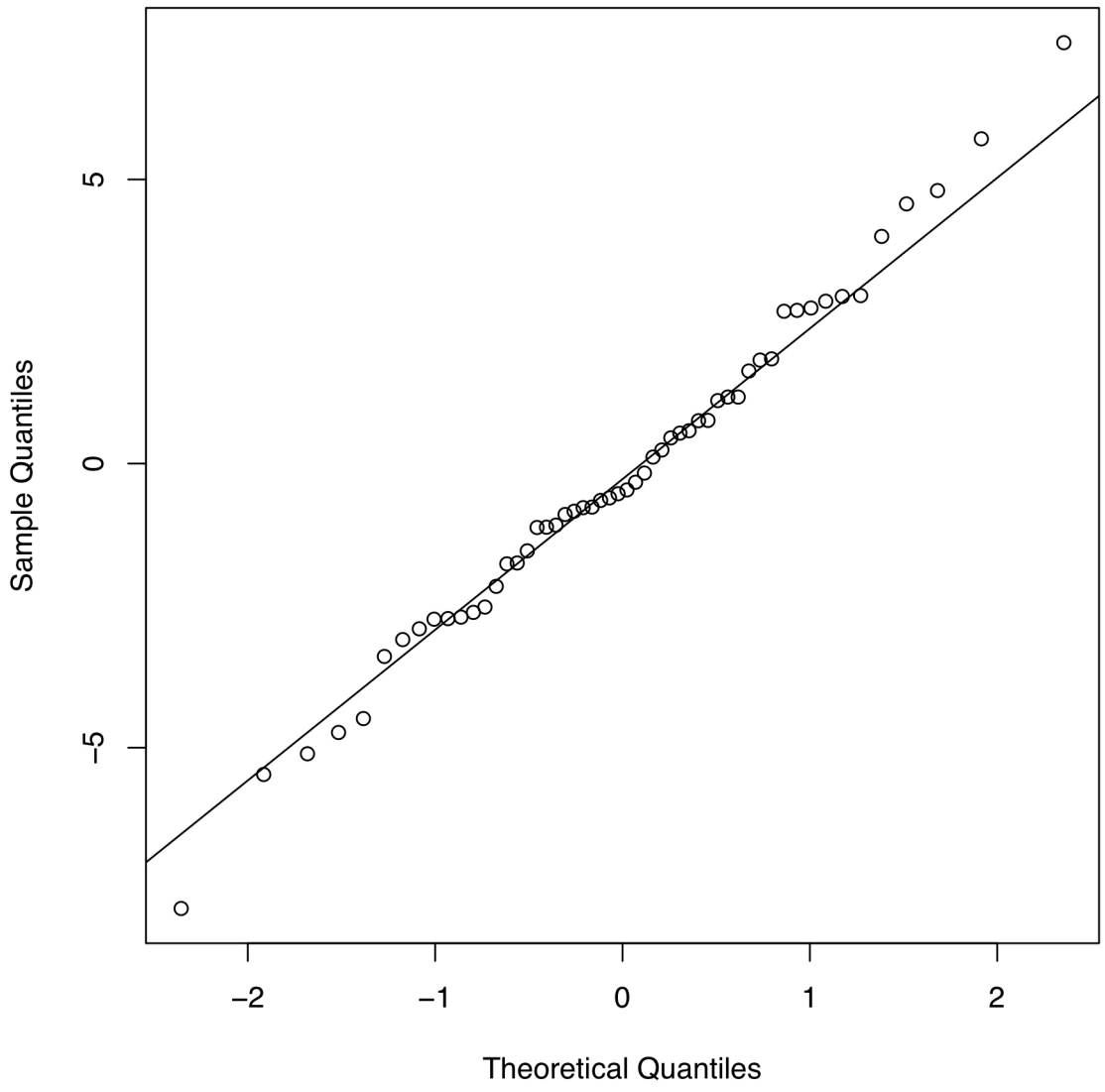

Figure S6: Q-Q norm plot of the residuals from the generalized linear model used in the survival reaction norm analysis.

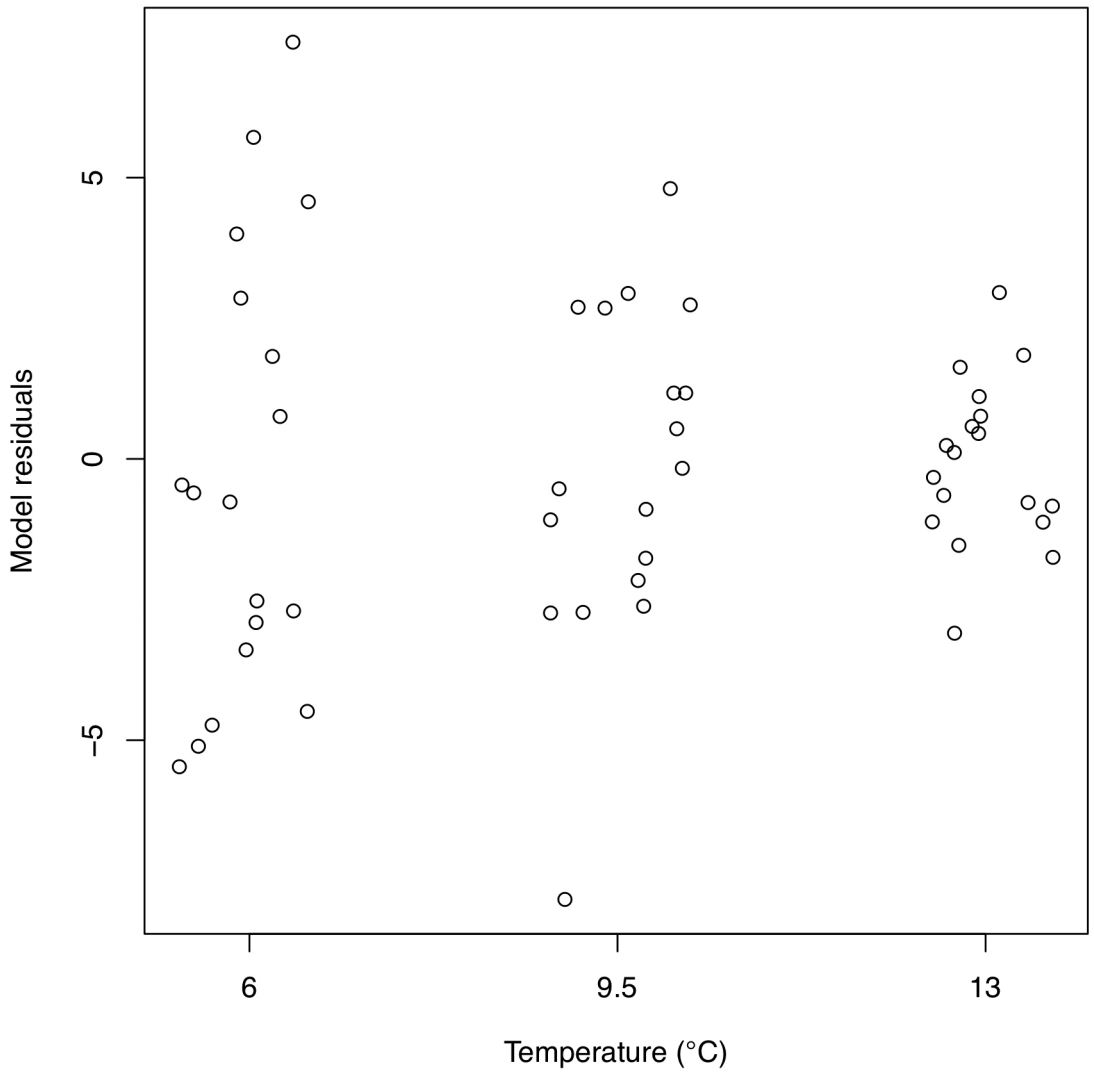

Figure S7: Generalized linear model residuals for each temperature in the survival reaction norm analysis.

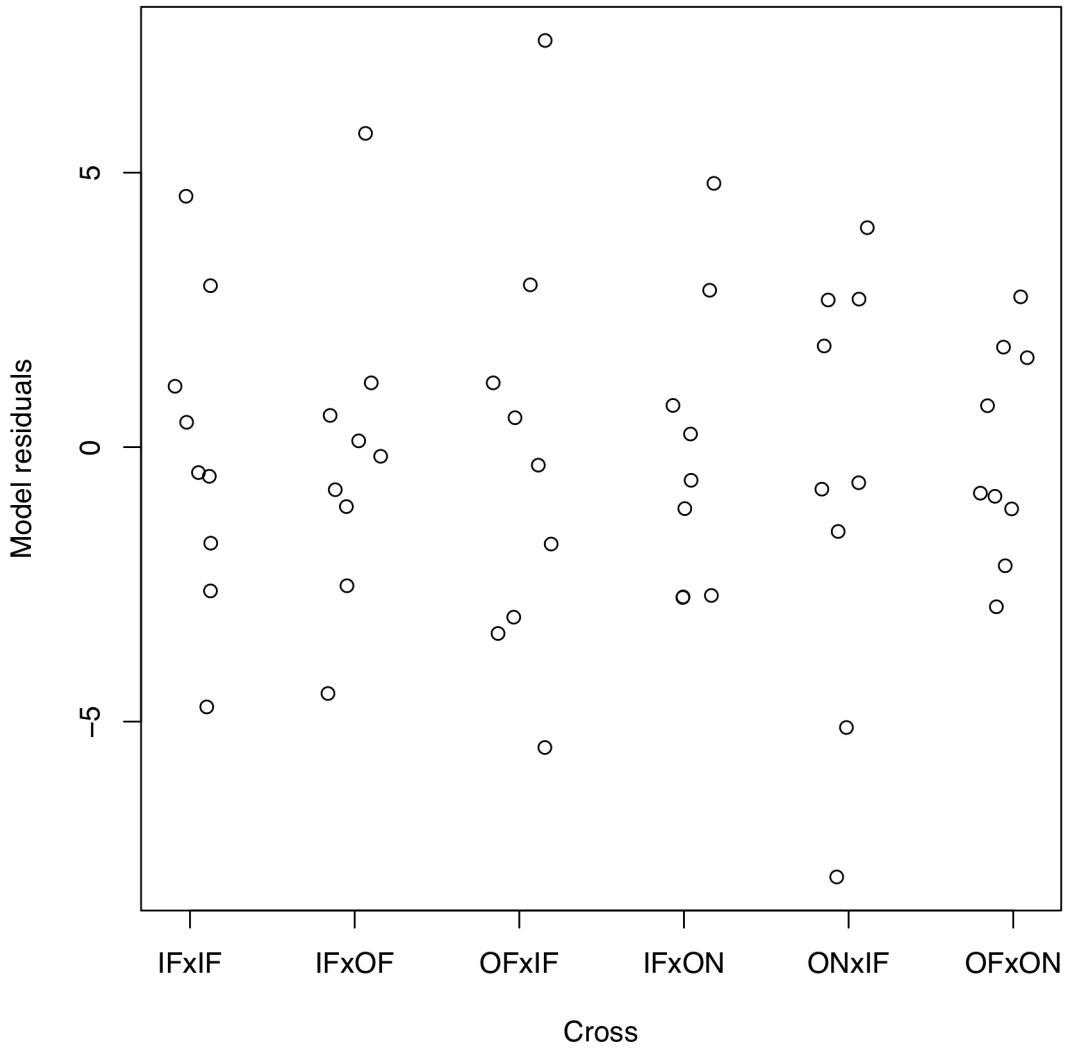

Figure S8: Generalized linear model residuals for each cross in the survival reaction norm analysis.

Appendix D: Supplementary Materials for Chapter 5

D.1 Supplementary Methods for Helgeland Experiment

Adult cod (n=29; 15 females and 14 males) > 40 cm in length (mean±SD = 49.2±5.8 cm) were collected from a semi-sheltered area outside a large fjord (Ranfjorden) near Helgeland, Norway by baited fyke nets and transported in chilled and aerated seawater by truck to the *Flødevigen Research Station, Institute of Marine Research*. Eggs were collected ~8 weeks after the adults were placed in the spawning basin and incubated in a 900 L flow-through seawater tank at 6°C until hatch. At 0 days post hatch (dph), larvae were randomly sampled and distributed among 40 L flow-through seawater tanks. Larvae were reared at 6°C, 9.5°C, and 13°C with 5 replicate tanks per temperature treatment (Table S1).

Three of the temperature replicates were initially stocked with exactly 2000 larvae each (50 larvae/L = 'low density') and two of the replicates were stocked with approximately 4000 larvae each (~100 larvae/L = 'high density'). Stocking densities of 50 to 300 larvae per litre have been shown to have no effect on survival or growth of cod larvae as long as food is not limiting (Baskerville-Bridges & Kling 2000), as was the case in the present study. Further, a previous study including five experiments on Northwest Atlantic cod larvae similar in design to the present study found that tank density was not related to patterns of growth and survival in response to temperature (Oomen & Hutchings 2015b). Thus, tanks of different initial stocking densities were considered to be experimental replicates for the growth and gene expression analyses.

At 0 dph, 20 larvae were randomly sampled from the incubation tank to serve as baseline samples prior to transfer and temperature exposure. At 2 and 7 dph, 20 larvae were randomly sampled from each of the low-density tanks. At 14 and 21 dph, 10 larvae were randomly sampled from each of the low and high-density tanks. At 28 dph, 20 larvae were randomly sampled from each of the low and high-density tanks. If fewer than 10 or 20 larvae were present in the tanks, all remaining larvae were sampled.

D.2 Supplementary Tables

Table S1: Details for three larval cod rearing experiments from 2013-2015 at the *Institute of Marine Research, Flødevigen*.

Experimental factor	2013	2014	2015
Region	Skagerrak	Skagerrak	Helgeland
Location	Flødevigen	Risør	Nesna
Broodstock collection	Dec. 2012 - Jan. 2013	Dec. 2013 - Jan. 2014	Jan. 2015
Egg collection	April 13, 2013	March 5, 2014	April 8, 2015
Experiment start (0 dph)	April 24, 2013	March 20, 2014	April 22, 2015
Ambient temperature (°C)	9	6	6
Number of tank replicates	3	4	5
Initial stocking density (larvae/L)	40	50	50 to ≈100
Water chiller used	no	yes	yes
Rearing temperatures (°C)	9, 11, 13	6, 9.5, 13	6, 9.5, 13
Sample time points (dph)	0, 2, 14, 29	0, 2, 14, 21, 28	0, 2, 7, 14, 21, 28
Sample per tank per time point	10 (30 at 0 dph)	40	10/20 (or remainder)
RNA-seq experiment	A	B	B
RNA-seq replicates (mean±SD)	3±0	5.6±0.9	5±0

Table S2: Results of a linear mixed effects model of larval Atlantic cod growth from 2 to 28 dph, including interactions between all genetic factors. Asterisks denote significance based on a Type III ANOVA (α=0.05).

Model term	χ2	d.f.	*P*-value	
Original model terms				
ecotype	0.74	2	0.692	
location	4.60	3	0.204	
LG02	2.22	1	0.136	
LG07	0.40	1	0.525	
LG12	0.08	1	0.779	
dph	0.30	3	0.959	
temperature	3.30	2	0.192	
ecotype×dph	1.88	6	0.930	
location×dph	3.68	8	0.884	
LG02×dph	3.27	3	0.352	
LG07×dph	0.02	3	0.999	
LG12×dph	5.25	3	0.155	
temperature×dph	8.05	6	0.235	
ecotype×dph×temperature	10.45	16	0.842	
location×dph×temperature	22.26	16	0.135	
LG02×dph×temperature	5.86	8	0.663	
LG07×dph×temperature	4.42	8	0.818	
LG12×dph×temperature	15.39	7	0.031	*
Interactions between genetic factors				
ecotype×LG02	3.46	2	0.177	
ecotype×LG07	3.08	2	0.214	
ecotype×LG12	5.78	2	0.056	
location×LG02	1.79	3	0.618	
location×LG07	0.53	3	0.913	
location×LG12	3.92	1	0.048	*
LG02×LG07	0.10	1	0.748	
LG02×LG12	0.30	1	0.584	
LG07×LG12	1.98	1	0.160	
ecotype×LG02×dph	7.48	3	0.058	
ecotype×LG07×dph	0.71	4	0.950	
ecotype×LG12×dph	2.03	2	0.362	
location×LG02×dph	3.24	6	0.778	
location×LG07×dph	0.98	5	0.964	
LG02×LG07×dph	0.44	3	0.932	
LG02×LG12×dph	6.40	3	0.094	
ecotype×LG02×dph×temperature	0.83	1	0.363	
ecotype×LG07×dph×temperature	3.56	4	0.469	
location×LG02×dph×temperature	5.66	9	0.773	
location×LG07×dph×temperature	2.74	5	0.741	
LG02×LG07×dph×temperature	0.01	1	0.936	

Model term	Variance	SD
father	0.06	0.24
mother	0.00	0.00
residual	0.26	0.51

Table S3: Shapiro-Wilk tests for deviations from normality of residuals from a generalized linear model of chromosomal inversion haplotype frequencies for all Risør larvae and for the two largest families. Asterisks denote significance at α=0.05.

Dataset	LG	W	*P*	
All	02	0.97	0.919	
All	07	0.93	0.300	
All	12	0.92	0.221	
F03×RIC5064	02	0.96	0.728	
F03×RIC5064	07	0.94	0.416	
F03×RIC5064	12	0.82	0.007	*
RIC5060×RIC5076	02	0.89	0.079	
RIC5060×RIC5076	07	0.92	0.182	
RIC5060×RIC5076	12	0.89	0.079	

Table S4: Comparison of reference genome-based transcriptome assembly with the reference genome annotation.

Statistic	Value(s)
Stringtie	
mRNAs	143890
Loci	60577
Multi-exon transcripts	114581
Multi-transcript loci	19909
Mean transcripts per locus	2.4
Reference	
mRNAs	23243
Loci	23243
Multi-exon transcripts	22139
Stringtie vs. Reference	
Super-loci w/ reference transcripts	18203
Base level sensitivity	100
Base level precision	45.1
Exon level sensitivity	100
Exon level precision	45.2
Intron level sensitivity	100
Intron level precision	55.4
Intron chain level sensitivity	100
Intron chain level precision	19.3
Transcript level sensitivity	100
Transcript level precision	16.2
Locus level sensitivity	100
Locus level precision	33
Matching intron chains	22139
Matching transcripts	23243
Matching loci	23243
Missed exons	0/223454 (0.0%)
Novel exons	175598/530333 (33.1%)
Missed introns	1/200211 (0.0%)
Novel introns	76626/361709 (21.2%)
Missed loci	0/23243 (0.0%)
Novel loci	39586/60577 (65.3%)
Total union super-loci	60577

Table S5: Number and percentage of read pairs retained after trimming and mapping.

		Initial	Trimmed	HISAT2 mapped		Trinity mapped	
Sample ID	Batch	# reads	# reads	# reads	%	# reads	%
13-C00000-11	A1	24436259	22797862	21619213	94.8	19877456	87.2
13-C00000-21	A1	24897254	23705966	22454291	94.7	20612337	87.0
13-C00000-30	A1	24120921	19073798	18038091	94.6	15898011	83.4
13-D02T09-01	A1	27823421	25904074	24619232	95.0	22694559	87.6
13-D02T09-02	A1	25964999	24426228	23043703	94.3	21123802	86.5
13-D02T09-04	A1	23590062	22255171	21040039	94.5	19402058	87.2
13-D02T11-03	A1	27296151	25411279	23980624	94.4	21874029	86.1
13-D02T11-17	A1	29852805	24494293	23205893	94.7	20952418	85.5
13-D02T11-18	A1	23296670	18635326	17638336	94.7	15886615	85.3
13-D02T13-16	A1	26356040	25133199	23049657	91.7	21810590	86.8
13-D02T13-19	A1	25437794	20275595	19016481	93.8	17143016	84.6
13-D02T13-20	A1	25857421	21012922	19823591	94.3	17608829	83.8
13-D14T09-06	A1	26615216	25257997	23904168	94.6	22335647	88.4
13-D14T09-08	A1	24246261	23084677	21791935	94.4	20055967	86.9
13-D14T09-09	A1	43185802	39854747	37503317	94.1	34119649	85.6
13-D14T11-10	A1	38553914	35770885	33241883	92.9	30991895	86.6
13-D14T11-22	A1	24261730	19937647	18123321	90.9	17196221	86.3
13-D14T11-23	A1	26816730	21761117	19843963	91.2	18542648	85.2
13-D14T13-05	A1	28514132	26604476	25143890	94.5	22746827	85.5
13-D14T13-07	A1	26959597	25706107	24297412	94.5	22521120	87.6
13-D14T13-24	A1	25532209	21007683	19848059	94.5	17837624	84.9
13-D29T09-12	A1	22731753	21594491	20037528	92.8	18653321	86.4
13-D29T09-13	A1	38305770	36468008	34079353	93.5	31406248	86.1
13-D29T09-25	A1	22432697	18955583	17609737	92.9	16017468	84.5
13-D29T11-14	A1	23688649	17854822	16967437	95.0	15174813	85.0
13-D29T11-26	A1	26328524	21290100	20085080	94.3	17800653	83.6
13-D29T11-27	A1	24848859	20932305	19691019	94.1	17486848	83.5
13-D29T13-15	A1	18984226	14755374	14005801	94.9	12663062	85.8
13-D29T13-28	A1	22414790	16919483	15865399	93.8	13958573	82.5
13-D29T13-29	A1	24098850	18907700	17856432	94.4	15888140	84.0
14-C00000-03	B4	29550480	22452125	21450760	95.5	18675678	83.2
14-C00000-05	B4	35873053	28660950	27322484	95.3	23957688	83.6
14-C00000-06	B1	27168165	17686531	16979070	96.0	14916820	84.3
14-C00000-08	B5	28307842	21716653	20776322	95.7	17987904	82.8
14-C00000-10	B4	24381382	18390664	17535498	95.4	15332297	83.4
14-C00000-12	B1	27966627	19155345	18368060	95.9	16197760	84.6
14-C00000-13	B4	21237357	16756285	16059224	95.8	14102089	84.2
14-C00000-14	B1	28963088	19926398	19107423	95.9	16881644	84.7
14-C00000-15	B1	26622615	18974401	18202143	95.9	16103574	84.9
14-C00000-18	B5	31567745	25254920	24214417	95.9	21350509	84.5
14-C00000-19	B1	24692356	16903631	16246080	96.1	14134816	83.6
14-C00000-21	B4	26639167	18472968	17636143	95.5	14990814	81.2
14-C00000-22	B4	26352163	20530965	19674824	95.8	17603249	85.7

		Initial	Trimmed	HISAT2 mapped		Trinity mapped	
Sample ID	Batch	# reads	# reads	# reads	%	# reads	%
14-C00000-24	B4	29285900	22607900	21619935	95.6	18947681	83.8
14-C00000-25	B4	35036977	27981710	26800882	95.8	23440278	83.8
14-C00000-27	B1	26762934	19383435	18549947	95.7	16483673	85.0
14-C00000-28	B1	25101723	19941147	19095642	95.8	16977893	85.1
14-C00000-29	B1	27980996	19594039	18731901	95.6	16317916	83.3
14-C00000-35	B1	19342879	13195104	12544585	95.1	10571917	80.1
14-C00000-37	B5	29745078	23866197	22737326	95.3	19546415	81.9
14-C00000-38	B4	23672429	18583551	17739858	95.5	15483815	83.3
14-C00000-39	B5	30155477	25160644	23988158	95.3	21104748	83.9
14-C00000-40	B5	29011074	22841740	21720211	95.1	18097511	79.2
14-D02HT1-02	B5	31126799	26245776	25177573	95.9	22689473	86.5
14-D02HT1-09	B4	30132488	23677823	22785169	96.2	20618648	87.1
14-D02HT1-18	B5	31697235	24756653	23773814	96.0	21119901	85.3
14-D02HT1-24	B5	31540801	25369225	24367141	96.1	21743963	85.7
14-D02HT1-28	B5	30283368	24925534	23931005	96.0	21515721	86.3
14-D02HT1-30	B4	20721551	16282379	15543159	95.5	13629979	83.7
14-D02HT1-34	B5	30509197	24366734	23301908	95.6	20687357	84.9
14-D02HT2-04	B3	24110143	19041317	18190170	95.5	16044214	84.3
14-D02HT2-06	B3	24057023	19130941	18258570	95.4	16238343	84.9
14-D02HT2-07	B3	27422772	21882629	20816945	95.1	18228230	83.3
14-D02HT2-08	B3	27804754	22061509	20967258	95.0	18348557	83.2
14-D02HT2-10	B3	31679322	24264007	23184259	95.6	20602568	84.9
14-D02HT2-23	B3	25984738	20491147	19577242	95.5	17269939	84.3
14-D02HT2-26	B3	31598150	24901530	23668904	95.1	20887403	83.9
14-D02HT2-28	B3	28344444	22619708	21674204	95.8	19319493	85.4
14-D02HT2-36	B3	27192316	22336789	21271324	95.2	18890222	84.6
14-D02HT2-37	B3	28411260	23382929	22356418	95.6	19954992	85.3
14-D02HT2-38	B3	24876163	19517774	18629715	95.5	16408593	84.1
14-D02HT2-39	B3	27679553	22067273	20886674	94.7	18412933	83.4
14-D02HT3-02	B4	36216583	29137602	27893426	95.7	24784444	85.1
14-D02HT3-21	B4	23463902	18488175	17425105	94.3	15437626	83.5
14-D02HT3-24	B5	30071557	24725521	23222209	93.9	21305981	86.2
14-D02HT3-28	B5	29996066	25353415	23307394	91.9	21611251	85.2
14-D02HT4-13	B1	22804733	15341864	14723587	96.0	12907110	84.1
14-D02HT4-14	B1	24689542	16623791	15915618	95.7	13880865	83.5
14-D02HT4-17	B5	29931626	24215980	21847657	90.2	19907957	82.2
14-D02HT4-21	B4	22649042	18225294	17408801	95.5	15564401	85.4
14-D02HT4-34	B1	22424639	16239792	15567465	95.9	13901262	85.6
14-D02HT4-40	B5	32661858	27514209	26416392	96.0	23967627	87.1
14-D02IT1-02	B4	21994457	17496993	16697380	95.4	14788458	84.5
14-D02IT1-03	B4	29363214	22327420	21342781	95.6	18645628	83.5
14-D02IT1-04	B4	22198675	17605814	16820595	95.5	14964942	85.0
14-D02IT1-05	B4	28939408	22166963	21142849	95.4	18684533	84.3
14-D02IT1-19	B3	29071205	22948478	21830887	95.1	19600295	85.4

		Initial	Trimmed	HISAT2 mapped		Trinity mapped	
Sample ID	Batch	# reads	# reads	# reads	%	# reads	%
14-D02IT1-20	B3	27079870	21524749	20493714	95.2	17938726	83.3
14-D02IT1-23	B3	27127392	21971614	20947737	95.3	18590183	84.6
14-D02IT1-25	B3	29834572	23330505	22282965	95.5	19569628	83.9
14-D02IT1-28	B3	28171345	22329046	21306376	95.4	18671548	83.6
14-D02IT1-30	B3	26894756	20597445	19662321	95.5	17223584	83.6
14-D02IT1-35	B3	24071437	19213190	18423528	95.9	16594432	86.4
14-D02IT2-15	B5	31360211	25095591	23966289	95.5	20937252	83.4
14-D02IT2-33	B4	21562385	15987859	15284393	95.6	13265127	83.0
14-D02IT2-38	B4	20690812	16152712	15406457	95.4	13661964	84.6
14-D02IT3-16	B5	30717877	21903709	20874235	95.3	17529538	80.0
14-D02IT3-23	B4	28342476	22972393	22012147	95.8	19636802	85.5
14-D02IT3-24	B5	31549448	26105825	23508295	90.1	22406630	85.8
14-D02IT3-25	B4	27168327	22170021	21218927	95.7	19090605	86.1
14-D02IT3-27	B1	25786251	17375344	16490939	94.9	14746454	84.9
14-D02IT3-29	B1	21448835	14609399	14020640	96.0	12537786	85.8
14-D02IT3-33	B4	24499934	19808752	18982727	95.8	16902808	85.3
14-D02IT4-14	B4	23186601	17822995	17040566	95.6	14928541	83.8
14-D02IT4-15	B1	25066409	15601839	14954363	95.9	12773226	81.9
14-D02IT4-16	B1	26729717	16875864	16190704	95.9	14035656	83.2
14-D02IT4-24	B1	22209689	15328481	14704612	95.9	13070596	85.3
14-D02IT4-25	B4	32010348	26039478	25016127	96.1	22516337	86.5
14-D02IT4-26	B1	24067587	16481828	15806073	95.9	13831550	83.9
14-D02IT4-27	B4	28552837	21833182	20972955	96.1	18575671	85.1
14-D02IT4-30	B1	20671804	14431531	13834066	95.9	12174440	84.4
14-D02LT1-03	B5	31111800	24804390	23603858	95.2	20478504	82.6
14-D02LT1-08	B5	29822929	22472130	21413693	95.3	18375461	81.8
14-D02LT1-19	B3	32943727	26173657	25037720	95.7	22326129	85.3
14-D02LT1-21	B3	29889369	23280752	22219150	95.4	19551176	84.0
14-D02LT1-23	B3	35661612	28455229	27151980	95.4	23873937	83.9
14-D02LT1-27	B3	28943538	22555114	21533367	95.5	18840287	83.5
14-D02LT1-28	B3	32029990	24631031	23510319	95.5	20623562	83.7
14-D02LT1-30	B3	30620695	23936032	22885240	95.6	20271426	84.7
14-D02LT1-32	B4	32993662	25270201	24170947	95.7	21055131	83.3
14-D02LT1-35	B5	30868933	22195519	20945911	94.4	17390189	78.4
14-D02LT2-02	B4	35497505	29088685	27930955	96.0	24998816	85.9
14-D02LT2-06	B4	33521730	26379563	25242604	95.7	22132453	83.9
14-D02LT2-16	B1	24822249	16937895	16016474	94.6	14210894	83.9
14-D02LT2-24	B4	31826966	24948007	23802893	95.4	20706846	83.0
14-D02LT2-25	B4	25662962	19230015	18370433	95.5	15920529	82.8
14-D02LT2-26	B4	20899120	15729253	15018291	95.5	13116624	83.4
14-D02LT2-33	B4	31447539	24820505	23792936	95.9	20871563	84.1
14-D02LT3-12	B5	31206516	23598712	22527330	95.5	19065399	80.8
14-D02LT4-02	B5	27799753	20757922	19715874	95.0	16413289	79.1
14-D02LT4-19	B1	28735034	19049266	18325394	96.2	16136633	84.7

		Initial	Trimmed	HISAT2 mapped		Trinity mapped	
Sample ID	Batch	# reads	# reads	# reads	%	# reads	%
14-D02LT4-20	B1	28951474	21104679	20277376	96.1	18004402	85.3
14-D02LT4-22	B4	22272353	18354595	17636930	96.1	15740901	85.8
14-D02LT4-23	B1	28233812	19525291	18755995	96.1	16602355	85.0
14-D02LT4-24	B4	24318262	18815074	17996618	95.7	15780203	83.9
14-D02LT4-28	B1	26312374	18924678	18175261	96.0	16108686	85.1
14-D02LT4-29	B1	25594121	17459689	16735112	95.9	14734232	84.4
14-D02LT4-32	B4	28926920	21918371	21046020	96.0	18667877	85.2
14-D02LT4-38	B4	26530282	21381041	20583528	96.3	18332105	85.7
14-D14HT2-01	B2	27551406	20819011	19898811	95.6	17462986	83.9
14-D14HT2-03	B2	26443408	20344232	19522325	96.0	17361768	85.3
14-D14HT2-05	B2	25321606	18938903	18130212	95.7	16088598	85.0
14-D14HT2-06	B2	26104595	20651024	19787811	95.8	17646300	85.5
14-D14HT2-14	B2	26707180	19220377	18351616	95.5	16062469	83.6
14-D14HT2-15	B2	27020382	20919515	20047171	95.8	17861082	85.4
14-D14HT2-16	B2	27006124	20269805	19388068	95.7	17089473	84.3
14-D14HT2-21	B2	27586119	20331998	19331664	95.1	17194771	84.6
14-D14HT2-25	B2	27245672	19363392	18339069	94.7	16259440	84.0
14-D14HT2-26	B2	27180396	19996632	19054791	95.3	16937147	84.7
14-D14HT2-27	B2	26354210	18927220	18001679	95.1	15978359	84.4
14-D14HT2-32	B2	26646948	19500368	18544850	95.1	16265257	83.4
14-D14HT2-35	B2	28186902	21413666	20482172	95.7	18109537	84.6
14-D14HT2-36	B2	28615382	19598972	18634703	95.1	16290666	83.1
14-D14HT2-38	B2	26532615	19824368	18825220	95.0	16551365	83.5
14-D14HT2-39	B2	26841456	20229244	19290607	95.4	16941992	83.8
14-D14HT3-14	B5	32683384	27543416	26400364	95.9	23734162	86.2
14-D14HT4-01	B3	27069326	21097096	20137178	95.5	17793291	84.3
14-D14HT4-04	B3	30425325	23511516	22491116	95.7	19996544	85.1
14-D14HT4-05	B5	31396124	26685240	25516426	95.6	23104081	86.6
14-D14HT4-06	B2	27445488	19136373	18315423	95.7	16147272	84.4
14-D14HT4-07	B2	25459286	18478856	17702744	95.8	15625721	84.6
14-D14HT4-08	B2	27345761	20126109	19202321	95.4	16863667	83.8
14-D14HT4-11	B3	27636660	21413685	20375121	95.2	18041030	84.3
14-D14HT4-14	B3	26964073	18550819	17643684	95.1	15664312	84.4
14-D14HT4-15	B3	25998931	19950424	19012754	95.3	16628678	83.4
14-D14HT4-16	B2	28249168	23429731	22194984	94.7	19596627	83.6
14-D14HT4-25	B2	27222886	20604411	19654548	95.4	17258255	83.8
14-D14HT4-26	B3	25904164	20498605	19274838	94.0	17019992	83.0
14-D14HT4-39	B2	27548900	20727832	19809589	95.6	17363705	83.8
14-D14IT2-01	B5	28877028	22210107	21137359	95.2	17941324	80.8
14-D14IT2-03	B2	23746127	14935216	14216832	95.2	12076616	80.9
14-D14IT2-04	B4	32236433	24670963	23595309	95.6	20474432	83.0
14-D14IT2-14	B4	23860685	19205723	18201264	94.8	16230757	84.5
14-D14IT2-19	B4	28044772	21030359	19837938	94.3	17352149	82.5
14-D14IT2-22	B5	33089899	25746664	24384665	94.7	21421224	83.2

		Initial	Trimmed	HISAT2 mapped		Trinity mapped	
Sample ID	Batch	# reads	# reads	# reads	%	# reads	%
14-D14IT2-31	B5	27263922	19940665	16802004	84.3	16056223	80.5
14-D14IT2-32	B3	35482987	27930310	26592448	95.2	23578768	84.4
14-D14IT2-33	B3	30112302	23739394	22485954	94.7	20064536	84.5
14-D14IT2-34	B3	33267881	21201776	20292220	95.7	17798891	84.0
14-D14IT2-36	B4	27454070	21170204	20164619	95.3	17965035	84.9
14-D14IT2-38	B3	28470090	22827431	21763673	95.3	19412447	85.0
14-D14IT2-39	B4	29008435	23077300	21944205	95.1	19359547	83.9
14-D14IT2-40	B3	29805391	24788545	23266528	93.9	21392514	86.3
14-D14IT3-04	B4	28413498	22533147	21534929	95.6	18839964	83.6
14-D14IT3-05	B2	24153894	16314908	15603578	95.6	13510375	82.8
14-D14IT3-09	B4	27650681	21110933	20177830	95.6	17722628	84.0
14-D14IT3-12	B4	33012817	25434379	24272028	95.4	21125795	83.1
14-D14IT3-18	B5	29968427	24399889	23297014	95.5	20598386	84.4
14-D14IT3-21	B4	25821131	21038593	20121310	95.6	17966958	85.4
14-D14IT3-32	B3	30522695	25378726	24178312	95.3	21762258	85.8
14-D14IT3-33	B3	30303150	24657859	23341129	94.7	20784109	84.3
14-D14IT3-34	B3	29051918	22724383	21654065	95.3	18988494	83.6
14-D14IT3-35	B3	29944223	23099251	21868061	94.7	19287875	83.5
14-D14IT3-40	B3	25799443	20626695	19395281	94.0	17448121	84.6
14-D14IT4-05	B3	28183627	22692549	21780309	96.0	19431630	85.6
14-D14IT4-09	B3	33431562	27155479	26031242	95.9	23361859	86.0
14-D14IT4-15	B3	25126752	19500857	18660370	95.7	16599129	85.1
14-D14IT4-21	B3	23597553	18038632	17203443	95.4	15042415	83.4
14-D14LT2-02	B4	31364678	24434374	23395913	95.8	20651933	84.5
14-D14LT2-03	B4	25902618	19859872	18948304	95.4	16648531	83.8
14-D14LT2-04	B5	31502000	23807748	22693545	95.3	19622346	82.4
14-D14LT2-05	B5	30976706	24594214	23322693	94.8	20041825	81.5
14-D14LT2-07	B2	26729357	15066871	14256273	94.6	12246353	81.3
14-D14LT2-08	B5	30784363	23390291	22281591	95.3	19182378	82.0
14-D14LT2-10	B5	32076916	25329954	24076121	95.1	20750298	81.9
14-D14LT2-11	B4	33970805	25322367	24084103	95.1	20860566	82.4
14-D14LT2-12	B2	21555013	12936240	12347641	95.5	10540448	81.5
14-D14LT2-13	B4	20638152	14493975	13822904	95.4	11931440	82.3
14-D14LT2-14	B5	28655241	22940990	21901763	95.5	19334666	84.3
14-D14LT2-20	B5	30776190	25835537	24732360	95.7	21965374	85.0
14-D14LT2-26	B5	30828432	24924922	23795823	95.5	20887085	83.8
14-D14LT2-27	B5	32170494	25143394	23888739	95.0	20745814	82.5
14-D14LT2-28	B4	35203764	26456747	24633877	93.1	21919415	82.9
14-D14LT2-30	B5	31326681	23552724	22210219	94.3	19214312	81.6
14-D14LT2-31	B5	31338010	23635526	22179578	93.8	19357496	81.9
14-D14LT4-02	B2	26309385	18135095	17328083	95.6	15010418	82.8
14-D14LT4-03	B2	27109356	17254581	16457419	95.4	13955505	80.9
14-D14LT4-04	B4	23165778	18698461	17948653	96.0	15861904	84.8
14-D14LT4-05	B4	23154247	16841954	16159855	96.0	14049558	83.4

		Initial	Trimmed	HISAT2 mapped		Trinity mapped	
Sample ID	Batch	# reads	# reads	# reads	%	# reads	%
14-D14LT4-09	B2	26270164	17569871	16691377	95.0	14198213	80.8
14-D14LT4-12	B4	21599422	16566136	15659968	94.5	13786338	83.2
14-D14LT4-13	B5	32866530	27177907	24549803	90.3	22924565	84.4
14-D14LT4-15	B4	31371708	24957538	23519984	94.2	20512600	82.2
14-D14LT4-16	B4	21552979	16452915	15610526	94.9	13649338	83.0
14-D14LT4-20	B4	35879001	26791458	24591879	91.8	22025258	82.2
14-D14LT4-22	B5	30437086	24574581	22947744	93.4	19971762	81.3
14-D14LT4-23	B4	33238939	27629501	26131982	94.6	23598357	85.4
14-D14LT4-25	B5	36443191	28875224	27269762	94.4	23934673	82.9
14-D14LT4-31	B5	30699256	26167799	24571563	93.9	22619445	86.4
14-D21HT1-02	B4	20120768	15688453	15023263	95.8	13493638	86.0
14-D21HT1-17	B2	27094117	19130893	18302525	95.7	16115864	84.2
14-D21HT1-23	B2	27448400	18277138	17037948	93.2	15456976	84.6
14-D21HT1-36	B3	28403827	23101262	21740598	94.1	19488225	84.4
14-D21HT3-01	B4	23436476	17568212	16245326	92.5	14242549	81.1
14-D21HT3-04	B2	23769277	17996850	17215787	95.7	15286524	84.9
14-D21HT3-07	B2	24889133	19154234	18344010	95.8	16440079	85.8
14-D21HT3-12	B2	26901966	21000932	20133594	95.9	18065002	86.0
14-D21HT3-14	B2	27957444	21209699	20331617	95.9	18369720	86.6
14-D21HT3-15	B2	25460931	19316571	18458915	95.6	16436470	85.1
14-D21HT3-16	B2	23289584	17812250	16998230	95.4	15044226	84.5
14-D21HT3-17	B2	27485611	19183788	18337783	95.6	16145076	84.2
14-D21HT3-18	B2	26457743	19523622	18635297	95.5	16489651	84.5
14-D21HT3-23	B2	28297294	21384620	20447974	95.6	18313789	85.6
14-D21HT3-24	B2	28352062	21406504	20456055	95.6	18379624	85.9
14-D21HT3-31	B2	28368126	21495918	20277099	94.3	18402655	85.6
14-D21HT3-32	B2	27786046	20632831	19405178	94.1	17601868	85.3
14-D21HT3-39	B3	29603442	23552590	22330211	94.8	19946688	84.7
14-D21HT4-01	B3	29198473	23038381	22006262	95.5	19372975	84.1
14-D21HT4-02	B3	29067011	22546798	21588559	95.8	19061063	84.5
14-D21HT4-03	B3	30055089	23585332	22549936	95.6	19981493	84.7
14-D21HT4-06	B3	23929686	19029587	18234150	95.8	16403504	86.2
14-D21HT4-07	B3	32250880	22459777	21408659	95.3	18679797	83.2
14-D21HT4-08	B3	28731013	23012172	21949010	95.4	19440683	84.5
14-D21HT4-10	B3	28062759	22133049	21123782	95.4	18582908	84.0
14-D21HT4-14	B3	28423130	23297611	22004594	94.5	19621248	84.2
14-D21HT4-16	B3	28912803	23026383	21785261	94.6	19521768	84.8
14-D21HT4-21	B3	32585985	25513841	24253457	95.1	21434178	84.0
14-D21IT2-01	B2	26973134	16024764	15359736	95.9	13342219	83.3
14-D21IT2-03	B2	25787259	13770338	13131394	95.4	10994238	79.8
14-D21IT2-06	B4	22369957	17846479	17052311	95.6	15074921	84.5
14-D21IT2-07	B2	23399992	17758063	16843523	94.9	15149404	85.3
14-D21IT2-08	B2	26650608	19324974	18494000	95.7	16242641	84.1
14-D21IT2-09	B2	25200252	16877224	16159942	95.8	14345640	85.0

		Initial	Trimmed	HISAT2 mapped		Trinity mapped	
Sample ID	Batch	# reads	# reads	# reads	%	# reads	%
14-D21IT2-15	B2	26826572	19009278	18226096	95.9	15889855	83.6
14-D21IT2-19	B2	25953179	19403072	18555158	95.6	16436342	84.7
14-D21IT2-21	B2	45923711	34792684	33171345	95.3	29949542	86.1
14-D21IT2-27	B2	27901120	20061364	19218787	95.8	17132405	85.4
14-D21IT2-31	B2	26582100	20101458	18720488	93.1	17072168	84.9
14-D21IT3-02	B2	25827468	19264146	18478169	95.9	16495888	85.6
14-D21IT3-03	B2	24427487	18366374	17609679	95.9	15721616	85.6
14-D21IT3-06	B4	20746959	16030768	15421599	96.2	13523556	84.4
14-D21IT3-07	B2	23814631	17399559	16707057	96.0	14833124	85.3
14-D21IT3-10	B2	25676315	19896873	19041307	95.7	16964074	85.3
14-D21IT3-12	B2	26610869	19291727	18521987	96.0	16424976	85.1
14-D21IT3-13	B2	27612558	19109739	18119855	94.8	15970009	83.6
14-D21IT3-15	B2	26104262	19744652	18808755	95.3	17213388	87.2
14-D21IT3-17	B2	28258774	19304020	18365845	95.1	16238542	84.1
14-D21IT3-23	B2	27816882	20822793	19958647	95.9	17591096	84.5
14-D21IT3-24	B2	26523937	20269400	19395789	95.7	17200613	84.9
14-D21IT3-25	B2	27519630	19920493	19040007	95.6	16663492	83.7
14-D21IT3-26	B2	26766470	20628700	19729289	95.6	17474572	84.7
14-D21LT1-05	B3	26344611	20747710	19776717	95.3	17733068	85.5
14-D21LT1-21	B3	26280671	20890655	19530673	93.5	17454142	83.6
14-D21LT1-24	B3	24961391	19479790	18556448	95.3	16600677	85.2
14-D21LT1-28	B3	25588638	20433117	18861810	92.3	17400842	85.2
14-D21LT2-01	B2	25923480	19519175	18705225	95.8	16854808	86.4
14-D21LT2-03	B2	23108029	14873033	14188873	95.4	12750651	85.7
14-D21LT2-04	B2	25599204	17755036	16973814	95.6	14939087	84.1
14-D21LT2-08	B2	26757505	19951750	19087839	95.7	16841272	84.4
14-D21LT2-11	B2	24522487	18151788	17418456	96.0	15581495	85.8
14-D21LT2-15	B2	25654758	18769981	17793942	94.8	15877527	84.6
14-D21LT2-19	B2	25975910	18579034	17789425	95.8	15747589	84.8
14-D21LT2-21	B2	24708560	17918687	17178645	95.9	15245219	85.1
14-D21LT2-27	B2	26444360	20067691	19188726	95.6	17216072	85.8
14-D21LT2-28	B2	27468213	20431680	19512254	95.5	17138093	83.9
14-D21LT2-30	B2	27075969	20484000	19648253	95.9	17481046	85.3
14-D21LT2-32	B2	26602877	20044042	18869461	94.1	16786885	83.8
14-D21LT2-33	B3	26916244	21674574	19539628	90.2	18473239	85.2
14-D21LT2-34	B3	27196843	19021690	17657835	92.8	15892622	83.6
14-D21LT2-39	B3	27730833	20731390	19557993	94.3	17706680	85.4
14-D21LT4-01	B2	23912555	18181480	17483311	96.2	15763343	86.7
14-D21LT4-02	B2	25525174	19756996	18978570	96.1	16987065	86.0
14-D21LT4-04	B2	27972135	17493514	16704557	95.5	14545857	83.2
14-D21LT4-06	B2	23488410	17545168	16824062	95.9	14999364	85.5
14-D21LT4-10	B2	27002259	17620214	16751537	95.1	14427431	81.9
14-D21LT4-11	B2	28402332	22374600	21101485	94.3	19143708	85.6
14-D21LT4-16	B2	24150944	16627384	15894116	95.6	13902156	83.6

		Initial	Trimmed	HISAT2 mapped		Trinity mapped	
Sample ID	Batch	# reads	# reads	# reads	%	# reads	%
14-D21LT4-17	B2	26634964	19673290	18774221	95.4	16470478	83.7
14-D21LT4-28	B2	27692589	20426887	18988834	93.0	17440476	85.4
14-D21LT4-30	B2	27824253	19840967	18870744	95.1	16882679	85.1
14-D21LT4-35	B3	30060699	23303311	22145136	95.0	19372042	83.1
14-D28HT1-02	B4	25814957	20914681	20084368	96.0	18022181	86.2
14-D28HT1-08	B1	26413439	18303499	17456047	95.4	15605563	85.3
14-D28HT1-25	B4	33181327	23231741	21389464	92.1	18822357	81.0
14-D28HT3-01	B1	27523540	20936216	20006648	95.6	17672260	84.4
14-D28HT3-03	B1	23882931	17470524	16729774	95.8	14827234	84.9
14-D28HT3-05	B1	22835862	15525700	14903119	96.0	13150268	84.7
14-D28HT3-06	B1	22411919	16123636	15399685	95.5	13506770	83.8
14-D28HT3-07	B1	25147747	16075378	15377707	95.7	13451876	83.7
14-D28HT3-13	B1	22688559	14535883	13894851	95.6	11920878	82.0
14-D28HT3-14	B1	26596282	17956844	17136216	95.4	14961642	83.3
14-D28HT3-19	B1	21207057	12949991	12365946	95.5	10664318	82.4
14-D28HT3-21	B1	26030330	18395149	17366860	94.4	15058269	81.9
14-D28HT3-25	B1	28882532	20120832	18853220	93.7	16599686	82.5
14-D28HT3-30	B1	25742464	17360185	16396695	94.5	14315209	82.5
14-D28HT3-31	B2	23028451	17266937	16434671	95.2	14350551	83.1
14-D28HT3-34	B5	24178000	9526388	8991958	94.4	7343893	77.1
14-D28HT4-03	B1	22930785	16698019	16045126	96.1	14291834	85.6
14-D28HT4-05	B1	24429229	17896592	17150304	95.8	15131569	84.6
14-D28HT4-09	B1	28132426	20116833	19267903	95.8	17129483	85.2
14-D28HT4-11	B1	27302653	19588167	18691029	95.4	16313025	83.3
14-D28HT4-12	B1	27291451	19954311	18958591	95.0	16572055	83.1
14-D28HT4-13	B1	21687173	15398019	14535730	94.4	12575562	81.7
14-D28HT4-14	B1	26258107	18748672	17886233	95.4	15580146	83.1
14-D28HT4-17	B1	27434478	19520166	18481693	94.7	16541389	84.7
14-D28HT4-22	B1	28916460	18400618	17440106	94.8	14873220	80.8
14-D28HT4-34	B4	23772278	18090378	17173196	94.9	14732804	81.4
14-D28HT4-37	B5	32365837	25273872	23959631	94.8	21134012	83.6
14-D28HT4-40	B2	24522892	17951393	17071775	95.1	14939149	83.2
14-D28IT2-01	B1	22901259	16946449	16261812	96.0	14482435	85.5
14-D28IT2-02	B1	27035604	20054578	19276460	96.1	17246937	86.0
14-D28IT2-03	B1	27272857	19565667	18710647	95.6	16497770	84.3
14-D28IT2-07	B1	26871872	19641298	18861538	96.0	16700996	85.0
14-D28IT2-09	B1	24873815	18104686	17362394	95.9	15227851	84.1
14-D28IT2-10	B1	26666199	19695417	18919418	96.1	16831703	85.5
14-D28IT2-11	B1	27598208	19616414	18837642	96.0	16505251	84.1
14-D28IT2-12	B1	26609316	18006566	17235885	95.7	15017476	83.4
14-D28IT2-14	B1	29014385	20013669	19159085	95.7	16795471	83.9
14-D28IT2-16	B1	22657122	16509910	15780172	95.6	13906297	84.2
14-D28IT2-22	B1	25181651	17737383	16644760	93.8	14885212	83.9
14-D28IT2-24	B2	25648017	16293230	15387326	94.4	13495682	82.8

		Initial	Trimmed	HISAT2 mapped		Trinity mapped	
Sample ID	Batch	# reads	# reads	# reads	%	# reads	%
14-D28IT2-29	B1	22181548	16425758	15655390	95.3	13692512	83.4
14-D28IT2-33	B2	23152847	17605363	16124752	91.6	14461045	82.1
14-D28IT3-06	B1	32196008	21178265	20282424	95.8	17855395	84.3
14-D28IT3-08	B1	22140724	15893712	15262732	96.0	13628858	85.8
14-D28IT3-10	B1	23675973	16268605	15590204	95.8	13605434	83.6
14-D28IT3-13	B1	21522536	15674240	14813724	94.5	13290188	84.8
14-D28IT3-14	B1	27391254	19188419	18267375	95.2	16108678	84.0
14-D28IT3-16	B1	27842592	20457852	19408364	94.9	17393266	85.0
14-D28IT3-18	B1	20148318	12520307	11841706	94.6	10376830	82.9
14-D28IT3-35	B5	31570020	23770054	22334343	94.0	18975634	79.8
14-D28IT4-07	B1	25920739	19459900	18691234	96.1	16636269	85.5
14-D28IT4-09	B1	22183856	16485181	15777967	95.7	13949760	84.6
14-D28IT4-11	B1	27915106	20202500	19079241	94.4	16990303	84.1
14-D28IT4-16	B1	24656862	17077856	16270073	95.3	14215607	83.2
14-D28IT4-17	B1	26714866	18162462	17198035	94.7	15122066	83.3
14-D28IT4-27	B2	25105071	17081613	16253155	95.2	14493749	84.9
14-D28IT4-30	B2	24811381	17778252	16791559	94.5	14987066	84.3
14-D28IT4-38	B2	23891060	17477740	16588123	94.9	14630616	83.7
14-D28LT2-01	B1	22957032	15986464	15315033	95.8	13526147	84.6
14-D28LT2-02	B1	26320218	18596610	17772780	95.6	15626731	84.0
14-D28LT2-03	B1	24290691	17887028	17184068	96.1	15300564	85.5
14-D28LT2-05	B1	26061644	18739570	17967500	95.9	15810575	84.4
14-D28LT2-08	B1	28007613	17560650	16786225	95.6	14477000	82.4
14-D28LT2-09	B1	25396234	18016231	17279367	95.9	15537198	86.2
14-D28LT2-10	B1	25935256	17636534	16954000	96.1	14973417	84.9
14-D28LT2-12	B1	26774096	18742708	17884292	95.4	15380266	82.1
14-D28LT2-17	B1	27024362	17561002	16830464	95.8	14512412	82.6
14-D28LT2-20	B1	19614420	13450003	12905278	96.0	11148707	82.9
14-D28LT2-30	B2	24809167	17704320	16714649	94.4	14970773	84.6
14-D28LT3-01	B1	27085663	18459079	17687489	95.8	15337649	83.1
14-D28LT3-02	B1	22421137	14900161	14250514	95.6	12386504	83.1
14-D28LT3-09	B1	23213668	15581625	14902266	95.6	13020006	83.6
14-D28LT3-13	B1	21658151	13652155	12936782	94.8	11250741	82.4
14-D28LT3-14	B1	26099517	18414143	17432669	94.7	15443942	83.9
14-D28LT3-17	B1	21169931	15887612	15229865	95.9	13493349	84.9
14-D28LT3-23	B2	24948410	18229363	17379875	95.3	15480375	84.9
14-D28LT4-03	B1	23813267	17012055	16311158	95.9	14339461	84.3
14-D28LT4-04	B1	25494009	16092905	15346194	95.4	13155950	81.8
14-D28LT4-06	B1	25811716	18893197	18137469	96.0	16085668	85.1
14-D28LT4-08	B1	27205155	20447430	19629533	96.0	17572521	85.9
14-D28LT4-09	B1	23567800	17551861	16809417	95.8	14940144	85.1
14-D28LT4-10	B1	25744382	18938615	18162132	95.9	16147063	85.3
14-D28LT4-12	B1	21336679	14470660	13721080	94.8	12133648	83.9
14-D28LT4-14	B1	28077632	19557659	18489811	94.5	16193742	82.8

		Initial	Trimmed	HISAT2 mapped		Trinity mapped	
Sample ID	Batch	# reads	# reads	# reads	%	# reads	%
14-D28LT4-16	B1	25626685	18302120	17328447	94.7	15307893	83.6
14-D28LT4-20	B1	27748062	17916383	16973981	94.7	14849098	82.9
15-C00000-05	B4	22904499	15641336	14978143	95.8	13037054	83.4
15-C00000-07	B4	23622811	17872118	17067873	95.5	14841007	83.0
15-C00000-10	B5	30687656	24070562	22919989	95.2	19781188	82.2
15-C00000-12	B4	32170913	25196700	24083006	95.6	20998930	83.3
15-C00000-17	B4	21779372	15786547	15087203	95.6	13087047	82.9
15-D02HT1-11	B3	25935980	19709295	18771133	95.2	16429668	83.4
15-D02HT1-13	B3	26042624	20029797	19130459	95.5	16887122	84.3
15-D02HT1-20	B3	25735944	19889657	18976722	95.4	16582007	83.4
15-D02HT3-08	B3	29169978	22407669	21325379	95.2	18844850	84.1
15-D02HT3-14	B4	29459420	21842550	20239307	92.7	17972050	82.3
15-D02IT1-09	B3	29534892	22179274	21190078	95.5	18626154	84.0
15-D02IT1-12	B4	21901857	16353213	15681096	95.9	13800476	84.4
15-D02IT1-16	B4	26188712	19330106	18539505	95.9	16652886	86.2
15-D02IT2-13	B5	33068497	26628011	25120866	94.3	21677864	81.4
15-D02IT2-18	B5	28216602	21224595	19961732	94.1	16848084	79.4
15-D02LT1-04	B4	22297217	17028570	16301450	95.7	14513450	85.2
15-D02LT1-10	B4	23240493	18407673	17238786	93.7	15683337	85.2
15-D02LT1-16	B4	22216822	16733438	16020594	95.7	14188282	84.8
15-D02LT3-17	B4	28685575	21946490	21020348	95.8	18674268	85.1
15-D02LT3-18	B4	34670382	25681921	24554485	95.6	21457245	83.6
15-D07HT1-01	B4	25062052	19137565	18308908	95.7	16127226	84.3
15-D07HT1-09	B4	33505223	26658312	25450690	95.5	22614246	84.8
15-D07HT3-05	B3	25851399	20726262	19435016	93.8	17250468	83.2
15-D07HT3-06	B3	25620717	19995991	18930205	94.7	16640664	83.2
15-D07HT3-10	B3	25996628	20791275	19379547	93.2	17290024	83.2
15-D14HT2-04	B3	22172263	18160957	17192978	94.7	14797548	81.5
15-D14HT2-06	B3	25584049	20117753	19150089	95.2	16806371	83.5
15-D14HT2-10	B3	25840640	17768614	16778902	94.4	14763941	83.1
15-D14HT3-05	B4	23111370	17040427	16224191	95.2	14136738	83.0
15-D14HT3-06	B4	23026048	17752125	16844991	94.9	14585146	82.2
15-D14IT1-03	B3	23320078	16090008	15374003	95.6	13517216	84.0
15-D14IT1-05	B3	26862617	21060423	18293083	86.9	16431342	78.0
15-D14IT2-04	B3	29793539	24003525	22803349	95.0	20261375	84.4
15-D14IT2-05	B3	29539036	23491894	22096475	94.1	19446590	82.8
15-D14IT2-07	B3	25342112	19847776	18781950	94.6	16560984	83.4
15-D14LT1-06	B3	25810239	20137578	19110562	94.9	16861194	83.7
15-D14LT1-07	B3	26454147	20133979	19197749	95.4	16793752	83.4
15-D14LT1-10	B3	26990186	21113928	19939994	94.4	17691360	83.8
15-D14LT3-01	B3	25916416	20086399	18571885	92.5	16717910	83.2
15-D14LT3-03	B4	20612818	16315914	15309222	93.8	13582998	83.3
15-D21HX1-04	B4	31019725	23447127	22478761	95.9	19976952	85.2
15-D21HX1-06	B4	24282131	19066283	18091996	94.9	16429416	86.2

		Initial	Trimmed	HISAT2 mapped		Trinity mapped	
Sample ID	Batch	# reads	# reads	# reads	%	# reads	%
15-D21HX2-01	B4	30357592	22891056	21959390	95.9	19672574	85.9
15-D21HX2-02	B3	29101458	22085399	21029717	95.2	18419223	83.4
15-D21HX2-10	B3	25285999	19272193	18289311	94.9	16196351	84.0
15-D21LT1-05	B4	29655192	22411650	21416573	95.6	19045420	85.0
15-D21LT1-06	B4	32800710	24710810	23319591	94.4	20880634	84.5
15-D21LT3-03	B3	28983226	22859513	21828549	95.5	19403155	84.9
15-D21LT3-08	B3	28709124	22813958	21709762	95.2	19232167	84.3
15-D21LT3-09	B4	30598773	23871539	22761512	95.4	20185773	84.6
15-D28HX1-09	B4	33136991	26404939	25351382	96.0	22916847	86.8
15-D28HX1-18	B4	33983505	26886021	25789071	95.9	23334378	86.8
15-D28HX2-03	B3	27263888	21220922	20081358	94.6	17532726	82.6
15-D28HX2-07	B3	23946861	19106652	18128391	94.9	16240654	85.0
15-D28HX2-09	B3	24405298	19421331	18450264	95.0	16465404	84.8
15-D28IT2-12	B4	27435522	21226562	20337169	95.8	18191164	85.7
15-D28IT2-13	B4	27404111	21762049	20750114	95.4	18639195	85.7
15-D28IX2-01	B4	25427364	20582260	19575787	95.1	17643113	85.7
15-D28IX2-03	B3	25584952	20484682	19294522	94.2	17264490	84.3
15-D28IX2-06	B3	27404647	22762946	21533747	94.6	19491911	85.6
15-D28LT1-09	B4	23288757	17882289	17120503	95.7	15040793	84.1
15-D28LT1-11	B4	30547450	23466744	22434207	95.6	19683905	83.9
15-D28LT1-12	B4	25163038	20051166	19190971	95.7	17161793	85.6
15-D28LT3-01	B3	25882816	20523572	19045875	92.8	17055088	83.1
15-D28LT3-10	B3	23668755	19118264	18257942	95.5	16365234	85.6
Average:		27085814	20563250	19546762	95.1	17315934.33	84.1
Standard deviation:		3572823	3617764	3403797	1.2	3136958.68	1.5
Minumum:		18984226	9526388	8991958	84.3	7343892.509	77.1
Maximum:		45923711	39854747	37503317	96.3	34119648.91	88.4

Table S6: Effect of increasing temperature on larval growth of Atlantic cod from Helgeland and differences in thermal plasticity between Helgeland and 6 crosses from Risør fjord. Estimates of interaction effects represent differences in slopes relative to Helgeland. Asterisks denote significance at $\alpha=0.05$. Larvae lacking parentage information were excluded from the analysis.

Contrast	Estimate	SEM	*t*	*P*-value	
Temperature effect					
6-9.5°C	0.45	0.31	1.48	0.079	
9.5-13°C	0.64	0.32	2.00	0.032	*
Cross-by-temperature interaction with Helgeland at 6-9.5°C					
IF×IF	-0.14	0.36	-0.37	0.358	
IF×OF	-0.30	0.43	-0.70	0.254	
OF×IF	-0.34	0.37	-0.94	0.182	
IF×ON	0.33	0.41	0.81	0.219	
ON×IF	-0.38	0.50	-0.76	0.245	
OF×ON	-0.28	0.42	-0.68	0.257	
Cross-by-temperature interaction with Helgeland at 9.5-13°C					
IF×IF	-0.94	0.39	-2.45	0.014	*
IF×OF	-0.93	0.53	-1.74	0.090	
OF×IF	-0.37	0.37	-1.01	0.165	
IF×ON	-1.52	0.42	-3.63	0.002	*
ON×IF	-0.35	0.44	-0.79	0.226	
OF×ON	-1.46	0.47	-3.09	0.014	*

Table S7: Numbers of enriched (FDR<0.05) gene ontology (GO) terms among transcripts that differ in mean expression and differentially plastic responses to temperature in pairwise contrasts among larvae from Risør fjord. Contrasts are denoted A - B where A is the point of contrast. Enrichment was computed using BiNGO v.3.0.3 (Maere *et al.* 2005) in Cytoscape v.3.2.1 (Shannon *et al.* 2003) to identify significantly enriched GO terms in the category 'biological processes'.

		Mean expression differences	Differences in transcriptomic plasticity							
		All dph	2 dph		14 dph		21 dph		28 dph	
factor	contrast	DE	6-9.5°C	6-13°C	6-9.5°C	6-13°C	6-9.5°C	6-13°C	6-9.5°C	6-13°C
location	I×I - I×O	0	3	99	0	0	10	2	50	45
	I×I - O×I	0	2	40	1	8	2	0	50	8
	I×I - O×O	0	0	0	3	26	1	0	0	.
	I×O - O×I	.	0	3	.	0	4	0	0	0
	I×O - O×O	0	0	0	0	8	0	0	0	3
	O×I - O×O	0	0	6	0	8	1	0	.	3
ecotype	F×F - F×N	16	0	.	0	0	0	0	.	.
	F×F - N×F	0	0	.	0	0	0	0	.	.
	F×N - N×F	1	.	.	19	.	.	.	.	.
LG02	AA - AB	0	-	-	-	-	-	-	33	-
	AA - BB	24	-	-	-	-	-	-	50	-
	AB - BB	8	0	0	0	0	4	0	.	0
LG07	AA - AB	0	0	0	0	40	.	0	0	.
LG12	AA - AB	0	0	74	0	0	1	0	8	3
	AA - BB	3	-	-	-	-	-	-	-	-
	AB - BB	3	-	-	-	-	-	-	-	-

- No differential expression test was performed.
. No differentially expressed genes were detected.

Table S8: Enriched (FDR<0.05) gene ontology (GO) terms among transcripts that differ in mean expression in pairwise contrasts among larvae from Risør fjord. Contrasts are denoted A - B where A is the point of contrast. Enrichment was computed using BiNGO v.3.0.3 (Maere et al. 2005) in Cytoscape v.3.2.1 (Shannon et al. 2003) to identify significantly enriched GO terms in the category 'biological processes'.

Contrast	GO-ID	Description	Corrected *P*-value
Ecotype effects			
F×F - F×N	7049	cell cycle	1.91E-02
F×F - F×N	279	M phase	2.40E-02
F×F - F×N	2244	hemopoietic progenitor cell differentiation	2.40E-02
F×F - F×N	819	sister chromatid segregation	2.40E-02
F×F - F×N	22402	cell cycle process	2.40E-02
F×F - F×N	3241	growth involved in heart morphogenesis	2.40E-02
F×F - F×N	48708	astrocyte differentiation	2.40E-02
F×F - F×N	51301	cell division	2.40E-02
F×F - F×N	278	mitotic cell cycle	2.75E-02
F×F - F×N	7059	chromosome segregation	2.75E-02
F×F - F×N	7067	mitosis	2.75E-02
F×F - F×N	280	nuclear division	2.75E-02
F×F - F×N	35265	organ growth	4.02E-02
F×F - F×N	22403	cell cycle phase	4.04E-02
F×F - F×N	87	M phase of mitotic cell cycle	4.04E-02
F×F - F×N	60856	establishment of blood-brain barrier	4.09E-02
F×N - N×F	2244	hemopoietic progenitor cell differentiation	1.30E-02
LG02 effects			
AA - BB	6418	tRNA aminoacylation for protein translation	8.89E-06
AA - BB	43038	amino acid activation	8.89E-06
AA - BB	43039	tRNA aminoacylation	8.89E-06
AA - BB	6520	cellular amino acid metabolic process	1.70E-05
AA - BB	6412	translation	3.27E-05
AA - BB	6519	cellular amino acid and derivative metabolic process	1.61E-04
AA - BB	44106	cellular amine metabolic process	3.16E-04
AA - BB	43436	oxoacid metabolic process	3.19E-04
AA - BB	19752	carboxylic acid metabolic process	3.19E-04
AA - BB	6082	organic acid metabolic process	3.50E-04
AA - BB	42180	cellular ketone metabolic process	3.50E-04
AA - BB	6399	tRNA metabolic process	1.64E-03
AA - BB	6417	regulation of translation	2.65E-03
AA - BB	6436	tryptophanyl-tRNA aminoacylation	3.26E-03
AA - BB	9308	amine metabolic process	4.20E-03
AA - BB	44281	small molecule metabolic process	8.45E-03
AA - BB	33014	tetrapyrrole biosynthetic process	1.10E-02
AA - BB	6779	porphyrin biosynthetic process	1.10E-02
AA - BB	6564	L-serine biosynthetic process	1.19E-02
AA - BB	6778	porphyrin metabolic process	3.13E-02
AA - BB	33013	tetrapyrrole metabolic process	3.18E-02
AA - BB	6563	L-serine metabolic process	3.74E-02
AA - BB	6879	cellular iron ion homeostasis	3.97E-02
AA - BB	10608	posttranscriptional regulation of gene expression	4.43E-02
AB - BB	6412	translation	8.79E-03
AB - BB	6418	tRNA aminoacylation for protein translation	1.57E-02

Contrast	GO-ID	Description	Corrected *P*-value
AB - BB	43038	amino acid activation	1.57E-02
AB - BB	43039	tRNA aminoacylation	1.57E-02
AB - BB	6520	cellular amino acid metabolic process	1.57E-02
AB - BB	6519	cellular amino acid and derivative metabolic process	1.57E-02
AB - BB	289	nuclear-transcribed mRNA poly(A) tail shortening	3.51E-02
AB - BB	31123	RNA 3'-end processing	4.23E-02
LG12 effects			
AA - BB	6843	mitochondrial citrate transport	1.36E-02
AA - BB	15746	citrate transport	1.36E-02
AA - BB	6842	tricarboxylic acid transport	1.36E-02

Table S9: Enriched (FDR<0.05) gene ontology (GO) terms among transcripts with differentially plastic responses to temperature in pairwise contrasts among larvae from Risør fjord. Contrasts are denoted A - B where A is the point of contrast. Enrichment was computed using BiNGO v.3.0.3 (Maere et al. 2005) in Cytoscape v.3.2.1 (Shannon et al. 2003) to identify significantly enriched GO terms in the category 'biological processes'.

Contrast	Temperature range	dph	GO-ID	Description	Corrected *P*-value
Location effects					
I×I - I×O	6-9.5°C	2	2000016	negative regulation of determination of dorsal identity	4.67E-02
I×I - I×O	6-9.5°C	2	60648	mammary gland bud morphogenesis	4.67E-02
I×I - I×O	6-9.5°C	2	2000015	regulation of determination of dorsal identity	4.67E-02
I×I - O×I	6-9.5°C	2	44319	wound healing, spreading of epithelial cells	2.80E-02
I×I - O×I	6-9.5°C	2	45765	regulation of angiogenesis	2.80E-02
I×I - O×I	6-9.5°C	14	43569	negative regulation of insulin-like growth factor receptor signaling pathway	1.63E-02
I×I - O×O	6-9.5°C	14	43569	negative regulation of insulin-like growth factor receptor signaling pathway	4.23E-02
I×I - O×O	6-9.5°C	14	16578	histone deubiquitination	4.23E-02
I×I - O×O	6-9.5°C	14	43567	regulation of insulin-like growth factor receptor signaling pathway	4.23E-02
I×I - I×O	6-9.5°C	21	45759	negative regulation of action potential	2.82E-02
I×I - I×O	6-9.5°C	21	14075	response to amine stimulus	2.82E-02
I×I - I×O	6-9.5°C	21	10243	response to organic nitrogen	2.82E-02
I×I - I×O	6-9.5°C	21	51001	negative regulation of nitric-oxide synthase activity	2.82E-02
I×I - I×O	6-9.5°C	21	32229	negative regulation of synaptic transmission, GABAergic	2.82E-02
I×I - I×O	6-9.5°C	21	33004	negative regulation of mast cell activation	2.82E-02
I×I - I×O	6-9.5°C	21	18344	protein geranylgeranylation	2.90E-02
I×I - I×O	6-9.5°C	21	32769	negative regulation of monooxygenase activity	3.38E-02
I×I - I×O	6-9.5°C	21	18342	protein prenylation	3.38E-02
I×I - I×O	6-9.5°C	21	51354	negative regulation of oxidoreductase activity	4.73E-02
I×I - O×I	6-9.5°C	21	18344	protein geranylgeranylation	2.40E-02
I×I - O×I	6-9.5°C	21	18342	protein prenylation	2.40E-02
I×I - O×O	6-9.5°C	21	154	rRNA modification	4.12E-02
I×O - O×I	6-9.5°C	21	32874	positive regulation of stress-activated MAPK cascade	4.73E-02
I×O - O×I	6-9.5°C	21	71526	semaphorin-plexin signaling pathway	4.73E-02
I×O - O×I	6-9.5°C	21	21535	cell migration in hindbrain	4.73E-02
I×O - O×I	6-9.5°C	21	32872	regulation of stress-activated MAPK cascade	4.73E-02
O×I - O×O	6-9.5°C	21	154	rRNA modification	4.12E-02
I×I - I×O	6-9.5°C	28	21824	cerebral cortex tangential migration using cell-axon interactions	1.08E-02
I×I - I×O	6-9.5°C	28	21828	gonadotrophin-releasing hormone	1.08E-02

Contrast	Temperature range	dph	GO-ID	Description	Corrected *P*-value
				neuronal migration to the hypothalamus	
I×I - I×O	6-9.5°C	28	21856	hypothalamic tangential migration using cell-axon interactions	1.08E-02
I×I - I×O	6-9.5°C	28	21886	hypothalamus gonadotrophin-releasing hormone neuron differentiation	1.08E-02
I×I - I×O	6-9.5°C	28	21888	hypothalamus gonadotrophin-releasing hormone neuron development	1.08E-02
I×I - I×O	6-9.5°C	28	21649	vestibulocochlear nerve structural organization	1.08E-02
I×I - I×O	6-9.5°C	28	21855	hypothalamus cell migration	1.28E-02
I×I - I×O	6-9.5°C	28	21979	hypothalamus cell differentiation	1.28E-02
I×I - I×O	6-9.5°C	28	21825	substrate-dependent cerebral cortex tangential migration	1.28E-02
I×I - I×O	6-9.5°C	28	21612	facial nerve structural organization	1.28E-02
I×I - I×O	6-9.5°C	28	21648	vestibulocochlear nerve morphogenesis	1.28E-02
I×I - I×O	6-9.5°C	28	21800	cerebral cortex tangential migration	1.28E-02
I×I - I×O	6-9.5°C	28	21561	facial nerve development	1.28E-02
I×I - I×O	6-9.5°C	28	21610	facial nerve morphogenesis	1.28E-02
I×I - I×O	6-9.5°C	28	21562	vestibulocochlear nerve development	1.30E-02
I×I - I×O	6-9.5°C	28	21604	cranial nerve structural organization	1.32E-02
I×I - I×O	6-9.5°C	28	21783	preganglionic parasympathetic nervous system development	1.63E-02
I×I - I×O	6-9.5°C	28	48846	axon extension involved in axon guidance	1.63E-02
I×I - I×O	6-9.5°C	28	6614	SRP-dependent cotranslational protein targeting to membrane	1.63E-02
I×I - I×O	6-9.5°C	28	48486	parasympathetic nervous system development	1.63E-02
I×I - I×O	6-9.5°C	28	6613	cotranslational protein targeting to membrane	1.70E-02
I×I - I×O	6-9.5°C	28	48532	anatomical structure arrangement	1.70E-02
I×I - I×O	6-9.5°C	28	21854	hypothalamus development	1.82E-02
I×I - I×O	6-9.5°C	28	21884	forebrain neuron development	1.82E-02
I×I - I×O	6-9.5°C	28	3148	outflow tract septum morphogenesis	1.82E-02
I×I - I×O	6-9.5°C	28	45047	protein targeting to ER	1.94E-02
I×I - I×O	6-9.5°C	28	21602	cranial nerve morphogenesis	1.99E-02
I×I - I×O	6-9.5°C	28	6929	substrate-bound cell migration	2.26E-02
I×I - I×O	6-9.5°C	28	70972	protein localization in endoplasmic reticulum	2.58E-02
I×I - I×O	6-9.5°C	28	48483	autonomic nervous system development	2.77E-02
I×I - I×O	6-9.5°C	28	21879	forebrain neuron differentiation	2.77E-02
I×I - I×O	6-9.5°C	28	3151	outflow tract morphogenesis	2.77E-02
I×I - I×O	6-9.5°C	28	21795	cerebral cortex cell migration	2.77E-02
I×I - I×O	6-9.5°C	28	50919	negative chemotaxis	2.77E-02
I×I - I×O	6-9.5°C	28	48675	axon extension	3.00E-02
I×I - I×O	6-9.5°C	28	6612	protein targeting to membrane	3.00E-02
I×I - I×O	6-9.5°C	28	21545	cranial nerve development	3.00E-02
I×I - I×O	6-9.5°C	28	60411	cardiac septum morphogenesis	3.00E-02
I×I - I×O	6-9.5°C	28	22029	telencephalon cell migration	3.00E-02
I×I - I×O	6-9.5°C	28	21872	generation of neurons in the forebrain	3.00E-02
I×I - I×O	6-9.5°C	28	21885	forebrain cell migration	3.01E-02
I×I - I×O	6-9.5°C	28	21954	central nervous system neuron	3.40E-02

Contrast	Temperature range	dph	GO-ID	Description	Corrected *P*-value
				development	
I×I - I×O	6-9.5°C	28	48588	developmental cell growth	3.66E-02
I×I - I×O	6-9.5°C	28	21675	nerve development	3.98E-02
I×I - I×O	6-9.5°C	28	16049	cell growth	4.16E-02
I×I - I×O	6-9.5°C	28	21536	diencephalon development	4.16E-02
I×I - I×O	6-9.5°C	28	3279	cardiac septum development	4.21E-02
I×I - I×O	6-9.5°C	28	21761	limbic system development	4.66E-02
I×I - I×O	6-9.5°C	28	21987	cerebral cortex development	4.83E-02
I×I - I×O	6-9.5°C	28	3206	cardiac chamber morphogenesis	4.83E-02
I×I - O×I	6-9.5°C	28	21824	cerebral cortex tangential migration using cell-axon interactions	1.08E-02
I×I - O×I	6-9.5°C	28	21828	gonadotrophin-releasing hormone neuronal migration to the hypothalamus	1.08E-02
I×I - O×I	6-9.5°C	28	21856	hypothalamic tangential migration using cell-axon interactions	1.08E-02
I×I - O×I	6-9.5°C	28	21886	hypothalamus gonadotrophin-releasing hormone neuron differentiation	1.08E-02
I×I - O×I	6-9.5°C	28	21888	hypothalamus gonadotrophin-releasing hormone neuron development	1.08E-02
I×I - O×I	6-9.5°C	28	21649	vestibulocochlear nerve structural organization	1.08E-02
I×I - O×I	6-9.5°C	28	21855	hypothalamus cell migration	1.28E-02
I×I - O×I	6-9.5°C	28	21979	hypothalamus cell differentiation	1.28E-02
I×I - O×I	6-9.5°C	28	21825	substrate-dependent cerebral cortex tangential migration	1.28E-02
I×I - O×I	6-9.5°C	28	21612	facial nerve structural organization	1.28E-02
I×I - O×I	6-9.5°C	28	21648	vestibulocochlear nerve morphogenesis	1.28E-02
I×I - O×I	6-9.5°C	28	21800	cerebral cortex tangential migration	1.28E-02
I×I - O×I	6-9.5°C	28	21561	facial nerve development	1.28E-02
I×I - O×I	6-9.5°C	28	21610	facial nerve morphogenesis	1.28E-02
I×I - O×I	6-9.5°C	28	21562	vestibulocochlear nerve development	1.30E-02
I×I - O×I	6-9.5°C	28	21604	cranial nerve structural organization	1.32E-02
I×I - O×I	6-9.5°C	28	21783	preganglionic parasympathetic nervous system development	1.63E-02
I×I - O×I	6-9.5°C	28	48846	axon extension involved in axon guidance	1.63E-02
I×I - O×I	6-9.5°C	28	6614	SRP-dependent cotranslational protein targeting to membrane	1.63E-02
I×I - O×I	6-9.5°C	28	48486	parasympathetic nervous system development	1.63E-02
I×I - O×I	6-9.5°C	28	6613	cotranslational protein targeting to membrane	1.70E-02
I×I - O×I	6-9.5°C	28	48532	anatomical structure arrangement	1.70E-02
I×I - O×I	6-9.5°C	28	21854	hypothalamus development	1.82E-02
I×I - O×I	6-9.5°C	28	21884	forebrain neuron development	1.82E-02
I×I - O×I	6-9.5°C	28	3148	outflow tract septum morphogenesis	1.82E-02
I×I - O×I	6-9.5°C	28	45047	protein targeting to ER	1.94E-02
I×I - O×I	6-9.5°C	28	21602	cranial nerve morphogenesis	1.99E-02
I×I - O×I	6-9.5°C	28	6929	substrate-bound cell migration	2.26E-02
I×I - O×I	6-9.5°C	28	70972	protein localization in endoplasmic reticulum	2.58E-02
I×I - O×I	6-9.5°C	28	48483	autonomic nervous system development	2.77E-02

Contrast	Temperature range	dph	GO-ID	Description	Corrected *P*-value
I×I - O×I	6-9.5°C	28	21879	forebrain neuron differentiation	2.77E-02
I×I - O×I	6-9.5°C	28	3151	outflow tract morphogenesis	2.77E-02
I×I - O×I	6-9.5°C	28	21795	cerebral cortex cell migration	2.77E-02
I×I - O×I	6-9.5°C	28	50919	negative chemotaxis	2.77E-02
I×I - O×I	6-9.5°C	28	48675	axon extension	3.00E-02
I×I - O×I	6-9.5°C	28	6612	protein targeting to membrane	3.00E-02
I×I - O×I	6-9.5°C	28	21545	cranial nerve development	3.00E-02
I×I - O×I	6-9.5°C	28	60411	cardiac septum morphogenesis	3.00E-02
I×I - O×I	6-9.5°C	28	22029	telencephalon cell migration	3.00E-02
I×I - O×I	6-9.5°C	28	21872	generation of neurons in the forebrain	3.00E-02
I×I - O×I	6-9.5°C	28	21885	forebrain cell migration	3.01E-02
I×I - O×I	6-9.5°C	28	21954	central nervous system neuron development	3.40E-02
I×I - O×I	6-9.5°C	28	48588	developmental cell growth	3.66E-02
I×I - O×I	6-9.5°C	28	21675	nerve development	3.98E-02
I×I - O×I	6-9.5°C	28	16049	cell growth	4.16E-02
I×I - O×I	6-9.5°C	28	21536	diencephalon development	4.16E-02
I×I - O×I	6-9.5°C	28	3279	cardiac septum development	4.21E-02
I×I - O×I	6-9.5°C	28	21761	limbic system development	4.66E-02
I×I - O×I	6-9.5°C	28	21987	cerebral cortex development	4.83E-02
I×I - O×I	6-9.5°C	28	3206	cardiac chamber morphogenesis	4.83E-02
I×I - I×O	6-13°C	2	44281	small molecule metabolic process	4.07E-07
I×I - I×O	6-13°C	2	6091	generation of precursor metabolites and energy	5.87E-07
I×I - I×O	6-13°C	2	46483	heterocycle metabolic process	7.10E-06
I×I - I×O	6-13°C	2	6082	organic acid metabolic process	5.50E-05
I×I - I×O	6-13°C	2	42180	cellular ketone metabolic process	5.50E-05
I×I - I×O	6-13°C	2	43436	oxoacid metabolic process	8.28E-05
I×I - I×O	6-13°C	2	19752	carboxylic acid metabolic process	8.28E-05
I×I - I×O	6-13°C	2	71688	striated muscle myosin thick filament assembly	1.24E-04
I×I - I×O	6-13°C	2	15980	energy derivation by oxidation of organic compounds	1.24E-04
I×I - I×O	6-13°C	2	31033	myosin filament assembly or disassembly	1.24E-04
I×I - I×O	6-13°C	2	31034	myosin filament assembly	1.24E-04
I×I - I×O	6-13°C	2	6119	oxidative phosphorylation	1.65E-04
I×I - I×O	6-13°C	2	45333	cellular respiration	1.65E-04
I×I - I×O	6-13°C	2	6599	phosphagen metabolic process	3.46E-04
I×I - I×O	6-13°C	2	46395	carboxylic acid catabolic process	3.46E-04
I×I - I×O	6-13°C	2	16054	organic acid catabolic process	3.46E-04
I×I - I×O	6-13°C	2	43648	dicarboxylic acid metabolic process	4.66E-04
I×I - I×O	6-13°C	2	9063	cellular amino acid catabolic process	5.68E-04
I×I - I×O	6-13°C	2	42396	phosphagen biosynthetic process	8.35E-04
I×I - I×O	6-13°C	2	55086	nucleobase, nucleoside and nucleotide metabolic process	1.07E-03
I×I - I×O	6-13°C	2	45214	sarcomere organization	1.09E-03
I×I - I×O	6-13°C	2	44282	small molecule catabolic process	1.09E-03
I×I - I×O	6-13°C	2	44283	small molecule biosynthetic process	1.09E-03
I×I - I×O	6-13°C	2	6519	cellular amino acid and derivative metabolic process	1.09E-03
I×I - I×O	6-13°C	2	34404	nucleobase, nucleoside and nucleotide biosynthetic process	1.10E-03
I×I - I×O	6-13°C	2	34654	nucleobase, nucleoside, nucleotide and	1.10E-03

Contrast	Temperature range	dph	GO-ID	Description	Corrected *P*-value
				nucleic acid biosynthetic process	
I×I - I×O	6-13°C	2	6412	translation	1.51E-03
I×I - I×O	6-13°C	2	9165	nucleotide biosynthetic process	1.97E-03
I×I - I×O	6-13°C	2	6941	striated muscle contraction	2.03E-03
I×I - I×O	6-13°C	2	55114	oxidation reduction	2.03E-03
I×I - I×O	6-13°C	2	9310	amine catabolic process	2.32E-03
I×I - I×O	6-13°C	2	30036	actin cytoskeleton organization	2.44E-03
I×I - I×O	6-13°C	2	22904	respiratory electron transport chain	2.49E-03
I×I - I×O	6-13°C	2	30239	myofibril assembly	2.49E-03
I×I - I×O	6-13°C	2	51146	striated muscle cell differentiation	3.64E-03
I×I - I×O	6-13°C	2	44271	cellular nitrogen compound biosynthetic process	3.64E-03
I×I - I×O	6-13°C	2	9109	coenzyme catabolic process	3.64E-03
I×I - I×O	6-13°C	2	22900	electron transport chain	3.64E-03
I×I - I×O	6-13°C	2	42775	mitochondrial ATP synthesis coupled electron transport	3.65E-03
I×I - I×O	6-13°C	2	6084	acetyl-CoA metabolic process	3.82E-03
I×I - I×O	6-13°C	2	31032	actomyosin structure organization	3.99E-03
I×I - I×O	6-13°C	2	44237	cellular metabolic process	4.60E-03
I×I - I×O	6-13°C	2	9308	amine metabolic process	4.62E-03
I×I - I×O	6-13°C	2	30029	actin filament-based process	4.62E-03
I×I - I×O	6-13°C	2	42773	ATP synthesis coupled electron transport	4.62E-03
I×I - I×O	6-13°C	2	2074	extraocular skeletal muscle development	4.62E-03
I×I - I×O	6-13°C	2	55002	striated muscle cell development	4.62E-03
I×I - I×O	6-13°C	2	8152	metabolic process	4.62E-03
I×I - I×O	6-13°C	2	6099	tricarboxylic acid cycle	4.62E-03
I×I - I×O	6-13°C	2	6754	ATP biosynthetic process	4.62E-03
I×I - I×O	6-13°C	2	51187	cofactor catabolic process	4.62E-03
I×I - I×O	6-13°C	2	6164	purine nucleotide biosynthetic process	4.62E-03
I×I - I×O	6-13°C	2	3012	muscle system process	4.62E-03
I×I - I×O	6-13°C	2	46356	acetyl-CoA catabolic process	5.00E-03
I×I - I×O	6-13°C	2	55001	muscle cell development	5.35E-03
I×I - I×O	6-13°C	2	6520	cellular amino acid metabolic process	5.35E-03
I×I - I×O	6-13°C	2	46314	phosphocreatine biosynthetic process	6.09E-03
I×I - I×O	6-13°C	2	6603	phosphocreatine metabolic process	6.09E-03
I×I - I×O	6-13°C	2	10927	cellular component assembly involved in morphogenesis	6.30E-03
I×I - I×O	6-13°C	2	6104	succinyl-CoA metabolic process	7.54E-03
I×I - I×O	6-13°C	2	6163	purine nucleotide metabolic process	7.98E-03
I×I - I×O	6-13°C	2	51186	cofactor metabolic process	8.49E-03
I×I - I×O	6-13°C	2	46034	ATP metabolic process	9.66E-03
I×I - I×O	6-13°C	2	15985	energy coupled proton transport, down electrochemical gradient	9.66E-03
I×I - I×O	6-13°C	2	15986	ATP synthesis coupled proton transport	9.66E-03
I×I - I×O	6-13°C	2	9117	nucleotide metabolic process	9.66E-03
I×I - I×O	6-13°C	2	6753	nucleoside phosphate metabolic process	9.66E-03
I×I - I×O	6-13°C	2	44238	primary metabolic process	1.01E-02
I×I - I×O	6-13°C	2	9075	histidine family amino acid metabolic process	1.15E-02
I×I - I×O	6-13°C	2	6547	histidine metabolic process	1.15E-02
I×I - I×O	6-13°C	2	6936	muscle contraction	1.15E-02

Contrast	Temperature range	dph	GO-ID	Description	Corrected *P*-value
I×I - I×O	6-13°C	2	9145	purine nucleoside triphosphate biosynthetic process	1.15E-02
I×I - I×O	6-13°C	2	9206	purine ribonucleoside triphosphate biosynthetic process	1.15E-02
I×I - I×O	6-13°C	2	44106	cellular amine metabolic process	1.15E-02
I×I - I×O	6-13°C	2	6732	coenzyme metabolic process	1.24E-02
I×I - I×O	6-13°C	2	9056	catabolic process	1.32E-02
I×I - I×O	6-13°C	2	9152	purine ribonucleotide biosynthetic process	1.32E-02
I×I - I×O	6-13°C	2	42692	muscle cell differentiation	1.63E-02
I×I - I×O	6-13°C	2	9144	purine nucleoside triphosphate metabolic process	1.66E-02
I×I - I×O	6-13°C	2	9060	aerobic respiration	1.91E-02
I×I - I×O	6-13°C	2	6807	nitrogen compound metabolic process	1.96E-02
I×I - I×O	6-13°C	2	9201	ribonucleoside triphosphate biosynthetic process	2.18E-02
I×I - I×O	6-13°C	2	7015	actin filament organization	2.37E-02
I×I - I×O	6-13°C	2	6536	glutamate metabolic process	2.37E-02
I×I - I×O	6-13°C	2	34641	cellular nitrogen compound metabolic process	2.62E-02
I×I - I×O	6-13°C	2	9083	branched chain family amino acid catabolic process	2.81E-02
I×I - I×O	6-13°C	2	31103	axon regeneration	2.81E-02
I×I - I×O	6-13°C	2	9260	ribonucleotide biosynthetic process	2.81E-02
I×I - I×O	6-13°C	2	7010	cytoskeleton organization	3.05E-02
I×I - I×O	6-13°C	2	6096	glycolysis	3.31E-02
I×I - I×O	6-13°C	2	14745	negative regulation of muscle adaptation	3.71E-02
I×I - I×O	6-13°C	2	19556	histidine catabolic process to glutamate and formamide	3.71E-02
I×I - I×O	6-13°C	2	19557	histidine catabolic process to glutamate and formate	3.71E-02
I×I - I×O	6-13°C	2	9141	nucleoside triphosphate metabolic process	3.74E-02
I×I - I×O	6-13°C	2	9142	nucleoside triphosphate biosynthetic process	3.74E-02
I×I - I×O	6-13°C	2	42273	ribosomal large subunit biogenesis	3.74E-02
I×I - I×O	6-13°C	2	9150	purine ribonucleotide metabolic process	4.41E-02
I×I - I×O	6-13°C	2	9205	purine ribonucleoside triphosphate metabolic process	4.58E-02
I×I - I×O	6-13°C	2	6725	cellular aromatic compound metabolic process	4.88E-02
I×I - O×I	6-13°C	2	46483	heterocycle metabolic process	3.33E-03
I×I - O×I	6-13°C	2	6163	purine nucleotide metabolic process	6.97E-03
I×I - O×I	6-13°C	2	9063	cellular amino acid catabolic process	6.97E-03
I×I - O×I	6-13°C	2	43648	dicarboxylic acid metabolic process	6.97E-03
I×I - O×I	6-13°C	2	46395	carboxylic acid catabolic process	6.97E-03
I×I - O×I	6-13°C	2	16054	organic acid catabolic process	6.97E-03
I×I - O×I	6-13°C	2	6164	purine nucleotide biosynthetic process	8.86E-03
I×I - O×I	6-13°C	2	6119	oxidative phosphorylation	9.18E-03
I×I - O×I	6-13°C	2	9310	amine catabolic process	1.06E-02
I×I - O×I	6-13°C	2	15985	energy coupled proton transport, down electrochemical gradient	1.06E-02

Contrast	Temperature range	dph	GO-ID	Description	Corrected *P*-value
I×I - O×I	6-13°C	2	15986	ATP synthesis coupled proton transport	1.06E-02
I×I - O×I	6-13°C	2	9152	purine ribonucleotide biosynthetic process	1.59E-02
I×I - O×I	6-13°C	2	6082	organic acid metabolic process	1.66E-02
I×I - O×I	6-13°C	2	31099	regeneration	1.66E-02
I×I - O×I	6-13°C	2	30036	actin cytoskeleton organization	1.83E-02
I×I - O×I	6-13°C	2	6091	generation of precursor metabolites and energy	1.83E-02
I×I - O×I	6-13°C	2	9260	ribonucleotide biosynthetic process	1.83E-02
I×I - O×I	6-13°C	2	6753	nucleoside phosphate metabolic process	1.83E-02
I×I - O×I	6-13°C	2	9117	nucleotide metabolic process	1.83E-02
I×I - O×I	6-13°C	2	6754	ATP biosynthetic process	1.83E-02
I×I - O×I	6-13°C	2	44281	small molecule metabolic process	1.83E-02
I×I - O×I	6-13°C	2	6108	malate metabolic process	2.21E-02
I×I - O×I	6-13°C	2	30029	actin filament-based process	2.30E-02
I×I - O×I	6-13°C	2	44282	small molecule catabolic process	2.30E-02
I×I - O×I	6-13°C	2	9165	nucleotide biosynthetic process	2.34E-02
I×I - O×I	6-13°C	2	44271	cellular nitrogen compound biosynthetic process	2.34E-02
I×I - O×I	6-13°C	2	6818	hydrogen transport	2.34E-02
I×I - O×I	6-13°C	2	15992	proton transport	2.34E-02
I×I - O×I	6-13°C	2	9144	purine nucleoside triphosphate metabolic process	2.68E-02
I×I - O×I	6-13°C	2	9145	purine nucleoside triphosphate biosynthetic process	2.68E-02
I×I - O×I	6-13°C	2	9206	purine ribonucleoside triphosphate biosynthetic process	2.68E-02
I×I - O×I	6-13°C	2	43436	oxoacid metabolic process	2.71E-02
I×I - O×I	6-13°C	2	19752	carboxylic acid metabolic process	2.71E-02
I×I - O×I	6-13°C	2	55086	nucleobase, nucleoside and nucleotide metabolic process	2.71E-02
I×I - O×I	6-13°C	2	34404	nucleobase, nucleoside and nucleotide biosynthetic process	2.71E-02
I×I - O×I	6-13°C	2	34654	nucleobase, nucleoside, nucleotide and nucleic acid biosynthetic process	2.71E-02
I×I - O×I	6-13°C	2	42180	cellular ketone metabolic process	2.95E-02
I×I - O×I	6-13°C	2	9201	ribonucleoside triphosphate biosynthetic process	3.48E-02
I×I - O×I	6-13°C	2	9141	nucleoside triphosphate metabolic process	3.87E-02
I×I - O×I	6-13°C	2	9150	purine ribonucleotide metabolic process	4.29E-02
I×O - O×I	6-13°C	2	46415	urate metabolic process	4.00E-02
I×O - O×I	6-13°C	2	8645	hexose transport	4.00E-02
I×O - O×I	6-13°C	2	15749	monosaccharide transport	4.00E-02
O×I - O×O	6-13°C	2	6096	glycolysis	2.54E-02
O×I - O×O	6-13°C	2	6007	glucose catabolic process	2.54E-02
O×I - O×O	6-13°C	2	19320	hexose catabolic process	2.54E-02
O×I - O×O	6-13°C	2	46365	monosaccharide catabolic process	2.82E-02
O×I - O×O	6-13°C	2	46164	alcohol catabolic process	3.90E-02
O×I - O×O	6-13°C	2	44275	cellular carbohydrate catabolic process	3.90E-02
I×I - O×I	6-13°C	14	43569	negative regulation of insulin-like growth factor receptor signaling	9.66E-04

Contrast	Temperature range	dph	GO-ID	Description	Corrected *P*-value
				pathway	
I×I - O×I	6-13°C	14	43567	regulation of insulin-like growth factor receptor signaling pathway	3.62E-03
I×I - O×I	6-13°C	14	35332	positive regulation of hippo signaling cascade	4.08E-02
I×I - O×I	6-13°C	14	45186	zonula adherens assembly	4.08E-02
I×I - O×I	6-13°C	14	18103	protein amino acid C-linked glycosylation	4.08E-02
I×I - O×I	6-13°C	14	18211	peptidyl-tryptophan modification	4.08E-02
I×I - O×I	6-13°C	14	18317	protein amino acid C-linked glycosylation via tryptophan	4.08E-02
I×I - O×I	6-13°C	14	18406	protein amino acid C-linked glycosylation via 2'-alpha-mannosyl-L-tryptophan	4.08E-02
I×I - O×O	6-13°C	14	1574	ganglioside biosynthetic process	1.63E-02
I×I - O×O	6-13°C	14	6677	glycosylceramide metabolic process	1.63E-02
I×I - O×O	6-13°C	14	1573	ganglioside metabolic process	1.63E-02
I×I - O×O	6-13°C	14	6688	glycosphingolipid biosynthetic process	1.63E-02
I×I - O×O	6-13°C	14	9312	oligosaccharide biosynthetic process	1.63E-02
I×I - O×O	6-13°C	14	9247	glycolipid biosynthetic process	1.63E-02
I×I - O×O	6-13°C	14	18279	protein amino acid N-linked glycosylation via asparagine	1.63E-02
I×I - O×O	6-13°C	14	18196	peptidyl-asparagine modification	1.63E-02
I×I - O×O	6-13°C	14	9988	cell-cell recognition	1.63E-02
I×I - O×O	6-13°C	14	6687	glycosphingolipid metabolic process	1.77E-02
I×I - O×O	6-13°C	14	6664	glycolipid metabolic process	1.95E-02
I×I - O×O	6-13°C	14	9311	oligosaccharide metabolic process	1.95E-02
I×I - O×O	6-13°C	14	6672	ceramide metabolic process	1.95E-02
I×I - O×O	6-13°C	14	30148	sphingolipid biosynthetic process	1.95E-02
I×I - O×O	6-13°C	14	6487	protein amino acid N-linked glycosylation	1.95E-02
I×I - O×O	6-13°C	14	46519	sphingoid metabolic process	1.95E-02
I×I - O×O	6-13°C	14	46467	membrane lipid biosynthetic process	2.01E-02
I×I - O×O	6-13°C	14	8037	cell recognition	2.53E-02
I×I - O×O	6-13°C	14	6665	sphingolipid metabolic process	2.62E-02
I×I - O×O	6-13°C	14	6643	membrane lipid metabolic process	2.82E-02
I×I - O×O	6-13°C	14	16051	carbohydrate biosynthetic process	3.50E-02
I×I - O×O	6-13°C	14	43413	macromolecule glycosylation	3.50E-02
I×I - O×O	6-13°C	14	6486	protein amino acid glycosylation	3.50E-02
I×I - O×O	6-13°C	14	70085	glycosylation	3.50E-02
I×I - O×O	6-13°C	14	9101	glycoprotein biosynthetic process	4.15E-02
I×I - O×O	6-13°C	14	9100	glycoprotein metabolic process	4.89E-02
I×O - O×O	6-13°C	14	6268	DNA unwinding involved in replication	1.93E-02
I×O - O×O	6-13°C	14	30174	regulation of DNA-dependent DNA replication initiation	1.93E-02
I×O - O×O	6-13°C	14	6270	DNA-dependent DNA replication initiation	1.93E-02
I×O - O×O	6-13°C	14	32508	DNA duplex unwinding	1.93E-02
I×O - O×O	6-13°C	14	32392	DNA geometric change	1.93E-02
I×O - O×O	6-13°C	14	90329	regulation of DNA-dependent DNA replication	2.33E-02
I×O - O×O	6-13°C	14	6261	DNA-dependent DNA replication	4.74E-02
I×O - O×O	6-13°C	14	6275	regulation of DNA replication	4.74E-02

Contrast	Temperature range	dph	GO-ID	Description	Corrected *P*-value
O×I - O×O	6-13°C	14	6268	DNA unwinding involved in replication	1.93E-02
O×I - O×O	6-13°C	14	30174	regulation of DNA-dependent DNA replication initiation	1.93E-02
O×I - O×O	6-13°C	14	6270	DNA-dependent DNA replication initiation	1.93E-02
O×I - O×O	6-13°C	14	32508	DNA duplex unwinding	1.93E-02
O×I - O×O	6-13°C	14	32392	DNA geometric change	1.93E-02
O×I - O×O	6-13°C	14	90329	regulation of DNA-dependent DNA replication	2.33E-02
O×I - O×O	6-13°C	14	6261	DNA-dependent DNA replication	4.74E-02
O×I - O×O	6-13°C	14	6275	regulation of DNA replication	4.74E-02
I×I - I×O	6-13°C	21	8360	regulation of cell shape	1.65E-02
I×I - I×O	6-13°C	21	31346	positive regulation of cell projection organization	4.08E-02
I×I - I×O	6-13°C	28	7193	inhibition of adenylate cyclase activity by G-protein signaling pathway	1.28E-02
I×I - I×O	6-13°C	28	7194	negative regulation of adenylate cyclase activity	1.28E-02
I×I - I×O	6-13°C	28	31280	negative regulation of cyclase activity	1.28E-02
I×I - I×O	6-13°C	28	51350	negative regulation of lyase activity	1.28E-02
I×I - I×O	6-13°C	28	30803	negative regulation of cyclic nucleotide biosynthetic process	1.28E-02
I×I - I×O	6-13°C	28	30809	negative regulation of nucleotide biosynthetic process	1.28E-02
I×I - I×O	6-13°C	28	30818	negative regulation of cAMP biosynthetic process	1.28E-02
I×I - I×O	6-13°C	28	6843	mitochondrial citrate transport	1.28E-02
I×I - I×O	6-13°C	28	45761	regulation of adenylate cyclase activity	1.28E-02
I×I - I×O	6-13°C	28	7188	G-protein signaling, coupled to cAMP nucleotide second messenger	1.28E-02
I×I - I×O	6-13°C	28	31279	regulation of cyclase activity	1.28E-02
I×I - I×O	6-13°C	28	51339	regulation of lyase activity	1.28E-02
I×I - I×O	6-13°C	28	30817	regulation of cAMP biosynthetic process	1.28E-02
I×I - I×O	6-13°C	28	7187	G-protein signaling, coupled to cyclic nucleotide second messenger	1.28E-02
I×I - I×O	6-13°C	28	30814	regulation of cAMP metabolic process	1.28E-02
I×I - I×O	6-13°C	28	30802	regulation of cyclic nucleotide biosynthetic process	1.28E-02
I×I - I×O	6-13°C	28	30808	regulation of nucleotide biosynthetic process	1.28E-02
I×I - I×O	6-13°C	28	19933	cAMP-mediated signaling	1.28E-02
I×I - I×O	6-13°C	28	30799	regulation of cyclic nucleotide metabolic process	1.28E-02
I×I - I×O	6-13°C	28	10523	negative regulation of calcium ion transport into cytosol	1.28E-02
I×I - I×O	6-13°C	28	30800	negative regulation of cyclic nucleotide metabolic process	1.28E-02
I×I - I×O	6-13°C	28	30815	negative regulation of cAMP metabolic process	1.28E-02
I×I - I×O	6-13°C	28	19935	cyclic-nucleotide-mediated signaling	1.32E-02
I×I - I×O	6-13°C	28	15746	citrate transport	1.32E-02
I×I - I×O	6-13°C	28	6842	tricarboxylic acid transport	1.32E-02

Contrast	Temperature range	dph	GO-ID	Description	Corrected *P*-value
I×I - I×O	6-13°C	28	45980	negative regulation of nucleotide metabolic process	1.45E-02
I×I - I×O	6-13°C	28	7195	inhibition of adenylate cyclase activity by dopamine receptor signaling pathway	1.74E-02
I×I - I×O	6-13°C	28	51967	negative regulation of synaptic transmission, glutamatergic	1.85E-02
I×I - I×O	6-13°C	28	60158	activation of phospholipase C activity by dopamine receptor signaling pathway	2.27E-02
I×I - I×O	6-13°C	28	48149	behavioral response to ethanol	2.51E-02
I×I - I×O	6-13°C	28	19932	second-messenger-mediated signaling	2.74E-02
I×I - I×O	6-13°C	28	1963	synaptic transmission, dopaminergic	2.79E-02
I×I - I×O	6-13°C	28	48148	behavioral response to cocaine	3.41E-02
I×I - I×O	6-13°C	28	14059	regulation of dopamine secretion	3.59E-02
I×I - I×O	6-13°C	28	51481	reduction of cytosolic calcium ion concentration	3.62E-02
I×I - I×O	6-13°C	28	6140	regulation of nucleotide metabolic process	3.63E-02
I×I - I×O	6-13°C	28	23050	consequence of signal transmission	4.31E-02
I×I - I×O	6-13°C	28	43266	regulation of potassium ion transport	4.32E-02
I×I - I×O	6-13°C	28	7212	dopamine receptor signaling pathway	4.45E-02
I×I - I×O	6-13°C	28	48512	circadian behavior	4.46E-02
I×I - I×O	6-13°C	28	7622	rhythmic behavior	4.46E-02
I×I - I×O	6-13°C	28	7268	synaptic transmission	4.49E-02
I×I - I×O	6-13°C	28	7186	G-protein coupled receptor protein signaling pathway	4.49E-02
I×I - I×O	6-13°C	28	43086	negative regulation of catalytic activity	4.49E-02
I×I - I×O	6-13°C	28	50433	regulation of catecholamine secretion	4.68E-02
I×I - O×I	6-13°C	28	6843	mitochondrial citrate transport	2.52E-03
I×I - O×I	6-13°C	28	15746	citrate transport	2.52E-03
I×I - O×I	6-13°C	28	6842	tricarboxylic acid transport	2.52E-03
I×I - O×I	6-13°C	28	15711	organic anion transport	2.67E-02
I×I - O×I	6-13°C	28	6839	mitochondrial transport	3.28E-02
I×I - O×I	6-13°C	28	6820	anion transport	3.28E-02
I×I - O×I	6-13°C	28	46942	carboxylic acid transport	3.30E-02
I×I - O×I	6-13°C	28	15849	organic acid transport	3.30E-02
I×O - O×O	6-13°C	28	6843	mitochondrial citrate transport	1.36E-02
I×O - O×O	6-13°C	28	15746	citrate transport	1.36E-02
I×O - O×O	6-13°C	28	6842	tricarboxylic acid transport	1.36E-02
O×I - O×O	6-13°C	28	6843	mitochondrial citrate transport	1.36E-02
O×I - O×O	6-13°C	28	15746	citrate transport	1.36E-02
O×I - O×O	6-13°C	28	6842	tricarboxylic acid transport	1.36E-02
Ecotype effects					
F×N - N×F	6-9.5°C	14	6853	carnitine shuttle	4.83E-02
F×N - N×F	6-9.5°C	14	32000	positive regulation of fatty acid beta-oxidation	4.83E-02
F×N - N×F	6-9.5°C	14	15879	carnitine transport	4.83E-02
F×N - N×F	6-9.5°C	14	15838	betaine transport	4.83E-02
F×N - N×F	6-9.5°C	14	9437	carnitine metabolic process	4.83E-02
F×N - N×F	6-9.5°C	14	46321	positive regulation of fatty acid oxidation	4.83E-02

Contrast	Temperature range	dph	GO-ID	Description	Corrected *P*-value
F×N - N×F	6-9.5°C	14	31998	regulation of fatty acid beta-oxidation	4.83E-02
F×N - N×F	6-9.5°C	14	15697	quaternary ammonium group transport	4.83E-02
F×N - N×F	6-9.5°C	14	70208	protein heterotrimerization	4.83E-02
F×N - N×F	6-9.5°C	14	6577	betaine metabolic process	4.83E-02
F×N - N×F	6-9.5°C	14	32365	intracellular lipid transport	4.83E-02
F×N - N×F	6-9.5°C	14	71398	cellular response to fatty acid	4.83E-02
F×N - N×F	6-9.5°C	14	51259	protein oligomerization	4.83E-02
F×N - N×F	6-9.5°C	14	42755	eating behavior	4.83E-02
F×N - N×F	6-9.5°C	14	3333	amino acid transmembrane transport	4.83E-02
F×N - N×F	6-9.5°C	14	45923	positive regulation of fatty acid metabolic process	4.83E-02
F×N - N×F	6-9.5°C	14	51181	cofactor transport	4.83E-02
F×N - N×F	6-9.5°C	14	50996	positive regulation of lipid catabolic process	4.92E-02
F×N - N×F	6-9.5°C	14	46320	regulation of fatty acid oxidation	4.99E-02
LG02 effects					
AB - BB	6-9.5°C	21	32874	positive regulation of stress-activated MAPK cascade	4.73E-02
AB - BB	6-9.5°C	21	71526	semaphorin-plexin signaling pathway	4.73E-02
AB - BB	6-9.5°C	21	21535	cell migration in hindbrain	4.73E-02
AB - BB	6-9.5°C	21	32872	regulation of stress-activated MAPK cascade	4.73E-02
AA - AB	6-9.5°C	28	6843	mitochondrial citrate transport	1.62E-02
AA - AB	6-9.5°C	28	21824	cerebral cortex tangential migration using cell-axon interactions	1.62E-02
AA - AB	6-9.5°C	28	21828	gonadotrophin-releasing hormone neuronal migration to the hypothalamus	1.62E-02
AA - AB	6-9.5°C	28	21856	hypothalamic tangential migration using cell-axon interactions	1.62E-02
AA - AB	6-9.5°C	28	21886	hypothalamus gonadotrophin-releasing hormone neuron differentiation	1.62E-02
AA - AB	6-9.5°C	28	21888	hypothalamus gonadotrophin-releasing hormone neuron development	1.62E-02
AA - AB	6-9.5°C	28	21649	vestibulocochlear nerve structural organization	1.62E-02
AA - AB	6-9.5°C	28	21855	hypothalamus cell migration	1.75E-02
AA - AB	6-9.5°C	28	15746	citrate transport	1.75E-02
AA - AB	6-9.5°C	28	6842	tricarboxylic acid transport	1.75E-02
AA - AB	6-9.5°C	28	21979	hypothalamus cell differentiation	1.75E-02
AA - AB	6-9.5°C	28	21825	substrate-dependent cerebral cortex tangential migration	1.75E-02
AA - AB	6-9.5°C	28	21612	facial nerve structural organization	1.75E-02
AA - AB	6-9.5°C	28	21648	vestibulocochlear nerve morphogenesis	1.83E-02
AA - AB	6-9.5°C	28	21800	cerebral cortex tangential migration	1.84E-02
AA - AB	6-9.5°C	28	21561	facial nerve development	1.84E-02
AA - AB	6-9.5°C	28	21610	facial nerve morphogenesis	1.84E-02
AA - AB	6-9.5°C	28	21562	vestibulocochlear nerve development	1.89E-02
AA - AB	6-9.5°C	28	21604	cranial nerve structural organization	1.94E-02
AA - AB	6-9.5°C	28	21783	preganglionic parasympathetic nervous system development	2.43E-02
AA - AB	6-9.5°C	28	48846	axon extension involved in axon guidance	2.43E-02
AA - AB	6-9.5°C	28	48486	parasympathetic nervous system	2.58E-02

Contrast	Temperature range	dph	GO-ID	Description	Corrected *P*-value
				development	
AA - AB	6-9.5°C	28	48532	anatomical structure arrangement	2.84E-02
AA - AB	6-9.5°C	28	21854	hypothalamus development	3.05E-02
AA - AB	6-9.5°C	28	21884	forebrain neuron development	3.05E-02
AA - AB	6-9.5°C	28	3148	outflow tract septum morphogenesis	3.05E-02
AA - AB	6-9.5°C	28	21602	cranial nerve morphogenesis	3.47E-02
AA - AB	6-9.5°C	28	6929	substrate-bound cell migration	3.95E-02
AA - AB	6-9.5°C	28	48483	autonomic nervous system development	4.98E-02
AA - AB	6-9.5°C	28	21879	forebrain neuron differentiation	4.98E-02
AA - AB	6-9.5°C	28	3151	outflow tract morphogenesis	4.98E-02
AA - AB	6-9.5°C	28	21795	cerebral cortex cell migration	4.98E-02
AA - AB	6-9.5°C	28	50919	negative chemotaxis	4.98E-02
AA - BB	6-9.5°C	28	6843	mitochondrial citrate transport	8.94E-03
AA - BB	6-9.5°C	28	21824	cerebral cortex tangential migration using cell-axon interactions	8.94E-03
AA - BB	6-9.5°C	28	21828	gonadotrophin-releasing hormone neuronal migration to the hypothalamus	8.94E-03
AA - BB	6-9.5°C	28	21856	hypothalamic tangential migration using cell-axon interactions	8.94E-03
AA - BB	6-9.5°C	28	21886	hypothalamus gonadotrophin-releasing hormone neuron differentiation	8.94E-03
AA - BB	6-9.5°C	28	21888	hypothalamus gonadotrophin-releasing hormone neuron development	8.94E-03
AA - BB	6-9.5°C	28	21649	vestibulocochlear nerve structural organization	8.94E-03
AA - BB	6-9.5°C	28	21855	hypothalamus cell migration	9.62E-03
AA - BB	6-9.5°C	28	15746	citrate transport	9.62E-03
AA - BB	6-9.5°C	28	6842	tricarboxylic acid transport	9.62E-03
AA - BB	6-9.5°C	28	21979	hypothalamus cell differentiation	9.62E-03
AA - BB	6-9.5°C	28	21825	substrate-dependent cerebral cortex tangential migration	9.62E-03
AA - BB	6-9.5°C	28	21612	facial nerve structural organization	9.62E-03
AA - BB	6-9.5°C	28	21648	vestibulocochlear nerve morphogenesis	1.01E-02
AA - BB	6-9.5°C	28	21800	cerebral cortex tangential migration	1.01E-02
AA - BB	6-9.5°C	28	21561	facial nerve development	1.01E-02
AA - BB	6-9.5°C	28	21610	facial nerve morphogenesis	1.01E-02
AA - BB	6-9.5°C	28	21562	vestibulocochlear nerve development	1.04E-02
AA - BB	6-9.5°C	28	21604	cranial nerve structural organization	1.07E-02
AA - BB	6-9.5°C	28	21783	preganglionic parasympathetic nervous system development	1.34E-02
AA - BB	6-9.5°C	28	48846	axon extension involved in axon guidance	1.34E-02
AA - BB	6-9.5°C	28	48486	parasympathetic nervous system development	1.42E-02
AA - BB	6-9.5°C	28	48532	anatomical structure arrangement	1.56E-02
AA - BB	6-9.5°C	28	21854	hypothalamus development	1.68E-02
AA - BB	6-9.5°C	28	21884	forebrain neuron development	1.68E-02
AA - BB	6-9.5°C	28	3148	outflow tract septum morphogenesis	1.68E-02
AA - BB	6-9.5°C	28	21602	cranial nerve morphogenesis	1.91E-02
AA - BB	6-9.5°C	28	6929	substrate-bound cell migration	2.18E-02
AA - BB	6-9.5°C	28	48483	autonomic nervous system development	2.74E-02

Contrast	Temperature range	dph	GO-ID	Description	Corrected *P*-value
AA - BB	6-9.5°C	28	21879	forebrain neuron differentiation	2.74E-02
AA - BB	6-9.5°C	28	3151	outflow tract morphogenesis	2.74E-02
AA - BB	6-9.5°C	28	21795	cerebral cortex cell migration	2.74E-02
AA - BB	6-9.5°C	28	50919	negative chemotaxis	2.74E-02
AA - BB	6-9.5°C	28	48675	axon extension	2.98E-02
AA - BB	6-9.5°C	28	21545	cranial nerve development	3.04E-02
AA - BB	6-9.5°C	28	60411	cardiac septum morphogenesis	3.04E-02
AA - BB	6-9.5°C	28	22029	telencephalon cell migration	3.04E-02
AA - BB	6-9.5°C	28	21872	generation of neurons in the forebrain	3.04E-02
AA - BB	6-9.5°C	28	21885	forebrain cell migration	3.04E-02
AA - BB	6-9.5°C	28	21954	central nervous system neuron development	3.43E-02
AA - BB	6-9.5°C	28	48588	developmental cell growth	3.67E-02
AA - BB	6-9.5°C	28	15711	organic anion transport	3.67E-02
AA - BB	6-9.5°C	28	21675	nerve development	3.91E-02
AA - BB	6-9.5°C	28	16049	cell growth	4.09E-02
AA - BB	6-9.5°C	28	21536	diencephalon development	4.09E-02
AA - BB	6-9.5°C	28	3279	cardiac septum development	4.13E-02
AA - BB	6-9.5°C	28	21761	limbic system development	4.57E-02
AA - BB	6-9.5°C	28	21987	cerebral cortex development	4.73E-02
AA - BB	6-9.5°C	28	3206	cardiac chamber morphogenesis	4.73E-02
AA - BB	6-9.5°C	28	6839	mitochondrial transport	4.79E-02
LG07 effects					
AA - AB	6-13°C	14	34637	cellular carbohydrate biosynthetic process	3.05E-03
AA - AB	6-13°C	14	16143	S-glycoside metabolic process	3.05E-03
AA - AB	6-13°C	14	16144	S-glycoside biosynthetic process	3.05E-03
AA - AB	6-13°C	14	19757	glycosinolate metabolic process	3.05E-03
AA - AB	6-13°C	14	19758	glycosinolate biosynthetic process	3.05E-03
AA - AB	6-13°C	14	19760	glucosinolate metabolic process	3.05E-03
AA - AB	6-13°C	14	19761	glucosinolate biosynthetic process	3.05E-03
AA - AB	6-13°C	14	9751	response to salicylic acid stimulus	5.12E-03
AA - AB	6-13°C	14	16051	carbohydrate biosynthetic process	5.12E-03
AA - AB	6-13°C	14	16138	glycoside biosynthetic process	5.82E-03
AA - AB	6-13°C	14	9753	response to jasmonic acid stimulus	5.82E-03
AA - AB	6-13°C	14	2000001	regulation of DNA damage checkpoint	1.25E-02
AA - AB	6-13°C	14	42754	negative regulation of circadian rhythm	1.37E-02
AA - AB	6-13°C	14	6975	DNA damage induced protein phosphorylation	1.37E-02
AA - AB	6-13°C	14	30321	transepithelial chloride transport	1.71E-02
AA - AB	6-13°C	14	16137	glycoside metabolic process	1.73E-02
AA - AB	6-13°C	14	44262	cellular carbohydrate metabolic process	1.74E-02
AA - AB	6-13°C	14	70633	transepithelial transport	2.13E-02
AA - AB	6-13°C	14	43153	entrainment of circadian clock by photoperiod	2.22E-02
AA - AB	6-13°C	14	5975	carbohydrate metabolic process	2.22E-02
AA - AB	6-13°C	14	9648	photoperiodism	2.22E-02
AA - AB	6-13°C	14	9725	response to hormone stimulus	2.22E-02
AA - AB	6-13°C	14	71380	cellular response to prostaglandin E stimulus	2.22E-02
AA - AB	6-13°C	14	9649	entrainment of circadian clock	2.22E-02
AA - AB	6-13°C	14	71379	cellular response to prostaglandin	2.30E-02

Contrast	Temperature range	dph	GO-ID	Description	Corrected *P*-value
				stimulus	
AA - AB	6-13°C	14	34695	response to prostaglandin E stimulus	2.38E-02
AA - AB	6-13°C	14	45744	negative regulation of G-protein coupled receptor protein signaling pathway	2.56E-02
AA - AB	6-13°C	14	19915	lipid storage	2.56E-02
AA - AB	6-13°C	14	34694	response to prostaglandin stimulus	2.56E-02
AA - AB	6-13°C	14	33762	response to glucagon stimulus	2.56E-02
AA - AB	6-13°C	14	18298	protein-chromophore linkage	2.59E-02
AA - AB	6-13°C	14	9719	response to endogenous stimulus	2.59E-02
AA - AB	6-13°C	14	6094	gluconeogenesis	2.59E-02
AA - AB	6-13°C	14	31397	negative regulation of protein ubiquitination	2.95E-02
AA - AB	6-13°C	14	6090	pyruvate metabolic process	2.99E-02
AA - AB	6-13°C	14	19319	hexose biosynthetic process	3.26E-02
AA - AB	6-13°C	14	6821	chloride transport	3.34E-02
AA - AB	6-13°C	14	71396	cellular response to lipid	3.70E-02
AA - AB	6-13°C	14	32922	circadian regulation of gene expression	3.83E-02
AA - AB	6-13°C	14	46364	monosaccharide biosynthetic process	3.89E-02
LG12 effects					
AA - AB	6-9.5°C	21	154	rRNA modification	4.12E-02
AA - AB	6-9.5°C	28	6843	mitochondrial citrate transport	2.52E-03
AA - AB	6-9.5°C	28	15746	citrate transport	2.52E-03
AA - AB	6-9.5°C	28	6842	tricarboxylic acid transport	2.52E-03
AA - AB	6-9.5°C	28	15711	organic anion transport	2.67E-02
AA - AB	6-9.5°C	28	6839	mitochondrial transport	3.28E-02
AA - AB	6-9.5°C	28	6820	anion transport	3.28E-02
AA - AB	6-9.5°C	28	46942	carboxylic acid transport	3.30E-02
AA - AB	6-9.5°C	28	15849	organic acid transport	3.30E-02
AA - AB	6-13°C	2	6091	generation of precursor metabolites and energy	6.66E-12
AA - AB	6-13°C	2	6119	oxidative phosphorylation	1.67E-08
AA - AB	6-13°C	2	9165	nucleotide biosynthetic process	2.78E-07
AA - AB	6-13°C	2	34404	nucleobase, nucleoside and nucleotide biosynthetic process	4.33E-07
AA - AB	6-13°C	2	34654	nucleobase, nucleoside, nucleotide and nucleic acid biosynthetic process	4.33E-07
AA - AB	6-13°C	2	9142	nucleoside triphosphate biosynthetic process	4.33E-07
AA - AB	6-13°C	2	6754	ATP biosynthetic process	4.33E-07
AA - AB	6-13°C	2	45333	cellular respiration	4.33E-07
AA - AB	6-13°C	2	46034	ATP metabolic process	5.57E-07
AA - AB	6-13°C	2	6164	purine nucleotide biosynthetic process	6.31E-07
AA - AB	6-13°C	2	9152	purine ribonucleotide biosynthetic process	8.51E-07
AA - AB	6-13°C	2	15980	energy derivation by oxidation of organic compounds	1.18E-06
AA - AB	6-13°C	2	9145	purine nucleoside triphosphate biosynthetic process	1.23E-06
AA - AB	6-13°C	2	9206	purine ribonucleoside triphosphate biosynthetic process	1.23E-06
AA - AB	6-13°C	2	15985	energy coupled proton transport, down	1.50E-06

Contrast	Temperature range	dph	GO-ID	Description	Corrected *P*-value
				electrochemical gradient	
AA - AB	6-13°C	2	15986	ATP synthesis coupled proton transport	1.50E-06
AA - AB	6-13°C	2	9150	purine ribonucleotide metabolic process	1.50E-06
AA - AB	6-13°C	2	9260	ribonucleotide biosynthetic process	1.67E-06
AA - AB	6-13°C	2	9201	ribonucleoside triphosphate biosynthetic process	2.43E-06
AA - AB	6-13°C	2	9259	ribonucleotide metabolic process	2.97E-06
AA - AB	6-13°C	2	9205	purine ribonucleoside triphosphate metabolic process	3.20E-06
AA - AB	6-13°C	2	9199	ribonucleoside triphosphate metabolic process	5.26E-06
AA - AB	6-13°C	2	6163	purine nucleotide metabolic process	5.41E-06
AA - AB	6-13°C	2	9144	purine nucleoside triphosphate metabolic process	5.41E-06
AA - AB	6-13°C	2	55086	nucleobase, nucleoside and nucleotide metabolic process	1.10E-05
AA - AB	6-13°C	2	44281	small molecule metabolic process	1.30E-05
AA - AB	6-13°C	2	9141	nucleoside triphosphate metabolic process	1.51E-05
AA - AB	6-13°C	2	6818	hydrogen transport	1.73E-05
AA - AB	6-13°C	2	15992	proton transport	1.73E-05
AA - AB	6-13°C	2	6753	nucleoside phosphate metabolic process	2.04E-05
AA - AB	6-13°C	2	9117	nucleotide metabolic process	2.04E-05
AA - AB	6-13°C	2	22904	respiratory electron transport chain	2.59E-05
AA - AB	6-13°C	2	55114	oxidation reduction	3.52E-05
AA - AB	6-13°C	2	22900	electron transport chain	3.85E-05
AA - AB	6-13°C	2	44271	cellular nitrogen compound biosynthetic process	4.00E-05
AA - AB	6-13°C	2	46483	heterocycle metabolic process	8.95E-05
AA - AB	6-13°C	2	42775	mitochondrial ATP synthesis coupled electron transport	1.60E-04
AA - AB	6-13°C	2	42773	ATP synthesis coupled electron transport	2.16E-04
AA - AB	6-13°C	2	44283	small molecule biosynthetic process	2.36E-04
AA - AB	6-13°C	2	45214	sarcomere organization	1.59E-03
AA - AB	6-13°C	2	71688	striated muscle myosin thick filament assembly	2.14E-03
AA - AB	6-13°C	2	31033	myosin filament assembly or disassembly	2.24E-03
AA - AB	6-13°C	2	31034	myosin filament assembly	2.24E-03
AA - AB	6-13°C	2	16310	phosphorylation	2.24E-03
AA - AB	6-13°C	2	6732	coenzyme metabolic process	6.32E-03
AA - AB	6-13°C	2	6099	tricarboxylic acid cycle	7.03E-03
AA - AB	6-13°C	2	46356	acetyl-CoA catabolic process	7.40E-03
AA - AB	6-13°C	2	30239	myofibril assembly	9.13E-03
AA - AB	6-13°C	2	6793	phosphorus metabolic process	1.09E-02
AA - AB	6-13°C	2	6796	phosphate metabolic process	1.09E-02
AA - AB	6-13°C	2	9109	coenzyme catabolic process	1.89E-02
AA - AB	6-13°C	2	51186	cofactor metabolic process	1.89E-02
AA - AB	6-13°C	2	9060	aerobic respiration	1.89E-02
AA - AB	6-13°C	2	6084	acetyl-CoA metabolic process	1.89E-02
AA - AB	6-13°C	2	55002	striated muscle cell development	1.89E-02

Contrast	Temperature range	dph	GO-ID	Description	Corrected *P*-value
AA - AB	6-13°C	2	15672	monovalent inorganic cation transport	1.97E-02
AA - AB	6-13°C	2	44237	cellular metabolic process	2.00E-02
AA - AB	6-13°C	2	6120	mitochondrial electron transport, NADH to ubiquinone	2.01E-02
AA - AB	6-13°C	2	51187	cofactor catabolic process	2.19E-02
AA - AB	6-13°C	2	34982	mitochondrial protein processing	2.22E-02
AA - AB	6-13°C	2	31032	actomyosin structure organization	2.61E-02
AA - AB	6-13°C	2	46688	response to copper ion	2.72E-02
AA - AB	6-13°C	2	6839	mitochondrial transport	2.72E-02
AA - AB	6-13°C	2	10927	cellular component assembly involved in morphogenesis	3.68E-02
AA - AB	6-13°C	2	55001	muscle cell development	3.82E-02
AA - AB	6-13°C	2	390	spliceosome disassembly	4.93E-02
AA - AB	6-13°C	2	35378	carbon dioxide transmembrane transport	4.93E-02
AA - AB	6-13°C	2	6747	FAD biosynthetic process	4.93E-02
AA - AB	6-13°C	2	85018	maintenance of symbiont-containing vacuole via substance secreted by host	4.93E-02
AA - AB	6-13°C	2	46443	FAD metabolic process	4.93E-02
AA - AB	6-13°C	2	71288	cellular response to mercury ion	4.93E-02
AA - AB	6-13°C	2	46878	positive regulation of saliva secretion	4.93E-02
AA - AB	6-13°C	2	51068	dihydrolipoamide metabolic process	4.93E-02
AA - AB	6-13°C	2	34220	ion transmembrane transport	4.96E-02
AA - AB	6-13°C	28	6843	mitochondrial citrate transport	1.36E-02
AA - AB	6-13°C	28	15746	citrate transport	1.36E-02
AA - AB	6-13°C	28	6842	tricarboxylic acid transport	1.36E-02

Table S10: Results of a linear mixed effects model for growth of larval Atlantic cod from Risør fjord of pure fjord ecotype from 2 to 28 dph. Asterisks denote significance at α=0.05.

Model term	χ2	d.f.	*P*-value	
location	2.93	2	0.23	
LG02	0.34	1	0.56	
LG07	0.11	1	0.736	
LG12	0.15	1	0.700	
dph	84.09	3	<0.001	*
temperature	0.31	2	0.857	
location×dph	3.89	6	0.691	
LG02×dph	5.55	3	0.136	
LG07×dph	7.15	3	0.067	
LG12×dph	5.60	3	0.133	
temperature×dph	6.26	6	0.395	
location×dph×temperature	22.79	16	0.119	
LG02×dph×temperature	7.01	8	0.535	
LG07×dph×temperature	7.11	8	0.525	
LG12×dph×temperature	16.17	8	0.040	*

Model term	Variance	SD
father	0.04	0.21
mother	<0.001	0.02
residual	0.29	0.54

Table S11: Results of a linear mixed effects model for growth of larval Atlantic cod from a cross between outer Risør mothers and inner Risør fathers (O×I) from 2 to 28 dph. Asterisks denote significance at α=0.05.

Model term	$\chi 2$	d.f.	*P*-value	
ecotype	2.72	1	0.099	
LG02	4.84	1	0.028	*
LG07	0.07	1	0.798	
LG12	1.40	1	0.237	
dph	11.95	3	0.008	*
temperature	0.12	2	0.940	
ecotype×dph	0.62	3	0.892	
LG02×dph	6.65	3	0.084	
LG07×dph	3.24	3	0.356	
LG12×dph	2.30	2	0.317	
temperature×dph	17.41	6	0.008	*
ecotype×dph×temperature	4.83	8	0.776	
LG02×dph×temperature	5.09	8	0.748	
LG07×dph×temperature	4.96	7	0.665	
LG12×dph×temperature	0.01	1	0.912	

Model term	Variance	SD
father	0.00	0.00
mother	0.00	0.00
residual	0.31	0.55

Table S12: Results of a linear mixed effects model for growth of larval Atlantic cod from inner Risør fjord of pure fjord ecotype from 2 to 28 dph. Asterisks denote significance at α=0.05.

Model term	$\chi 2$	d.f.	*P*-value	
LG02	1.87	1	0.172	
LG07	2.82	1	0.093	
LG12	0.20	1	0.651	
dph	26.85	3	<0.001	*
temperature	13.13	2	0.001	*
LG02×dph	10.85	3	0.013	*
LG07×dph	4.19	2	0.123	
LG12×dph	8.59	3	0.035	*
temperature×dph	7.23	6	0.300	
LG02×dph×temperature	17.45	7	0.015	*
LG07×dph×temperature	0.03	1	0.872	
LG12×dph×temperature	55.49	7	<0.001	*

Model term	Variance	SD
father	0.20	0.45
mother	0.78	0.88
residual	0.07	0.26

D.3 Supplementary Figures

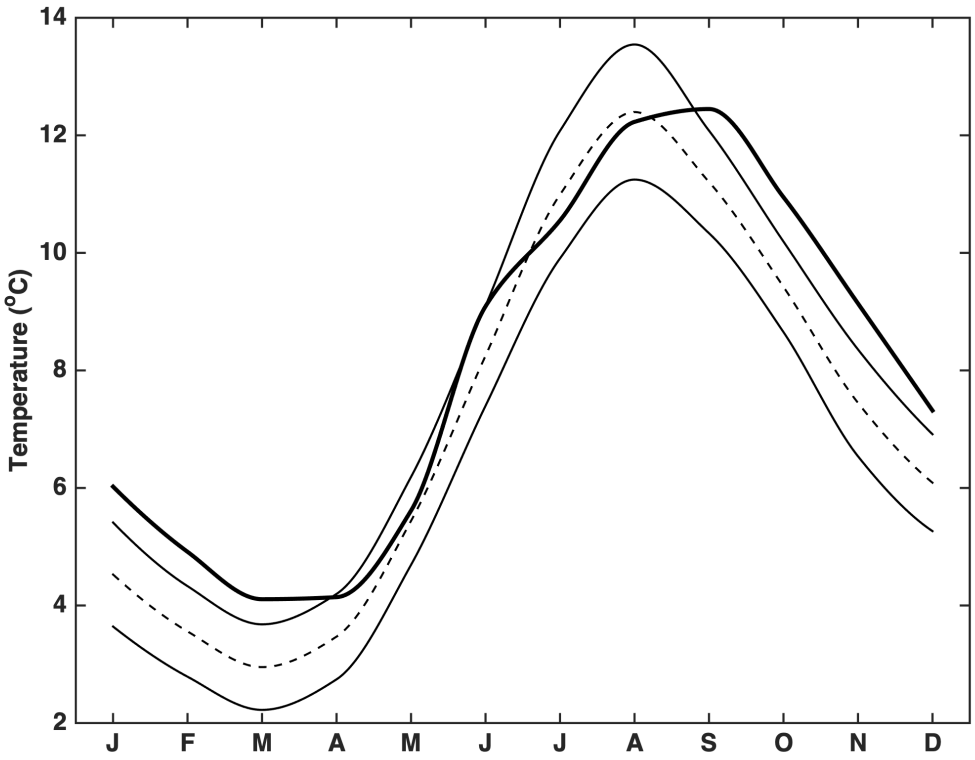

Figure S1: Temperature at 10 m depth in the coastal Norwegian Sea. Thin dashed and solid lines represent historical (1981-2010) means and standard deviations. The thick solid line represents climatological means for 2015. Data were obtained from the Skrova fixed hydrographical station of the Institute of Marine Research (available at http://www.imr.no/forskning/forskningsdata/stasjoner/view?station).

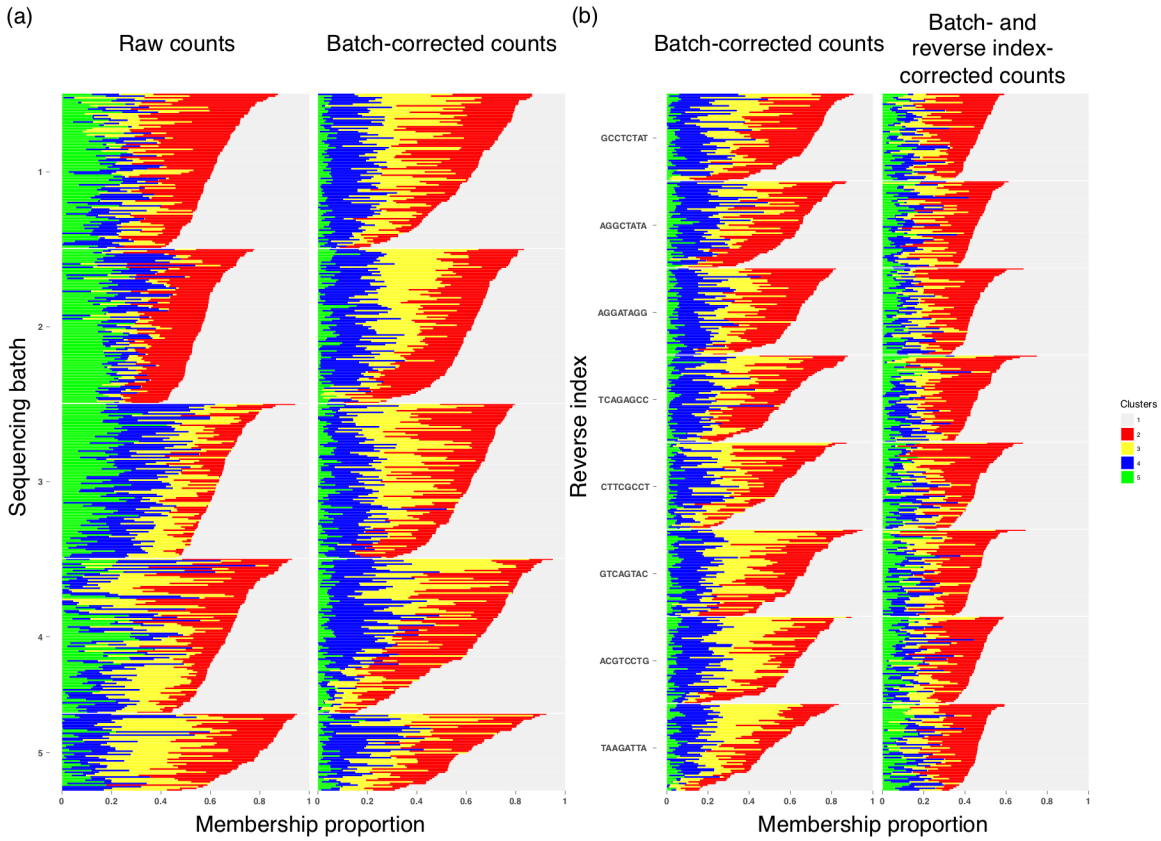

Figure S2: Grade of membership model proportions for Risør and Helgeland reference-based transcriptomes illustrating the BatchCorrectedCounts() adjustment for (a) batch effects and (b) reverse sequencing index effects with K=5.

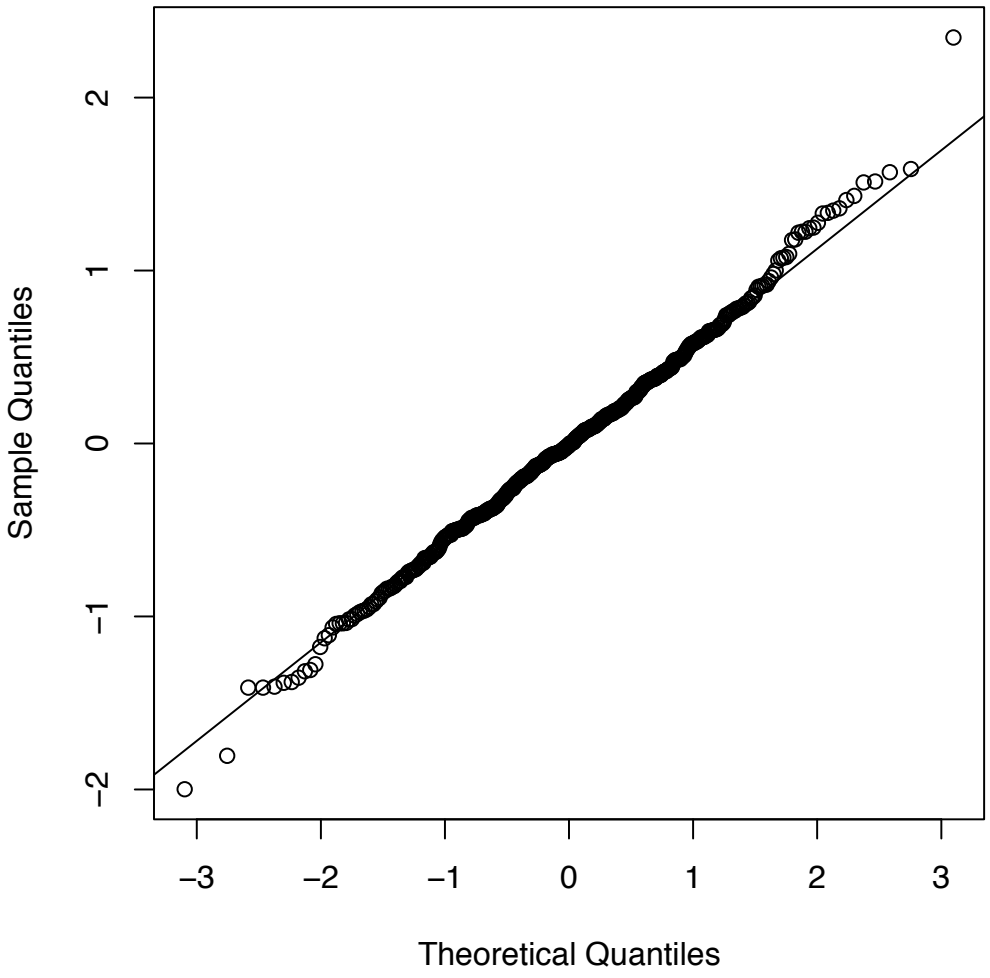

Figure S3: Q-Q norm plot of the residuals from the linear model used in the length-at-day reaction norm analysis of all larvae.

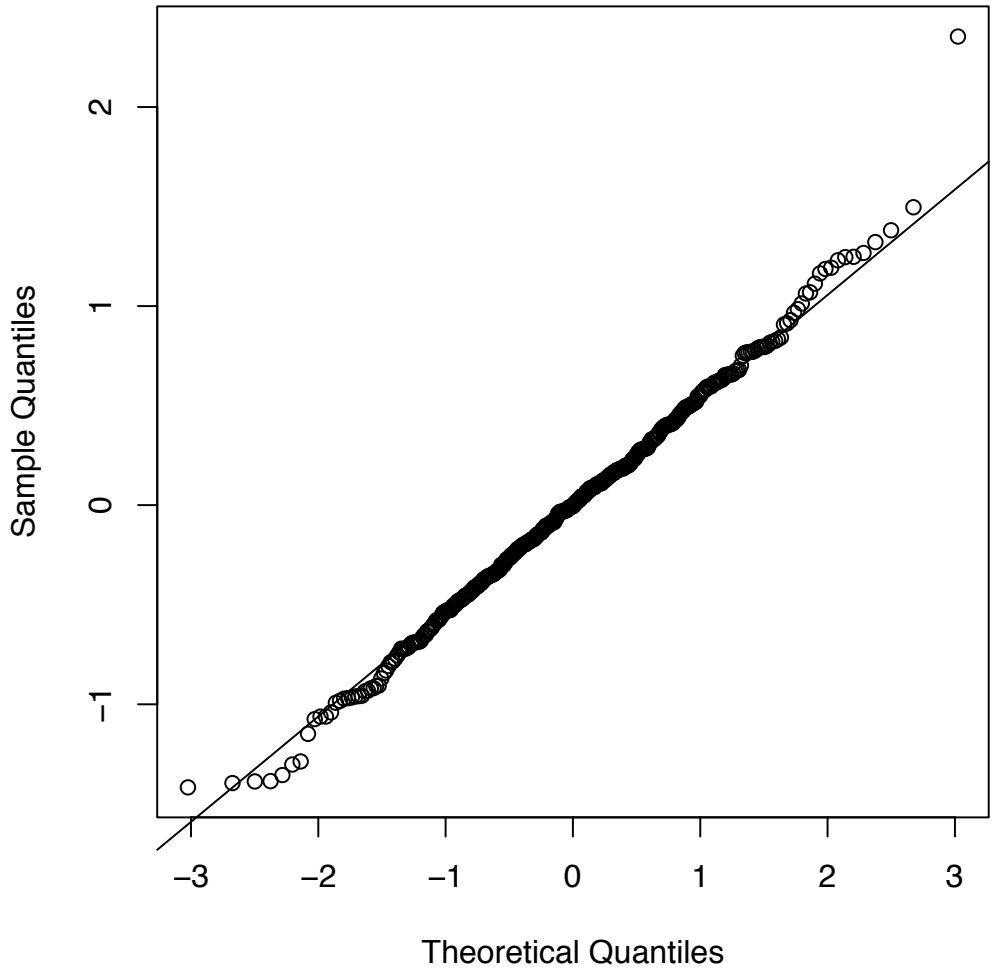

Figure S4: Q-Q norm plot of the residuals from the linear model used in the length-at-day reaction norm analysis of all larvae for which parentage information was available.

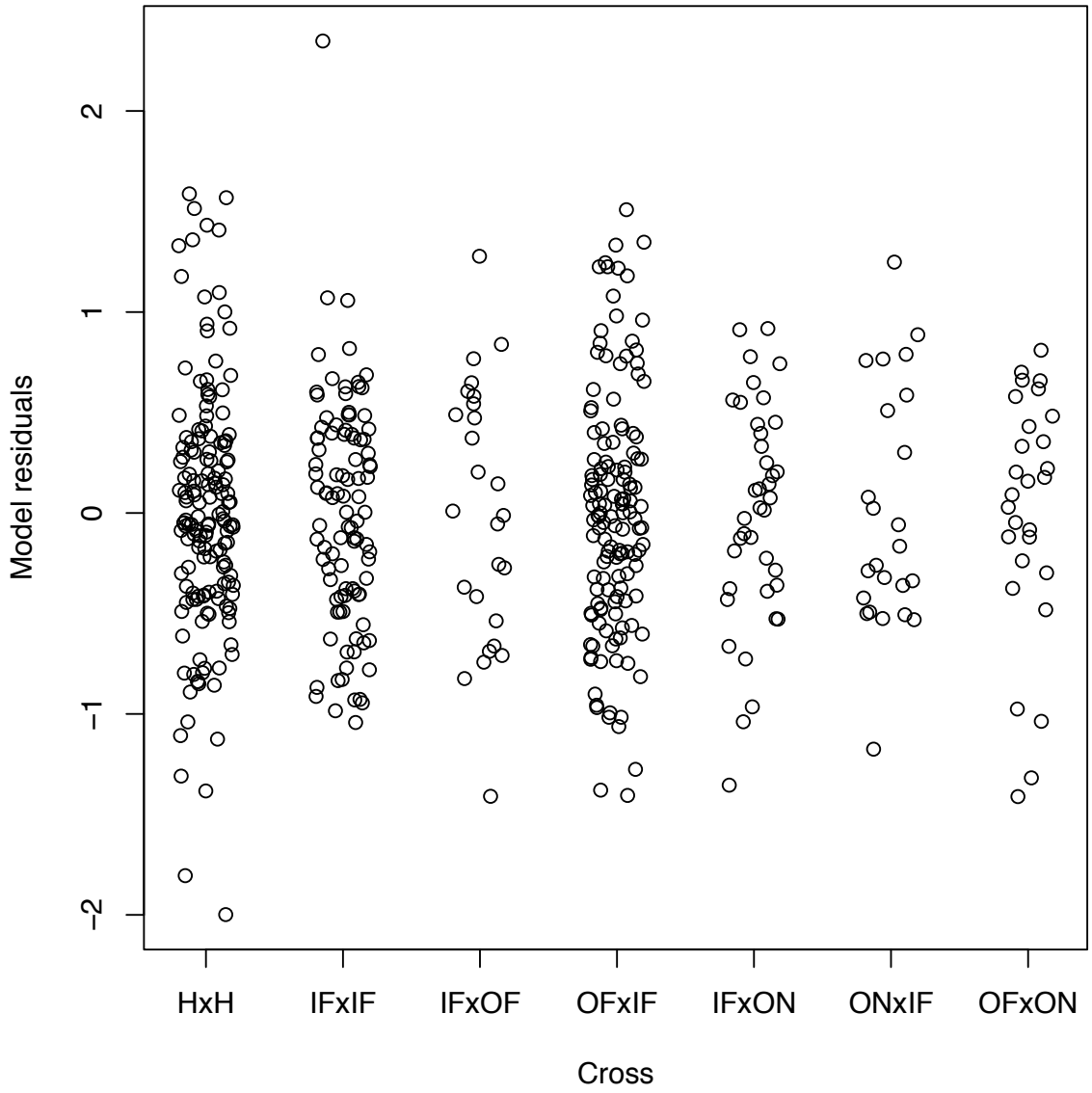

Figure S5: Linear model residuals for each cross in the length-at-day reaction norm analysis of all larvae.

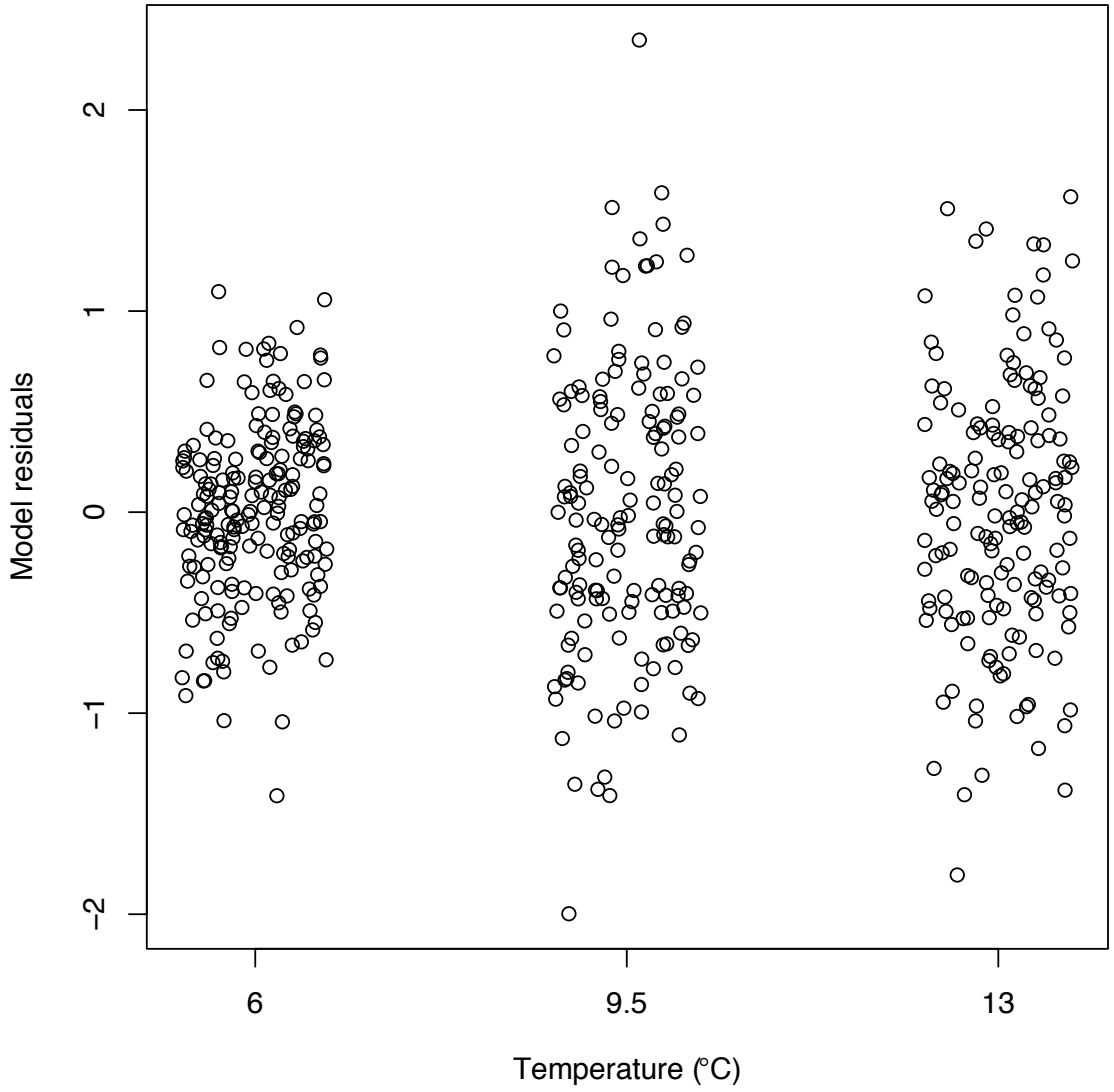

Figure S6: Linear model residuals for each temperature in the length-at-day reaction norm analysis of all larvae.

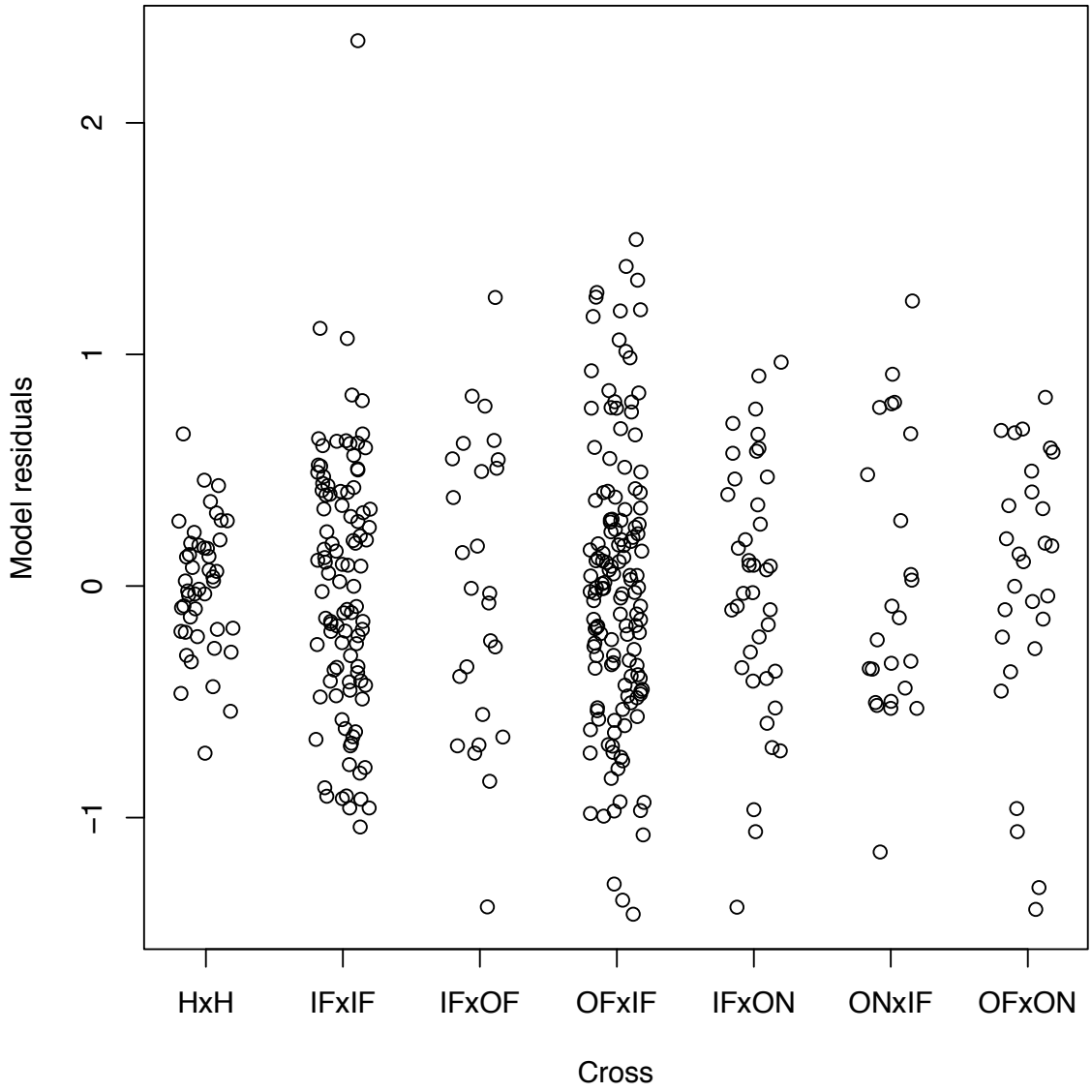

Figure S7: Linear model residuals for each cross in the length-at-day reaction norm analysis of all larvae for which parentage information was available.

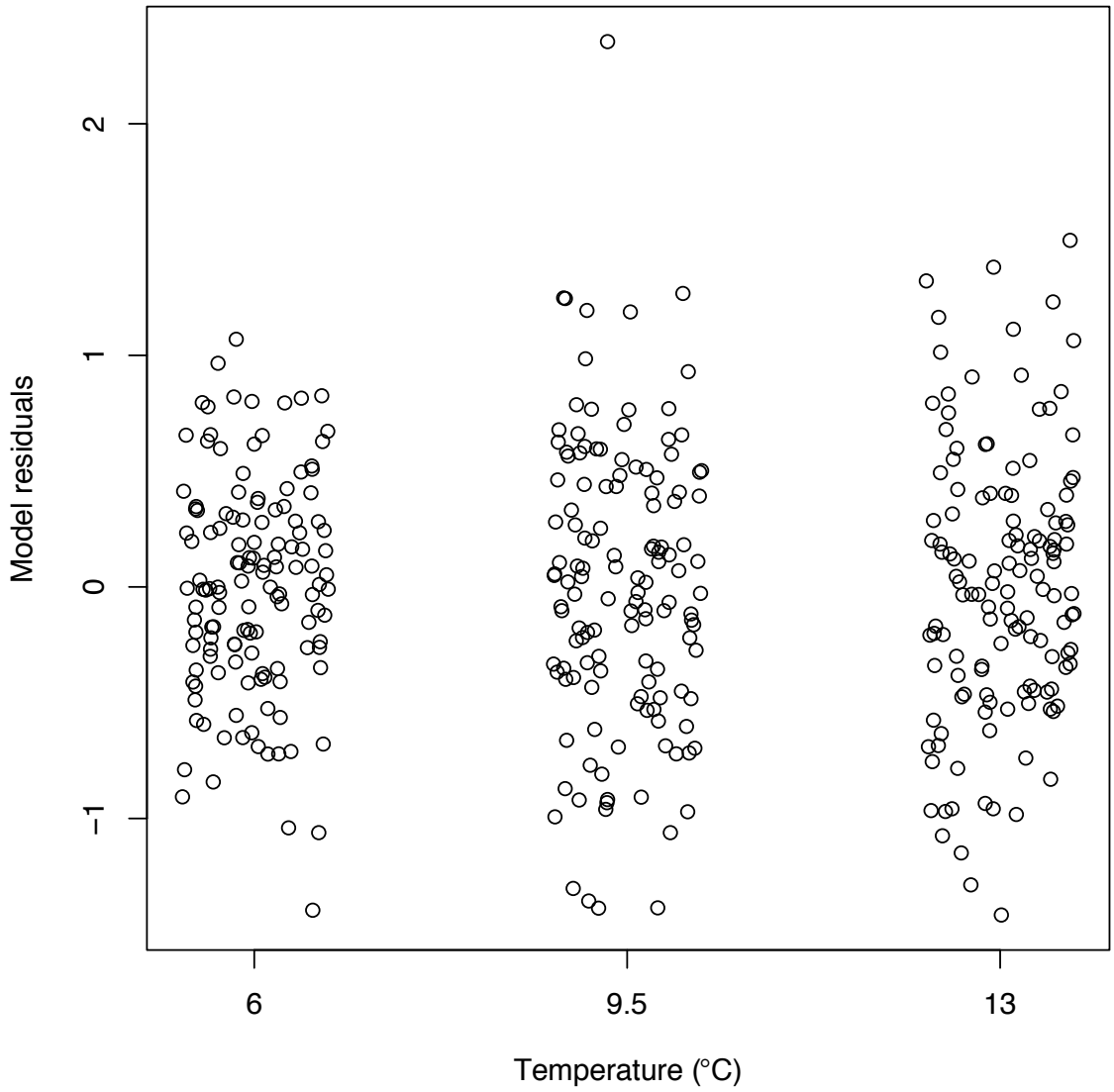

Figure S8: Linear model residuals for each temperature in the length-at-day reaction norm analysis of all larvae for which parentage information was available.

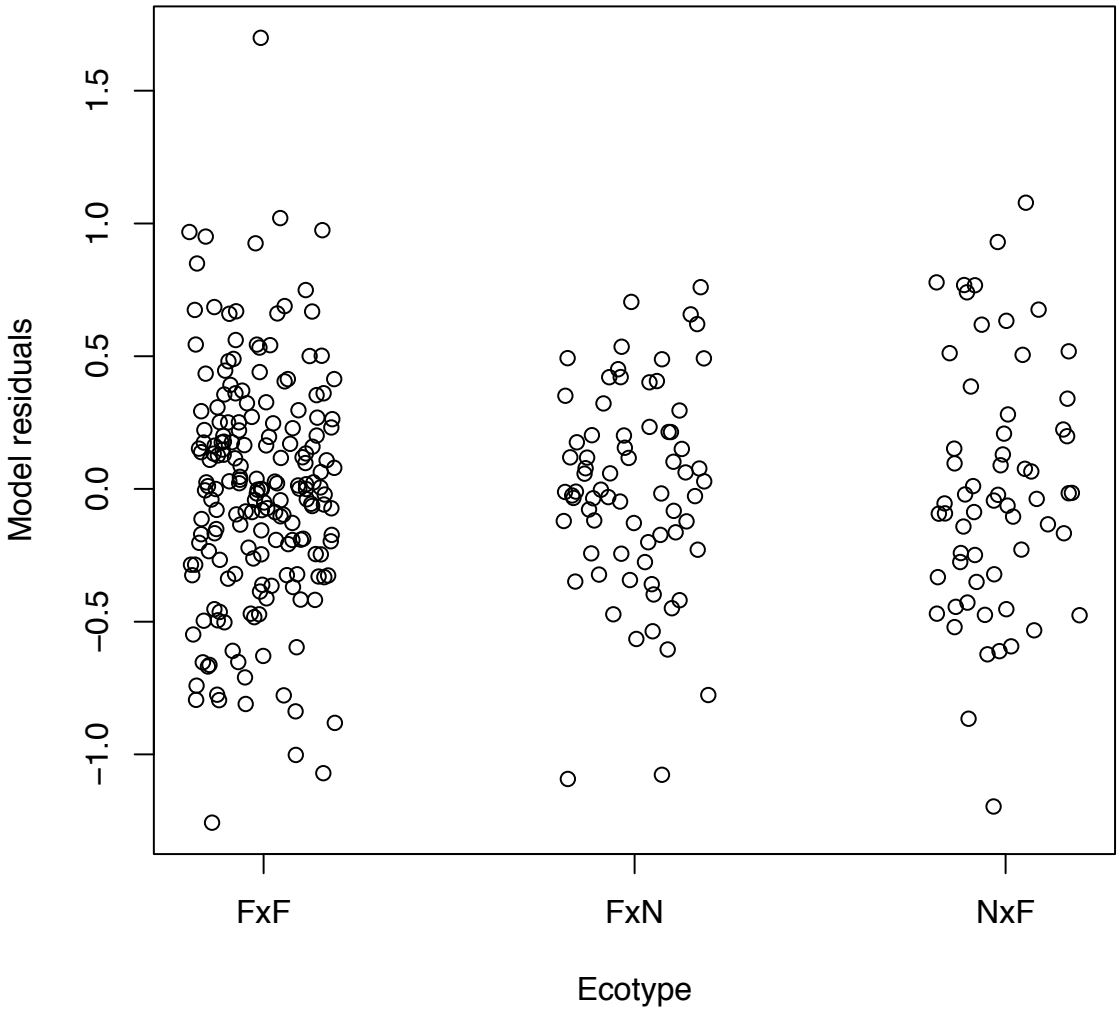

Figure S9: Linear model residuals for each ecotype in the microgeographic scale length-at-day reaction norm analysis for all dph combined.

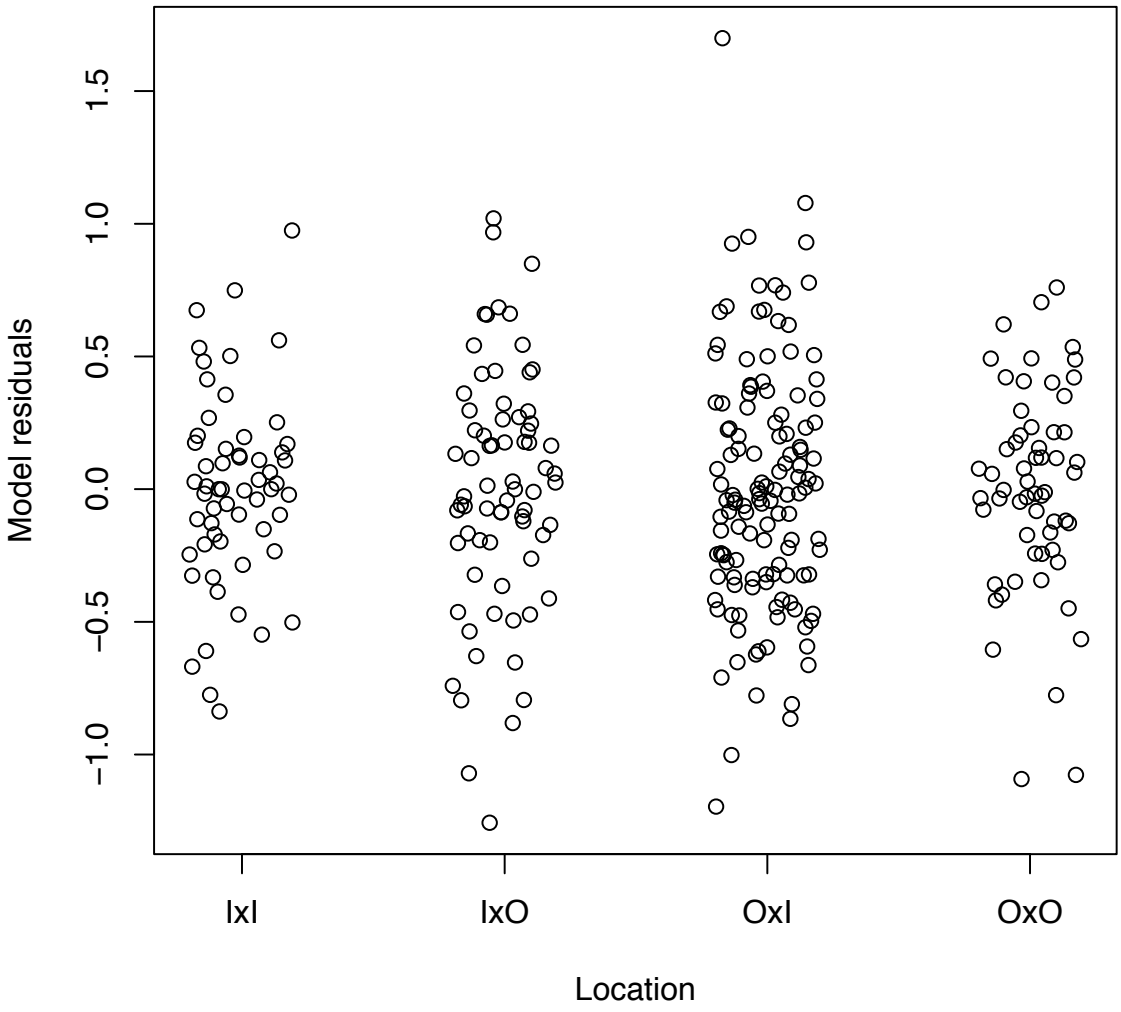

Figure S10: Linear model residuals for each location in the microgeographic scale length-at-day reaction norm analysis for all dph combined.

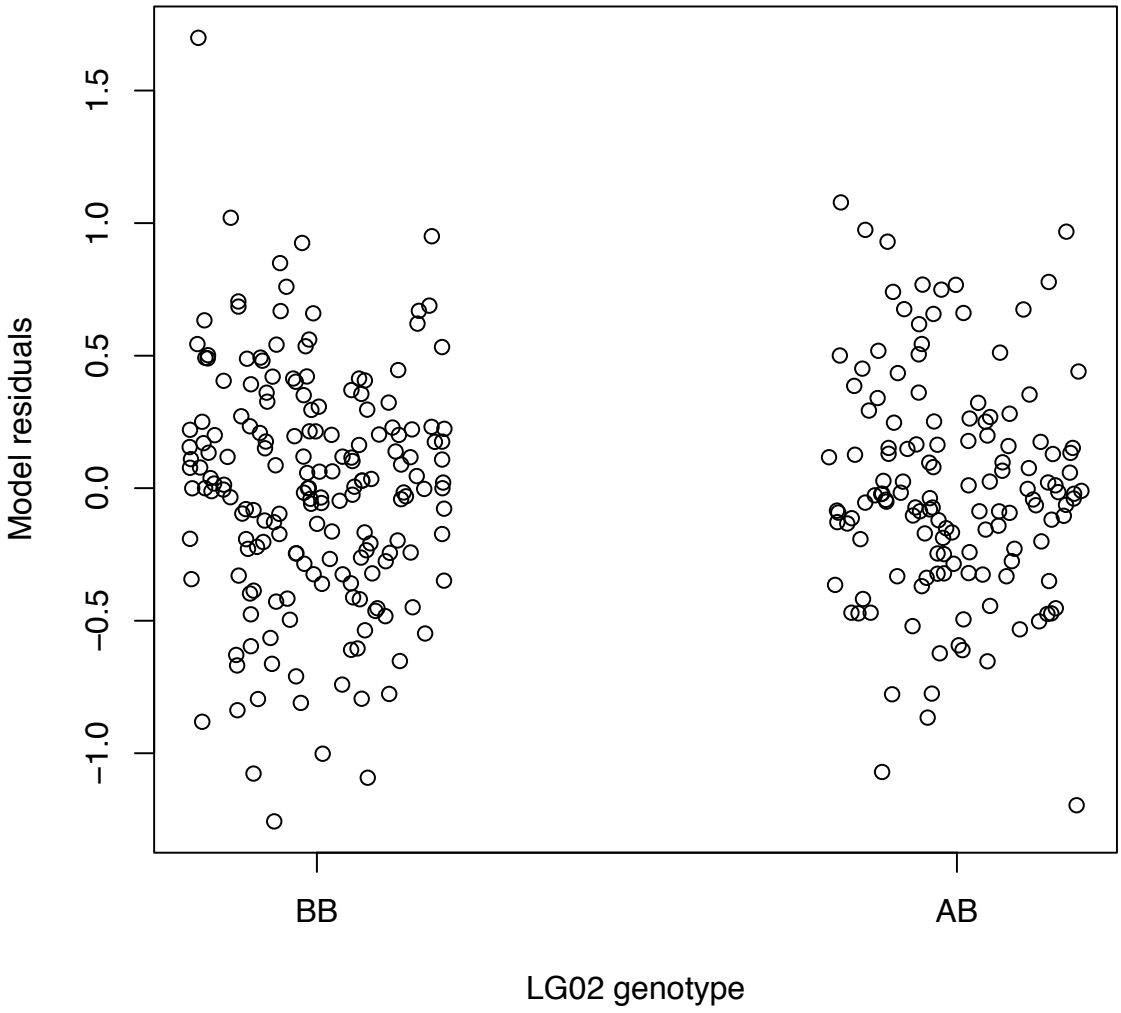

Figure S11: Linear model residuals for each LG02 genotype in the microgeographic scale length-at-day reaction norm analysis for all dph combined.

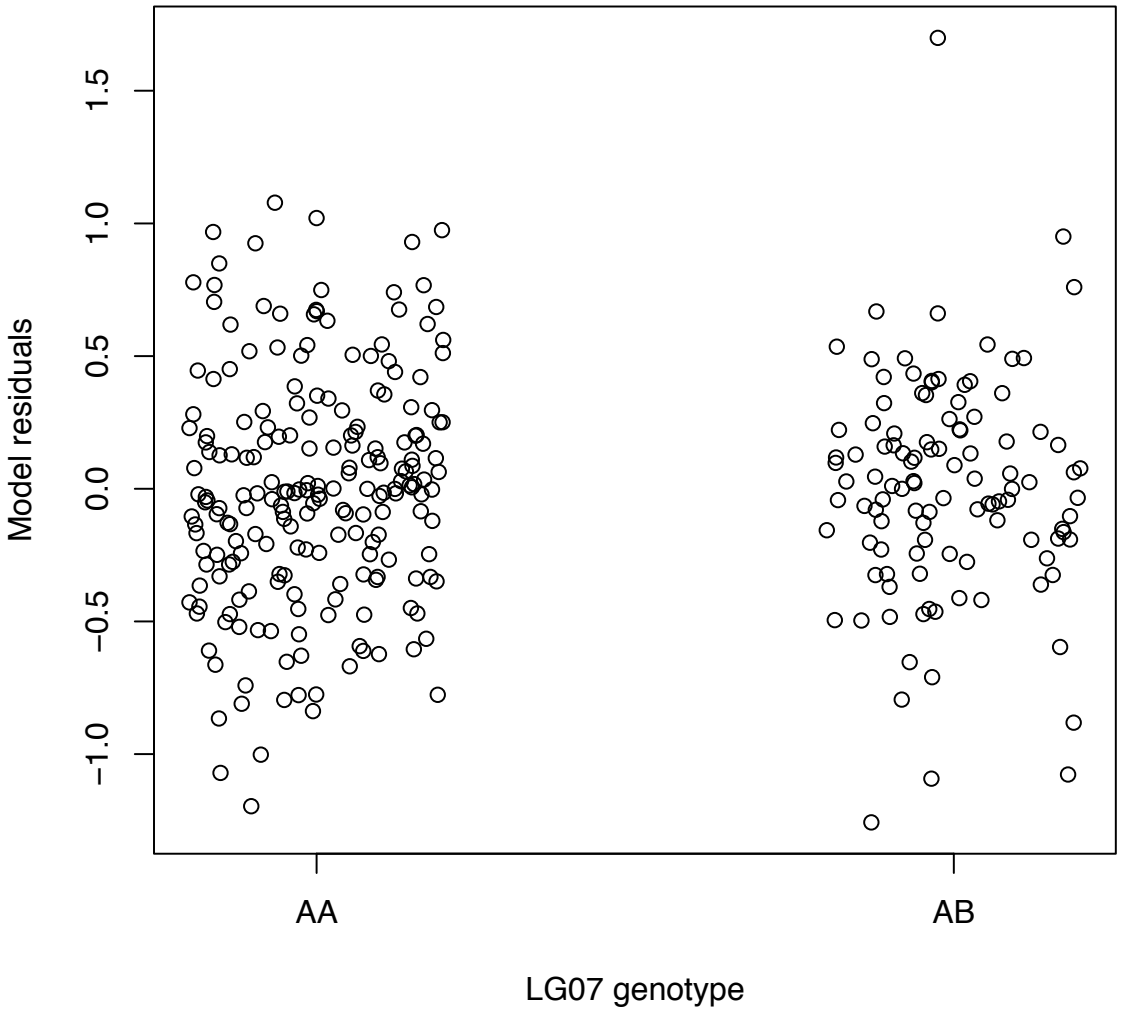

Figure S12: Linear model residuals for each LG07 genotype in the microgeographic scale length-at-day reaction norm analysis for all dph combined.

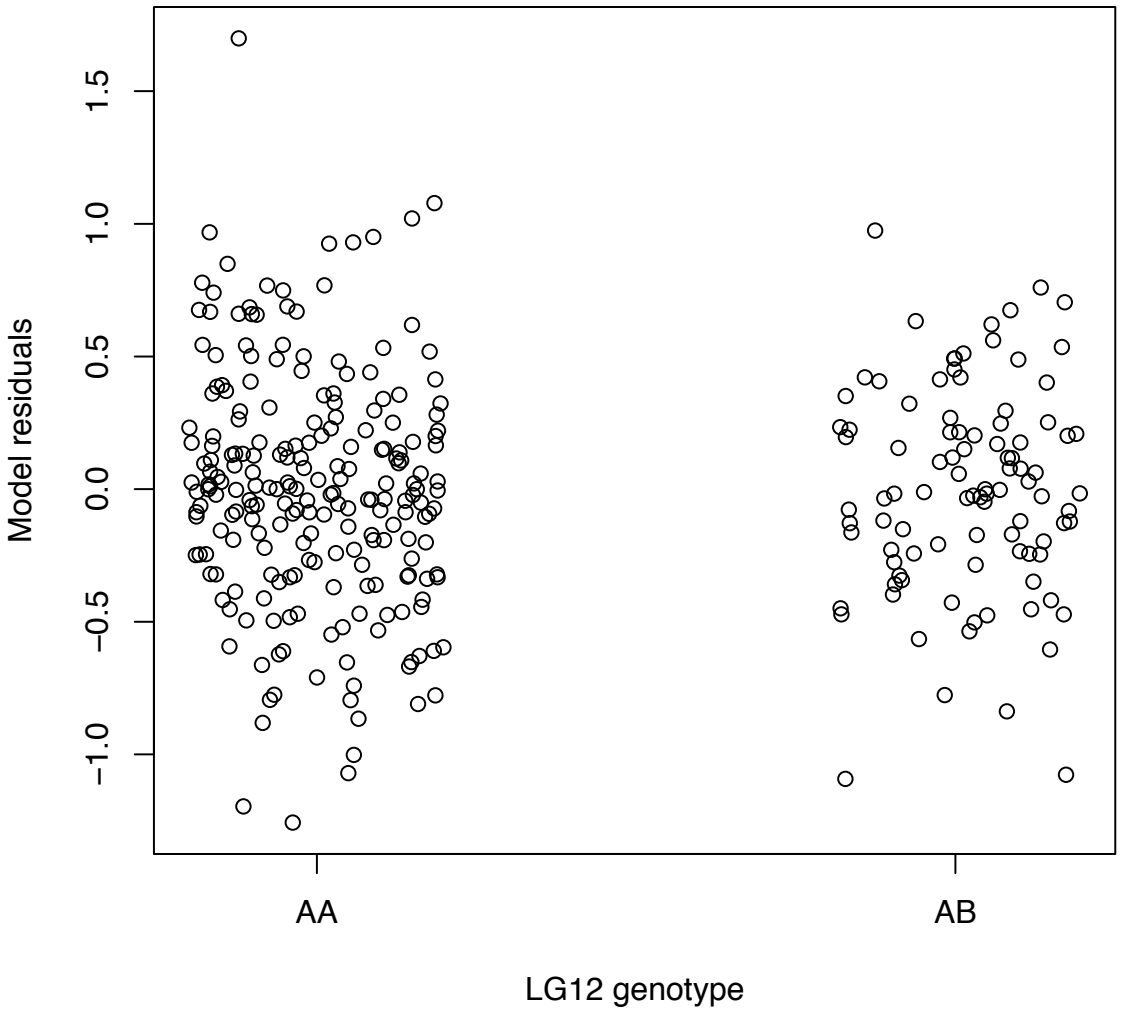

Figure S13: Linear model residuals for each LG12 genotype in the microgeographic scale length-at-day reaction norm analysis for all dph combined.

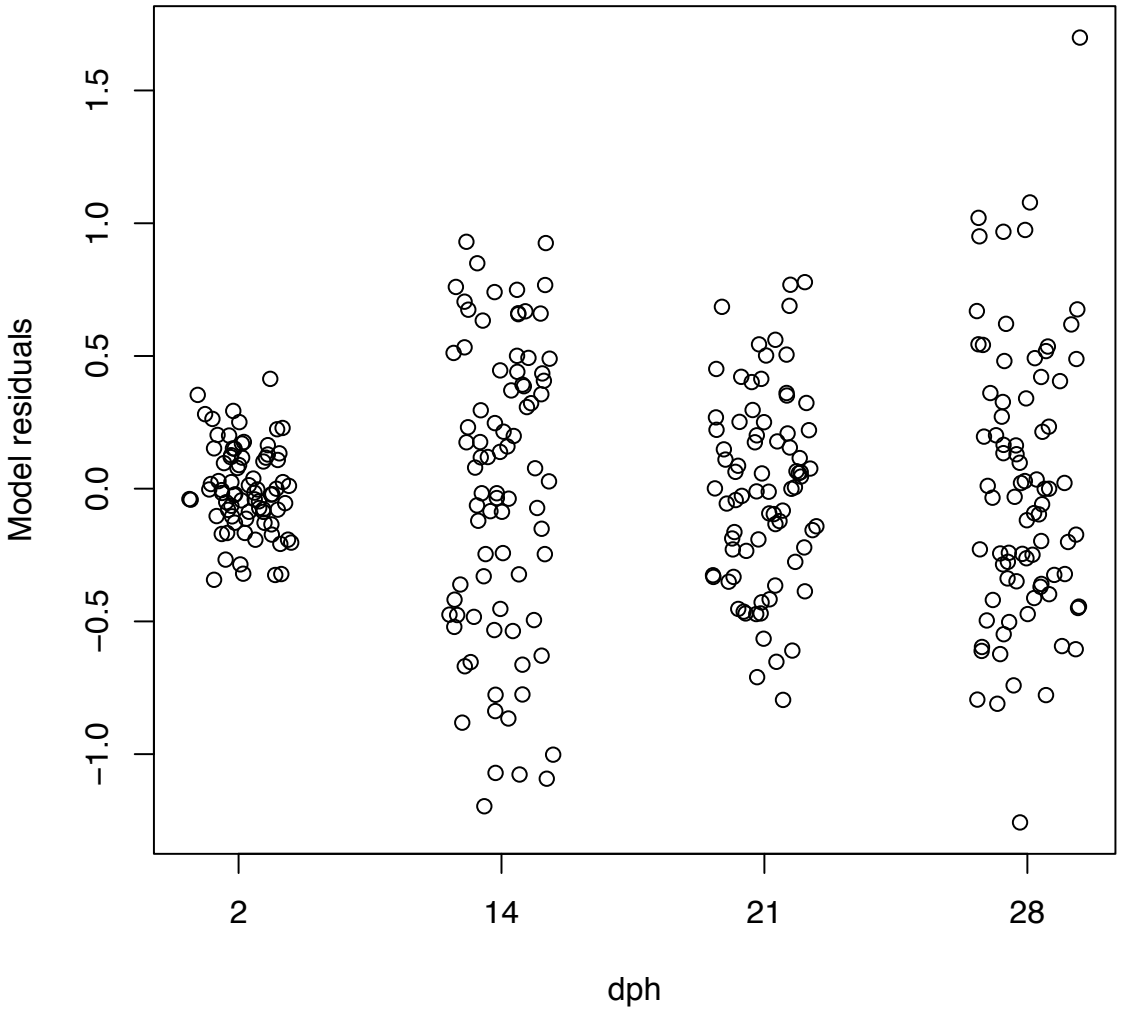

Figure S14: Linear model residuals for each day post hatch in the microgeographic scale length-at-day reaction norm analysis for all dph combined.

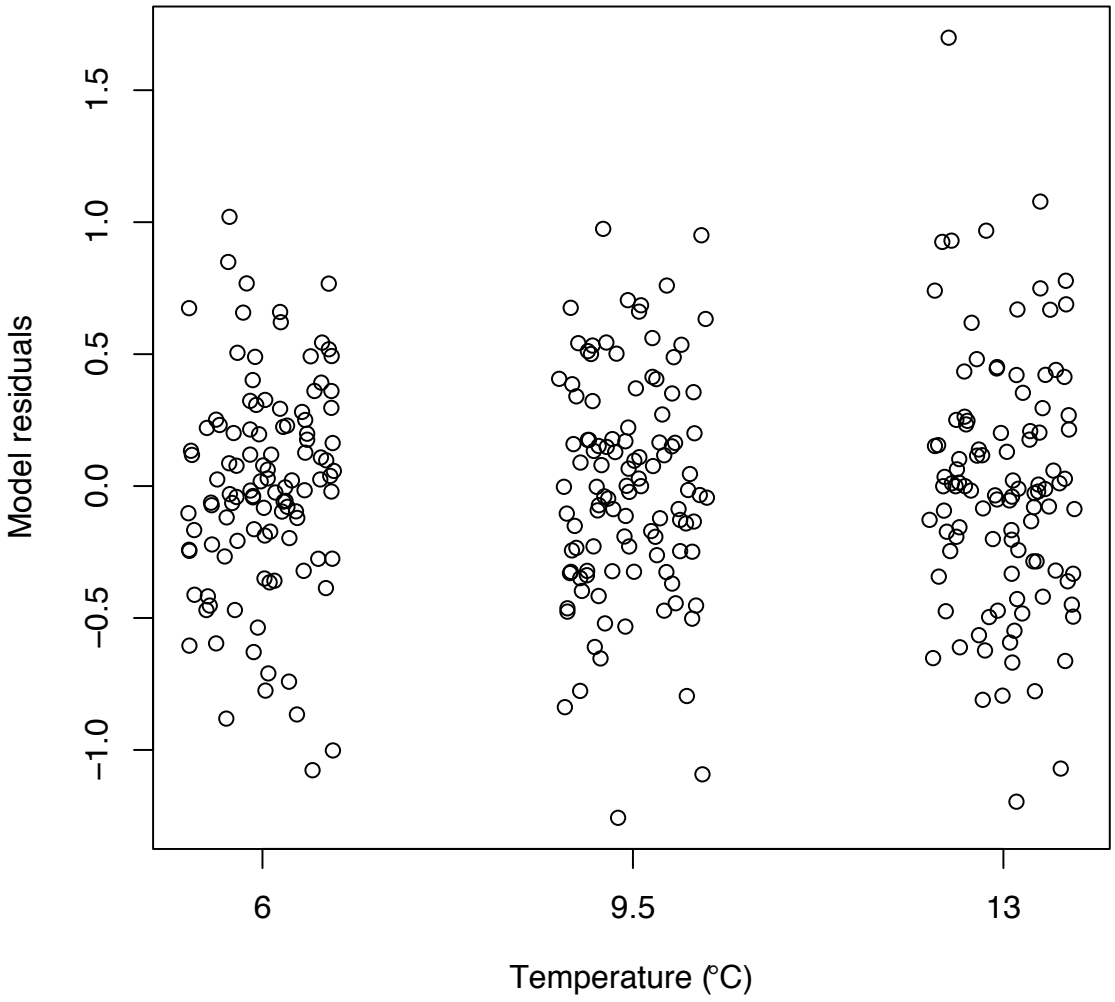

Figure S15: Linear model residuals for each temperature in the microgeographic scale length-at-day reaction norm analysis for all dph combined.

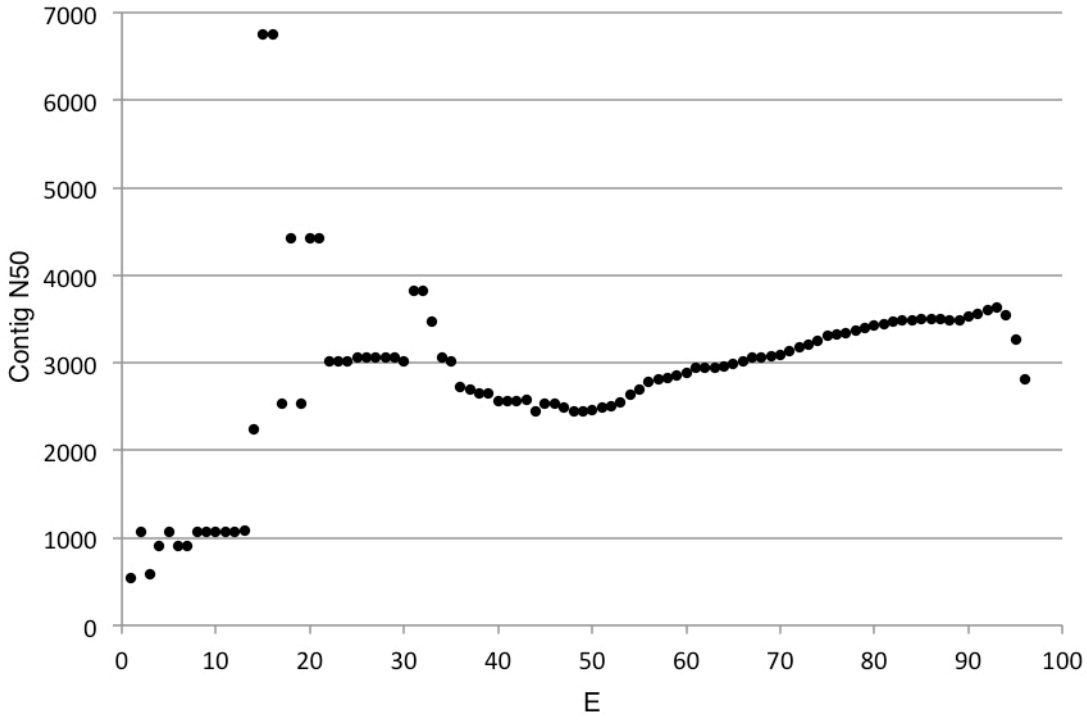

Figure S16: The minimum length of contig in which 50% of all assembled bases are contained (Contig N50) as a function of the percentage of total normalized expression data represented by the most highly expressed trancripts (E) in the *de novo* transcriptome assembled using Trinity and refined using PASA.

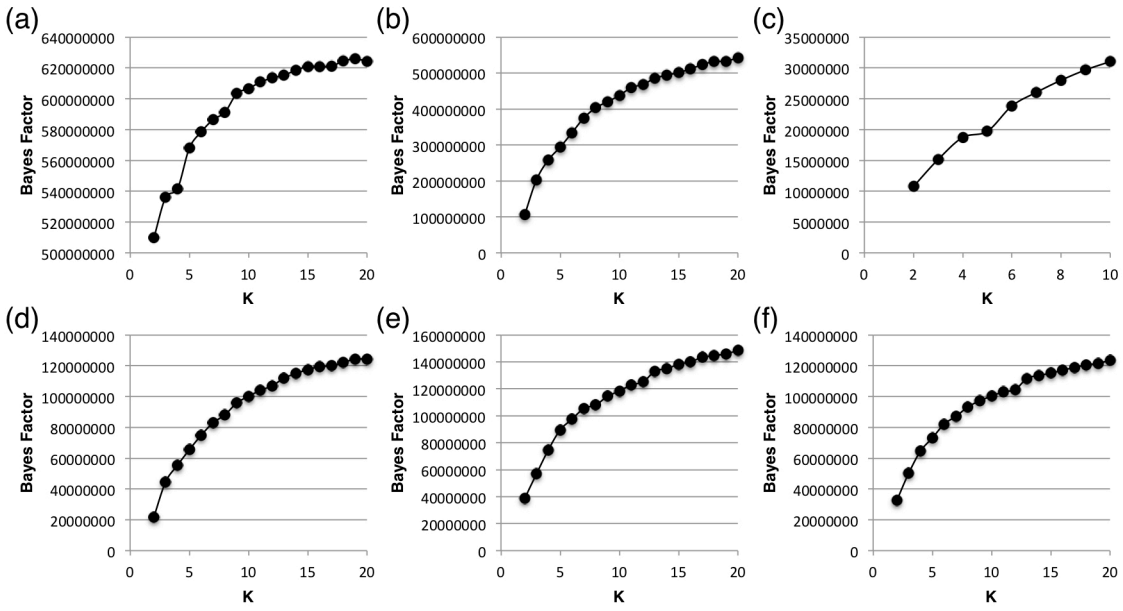

Figure S17: K-plots of the number of clusters, K, and grade of membership model Bayes Factors. (a) *de novo* analysis of all samples (b) reference-based analysis of batch- and index- corrected Risør and Helgeland samples (c) 0 dph, (d) 2 dph, (e) 14 dph, and (f) 28 dph.

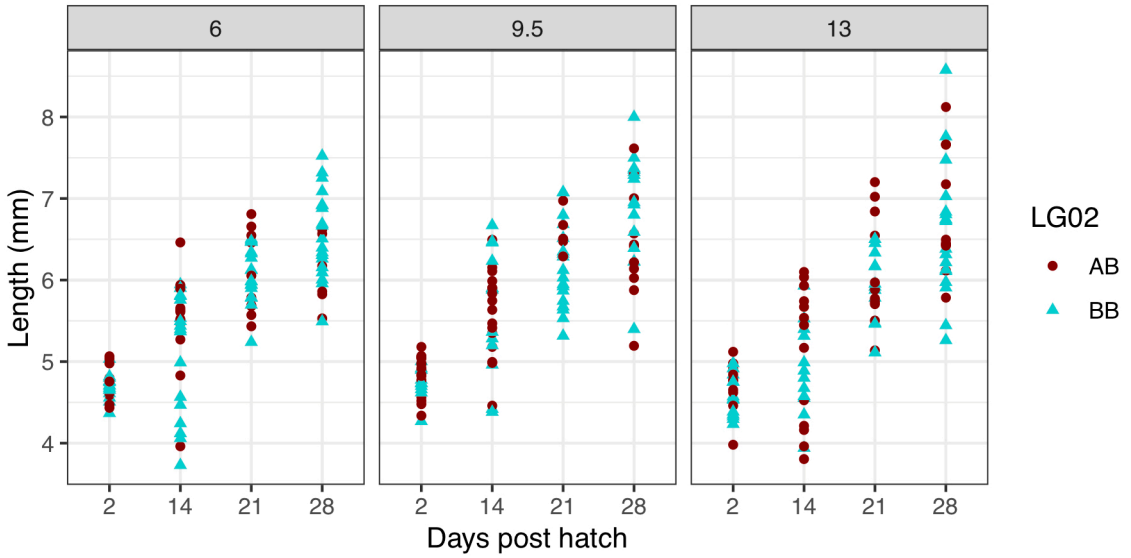

Figure S18: Individual lengths-at-day for Risør larvae possessing different LG02 genotypes at 6, 9.5, and 13°C.

D.4 List of Supplementary Data Files

All files located at: https://github.com/rebekahoomen/PhD-thesis

Data S1: Enriched gene ontology terms based on genes differentially expressed between Helgeland and Skagerrak.

<D_Data_S1_ClueGO_region_DE.xlsx>

Data S2: Enriched gene ontology terms based on genes differentially plastic in response to temperature between Helgeland and Skagerrak.

<D_Data_S2_ ClueGO_region_DP.xlsx>

References

Abele D (2012) Temperature adaptation in changing climate: marine fish and invertebrates. In: *Temperature adaptation in a changing climate: nature at risk* (eds Storey KB, Tanino S, Tanino KK), pp. 67–79. Centre for Agriculture and Biosciences International, Wallingford, UK.

Abele D, Puntarulo S (2004) Formation of reactive species and induction of antioxidant defence systems in polar and temperate marine invertebrates and fish. *Comparative Biochemistry and Physiology - A Molecular and Integrative Physiology*, **138**, 405–415.

Abràmoff MD, Magalhães PJ, Ram SJ (2004) Image Processing with ImageJ. *Biophotonics International*, **11**, 36–42.

Aeschbacher S, Bürger R (2014) The effect of linkage on establishment and survival of locally beneficial mutations. *Genetics*, **197**, 317–336.

Aird D, Ross MG, Chen W-S *et al.* (2011) Analyzing and minimizing PCR amplification bias in Illumina sequencing libraries. *Genome Biology*, **12**, R18.

Aitken SN, Yeaman S, Holliday JA, Wang T, Curtis-McLane S (2008) Adaptation, migration or extirpation: climate change outcomes for tree populations. *Evolutionary Applications*, **1**, 95–111.

Akbarzadeh A, Günther OP, Houde AL *et al.* (2018) Developing specific molecular biomarkers for thermal stress in salmonids. *BMC Genomics*.

Akerman A, Bürger R (2014) The consequences of gene flow for local adaptation and differentiation: a two-locus two-deme model. *Journal of Mathematical Biology*, **68**, 1135–1198.

Albretsen J, Aure J, Sætre R, Danielssen DS (2012) Climatic variability in the Skagerrak and coastal waters of Norway. *ICES Journal of Marine Science*, **69**, 758–763.

Allendorf FW, Hohenlohe PA, Luikart G (2010) Genomics and the future of conservation genetics. *Nature Reviews Genetics*, **11**, 697–709.

Alvarez M, Schrey AW, Richards CL (2015) Ten years of transcriptomics in wild populations: what have we learned about their ecology and evolution? *Molecular Ecology*, **24**, 710–725.

Andersen Ø, Wetten OF, Rosa MC De *et al.* (2009) Haemoglobin polymorphisms affect the oxygen-binding properties in Atlantic cod populations. *Proceedings of the Royal Society B: Biological Sciences*, **276**, 833–841.

Anderson JT (1988) A review of size dependent survival during pre-recruit stages of fishes in relation to recruitment. *Journal of Northwest Atlantic Fishery Science*, **8**, 55–66.

André C, Svedäng H, Knutsen H *et al.* (2016) Population structure in Atlantic cod in the eastern North Sea-Skagerrak-Kattegat: early life stage dispersal and adult migration. *BMC Research Notes*, **9**, 63.

Andrew RL, Bernatchez L, Bonin A *et al.* (2013) A road map for molecular ecology. *Molecular Ecology*, **22**, 2605–2626.

Andrews S (2011) The FastQC Project.

Ao J, Mu Y, Xiang L-X *et al.* (2015) Genome sequencing of the perciform fish *Larimichthys crocea* provides insights into molecular and genetic mechanisms of stress adaptation. *PLoS Genetics*, **11**, e1005118.

Aubin-Horth N, Renn SCP (2009) Genomic reaction norms: using integrative biology to understand molecular mechanisms of phenotypic plasticity. *Molecular Ecology*, **18**, 3763–3780.

Barat A, Sahoo PK, Kumar R, Goel C, Singh AK (2016) Transcriptional response to heat shock in liver of snow trout (*Schizothorax richardsonii*) - a vulnerable Himalayan Cyprinid fish. *Functional and Integrative Genomics*, **16**, 203–213.

Barceló C, Ciannelli L, Olsen EM, Johannessen T, Knutsen H (2016) Eight decades of sampling reveal a contemporary novel fish assemblage in coastal nursery habitats. *Global Change Biology*, **22**, 1155–1167.

Barlow SL, Metcalfe J, Righton DA, Berenbrink M (2017) Life on the edge: O_2 binding in Atlantic cod red blood cells near their southern distribution limit is not sensitive to temperature or haemoglobin genotype. *Journal of Experimental Biology*, **220**, 414–424.

Barrett RDH, Hoekstra HE (2011) Molecular spandrels: tests of adaptation at the genetic level. *Nature Reviews Genetics*, **12**, 767–780.

Barrett RDH, Rogers SM, Schluter D (2008) Natural selection on a major armor gene in threespine stickleback. *Science*, **322**, 255–257.

Barson NJ, Aykanat T, Hindar K *et al.* (2015) Sex-dependent dominance at a single locus maintains variation in age at maturity in salmon. *Nature*, **528**, 405–408.

Barth JMI, Berg PR, Jonsson PR *et al.* (2017) Genome architecture enables local adaptation of Atlantic cod despite high connectivity. *Molecular Ecology*, **26**, 4452–4466.

Barth JMI, Villegas-Ríos D, Freitas C *et al.* (2019) Disentangling structural genomic and behavioral barriers in a sea of connectivity. *Molecular Ecology*.

Baskerville-Bridges B, Kling LJ (2000) Larval culture of Atlantic cod (*Gadus morhua*) at high stocking densities. *Aquaculture*, **181**, 61–69.

Baumann H, Conover DO (2011) Adaptation to climate change: contrasting patterns of thermal-reaction-norm evolution in Pacific versus Atlantic silversides. *Proceedings of the Royal Society B: Biological Sciences*, **278**, 2265–2273.

Bay RA, Harrigan RJ, Underwood V Le *et al.* (2018) Genomic signals of selection predict climate-driven population declines in a migratory bird. *Science*, **86**, 83–86.

Bay RA, Rose N, Barrett R *et al.* (2017a) Predicting responses to contemporary environmental change using evolutionary response architectures. *The American Naturalist*, **189**, 463–473.

Bay RA, Rose NH, Logan CA, Palumbi SR (2017b) Genomic models predict successful coral adaptation if future ocean warming rates are reduced. *Science Advances*, **3**, e1701413.

Beck BH, Fuller SA, Li C *et al.* (2016) Hepatic transcriptomic and metabolic responses of hybrid striped bass (*Morone saxatilis* × *Morone chrysops*) to acute and chronic hypoxic insult. *Comparative Biochemistry and Physiology, Part D, Genomics & Proteomics*, **18**, 1–9.

van Belleghem SM, Roelofs D, van Houdt J, Hendrickx F (2012) De novo transcriptome assembly and SNP discovery in the wing polymorphic salt marsh beetle *Pogonus chalceus* (Coleoptera, Carabidae). *PLoS ONE*, **7**, e42605.

Benjamini Y, Hochberg Y (1995) Controlling the false discovery rate: a practical and powerful approach to multiple testing. *Journal of the Royal Statistical Society. Series B (Methodological)*, **57**, 289–300.

Berg PR, Jentoft S, Star B *et al.* (2015) Adaptation to low salinity promotes genomic divergence. *Genome Biology & Evolution*, **7**, 1644–1663.

Berg PR, Star B, Pampoulie C *et al.* (2016) Three chromosomal rearrangements promote genomic divergence between migratory and stationary ecotypes of Atlantic cod. *Scientific Reports*, 23246.

Berg PR, Star B, Pampoulie C *et al.* (2017) Trans-oceanic genomic divergence of Atlantic cod ecotypes is associated with large inversions. *Heredity*, **119**, 418–428.

Bergmann C (1847) *Ueber die verhaltnisse der warmeokonomie der thiere zu ihrer grosse*. Göttinger Studies, Göttingen, Germany.

Bergstad OA, Torstensen E, Bjørn Bøhle (1996) *Micronekton and pelagic fishes in fjords on the Norwegian Skagerrak coast in winter*. Institute of Marine Research, Flødevigen.

Bernatchez L (2016) On the maintenance of genetic variation and adaptation to environmental change: considerations from population genomics in fishes. *Journal of Fish Biology*, **89**, 2519–2556.

Bernatchez L, Wellenreuther M, Araneda C *et al.* (2017) Harnessing the power of genomics to secure the future of seafood. *Trends in Ecology and Evolution*, **32**, 665–680.

Billerbeck JM, Lankford TE, Conover DO (2001) Evolution of intrinsic growth and energy acquisition rates. I. Trade-offs with swimming performance in *Menidia menidia*. *Evolution*, **55**, 1863–1872.

Bilyk KT, Cheng CHC (2014) RNA-seq analyses of cellular responses to elevated body temperature in the high Antarctic cryopelagic nototheniid fish *Pagothenia borchgrevinki*. *Marine Genomics*, **18**, 163–171.

Bindea G, Mlecnik B, Hackl H *et al.* (2009) ClueGO: a Cytoscape plug-in to decipher functionally grouped gene ontology and pathway annotation networks. *Bioinformatics*, **25**, 1091–1093.

Björnsson B, Steinarsson A (2002) The food-unlimited growth rate of Atlantic cod (*Gadus morhua*). *Canadian Journal of Fisheries and Aquatic Sciences*, **59**, 494–502.

Bolger AM, Lohse M, Usadel B (2014) Trimmomatic: a flexible trimmer for Illumina sequence data. *Bioinformatics*, 1–7.

Bonanomi S, Pellissier L, Therkildsen NO *et al.* (2015) Archived DNA reveals fisheries and climate induced collapse of a major fishery. *Scientific Reports*, **5**, 15395.

Bougas B, Audet C, Bernatchez L (2013) The influence of parental effects on transcriptomic landscape during early development in brook charr (*Salvelinus fontinalis*, Mitchill). *Heredity*, **110**, 484–91.

Bradbury IR, Bowman S, Borza T *et al.* (2014) Long distance linkage disequilibrium and limited hybridization suggest cryptic speciation in Atlantic cod. *PLoS ONE*, **9**, e106380.

Bradbury IR, Hubert S, Higgins B *et al.* (2010) Parallel adaptive evolution of Atlantic cod on both sides of the Atlantic Ocean in response to temperature. *Proceedings of the Royal Society B: Biological Sciences*, **277**, 3725–3734.

Bradshaw AD (1965) Evolutionary significance of phenotypic plasticity in plants. *Advances in Genetics*, **13**, 115–155.

Bradshaw WE, Holzapfel CM (2001) Genetic shift in photoperiodic response correlated with global warming. *Proceedings of the National Academy of Sciences USA*, **98**, 14509–14511.

Brander KM (2007) Global fish production and climate change. *Proceedings of the National Academy of Sciences USA*, **104**, 19709–19714.

Brito-Morales I, Molinos JG, Schoeman DS *et al.* (2018) Climate velocity can inform conservation in a warming world. *Trends in Ecology and Evolution*, **33**, 441–457.

Buckley LB, Nufio CR, Kingsolver JG (2014) Phenotypic clines, energy balances and ecological responses to climate change. *Journal of Animal Ecology*, **83**, 41–50.

Bulmer MG (1972) The genetic variability of polygenic characters under optimizing selection, mutation and drift. *Genetics Research*, **19**, 17–25.

Buonocore F, Gerdol M (2016) Alternative adaptive immunity strategies: coelacanth, cod and shark immunity. *Molecular Immunology*, **69**, 157–169.

Bürger R, Akerman A (2011) The effects of linkage and gene flow on local adaptation: a two-locus continent–island model. *Theoretical Population Biology*, **80**, 272–288.

Busby MA, Stewart C, Miller CA, Grzeda KR, Marth GT (2013) Scotty: a web tool for designing RNA-seq experiments to measure differential gene expression. *Bioinformatics*, **29**, 656–657.

Canale CI, Henry P-Y (2010) Adaptive phenotypic plasticity and resilience of vertebrates to increasing climatic unpredictability. *Climate Research*, **43**, 135–147.

Cardinale M, Svenson A, Hjelm J (2017) The “easy restriction” syndrome drive local fish stocks to extinction: the case of the management of Swedish coastal populations. *Marine Policy*, **83**, 179–183.

Chandra V, Fetter-Pruneda I, Oxley PR *et al.* (2018) Social regulation of insulin signaling and the evolution of eusociality in ants. *Science*, **361**, 398–402.

Charlesworth D (2016) The status of supergenes in the 21st century: recombination suppression in Batesian mimicry and sex chromosomes and other complex adaptations. *Evolutionary Applications*, **9**, 74–90.

Charmantier A, McCleery RH, Cole LR *et al.* (2008) Adaptive phenotypic plasticity in response to climate change in a wild bird population. *Science*, **320**, 800–803.

Chaui-Berlinck JG, Navas CA, Monteiro LHA, Bicudo JEPW (2004) Temperature effects on a whole metabolic reaction cannot be inferred from its components. *Proceedings of the Royal Society B: Biological Sciences*, **271**, 1415–1419.

Chen B, Feder ME, Kang L (2018) Evolution of heat-shock protein expression underlying adaptive responses to environmental stress. *Molecular Ecology*, **27**, 3040–3054.

Chen Y, Mccarthy D, Robinson M, Smyth GK (2014) edgeR: differential expression analysis of digital gene expression data - User’s Guide.

Chevin L-M, Lande R, Mace GM (2010) Adaptation, plasticity, and extinction in a changing environment: towards a predictive theory. *PloS Biology*, **8**, e1000357.

Ciannelli L, Knutsen H, Olsen EM *et al.* (2010) Small-scale genetic structure in a marine population in relation to water circulation and egg characteristics. *Ecology*, **91**, 2918–2930.

Claireaux G, Lefrançois C (2007) Linking environmental variability and fish performance: integration through the concept of scope for activity. *Philosophical Transactions of the Royal Society B: Biological Sciences*, **362**, 2031–2041.

Clark TD, Sandblom E, Jutfelt F (2013) Aerobic scope measurements of fishes in an era of climate change: respirometry, relevance and recommendations. *The Journal of Experimental Biology*, **216**, 2771–2782.

Clarke A, Fraser KPP (2004) Why does metabolism scale with temperature? *Functional Ecology*, **18**, 243–251.

Clarke LM, Munch SB, Thorrold SR, Conover DO (2010) High connectivity among locally adapted populations of a marine fish (*Menidia menidia*). *Ecology*, **91**, 3526–3537.

Coates DJ, Byrne M, Moritz C (2018) Genetic diversity and conservation units: dealing with the species-population continuum in the age of genomics. *Frontiers in Ecology and Evolution*, **6**, 165.

Coghlan A, Eichler EE, Oliver SG, Paterson AH, Stein L (2005) Chromosome evolution in eukaryotes: a multi-kingdom perspective. *Trends in Genetics*, **21**, 673–682.

Conesa A, Madrigal P, Tarazona S *et al.* (2016) A survey of best practices for RNA-seq data analysis. *Genome Biology*, **17**, 13.

Conover DO (1998) Local adaptation in marine fishes: evidence and implications for stock enhancement. *Bulletin of Marine Science*, **62**, 477–493.

Conover DO, Baumann H (2009) The role of experiments in understanding fishery-induced evolution. *Evolutionary Applications*, **2**, 276–290.

Conover DO, Clarke LM, Munch SB, Wagner GN (2006) Spatial and temporal scales of adaptive divergence in marine fishes and the implications for conservation. *Journal of Fish Biology*, **69**, 21–47.

Conover DO, Munch SB (2002) Sustaining fisheries yields over evolutionary time scales. *Science*, **297**, 94–96.

Conover DO, Present TMC (1990) Countergradient variation in growth rate: compensation for length of the growing season among Atlantic silversides from different latitudes. *Oecologia*, **83**, 316–324.

Cooper KW (1945) Normal segregation without chiasmata in female *Drosophila melanogaster*. *Genetics*, **30**, 472–484.

Costa V, Angelini C, De Feis I, Ciccodicola A (2010) Uncovering the complexity of transcriptomes with RNA-seq. *Journal of Biomedicine and Biotechnology*, **2010**, 853916.

Costa V, Aprile M, Esposito R, Ciccodicola A (2013) RNA-seq and human complex diseases: recent accomplishments and future perspectives. *European Journal of Human Genetics*, **21**, 134–142.

Costanzo M, Baryshnikova A, Bellay J *et al.* (2010) The genetic landscape of a cell. *Science*, **327**, 425–431.

Costello C, Ovando D, Hilborn R *et al.* (2012) Reports status and solutions for the world's unassessed fisheries. *Science*, 1224768.

Coughlan JM, Willis JH (2018) Dissecting the role of a large chromosomal inversion in life history divergence throughout the *Mimulus guttatus* species complex. *Molecular Ecology*, 1–15.

Coulson T, Kendall BE, Barthold J *et al.* (2017) Modeling adaptive and nonadaptive responses of populations to environmental change. *American Naturalist*, **190**, 313–336.

Crozier LG, Hutchings JA (2014) Plastic and evolutionary responses to climate change in fish. *Evolutionary Applications*, **7**, 68–87.

Cushman SA (2014) Grand challenges in evolutionary and population genetics: the importance of integrating epigenetics, genomics, modeling, and experimentation. *Frontiers in Genetics*, **5**, 197.

Dahle G, Jorstad K, Rusaas H, Ottera H (2006) Genetic characteristics of broodstock collected from four Norwegian coastal cod (*Gadus morhua*) populations. *ICES Journal of Marine Science*, **63**, 209–215.

Dahle G, Quintela M, Johansen T *et al.* (2018) Analysis of coastal cod (*Gadus morhua* L.) sampled on spawning sites reveals a genetic gradient throughout Norway's coastline. *BMC Genetics*, **19**, 42.

Dahlke FT, Leo E, Mark FC *et al.* (2017) Effects of ocean acidification increase embryonic sensitivity to thermal extremes in Atlantic cod, *Gadus morhua*. *Global Change Biology*, **23**, 1499–1510.

Dahlke FT, Politis SN, Butts IAE, Trippel EA, Peck MA (2016) Fathers modify thermal reaction norms for hatching success in Atlantic cod, *Gadus morhua*. *Journal of Experimental Marine Biology and Ecology*, **474**, 148–155.

Dalziel AC, Rogers SM, Schulte PM (2009) Linking genotypes to phenotypes and fitness: how mechanistic biology can inform molecular ecology. *Molecular Ecology*, **18**, 4997–5017.

Danecek P, Auton A, Abecasis G *et al.* (2011) The variant call format and VCFtools. *Bioinformatics*, **27**, 2156–2158.

Delghandi M, Mortensen A, Westgaard J-I (2003) Simultaneous analysis of six microsatellite markers in Atlantic cod (*Gadus morhua*): a novel multiplex assay system for use in selective breeding studies. *Marine Biotechnology*, **5**, 141–148.

Denton JF, Lugo-Martinez J, Tucker AE *et al.* (2014) Extensive error in the number of genes inferred from draft genome assemblies. *PLoS Computational Biology*, **10**, e1003998.

Derry AM, Arnott SE (2007) Adaptive reversals in acid tolerance in copepods from lakes recovering from historical stress. *Ecological Applications*, **17**, 1116–1126.

Dey KK, Hsiao CJ, Stephens M (2017) Visualizing the structure of RNA-seq expression data using grade of membership models. *PLoS Genetics*, **13**, 1–23.

Dobzhansky T (1940) Speciation as a stage in evolutionary divergence. *The American Naturalist*, **74**, 312–321.

Donelson JM, Munday PL, McCormick MI, Pitcher CR (2012) Rapid transgenerational acclimation of a tropical reef fish to climate change. *Nature Climate Change*, **2**, 30–32.

Donelson JM, Salinas S, Munday PL, Shama LNS (2018) Transgenerational plasticity and climate change experiments: where do we go from here? *Global Change Biology*, **24**, 13–34.

Duncan EJ, Gluckman PD, Dearden PK (2014) Epigenetics, plasticity, and evolution: how do we link epigenetic change to phenotype? *Journal of Experimental Zoology Part B: Molecular and Developmental Evolution*, **322**, 208–220.

Dunlap JC (1999) Molecular bases for circadian clocks. *Cell*, **96**, 271–290.

Engström PG, Steijger T, Sipos B *et al.* (2013) Systematic evaluation of spliced alignment programs for RNA-seq data. *Nature Methods*, **10**, 1185–1193.

Ern R, Huong DTT, Phuong NT *et al.* (2015) Some like it hot: thermal tolerance and oxygen supply capacity in two eurythermal crustaceans. *Scientific Reports*, **5**, 10743.

Espeland SH, Gundersen AF, Olsen EM *et al.* (2007) Home range and elevated egg densities within an inshore spawning ground of coastal cod. *ICES Journal of Marine Science*, **64**, 920–928.

Espeland S, Olsen E, Knutsen H *et al.* (2008) New perspectives on fish movement: kernel and GAM smoothers applied to a century of tagging data on coastal Atlantic cod. *Marine Ecology Progress Series*, **372**, 231–241.

Evans TG (2015) Considerations for the use of transcriptomics in identifying the "genes that matter" for environmental adaptation. *Journal of Experimental Biology*, **218**, 1925–1935.

Evans TG, Hofmann GE (2012) Defining the limits of physiological plasticity: how gene expression can assess and predict the consequences of ocean change. *Philosophical transactions of the Royal Society of London. Series B, Biological sciences*, **367**, 1733–45.

Fan Z, Wu Z, Wang L *et al.* (2016) Characterization of embryo transcriptome of gynogenetic olive flounder *Paralichthys olivaceus*. *Marine Biotechnology*, **18**, 545–553.

Fang Z, Cui X (2011) Design and validation issues in RNA-seq experiments. *Briefings in Bioinformatics*, **12**, 280–287.

Feder ME, Mitchell-Olds T (2003) Evolutionary and ecological functional genomics. *Nature Reviews Genetics*, **4**, 649–655.

Feder JL, Roethele JB, Filchak K, Niedbalski J, Romero-Severson J (2003) Evidence for inversion polymorphism related to sympatric host race formation in the apple maggot fly, *Rhagoletis pomonella*. *Genetics*, **163**, 939–953.

Feder ME, Walser J (2005) The biological limitations of transcriptomics in elucidating stress and stress responses. *Journal of Evolutionary Biology*, **18**, 901–910.

Felsenstein J (1976) The theoretical population genetics of variable selection and migration. *Annual Review of Genetics*, **10**, 253–280.

Fernández-Chacón A, Moland E, Espeland SH, Olsen EM (2015) Demographic effects of full versus partial protection from harvesting: inference from an empirical before-after control-impact study on Atlantic cod. *Journal of Applied Ecology*, **52**, 1206–1215.

Fisher RA (1930) *The genetical theory of natural selection*. Dover Publications, Inc., New York, NY.

Francis WR, Wörheide G (2017) Similar ratios of introns to intergenic sequence across animal genomes. *Genome Biology and Evolution*, **9**, 1582–1598.

Frank KT, Brickman D (2000) Allee effects and compensatory population dynamics within a stock complex. *Canadian Journal of Fisheries and Aquatic Sciences*, **57**, 513–517.

Franks SJ, Hoffman AA (2012) Genetics of climate change adaptation. *Annual Review of Genetics*, **46**, 185–208.

Fraser DJ, Bernatchez L (2001) Adaptive evolutionary conservation: towards a unified concept for defining conservation units. *Molecular Ecology*, **10**, 2741–2752.

Fry FEJ, Hart JS (1948) Cruising speed of goldfish in relation to water temperature. *Journal of the Fisheries Research Board of Canada*, **7b**, 169–175.

Fu X, Sun Y, Wang J *et al.* (2014) Sequencing-based gene network analysis provides a core set of gene resource for understanding thermal adaptation in Zhikong scallop *Chlamys farreri*. *Molecular Ecology Resources*, **14**, 184–198.

Gamble JC, Houde ED (1984) Growth, mortality and feeding of cod (*Gadus morhua* L.) larvae in enclosed water columns and in laboratory tanks. In: *The Propagation of Cod Gadus Morhua L., Vol. 1*, pp. 123–143.

Gao X, Starmer J, Martin ER (2008) A multiple testing correction method for genetic association studies using correlated single nucleotide polymorphisms. *Genetic Epidemiology*, **32**, 361–369.

Gasch AP, Spellman PT, Kao CM *et al.* (2000) Genomic expression programs in the response of yeast cells to environmental changes. *Molecular Biology of the Cell*, **11**, 4241–57.

Gayral P, Melo-Ferreira J, Glemin S *et al.* (2013) Reference-free population genomics from next-generation transcriptome data and the vertebrate–invertebrate gap. *PLoS Genetics*, **94**, e1003457.

Ghalambor CK, Hoke KL, Ruell EW *et al.* (2015) Non-adaptive plasticity potentiates rapid adaptive evolution of gene expression in nature. *Nature*, **525**, 372–375.

Ghalambor CK, McKay JK, Carroll SP, Reznick DN (2007) Adaptive versus non-adaptive phenotypic plasticity and the potential for contemporary adaptation in new environments. *Functional Ecology*, **21**, 394–407.

Gillooly JF, Brown JH, West GB, Savage VM, Charnov EL (2001) Effects of size and temperature on metabolic rate. *Science*, **293**, 2248–2251.

Glover KA, Dahle G, Westgaard JI *et al.* (2010) Genetic diversity within and among Atlantic cod (*Gadus morhua*) farmed in marine cages: a proof-of-concept study for the identification of escapees. *Animal Genetics*, **41**, 515–522.

Griswold CK (2006) Gene flow's effect on the genetic architecture of a local adaptation and its consequences for QTL analyses. *Heredity*, **96**, 445–453.

Gu J, Li J-W, Tse WK-F *et al.* (2015) Transcriptomic responses of corpuscle of Stannius gland of Japanese eels (*Anguilla japonica*) to changes in water salinity. *Scientific Reports*, **5**, 9836.

Guo L, Wang Y, Liang S *et al.* (2016) Tissue-overlapping response of half-smooth tongue sole (*Cynoglossus semilaevis*) to thermostressing based on transcriptome profiles. *Gene*, **586**, 97–104.

Haas BJ, Delcher AL, Mount SM *et al.* (2003) Improving the *Arabidopsis* genome annotation using maximal transcript alignment assemblies. *Nucleic Acids Research*, **31**, 5654–5666.

Hansen MM (2010) Expression of interest: transcriptomics and the designation of conservation units. *Molecular Ecology*, **19**, 1757–1759.

Hansen MM, Olivieri I, Waller DM, Nielsen EE (2012) Monitoring adaptive genetic responses to environmental change. *Molecular Ecology*, **21**, 1311–1329.

Hard JJ (1995) A quantitative genetic perspective on the conservation of intraspecific diversity. *American Fisheries Society Symposium*, **17**, 304–326.

Hemmer-Hansen J, Nielsen EE, Therkildsen NO *et al.* (2013) A genomic island linked to ecotype divergence in Atlantic cod. *Molecular Ecology*, **22**, 2653–2667.

Hice LA, Duffy TA, Munch SB, Conover DO (2012) Spatial scale and divergent patterns of variation in adapted traits in the ocean. *Ecology Letters*, **15**, 568–575.

Hilbish TJ (1996) Population genetics of marine species: the interaction of natural selection and historically differentiated populations. *Journal of Experimental Marine Biology and Ecology*, **200**, 67–83.

Hilborn R, Quinn TP, Schindler DE, Rogers DE (2003) Biocomplexity and fisheries sustainability. *Proceedings of the National Academy of Sciences of the United States of America*, **100**, 6564–6568.

Hoban S, Kelley JL, Lotterhos KE *et al.* (2016) Finding the genomic basis of local adaptation: pitfalls, practical solutions, and future directions. *The American Naturalist*, **188**, 379–397.

Hoff SNK, Baalsrud HT, Klunderud AT *et al.* (2018) Long-read sequence capture of the haemoglobin gene clusters across codfish species. *Molecular Ecology Resources*, 1–15.

Hoffmann A, Griffin P, Dillon S *et al.* (2015) A framework for incorporating evolutionary genomics into biodiversity conservation and management. *Climate Change Responses*, **2**, 1.

Hoffmann AA, Rieseberg LH (2008) Revisiting the impact of inversions in evolution: from population genetic markers to drivers of adaptive shifts and speciation? *Annual Review of Ecology, Evolution, and Systematics*, **39**, 21–42.

Hoffmann AA, Sgrò CM (2011) Climate change and evolutionary adaptation. *Nature*, **470**, 479–485.

Hoffmann AA, Sgrò CM, Kristensen TN (2017) Revisiting adaptive potential, population size, and conservation. *Trends in Ecology and Evolution*, **32**, 506–517.

Hoffmann AA, Willi Y (2008) Detecting genetic responses to environmental change. *Nature Reviews Genetics*, **9**, 421–432.

Houde ED, Zastrow CE (1993) Ecosystem- and taxon-specific dynamic and energetics properties of larval fish assemblages. *Bulletin of Marine Science*, **53**, 290–335.

Hu Y-C, Kang C-K, Tang C-H, Lee T-H (2015a) Transcriptomic analysis of metabolic pathways in milkfish that respond to salinity and temperature changes. *PloS One*, **10**, e0134959.

Hu P, Liu M, Zhang D *et al.* (2015b) Global identification of the genetic networks and cis-regulatory elements of the cold response in zebrafish. *Nucleic Acids Research*, **43**, 9198–9213.

Huey RB, Berrigan D (2001) Temperature, demography, and ectotherm fitness. *The American Naturalist*, **158**, 204–210.

Hulsen T, de Vlieg J, Alkema W (2008) BioVenn – a web application for the comparison and visualization of biological lists using area-proportional Venn diagrams. *BMC Genomics*, **9**, 488.

Hung I-C, Hsiao Y-C, Sun HS, Chen T-M, Lee S-J (2016) MicroRNAs regulate gene plasticity during cold shock in zebrafish larvae. *BMC Genomics*, **17**, 922.

Hurst TP, Munch SB, Lavelle KA (2012) Thermal reaction norms for growth vary among cohorts of Pacific cod (*Gadus macrocephalus*). *Marine Biology*, **159**, 2173–2183.

Hutchings JA (1993) Reaction norms for reproductive traits in brook trout and their influence on life history evolution effected by size-selective harvesting. In: *The exploitation of evolving resources* (eds Stokes TK, McGlade JM, Law R), pp. 107-125. Springer, Berlin, Germany.

Hutchings JA (2000) Collapse and recovery of marine fishes. *Nature*, **406**, 882–885.

Hutchings JA (2011) Old wine in new bottles: reaction norms in salmonid fishes. *Heredity*, **106**, 421–37.

Hutchings JA, Rangeley RW (2011) Correlates of recovery for Canadian Atlantic cod (*Gadus morhua*). *Canadian Journal of Zoology*, **89**, 386–400.

Hutchings JA, Swain DP, Rowe S *et al.* (2007) Genetic variation in life-history reaction norms in a marine fish. *Proceedings of the Royal Society B: Biological Sciences*, **274**, 1693–1699.

Huth TJ, Place SP (2016a) RNA-seq reveals a diminished acclimation response to the combined effects of ocean acidification and elevated seawater temperature in *Pagothenia borchgrevinki*. *Marine Genomics*, **28**, 87–97.

Huth TJ, Place SP (2016b) Transcriptome wide analyses reveal a sustained cellular stress response in the gill tissue of *Trematomus bernacchii* after acclimation to multiple stressors. *BMC Genomics*, **17**, 127.

Huxley J (1942) *Evolution: the modern synthesis*. George Allen and Unwin.

ICES (2018) *Report of the Arctic Fisheries Working Group (AFWG)*. International Council for the Exploration of the Sea. Ispra, Italy.

Imsland AK, Foss A, Nævdal G, Stefansson SO (2001) Selection or adaptation: differences in growth performance of juvenile turbot (*Scophthalmus maximus* Rafinesque) from two close-by localities off Norway. *Sarsia*, **86**, 43–51.

IPCC (2013) IPCC, 2013: Summary for Policymakers. In: *Climate Change 2013: The Physical Science Basis. Contribution of Working Group I to the Fifth Assessment Report of the Intergovernmental Panel on Climate Change* (eds Stocker TF, Qin D, Plattner G-K, et al.). Cambridge University Press, Cambridge, United Kingdom and New York, NY, USA.

Jeffries KM, Connon RE, Davis BE *et al.* (2016) Effects of high temperatures on threatened estuarine fishes during periods of extreme drought. *Journal of Experimental Biology*, **219**, 1705–1716.

Jesus TF, Grosso AR, Almeida-Val VMF, Coelho MM (2016) Transcriptome profiling of two Iberian freshwater fish exposed to thermal stress. *Journal of Thermal Biology*, **55**, 54–61.

Johannessen T, Dahl E (1996) Historical changes in oxygen concentrations along the Norwegian Skagerrak coast: Reply to the comment by Gray and Abdullah. *Limnology and Oceanography*, **41**, 1847–1852.

Jones FC, Grabherr MG, Chan YF *et al.* (2012) The genomic basis of adaptive evolution in threespine sticklebacks. *Nature*, **484**, 55–61.

Jones OR, Wang J (2010) COLONY: a program for parentage and sibship inference from multilocus genotype data. *Molecular Ecology Resources*, **10**, 551–555.

Jorde PE, Kleiven AR, Sodeland M *et al.* (2018) Who is fishing on what stock: population-of-origin of individual cod (*Gadus morhua*) in commercial and recreational fisheries. *ICES Journal of Marine Science*, **75**, 2153–2162.

Joron M, Frezal L, Jones RT *et al.* (2013) Chromosomal rearrangements maintain a polymorphic supergene controlling butterfly mimicry. *Nature*, **477**, 203–206.

Juliussen EH (2016) Thermal reaction norms for larval Atlantic cod (*Gadus morhua*): exploring population differences on a micro-geographic scale. MSc thesis. University of Oslo.

Kahn RG, Pearson DE, Dick EJ (2004) Comparison of standard length, fork length, and total length for measuring west coast marine fishes. *Marine Fisheries Review*, **66**, 31–33.

Kalinowski ST, Taper ML, Marshall TC (2007) Revising how the computer program CERVUS accommodates genotyping error increases success in paternity assignment. *Molecular Ecology*, **16**, 1099–1106.

Kapuscinski AR, Miller LM (2007) *Genetic guidelines for fisheries management* (eds S Moen, M Zhuikov). University of Minnesota Sea Grant Program, Duluth, Minnesota, USA.

Kassahn KS, Crozier RH, Ward AC, Stone G, Caley MJ (2007) From transcriptome to biological function: environmental stress in an ectothermic vertebrate, the coral reef fish *Pomacentrus moluccensis*. *BMC Genomics*, **8**, 358.

Kavembe GD, Franchini P, Irisarri I, Machado-Schiaffino G, Meyer A (2015) Genomics of adaptation to multiple concurrent stresses: insights from comparative transcriptomics of a cichlid fish from one of Earth's most extreme environments, the hypersaline soda Lake Magadi in Kenya, East Africa. *Journal of Molecular Evolution*, **81**, 90–109.

Kawecki TJ, Ebert D (2004) Conceptual issues in local adaptation. *Ecology Letters*, **7**, 1225–1241.

Kelty JD, Lee Jr. RE (2001) Rapid cold-hardening of *Drosophila melanogaster* (Diptera: Drosophilidae) during ecologically based thermoperiodic cycles. *The Journal of Experimental Biology*, **204**, 1659–1666.

Killen SS, Brown JA (2006) Energetic cost of reduced foraging under predation threat in newly hatched ocean pout. *Marine Ecology Progress Series*, **321**, 255–266.

Kim D, Langmead B, Salzberg SL (2015) HISAT: a fast spliced aligner with low memory requirements. *Nature Methods*, **12**, 357–360.

Kim D, Pertea G, Trapnell C *et al.* (2013) TopHat2: accurate alignment of transcriptomes in the presence of insertions, deletions and gene fusions. *Genome Biology*, **14**, R36.

Kingsolver JG, Woods HA (2016) Beyond thermal performance curves: modeling time-dependent effects of thermal stress on ectotherm growth rates. *The American Naturalist*, **187**, 283–294.

Kirkpatrick M (2010) How and why chromosome inversions evolve. *PLoS Biology*, **8**, e1000501.

Kirkpatrick M (2017) The evolution of genome structure by natural and sexual selection. *Journal of Heredity*, **108**, 3–11.

Kirubakaran TG, Grove H, Kent MP *et al.* (2016) Two adjacent inversions maintain genomic differentiation between migratory and stationary ecotypes of Atlantic cod. *Molecular Ecology*, **25**, 2130–2143.

Kleiven AR, Fernandez-Chacon A, Nordahl JH *et al.* (2016) Harvest pressure on coastal Atlantic cod (*Gadus morhua*) from recreational fishing relative to commercial fishing assessed from tag-recovery data. *PLoS ONE*, **11**, 1–14.

Klepsatel P, Gáliková M, Xu Y, Kühnlein RP (2016) Thermal stress depletes energy reserves in *Drosophila*. *Scientific Reports*, **6**, 33667.

Knutsen H, André C, Jorde PE *et al.* (2004) Transport of North Sea cod larvae into the Skagerrak coastal populations. *Proceedings of the Royal Society B: Biological Sciences*, **271**, 1337–1344.

Knutsen H, Jorde PE, Hutchings JA *et al.* (2018) Stable coexistence of genetically divergent Atlantic cod ecotypes at multiple spatial scales. *Evolutionary Applications*, 1–13.

Knutsen H, Olsen EM, Ciannelli L *et al.* (2007) Egg distribution, bottom topography and small-scale cod population structure in a coastal marine system. *Marine Ecology Progress Series*, **333**, 249–255.

Knutsen H, Olsen EM, Jorde PE *et al.* (2011) Are low but statistically significant levels of genetic differentiation in marine fishes "biologically meaningful"? A case study of coastal Atlantic cod. *Molecular Ecology*, **20**, 768–783.

Kolder ICRM, van der Plas-Duivesteijn SJ, Tan G *et al.* (2016) A full-body transcriptome and proteome resource for the European common carp. *BMC Genomics*, **17**, 701.

Kültz D (2005) Molecular and evolutionary basis of the cellular stress response. *Annual Review of Physiology*, **67**, 225–257.

Kuparinen A, Hutchings JA (2017) Genetic architecture of age at maturity can generate divergent and disruptive harvest-induced evolution. *Philosophical Transactions of the Royal Society of London - Series B: Biological Sciences*, **372**, 20160035.

Kuparinen A, Merilä J (2007) Detecting and managing fisheries-induced evolution. *Trends in Ecology and Evolution*, **22**, 652–659.

Kuparinen A, Roney NE, Oomen RA, Hutchings JA, Olsen EM (2015) Small-scale life history variability suggests potential for spatial mismatches in Atlantic cod management units. *ICES Journal of Marine Science*, **73**, 286–292.

Kurlansky M (1997) *Cod: a biography of the fish that changed the world*. A.A. Knopf Canada.

Lai KP, Li J-W, Tse AC-K *et al.* (2016a) Differential responses of female and male brains to hypoxia in the marine medaka *Oryzias melastigma*. *Aquatic Toxicology*, **172**, 36–43.

Lai KP, Li J-W, Tse AC-K, Chan T-F, Wu RS-S (2016b) Hypoxia alters steroidogenesis in female marine medaka through miRNAs regulation. *Aquatic Toxicology*, **172**, 1–8.

Lam SH, Lui EY, Li Z *et al.* (2014) Differential transcriptomic analyses revealed genes and signaling pathways involved in iono-osmoregulation and cellular remodeling in the gills of euryhaline Mozambique tilapia, *Oreochromis mossambicus*. *BMC Genomics*, **15**, 921.

Lande R (2009) Adaptation to an extraordinary environment by evolution of phenotypic plasticity and genetic assimilation. *Journal of Evolutionary Biology*, **22**, 1435–1446.

Lande R, Shannon S (1996) The role of genetic variation in adaptation and population persistence in a changing environment. *Evolution*, **50**, 434–437.

Langmead B, Salzberg SL (2012) Fast gapped-read alignment with Bowtie 2. *Nature Methods*, **9**, 357–360.

Langmead B, Trapnell C, Pop M, Salzberg SL (2009) Ultrafast and memory-efficient alignment of short DNA sequences to the human genome. *Genome Biology*, **10**, R25.

St. Laurent G, Shtokalo D, Tackett MR *et al.* (2013) On the importance of small changes in RNA expression. *Methods*, **63**, 18–24.

Law CW, Alhamdoosh M, Su S, Smyth GK, Ritchie ME (2016) RNA-seq analysis is easy as 1-2-3 with limma, Glimma and edgeR. *F1000Research*, 1–26.

Law CW, Chen Y, Shi W, Smyth GK (2014) voom: precision weights unlock linear model analysis tools for RNA-seq read counts. *Genome Biology*, **15**, R29.

Lenormand T (2002) Gene flow and the limits to natural selection. *Trends in Ecology and Evolution*, **17**, 183–189.

Levin LA (2006) Recent progress in understanding larval dispersal: new directions and digressions. *Integrative and Comparative Biology*, **46**, 282–297.

Lewis P, Zaykin D (2001) "Genetic Data Analysis: computer program for the analysis of allelic data, version 1.0 (d16c)." Free program distributed by the authors over the internet from http://lewis.eeb.uconn.edu/lewishome/software.html.

Li H, Durbin R (2010) Fast and accurate long-read alignment with Burrows-Wheeler transform. *Bioinformatics*, **26**, 589–595.

Li H, Handsaker B, Wysoker A *et al.* (2009) The Sequence Alignment/Map format and SAMtools. *Bioinformatics*, **25**, 2078–2079.

Li C, Ling Q, Ge C, Ye Z, Han X (2015) Transcriptome characterization and SSR discovery in large-scale loach *Paramisgurnus dabryanus* (Cobitidae, Cypriniformes). *Gene*, **557**, 201–208.

Limborg MT, Helyar SJ, De Bruyn M *et al.* (2012) Environmental selection on transcriptome-derived SNPs in a high gene flow marine fish, the Atlantic herring (*Clupea harengus*). *Molecular Ecology*, **21**, 3686–3703.

Lindgreen S (2012) AdapterRemoval: easy cleaning of next generation sequencing reads. *BMC Research Notes*, **5**, 337–343.

Lindholm AK, Hunt J, Brooks R (2006) Where do all the maternal effects go? Variation in offspring body size through ontogeny in the live-bearing fish *Poecilia parae*. *Biology Letters*, **2**, 586–589.

Liu R, Holik AZ, Su S *et al.* (2015) Why weight? Modelling sample and observational level variability improves power in RNA-seq analyses. *Nucleic Acids Research*, **43**, e97.

Liu S, Wang X, Sun F *et al.* (2013) RNA-seq reveals expression signatures of genes involved in oxygen transport, protein synthesis, folding, and degradation in response to heat stress in catfish. *Physiological Genomics*, **45**, 462–476.

Logan CA, Buckley BA (2015) Transcriptomic responses to environmental temperature in eurythermal and stenothermal fishes. *Journal of Experimental Biology*, **218**, 1915–1924.

Logan CA, Somero GN (2010) Transcriptional responses to thermal acclimation in the eurythermal fish *Gillichthys mirabilis* (Cooper 1864). *American Journal of Physiology - Regulatory, Integrative and Comparative Physiology*, **299**, 843–852.

Long Y, Li L, Li Q, He X, Cui Z (2012) Transcriptomic characterization of temperature stress responses in larval zebrafish. *PLoS ONE*, **7**, e37209.

Long Y, Song G, Yan J *et al.* (2013) Transcriptomic characterization of cold acclimation in larval zebrafish. *BMC Genomics*, **14**, 612.

Long Y, Yan J, Song G *et al.* (2015) Transcriptional events co-regulated by hypoxia and cold stresses in Zebrafish larvae. *BMC Genomics*, **16**, 385.

Lopez-Maestre H, Brinza L, Marchet C *et al.* (2016) SNP calling from RNA-seq data without a reference genome: identification, quantification, differential analysis and impact on the protein sequence. *Nucleic Acids Research*, **44**, e148.

Lowe WH, Kovach RP, Allendorf FW (2017) Population genetics and demography unite ecology and evolution. *Trends in Ecology and Evolution*, **32**, 141–152.

Lowry DB, Willis JH (2010) A widespread chromosomal inversion polymorphism contributes to a major life-history transition, local adaptation, and reproductive isolation. *PLoS Biology*, **8**, e1000500.

Ma J, Amos CI (2012) Investigation of inversion polymorphisms in the human genome using principal components analysis. *PLoS ONE*, **7**, e40224.

Macbeath JRE, Shackleton DR, Hulmes DJS (1993) Tyrosine-rich acidic matrix protein (TRAMP) accelerates collagen fibril formation in vitro. *The Journal of Biological Chemistry*, **268**, 19826–19832.

Maere S, Heymans K, Kuiper M (2005) BiNGO: a Cytoscape plugin to assess overrepresentation of Gene Ontology categories in Biological Networks. *Bioinformatics*, **21**, 3448–3449.

Marshall DJ (2008) Transgenerational plasticity in the sea: context-dependent maternal effects across the life history. *Ecology*, **89**, 418–427.

Martin M (2011) Cutadapt removes adapter sequences from high-throughput sequencing reads. *Bioinformatics in Action*, **17**, 10–12.

Maynard Smith J (1989) The causes of extinction. *Philosophical Transactions of the Royal Society B: Biological Sciences*, **325**, 241–252.

McCairns RJS, Bernatchez L (2010) Adaptive divergence between freshwater and marine sticklebacks: insights into the role of phenotypic plasticity from an integrated analysis of candidate gene expression. *Evolution*, **64**, 1029–1047.

McCairns RJS, Smith S, Sasaki M, Bernatchez L, Beheregaray LB (2016) The adaptive potential of subtropical rainbowfish in the face of climate change: heritability and heritable plasticity for the expression of candidate genes. *Evolutionary Applications*, **9**, 531–545.

McKenna A, Hanna M, Banks E *et al.* (2010) The Genome Analysis Toolkit: a MapReduce framework for analyzing next-generation DNA sequencing data. *Genome Research*, **20**.

Meier K, Hansen MM, Normandeau E *et al.* (2014) Local adaptation at the transcriptome level in brown trout: evidence from early life history temperature genomic reaction norms. *PLoS ONE*, **9**, e85171.

Meissner A, Gnirke A, Bell GW *et al.* (2005) Reduced representation bisulfite sequencing for comparative high-resolution DNA methylation analysis. *Nucleic Acids Research*, **33**, 5868–5877.

Merilä J, Hendry AP (2014) Climate change, adaptation, and phenotypic plasticity: the problem and the evidence. *Evolutionary Applications*, **7**, 1–14.

Milano I, Babbucci M, Cariani A *et al.* (2014) Outlier SNP markers reveal fine-scale genetic structuring across European hake populations (*Merluccius merluccius*). *Molecular Ecology*, **23**, 118–135.

Miller GM, Watson S-A, Donelson JM, McCormick MI, Munday PL (2012) Parental environment mediates impacts of increased carbon dioxide on a coral reef fish. *Nature Climate Change*, **2**, 858–861.

Mousseau TA, Fox CW (1998) The adaptive significance of maternal effects. *Trends in Ecology and Evolution*, **13**, 403–407.

Moyano M, Candebat C, Ruhbaum Y *et al.* (2017) Effects of warming rate, acclimation temperature and ontogeny on the critical thermal maximum of temperate marine fish larvae. *PLoS ONE*, **12**, e0179928.

Munday PL, McCormick MI, Nilsson GE (2012) Impact of global warming and rising CO_2 levels on coral reef fishes: what hope for the future? *The Journal of Experimental Biology*, **215**, 3865–73.

Murren CJ, Maclean HJ, Diamond SE *et al.* (2014) Evolutionary change in continuous reaction norms. *The American Naturalist*, **183**, 453–467.

Narum SR, Campbell NR (2015) Transcriptomic response to heat stress among ecologically divergent populations of redband trout. *BMC Genomics*, **16**, 103.

Nei M (1973) Analysis of gene diversity in subdivided populations. *Proceedings of the National Academy of Sciences*, **70**, 3321–3323.

Nei M, Chesser RK (1983) Estimation of fixation indices and gene diversities. *Annals of Human Genetics*, **47**, 253–259.

Neuheimer AB, Taggart CT (2007) The growing degree-day and fish size-at-age: the overlooked metric. *Canadian Journal of Fisheries and Aquatic Sciences*, **64**, 375–385.

Nguyen TV, Jung H, Nguyen TM, Hurwood D, Mather P (2016) Evaluation of potential candidate genes involved in salinity tolerance in striped catfish (*Pangasianodon hypophthalmus*) using an RNA-seq approach. *Marine Genomics*, **25**.

Nielsen EE, Hemmer-Hansen J, Poulsen NA *et al.* (2009) Genomic signatures of local directional selection in a high gene flow marine organism; the Atlantic cod (*Gadus morhua*). *BMC Evolutionary Biology*, **9**, 276.

Nilsson GE, Lefevre S (2016) Physiological challenges to fishes in a warmer and acidified future. *Physiology*, **31**, 409–417.

Norman JD, Ferguson MM, Danzmann RG (2014a) Transcriptomics of salinity tolerance capacity in Arctic charr (*Salvelinus alpinus*): a comparison of gene expression profiles between divergent QTL genotypes. *Physiological Genomics*, **46**, 123–137.

Norman JD, Ferguson MM, Danzmann RG (2014b) An integrated transcriptomic and comparative genomic analysis of differential gene expression in Arctic charr (*Salvelinus alpinus*) following seawater exposure. *Journal of Experimental Biology*, **217**, 4029–4042.

Nosil P, Funk DJ, Ortiz-Barrientos D (2009) Divergent selection and heterogeneous genomic divergence. *Molecular Ecology*, **18**, 375–402.

Nussey DH, Postma E, Gienapp P, Visser ME (2005) Selection on heritable phenotypic plasticity in a wild bird population. *Science*, **310**, 304–306.

O'Brien-Macdonald K, Brown JA, Parrish CC (2006) Growth, behaviour, and digestive enzyme activity in larval Atlantic cod (*Gadus morhua*) in relation to rotifer lipid. *ICES Journal of Marine Science*, **63**, 275–284.

O'Brien CM, Fox CJ, Planque B, Casey J (2000) Climate variability and North Sea cod. *Nature*, **404**, 142–143.

Okoniewski MJ, Miller CJ (2006) Hybridization interactions between probesets in short oligo microarrays lead to spurious correlations. *BMC Bioinformatics*, **7**, 276.

Olsen EM, Carlson SM, Gjøsæter J, Stenseth NC (2009) Nine decades of decreasing phenotypic variability in Atlantic cod. *Ecology Letters*, **12**, 622–631.

Olsen EM, Knutsen H, Gjøsaeter J *et al.* (2008) Small-scale biocomplexity in coastal Atlantic cod supporting a Darwinian perspective on fisheries management. *Evolutionary Applications*, **1**, 524–533.

Olsen EM, Knutsen H, Gjøsæter J *et al.* (2004) Life-history variation among local populations of Atlantic cod from the Norwegian Skagerrak coast. *Journal of Fish Biology*, **64**, 1725–1730.

Olsen EM, Moland E (2011) Fitness landscape of Atlantic cod shaped by harvest selection and natural selection. *Evolutionary Ecology*, **25**, 695–710.

Oomen RA, Hutchings JA (2015a) Genetic variability in reaction norms in fishes. *Environmental Reviews*, **23**, 353–366.

Oomen RA, Hutchings JA (2015b) Variation in spawning time promotes genetic variability in population responses to environmental change in a marine fish. *Conservation Physiology*, **3**, 1–12.

Oomen RA, Hutchings JA (2016) Genetic variation in plasticity of life-history traits between Atlantic cod (*Gadus morhua*) populations exposed to contrasting thermal regimes. *Canadian Journal of Zoology*, **94**, 257–264.

Oomen RA, Hutchings JA (2017) Transcriptomic responses to environmental change in fishes: insights from RNA sequencing. *FACETS*, **2**, 610–641.

Orr HA, Unckless RL (2008) Population extinction and the genetics of adaptation. *The American Naturalist*, **172**, 160–169.

Orr HA, Unckless RL (2014) The population genetics of evolutionary rescue. *PLoS Genetics*, **10**, e1004551.

Otterlei E, Nyhammer G, Folkvord A, Stefansson SO (1999) Temperature- and size-dependent growth of larval and early juvenile Atlantic cod (*Gadus morhua*): a comparative study of Norwegian coastal cod and northeast Arctic cod. *Canadian Journal of Fisheries and Aquatic Sciences*, **56**, 2099–2111.

Ozsolak F, Milos PM (2011) RNA sequencing: advances, challenges and opportunities. *Nature Reviews Genetics*, **12**, 87–98.

Pacifici M, Foden WB, Visconti P *et al.* (2015) Assessing species vulnerability to climate change. *Nature Climate Change*, **5**, 215–225.

Padilla DK, Adolph SC (1996) Plastic inducible morphologies are not always adaptive: the importance of time delays in a stochastic environment. *Evolutionary Ecology*, **10**, 105–117.

Palumbi SR, Barshis DJ, Traylor-Knowles N, Bay RA (2014) Mechanisms of reef coral resistance to future climate change. *Science*, **344**, 895–899.

Patterson N, Price AL, Reich D (2006) Population structure and eigenanalysis. *PLoS Genetics*, **2**, 2074–2093.

Pavey SA, Bernatchez L, Aubin-Horth N, Landry CR (2012) What is needed for next-generation ecological and evolutionary genomics? *Trends in Ecology and Evolution*, **27**, 673–678.

Pearse DE (2016) Saving the spandrels? Adaptive genomic variation in conservation and fisheries management. *Journal of Fish Biology*, **89**, 2697–2716.

Pepin P (1991) Effect of temperature and size on development, mortality, and survival rates of the pelagic early life history stages of marine fish. *Canadian Journal of Fisheries and Aquatic Sciences*, **48**, 503–518.

Pertea M, Kim D, Pertea GM, Leek JT, Salzberg SL (2016) Transcript-level expression analysis of RNA-seq experiments with HISAT, StringTie and Ballgown. *Nature Protocols*, **11**, 1650–1667.

Pertea M, Pertea GM, Antonescu CM *et al.* (2015) StringTie enables improved reconstruction of a transcriptome from RNA-seq reads. *Nature Biotechnology*, **33**, 290–295.

Perutz MF (1979) Regulation of oxygen affinity of hemoglobin: influence of structure of the globin on the heme iron. *Annual Review of Biochemistry*, **48**, 327–386.

Pespeni MH, Palumbi SR (2013) Signals of selection in outlier loci in a widely dispersing species across an environmental mosaic. *Molecular Ecology*, **22**, 3580–3597.

Piiper J (1982) Respiratory gas exchange at lungs, gills and tissues: mechanisms and adjustments. *Journal of Experimental Biology*, **100**, 5–22.

Pinsky ML, Byler D (2015) Fishing, fast growth and climate variability increase the risk of collapse. *Proceedings of the Royal Society B: Biological Sciences*, **282**, 20151053.

Pinsky ML, Mantua NJ (2014) Emerging adaptation approaches for climate-ready fisheries management. *Oceanography*, **27**, 146–159.

Pinsky ML, Palumbi SR (2014) Meta-analysis reveals lower genetic diversity in overfished populations. *Molecular Ecology*, **23**, 29–39.

Pinsky ML, Worm B, Fogarty MJ, Sarmiento JL, Levin SA (2013) Marine taxa track local climate velocities. *Science*, **341**, 1239–1243.

Piry S, Alapetite A, Cornuet J-M *et al.* (2004) GENECLASS2: a software for genetic assignment and first-generation migrant detection. *Journal of Heredity*, **95**, 536–539.

Piskol R, Ramaswami G, Li JB (2013) Reliable identification of genomic variants from RNA-seq data. *American Journal of Human Genetics*, **93**, 641–651.

Podrabsky JE, Somero GN (2004) Changes in gene expression associated with acclimation to constant temperatures and fluctuating daily temperatures in an annual killifish *Austrofundulus limnaeus*. *The Journal of Experimental Biology*, **207**, 2237–2254.

Polato NR, Altman NS, Baums IB (2013) Variation in the transcriptional response of threatened coral larvae to elevated temperatures. *Molecular Ecology*, **22**, 1366–1382.

Pörtner HO (2002) Climate variations and the physiological basis of temperature dependent biogeography: systemic to molecular hierarchy of thermal tolerance in animals. *Comparative Biochemistry and Physiology Part A: Molecular & Integrative Physiology*, **132**, 739–761.

Pörtner HO, Bennett AF, Bozinovic F *et al.* (2006) Trade-offs in thermal adaptation: the need for a molecular to ecological integration. *Physiological and Biochemical Zoology*, **79**, 295–313.

Pörtner HO, Bock C, Knust R *et al.* (2008) Cod and climate in a latitudinal cline: physiological analyses of climate effects in marine fishes. *Climate Research*, **37**, 253–270.

Pörtner HO, Farrell AP (2008) Physiology and climate change. *Science*, **322**, 690–693.

Pörtner HO, Langenbuch M, Reipschlager A (2004) Biological impact of elevated ocean CO_2 concentrations: lessons from animal physiology and earth history. *Journal of Oceanography*, **60**, 705–718.

Pörtner HO, Peck MA (2010) Climate change effects on fishes and fisheries: towards a cause-and-effect understanding. *Journal of Fish Biology*, **77**, 1745–1779.

Poulsen NA, Nielsen EE, Schierup MH, Loeschcke V, Grønkjær P (2006) Long-term stability and effective population size in North Sea and Baltic Sea cod (*Gadus morhua*). *Molecular Ecology*, **15**, 321–331.

Prado-Lima M, Val AL (2016) Transcriptomic characterization of Tambaqui (*Colossoma macropomum*, Cuvier, 1818) exposed to three climate change scenarios. *PLoS ONE*, **11**, e0152366.

Pritchard JK, Di Rienzo A (2010) Adaptation – not by sweeps alone. *Nature Reviews Genetics*, **11**, 665–667.

Pujolar JM, Jacobsen MW, Als TD *et al.* (2014) Genome-wide single-generation signatures of local selection in the panmictic European eel. *Molecular Ecology*, **23**, 2514–2528.

Purcell S, Neale B, Todd-Brown K *et al.* (2007) PLINK: A tool set for whole-genome association and population-based linkage analyses. *The American Journal of Human Genetics*, **81**, 559–575.

Qian X, Ba Y, Zhuang Q, Zhong G (2014) RNA-seq technology and its application in fish transcriptomics. *OMICS: A Journal of Integrative Biology*, **18**, 98–110.

R Development Core Team (2014) R: a language and environment for statistical computing. ISBN 3-900051-07-0. Available from http://www.R-pr.

Rahmstorf S, Coumou D (2011) Increase of extreme events in a warming world. *Proceedings of the National Academy of Sciences USA*, **109**, 17905–17909.

Razgour O, Taggart JB, Manel S *et al.* (2018) An integrated framework to identify wildlife populations under threat from climate change. *Molecular Ecology Resources*, **18**, 18–31.

Reiss H, Hoarau G, Dickey-Collas M, Wolff WJ (2009) Genetic population structure of marine fish: mismatch between biological and fisheries management units. *Fish and Fisheries*, **10**, 361–395.

Reusch TBH (2014) Climate change in the oceans: evolutionary versus phenotypically plastic responses of marine animals and plants. *Evolutionary Applications*, **7**, 104–122.

Righton D, Andersen K, Neat F *et al.* (2010) Thermal niche of Atlantic cod *Gadus morhua*: limits, tolerance and optima. *Marine Ecology Progress Series*, **420**, 1–13.

Ritchie ME, Phipson B, Wu D *et al.* (2015) limma powers differential expression analyses for RNA-sequencing and microarray studies. *Nucleic Acids Research*, **43**, e47.

Roberts A, Pimentel H, Trapnell C, Pachter L (2011a) Identification of novel transcripts in annotated genomes using RNA-seq. *Bioinformatics*, **27**, 2325–2329.

Roberts A, Trapnell C, Donaghey J, Rinn JL, Pachter L (2011b) Improving RNA-seq expression estimates by correcting for fragment bias. *Genome Biology*, **12**, R22.

Robles JA, Qureshi SE, Stephen SJ *et al.* (2012) Efficient experimental design and analysis strategies for the detection of differential expression using RNA-sequencing. *BMC Genomics*, **13**, 484.

Roches S Des, Post DM, Turley NE *et al.* (2018) The ecological importance of intraspecific variation. *Nature Ecology & Evolution*, **2**, 57–64.

Roesti M, Kueng B, Moser D, Berner D (2015) The genomics of ecological vicariance in threespine stickleback fish. *Nature Communications*, **6**, 8767.

Rogers LA, Olsen EM, Knutsen H, Stenseth NC (2014) Habitat effects on population connectivity in a coastal seascape. *Marine Ecology Progress Series*, **511**, 153–163.

Rogers LA, Stenseth NC (2017) Fine-scale population dynamics in a marine fish species inferred from dynamic state-space models. *Journal of Animal Ecology*, **86**, 888–898.

Rogers LA, Stige LC, Olsen EM *et al.* (2011) Climate and population density drive changes in cod body size throughout a century on the Norwegian coast. *Proceedings of the National Academy of Sciences*, **108**, 1961–1966.

Romiguier J, Gayral P, Ballenghien M *et al.* (2014) Comparative population genomics in animals uncovers the determinants of genetic diversity. *Nature*, **515**, 261–263.

Roney NE (2016) Reproductive success in Atlantic cod, *Gadus morhua*. MSc thesis. Dalhousie University.

Roney NE, Hutchings JA, Olsen EM *et al.* (2016) Fine-scale life-history structure in a highly mobile marine fish. *Evolutionary Ecology Research*, **17**, 95–109.

Roney NE, Oomen RA, Knutsen H, Olsen EM, Hutchings JA (2018a) Temporal variability in offspring quality and individual reproductive output in a broadcast-spawning marine fish. *ICES Journal of Marine Science*, **75**, 1353–1361.

Roney NE, Oomen RA, Knutsen H, Olsen EM, Hutchings JA (2018b) Fine-scale population differences in Atlantic cod reproductive success: a potential mechanism for ecological speciation in a marine fish. *Ecology and Evolution*, **8**, 11634–11644.

Rousset F (2008) GENEPOP'007: a complete re-implementation of the GENEPOP software for Windows and Linux. *Molecular Ecology Resources*, **8**, 103–106.

Rowe S, Hutchings JA, Skjæraasen JE (2007) Nonrandom mating in a broadcast spawner: mate size influences reproductive success in Atlantic cod (*Gadus morhua*). *Canadian Journal of Fisheries and Aquatic Sciences*, **226**, 219–226.

Rowe S, Hutchings J, Skjæraasen J, Bezanson L (2008) Morphological and behavioural correlates of reproductive success in Atlantic cod *Gadus morhua*. *Marine Ecology Progress Series*, **354**, 257–265.

Ruegg K, Bay RA, Anderson EC *et al.* (2018) Ecological genomics predicts climate vulnerability in an endangered southwestern songbird. *Ecology Letters*, **21**, 1085–1096.

Ryder OA (1986) Species conservation and systematics: the dilemma of subspecies. *Trends in Ecology and Evolution*, **1**, 9–10.

Salem M, Paneru B, Al-Tobasei R *et al.* (2015) Transcriptome assembly, gene annotation and tissue gene expression atlas of the rainbow trout. *PloS One*, **10**, e0121778.

Salinas S, Munch SB (2012) Thermal legacies: transgenerational effects of temperature on growth in a vertebrate. *Ecology Letters*, **15**, 159–163.

Salisbury JP, Sîrbulescu RF, Moran BM *et al.* (2015) The central nervous system transcriptome of the weakly electric brown ghost knifefish (*Apteronotus leptorhynchus*): de novo assembly, annotation, and proteomics validation. *BMC Genomics*, **16**, 166.

Savolainen O, Lascoux M, Merilä J (2013) Ecological genomics of local adaptation. *Nature Reviews Genetics*, **14**, 807–820.

Schena M, Shalon D, Davis RW, Brown PO (1995) Quantitative monitoring of gene expression patterns with a complementary DNA microarray. *Science*, **270**, 467–470.

Schindler DE, Hilborn R, Chasco B *et al.* (2010) Population diversity and the portfolio effect in an exploited species. *Nature*, **465**, 609–612.

Schlichting CD (1986) The evolution of phenotypic plasticity in plants. *Annual Review of Ecology and Systematics*, **17**, 667–693.

Schmalhausen II (1949) *Factors of evolution: the theory of stabilizing selection*. The Blakiston Co., Philadelphia, PA.

Schubert M, Ermini L, Der Sarkissian C *et al.* (2014) Characterization of ancient and modern genomes by SNP detection and phylogenomic and metagenomic analysis using PALEOMIX. *Nature Protocols*, **9**, 1056–1082.

Schulte PM (2004) Responses to environmental stressors in an estuarine fish: interacting stressors and the impacts of local adaptation. *Journal of Thermal Biology*, **32**, 152–161.

Schulte PM (2014) What is environmental stress? Insights from fish living in a variable environment. *The Journal of Experimental Biology*, **217**, 23–34.

Schulte PM, Healy TM, Fangue NA (2011) Thermal performance curves, phenotypic plasticity, and the time scales of temperature exposure. *Integrative and Comparative Biology*, **51**, 691–702.

Schwander T, Libbrecht R, Keller L (2014) Supergenes and complex phenotypes. *Current Biology*, **24**, R288–R294.

Scott GR, Johnston IA (2012) Temperature during embryonic development has persistent effects on thermal acclimation capacity in zebrafish. *Proceedings of the National Academy of Sciences USA*, **109**, 14247–14252.

Sendler E, Johnson GD, Krawetz SA (2011) Local and global factors affecting RNA sequencing analysis. *Analytical Biochemistry*, **419**, 317–322.

Shama LNS, Mark FC, Strobel A *et al.* (2016) Transgenerational effects persist down the maternal line in marine sticklebacks: gene expression matches physiology in a warming ocean. *Evolutionary Applications*, **9**, 1096–1111.

Shannon P, Markiel A, Ozier O *et al.* (2003) Cytoscape: a software environment for integrated models of biomolecular interaction networks. *Genome Research*, **13**, 2498–2504.

Sick K (1965) Haemoglobin polymorphism of cod in the North Sea and the north Atlantic ocean. *Hereditas*, **54**, 49–69.

Simão FA, Waterhouse RM, Ioannidis P, Kriventseva E V, Zdobnov EM (2015) Genome analysis BUSCO: assessing genome assembly and annotation completeness with single-copy orthologs. *Bioinformatics*, **31**, 3210–3212.

Sinclair-Waters M, Bradbury IR, Morris CJ *et al.* (2018) Ancient chromosomal rearrangement associated with local adaptation of a postglacially colonized population of Atlantic Cod in the northwest Atlantic. *Molecular Ecology*, **27**, 339–351.

Skiftesvik AB (1992) Changes in behaviour at onset of exogenous feeding in marine fish larvae. *Canadian Journal of Fisheries and Aquatic Sciences*, **49**, 1570–1572.

Slimen IB, Najar T, Ghram A *et al.* (2014) Reactive oxygen species, heat stress and oxidative-induced mitochondrial damage. A review. *International Journal of Hyperthermia*, **30**, 513–523.

Smith S, Bernatchez L, Beheregaray LB (2013) RNA-seq analysis reveals extensive transcriptional plasticity to temperature stress in a freshwater fish species. *BMC Genomics*, **14**, 375.

Sodeland M, Jentoft S, Jorde PE *et al.* Genomic divergence of coexisting Atlantic cod (*Gadus morhua*) populations testify of historic allopatry, post-glacial expansions and ongoing selection. *In review*, 1–25.

Sodeland M, Jorde PE, Lien S *et al.* (2016) "Islands of Divergence" in the Atlantic cod genome represent polymorphic chromosomal rearrangements. *Genome Biology & Evolution*, **8**, 1012–1022.

Staal FJT, Luis TC, Tiemessen MM (2008) WNT signalling in the immune system: WNT is spreading its wings. *Nature Reviews Immunology*, **8**, 581–593.

Star B, Boessenkool S, Gondek AT *et al.* (2017) Ancient DNA reveals the Arctic origin of Viking Age cod from Haithabu, Germany. *Proceedings of the National Academy of Sciences*, **114**, 9152–9157 |.

Star B, Jentoft S (2012) Why does the immune system of Atlantic cod lack MHC II? *Bioessays*, **34**, 648–51.

Star B, Nederbragt AJ, Jentoft S *et al.* (2011) The genome sequence of Atlantic cod reveals a unique immune system. *Nature*, **477**, 207–210.

Steinarsson A, Björnsson B (1999) The effects of temperature and size on growth and mortality of cod larvae. *Journal of Fish Biology*, **55**, 100–109.

Stenseth NC, Jorde PE, Chan KS *et al.* (2006) Ecological and genetic impact of Atlantic cod larval drift in the Skagerrak. *Proceedings of the Royal Society B: Biological Sciences*, **273**, 1085–1092.

Stenseth NC, Mysterud A (2002) Climate, changing phenology, and other life history traits: nonlinearity and match–mismatch to the environment. *Proceedings of the National Academy of Sciences of the United States of America*, **99**, 13379–13381.

Storfer A (1996) Quantitative genetics: a promising approach for the assessment of genetic variation in endangered species. *Trends in Ecology and Evolution*, **11**, 343–348.

van Straalen NM, Feder ME (2012) Ecological and evolutionary functional genomics — how can it contribute to risk assessment of chemicals? *Environmental Science & Technology*, **46**, 3–9.

Struhl K (2007) Transcriptional noise and the fidelity of initiation by RNA polymerase II. *Nature Structural and Molecular Biology*, **14**, 103–105.

Sturtevant AH (1921) A case of rearrangement of genes in *Drosophila*. *Proceedings of the National Academy of Sciences*, **7**, 235–237.

Subramanian A, Tamayo P, Mootha VK *et al.* (2005) Gene set enrichment analysis: a knowledge-based approach for interpreting genome-wide expression profiles. *Proceedings of the National Academy of Sciences USA*, **102**, 15545–15550.

Sun L, Liu S, Bao L *et al.* (2015) Claudin multigene family in channel catfish and their expression profiles in response to bacterial infection and hypoxia as revealed by meta-analysis of RNA-seq datasets. *Comparative Biochemistry and Physiology Part D: Genomics and Proteomics*, **13**, 60–69.

Sundby S, Bjørke H, Soldai AV, Olsen S (1989) Mortality rates during the early life stages and year-class strength of northeast Arctic cod (*Gadus morhua* L.). *Rapports et Procès-verbaux des Réunions Conseil International pour l'Exploration de la Mer*, **191**, 351–358.

Svåsand T, Kristiansen TS, Pedersen T *et al.* (2000) The enhancement of cod stocks. *Fish and Fisheries*, **1**, 173–205.

Svedäng H, Bardon G (2003) Spatial and temporal aspects of the decline in cod (*Gadus morhua* L.) abundance in the Kattegat and eastern Skagerrak. *ICES Journal of Marine Science*, **60**, 32–37.

Svedäng H, Righton D, Jonsson P (2007) Migratory behaviour of Atlantic cod *Gadus morhua*: natal homing is the prime stock-separating mechanism. *Marine Ecology Progress Series*, **345**, 1–12.

Tallmon DA, Luikart G, Waples RS (2004) The alluring simplicity and complex reality of genetic rescue. *Trends in Ecology and Evolution*, **19**, 489–496.

Therkildsen NO, Nielsen EE, Swain DP (2010) Large effective population size and temporal genetic stability in Atlantic cod (*Gadus morhua*) in the southern Gulf of St. Lawrence. *Canadian Journal of Fisheries and Aquatic Sciences*, **67**, 1585–1595.

Tigano A, Friesen VL (2016) Genomics of local adaptation with gene flow. *Molecular Ecology*, **25**, 2144–2164.

Todd E V, Black MA, Gemmell NJ (2016) The power and promise of RNA-seq in ecology and evolution. *Molecular Ecology*, **25**, 1224–1241.

Tomanek L (2010) Variation in the heat shock response and its implication for predicting the effect of global climate change on species' biogeographical distribution ranges and metabolic costs. *The Journal of Experimental Biology*, **213**, 971–979.

Tørresen OK, Star B, Jentoft S *et al.* (2017) An improved genome assembly uncovers prolific tandem repeats in Atlantic cod. *BMC Genomics*, **18**, 95.

Trapnell C, Roberts A, Goff L *et al.* (2012) Differential gene and transcript expression analysis of RNA-seq experiments with TopHat and Cufflinks. *Nature Protocols*, **7**, 562–578.

Trapnell C, Williams BA, Pertea G *et al.* (2010) Transcript assembly and quantification by RNA-seq reveals unannotated transcripts and isoform switching during cell differentiation. *Nature Biotechnology*, **28**, 511–515.

Tse AC-K, Li J-W, Wang SY *et al.* (2016) Hypoxia alters testicular functions of marine medaka through microRNAs regulation. *Aquatic Toxicology*, **180**, 266–273.

Umina PA, Weeks AR, Kearney MR, Mckechnie SW, Hoffmann AA (2005) A rapid shift in a classic clinal pattern in *Drosophila* reflecting climate change. *Science*, **308**, 691–693.

Valladares F, Matesanz S, Guilhaumon F *et al.* (2014) The effects of phenotypic plasticity and local adaptation on forecasts of species range shifts under climate change. *Ecology Letters*, **17**, 1351–1364.

Vallone D, Lahiri K, Dickmeis T, Foulkes NS (2007) Start the clock! Circadian rhythms and development. *Developmental Dynamics*, **236**, 142–155.

Vandersteen Tymchuk W, O'Reilly P, Bittman J, MacDonald D, Schulte P (2010) Conservation genomics of Atlantic salmon: variation in gene expression between and within regions of the Bay of Fundy. *Molecular Ecology*, **19**, 1842–1859.

Veilleux HD, Ryu T, Donelson JM *et al.* (2015) Molecular processes of transgenerational acclimation to a warming ocean. *Nature Climate Change*, **5**, 1074–1078.

Villegas-Ríos D, Réale D, Freitas C, Moland E, Olsen EM (2017) Individual level consistency and correlations of fish spatial behaviour assessed from aquatic animal telemetry. *Animal Behaviour*, **124**, 83–94.

Villegas-Ríos D, Réale D, Freitas C, Moland E, Olsen EM (2018) Personalities influence spatial responses to environmental fluctuations in wild fish. *Journal of Animal Ecology*, **87**, 1309–1319.

de Villemereuil P, Gaggiotti OE, Mouterde M, Till-Bottraud I (2016) Common garden experiments in the genomic era: new perspectives and opportunities. *Heredity*, **116**, 249–254.

Visser ME (2008) Keeping up with a warming world; assessing the rate of adaptation to climate change. *Proceedings of the Royal Society B: Biological Sciences*, **275**, 649–659.

Wagner A (2005) Energy constraints on the evolution of gene expression. *Molecular Biology and Evolution*, **22**, 1365–1374.

Wang Z, Gerstein M, Snyder M (2009) RNA-seq: a revolutionary tool for transcriptomics. *Nature Reviews Genetics*, **10**, 57–63.

Wang L, Liu P, Wan ZY *et al.* (2016) RNA-seq revealed the impairment of immune defence of tilapia against the infection of *Streptococcus agalactiae* with simulated climate warming. *Fish & Shellfish Immunology*, **55**, 679–689.

Wang G, Yang E, Smith KJ *et al.* (2014) Gene expression responses of threespine stickleback to salinity: implications for salt-sensitive hypertension. *Frontiers in Genetics*, **5**, 312.

Waples RS, Lindley ST (2018) Genomics and conservation units: the genetic basis of adult migration timing in Pacific salmonids. *Evolutionary Applications*, 1518–1526.

Ward RD (2000) Genetics in fisheries management. *Hydrobiologia*, **420**, 191–201.

Ward RD, Woodwark M, Skibinski DOF (1994) A comparison of genetic diversity levels in marine, freshwater, and anadramous fishes. *Journal of Fish Biology*, **44**, 213–232.

Weir BS, Cockerham CC (1984) Estimating F-statistics for the analysis of population structure. *Evolution*, **38**, 1358–1370.

Wellband K, Mérot C, Linnansaari T *et al.* (2019) Chromosomal fusion and life history-associated genomic variation contribute to within-river local adaptation of Atlantic salmon. *Molecular Ecology*, doi: 10.1111/mec.14965.

Wellenreuther M, Bernatchez L (2018) Eco-evolutionary genomics of chromosomal inversions. *Trends in Ecology and Evolution*, **33**, 427–440.

West-Eberhard MJ (2003) *Developmental plasticity and evolution*. Oxford University Press, New York, NY.

Williams GC (1966) *Adaptation and natural selection*. Princeton University Press, Princeton, NJ.

Williams SE, Shoo LP, Isaac JL, Hoffmann AA, Langham G (2008) Towards an integrated framework for assessing the vulnerability of species to climate change. *PLoS Biology*, **6**, e325.

Woltereck R (1909) Weiterer experimentelle untersuchungen uber artveranderung, speziell uber das wessen quantitativer artunterschiede bei daphniden. *Verhandlungen der Deutschen Zoologischen Gesellschaft*, **19**, 110–172.

Wong MK-S, Ozaki H, Suzuki Y, Iwasaki W, Takei Y (2014) Discovery of osmotic sensitive transcription factors in fish intestine via a transcriptomic approach. *BMC Genomics*, **15**, 1134.

Wood AW, Duan C, Bern HA (2005) Insulin-like growth factor signaling in fish. *International Review of Cytology*, **243**, 215–285.

Worm B, Hilborn R, Baum JK *et al.* (2009) Rebuilding global fisheries. *Science*, **325**, 578–585.

Wright S (1931) Evolution in Mendelian populations. *Genetics*, **16**, 97–159.

Xia JH, Liu P, Liu F *et al.* (2013) Analysis of stress-responsive transcriptome in the intestine of Asian seabass (*Lates calcarifer*) using RNA-seq. *DNA Research*, **20**, 449–460.

Xu Z, Gan L, Li T *et al.* (2015) Transcriptome profiling and molecular pathway analysis of genes in association with salinity adaptation in Nile tilapia *Oreochromis niloticus*. *PloS One*, **10**, e0136506.

Xu J, Li Q, Xu L *et al.* (2013) Gene expression changes leading extreme alkaline tolerance in Amur ide (*Leuciscus waleckii*) inhabiting soda lake. *BMC Genomics*, **14**, 682.

Yeaman S (2013) Genomic rearrangements and the evolution of clusters of locally adaptive loci. *Proceedings of the Royal Society B: Biological Sciences*, **110**, E1743– E1751.

Yeaman S, Otto SP (2011) Establishment and maintenance of adaptive genetic divergence under migration, selection, and drift. *Evolution*, **65**, 2123–2129.

Yeaman S, Whitlock MC (2011) The genetic architecture of adaptation under migration-selection balance. *Evolution*, **65**, 1897–1911.

Yuan Z, Liu S, Yao J *et al.* (2016) Expression of Bcl-2 genes in channel catfish after bacterial infection and hypoxia stress. *Developmental & Comparative Immunology*, **65**, 79–90.

Yue H, Li C, Du H, Zhang S, Wei Q (2015) Sequencing and de novo assembly of the gonadal transcriptome of the endangered Chinese sturgeon (*Acipenser sinensis*). *PloS One*, **10**, e0127332.

Zhang R, Ludwig A, Zhang C *et al.* (2015) Local adaptation of *Gymnocypris przewalskii* (Cyprinidae) on the Tibetan Plateau. *Scientific Reports*, **5**, 9780.